THE METAMORPHIC ENVIRONMENTS OF THE STRONTIAN, FOYERS
AND DALBEATTIE INTRUSIONS, SCOTLAND

BY IAN MICHAEL TYLER

Ph.D THESIS

UNIVERSITY OF ASTON IN BIRMINGHAM

AUGUST, 1981

SUMMARY

THE METAMORPHIC ENVIRONMENTS OF THE STRONTIAN, FOYERS AND
DALBEATTIE INTRUSIONS, SCOTLAND.

BY IAN MICHAEL TYLER.

SUBMITTED FOR THE DEGREE OF DOCTOR OF PHILOSOPHY, 1981.

Three metamorphic aureoles around intrusions of the Caledonian
'Newer Granite' suite are described. Each represents a diff-
erent orogenic environment.

The Strontian complex is intruded into sillimanite grade
Moinian metasediments at the core of the orogen. The aureole
comprises three zones; a transitional muscovite + sillimanite
+ K-feldspar zone, a sillimanite + K-feldspar zone and an inner
cordierite + K-feldspar zone. Contact migmatization occurs in
the inner part of the aureole.

Zoning profiles from garnets in both regional and aureole assem-
blages show retrograde Mn-rich rims. Fe and Mg compositions
are re-equilibrated to contact conditions. Apparent re-equil-
ibration of Ca compositions results from increasingly ideal
solid solution behaviour of Ca in plagioclase and garnet with
increasing temperature. Temperatures of $690^{\circ}C$ at 4.1 kbar
(X_{H_2O} = 0.53) are estimated in the cordierite + K-feldspar zone,
dropping to $630^{\circ}C$ (X_{H_2O} = 0.69) at the sillimanite + K-feldspar
isograd.

The zones increase in width to the east, influenced by the
regional thermal gradient at the time of intrusion. The time-
scale of the contact event, t_2, relative to the regional, t_1,
is estimated as $t_2/t_1 = 10^{-1.1\pm0.7}$ and is consistent with
intrusion at an early stage of regional uplift and cooling.

The Foyers complex intrudes Moinian rocks at a higher struc-
tural level. Regional assemblages range from garnet to sill-
imanite grade. Three contact zones are recognised; a silliman-
ite zone, a sillimanite + K-feldspar zone and an inner cordier-
ite + K-feldspar zone. The limit of the aureole is marked by
the breakdown of garnet which shows disequilibrium, both tex-
turally, and in complex zoning profiles, within it. Temperatu-
res of $660^{\circ}C$ at 3.9 kbar (X_{H_2O} = 0.14) are estimated in the
cordierite + K-feldspar zone.

The Dalbeattie complex is at the margin of the orogen, intruded
into low grade Silurian metasediments. Two zones are recog-
nised; a biotite zone and an inner hornblende zone. Cordierite
and diopside are present in the inner zone.

Key Words: SCOTLAND, CALEDONIAN OROGENY, METAMORPHIC AUREOLES,
             GEOTHERMOMETRY, GEOBAROMETRY.

CONTENTS

LIST OF FIGURES AND TABLES

Maps 1, 2, and 3 in folder inside back cover.

ACKNOWLEDGEMENTS

CHAPTER 1

INTRODUCTION

The Caledonian orogenic event has been recognised in
Scandanavia, East Greenland, Britain, Ireland and eastern
North America, and these now separate fragments originally
formed one continuous fold belt.

The Caledonides in Britain can be divided into two parts
(fig. 1.1); the northern belt or orthotectonic zone, occupying
the terrain between the Moine thrust and the Highland Bound-
ary fault; and the southern belt or paratectonic zone, which
includes the Southern Uplands, the Lake District and Wales
(cf. Johnson et.al., 1979; Fettes, 1979). These zones have
been related to a plate tectonic model, involving closure of
a proto-Atlantic Ocean, Iapetus, by several authors. Dewey
(1969) interpreted the orthotectonic belt, which is extensively
deformed and metamorphosed, as representing a Cordillera rel-
ated to the subduction of the Iapetus oceanic crust. The
paratectonic belt was associated with the final stages of
closure, and, although deformed, showed only low grade meta-
morphism. Later models follow the same broad pattern, but
closure was suggested to be diachronous, occurring at an
earlier stage to the northeast than to the southwest (Phillips
et.al., 1976; Lambert & McKerrow, 1976).

One of the major components of the orogen is a suite of calc-
alkaline intrusions which, although dominantly granitic, range
from gabbro and diorite through tonalite to adamellite. Their
emplacement occurred during a period between 600 and 390 Ma
(Brown, 1979) and they may be divided into two groups. Those
in the first group are relatively small and are deformed.
They are therefore regarded as pre-tectonic. The second
group are volumetrically more important and are post-tectonic.

FIGURE 1.1

The Scottish Caledonian 'Newer Granite' suite.

D.- Dalbeattie granite complex; F.- Foyers complex;

G.G.F. - Great Glen Fault; H.B.F. - Highland Boundary

Fault; M.T. - Moine Thrust; S. - Strontian complex;

S.U.F. - Southern Uplands Fault.

50 km

N

M.T.

G.G.F.

Orthotectonic Zone

H.B.F.

S

Midland

Valley

S.U.F.

Paratectonic Zone

D

11
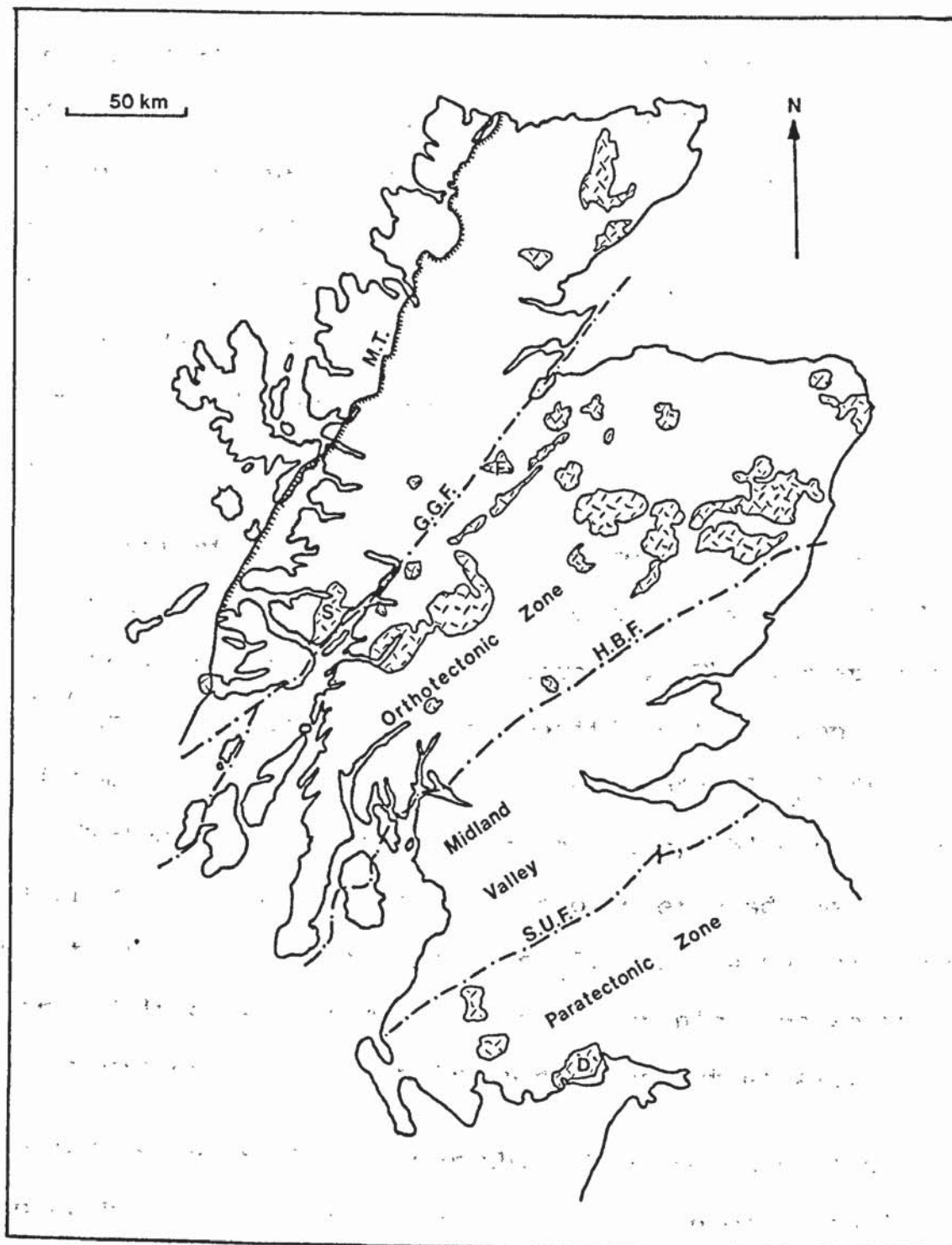
The post-tectonic granites are often referred to as the 'Newer Granite' suite, and generally give radiometric ages of c.400 Ma. Intrusion had taken place in uppermost Silurian and lower Devonian times after the closure of Iapetus, and little difference is seen in the petrography of intrusions on different sides of the suture. From an investigation of U-Pb isotopic systems in zircons, Pidgeon & Aftalion (1978) have established the nature of the source rocks from which various granites were derived. Those in the orthotectonic zone to the north of the Highland Boundary fault, showed evidence of having been derived from a dominantly Proterozoic crust, while those in the paratectonic zone were derived from new, Palaeozoic crust.

In the present study the metamorphic aureoles developed around three granitic intrusions belonging to the 'Newer Granite' suite in Scotland, have been investigated. The Strontian complex has been intruded into migmatitic metasediments at the core of the orogen at an early stage of regional uplift and cooling (Watson, 1964). The Foyers complex, while outcropping in the orogenic core, is intruded into lower grade metasediments representing a higher structural level. The Dalbeattie complex is intruded into sediments in the paratectonic zone which represent an orogenic margin environment (Leggett et.al., 1979).

A detailed study of the petrography of the country rocks around each intrusion has been carried out in order to identify the metamorphic zones, and their intervening isogradic reactions, present within each aureole. Electron microprobe analyses of silicate minerals, together with published experimental and theoretical calibrations of mineral equilibria within the

metasediments, have been used to establish the physical conditions of contact metamorphism, and where possible of the preceding Caledonian regional metamorphism. As the three intrusions concerned have similar igneous mineralogies little difference would be expected in initial magma temperatures. Any differences in temperature and pressure between the aureoles may therefore be interpreted in terms of their depth of intrusion, and of variations in the background regional temperature at the time of intrusion.

CHAPTER 2

THE STRONTIAN AUREOLE

2.1 INTRODUCTION

The Strontian "granitic" complex forms the largest of the Caledonian "Newer Granite" suite of intrusions northwest of the Great Glen. It occupies some 130 square kilometres of relatively low lying ground at the southwest end of Loch Linnhe, extending northwards as a tongue shaped body, to Strontian and the disused lead mines at Bellsgrove Lodge.

A detailed description of the igneous petrology of the complex has been given by Sabine (1963). It intrudes Moine schists and gneisses and consists of three main intrusive bodies; a tonalitic granodiorite, a porphyritic granodiorite, and a porphyritic biotite granite (fig 2.1). The two grano-diorites are roughly concentric, the tonalitic granodiorite forming the outer shell of the complex. A foliation can be seen within them and is particularly well developed near to the contact with the country rocks. The outcrop of the tonalite is relatively narrow on the western side of the pluton and a chilled margin is observed between it and the porphyritic granodiorite. By contrast, this contact on the eastern side is gradational over several tens of metres, suggesting that the intrusion of the two bodies took place over a relatively short time interval. The biotite granite forms a much later body cutting across both the granodiorites and extending into the country rocks. It displays no foliation or preferred mineral orientation. Within all three bodies xenoliths of appinitic material, ranging in size from a few centimetres to several hundreds of metres, are common. These probably represent the remnants of an early, dioritic phase. Xenoliths of country rock are also present.

The age of the granodiorites has been determined by Pidgeon

14

FIGURE 2.1

Geological map of the Strontian complex.

After: Phemister (1936) and Munro (1965).

5 km

N

Glen Tarbert

Camas
Chil-Mhalieu

Beinn
Mheadhoin

Tertiary

	Tonalitic Granodiorite
	Granodiorite
	Biotite Granite
	Appinite
	Moine Metasediments
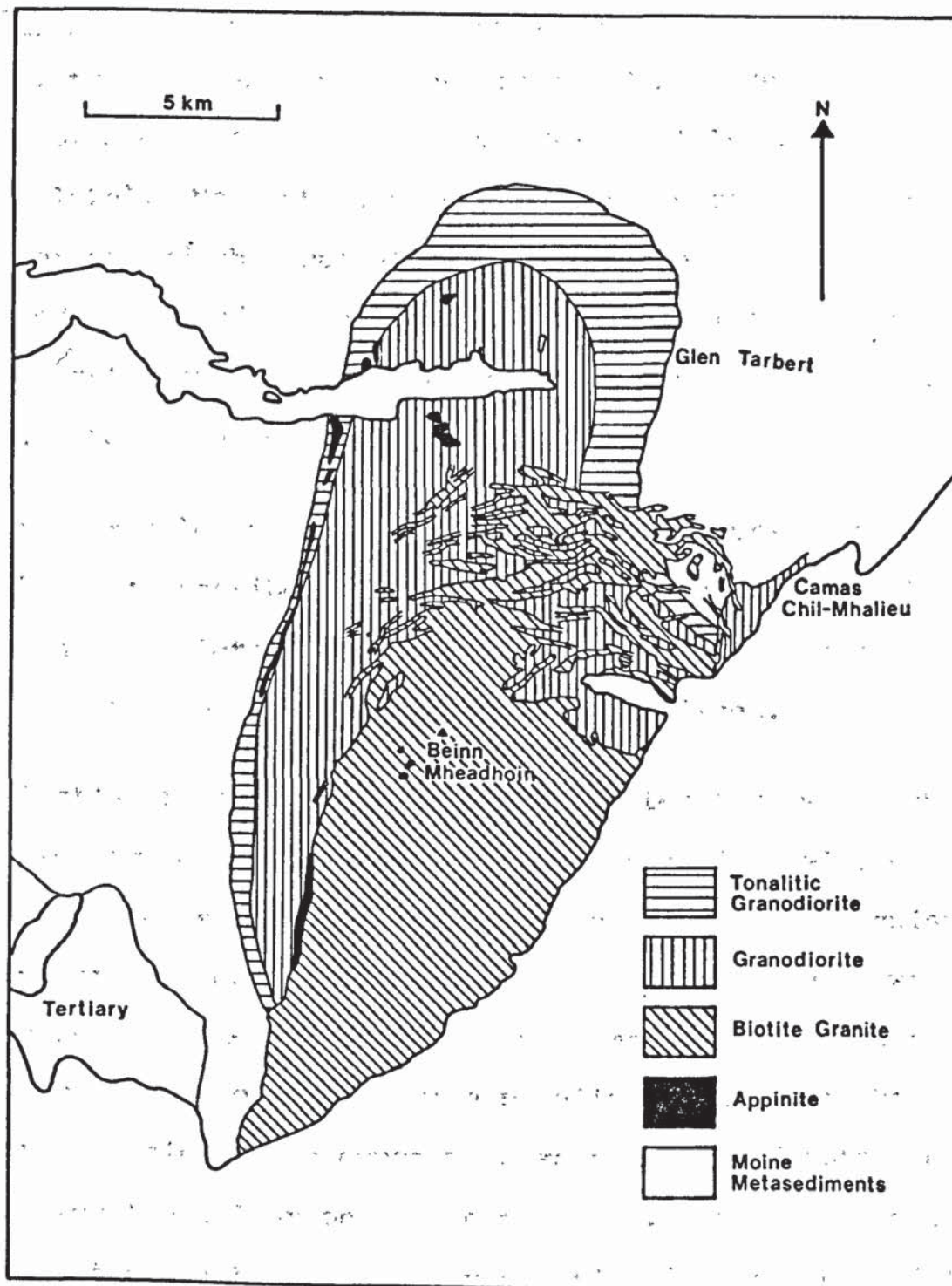
& Aftalion (1978) at 435 ± 10 Ma based on U-Pb ratios in zircons. Halliday et.al. (1979) have suggested a 54 ± 15 Ma gap between the intrusion of the tonalitic granodiorite and the biotite granite.

2.2 PREVIOUS RESEARCH ON THE AUREOLE ROCKS

Parts of the complex were mapped by the Survey during preparation of Sheets 44 & 53 (Bailey & Maufe, 1916; Lee & Bailey, 1925). No contact alteration of the country rocks was observed and this was attributed to "the highly crystallised nature of the gneiss, and the relative stability of its constituent minerals, among which muscovite does not occur". (Lee & Bailey, 1925, p46).

The first detailed survey, carried out during preparation of Sheet 52, was described by MacGregor & Kennedy (1932). A sketch map, complete except for the area to the east and northeast of Beinn Mheadhoin, was also published.

Again, little or no evidence of contact alteration was found which was regarded as unusual, particularly with reference to the pelitic rocks. The margin of the complex was recognised as being transgressive to the country rocks. However, where the regional strike had been nearly normal to the contact, it now swung around so as to strike parallel to it. At the contact, the dip of the country rocks parallelled both the contact and the foliation in the tonalite. Where the complex was in contact with a dominantly pelitic lithology containing bands of granular psammite and amphibolite, disruption and disorientation had resulted in the formation of "breccias" with angular blocks of siliceous or hornblendic rocks embedded in a matrix of injection gneiss. These observations

17

were attributed to flowage of the country rocks under the
influence of magma pressure. As the intruding magma forced
the country rock aside, the pelites yielded plastically,
while more resistant lithologies were broken into angular
blocks around which the foliation in the pelite flowed. It
was concluded that, "as the Morvern 'Granite' shows neither
an injecting nor a hornfels type of contact, the physical
conditions prevailing during intrusion must have been
abnormal".

A more complete version of the sketch map appeared in the
Survey's Northern Highlands Regional Guide (Phemister, 1936).

Although primarily concerned with the igneous petrology of
the complex, Sabine (1963) included a description of the
contact and of the schists immediately adjacent to it. In
general the margin of the complex dipped inwards so that
the tonalite overlay the schists. The angle of dip was
generally between 60° and 80°. South of Glen Tarbert the
angle decreased to about 45° or less. Five analyses of
schists collected from within 45 feet of the contact were
presented. All were of feldspathic type containing quartz,
oligoclase, orthoclase and biotite. One sample contained
garnet. It was concluded that there had been definite but
limited metasomatism of the schists at the margin.

Watson (1964) used variations in the nature of contact
metamorphism around Caledonian granites to draw conclusions
concerning the thermal structure of the Caledonides at the
time of their emplacement. The observations of MacGregor
& Kennedy (1932) on the lack of contact minerals at
Strontian were cited as evidence that "intrusion took place

18

while the country rocks were still relatively hot and in the same general environment as that in which regional metamorphism had ended".

Munro (1965, 1973) carried out a detailed study of the flow fabric developed within the complex, and of the structural effect of the intrusion on the adjacent country rocks. A zone of deformation, up to 1km wide, within which the bedding and schistosity of the schists and gneisses, the axial planes of small folds and the planes on which shearing occurred tended to be orientated to the contact, was identified. Large scale structures were also found to be deflected. This deformation was not uniform, and areas of intense shearing were separated by areas of virtually undeformed rocks. A zone of strongly sheared rocks, up to 100 metres wide, was commonly found at the contact. Small scale folds in this zone were either formed by deformation during intrusion, or by reorientation of pre-existing regional folds.

The contact was generally found to be sharp, but could become gradational over several metres particularly against semi-pelitic schists, attributed to local contact metasomatism. Extensive evidence of small scale stoping at the contact was recognised.

It was concluded that intrusion of the granodiorite occurred at considerable depth in the crust, where its forcible emplacement produced plastic deformation of the country rocks at the contact. Extensive displacement of the schists had occurred, primarily through vertical movement on relatively restricted shear zones.

The flow fabric developed within the granodiorite was

assumed to be orientated parallel to the nearest contact surface. This allowed the overall pattern of the flow fabric to be interpreted in terms of the shape of the pluton. It was found that the intrusion took the form of a harpolith, a cylindrical stock-like body centred on Kingairloch in the south, extending northwards as a sub-horizontal, tongue-like mass. The initial ascent of the magma is assumed to have been controlled by the Loch Quoich line, a major structural boundary in the Moines, lateral extension to the north apparently taking place along it. A further wedge-like extension was inferred to the northeast, between Loch a'Choire and Camas Chil Mhalieu on Loch Linnhe. This was thought to have been controlled by the generally flat lying orientation of the schists in this area.

An intrusion model was presented to explain the inferred shape of the pluton. The viscosity of the ascending granodiorite magma increased as it cooled and crystallisation proceeded. Eventually, the increasing viscosity inhibited the rise of the magma and it became emplaced. A fresh influx of magma into the emplaced body resulted in a mushrooming of its upper part. This tended to exploit pre-existing structures in the country rocks. Such a model suggested that the roof of the granodiorite may have been no more than a few thousand metres above the present erosion level. A gravity survey of the complex carried out by Blythe (1975) provides supporting evidence for the harpolithic form of the pluton.

The presence of cordierite co-existing with garnet in the country rocks at the margin of the complex was first recognised by P.D. Marsh (personal communication to J. R.

20

Ashworth). Ashworth & Chinner (1978) used Fe-Mg distribution between these two minerals to obtain estimates for the temperature and pressure of formation of the assemblage. These were found to be 4.2Kb at 700°C. It was also found that P_{H_2O} was considerably less than P_{TOTAL} (P_{H_2O} /P_{TOTAL} = 0.6). As the cordierite-garnet assemblages had only a localised occurrence near the granodiorite, they were interpreted as being a product of contact metamorphism by the granodiorite. The samples studied contained sillimanite and potash feldspar and were migmatitic, having leucosomes up to 1cm. thick. Both the cordierite and the leucosomes were considered to have been produced by operation of the reaction

Al_2SiO_5 + biotite + quartz

= cordierite + garnet + K-feldspar + melt.
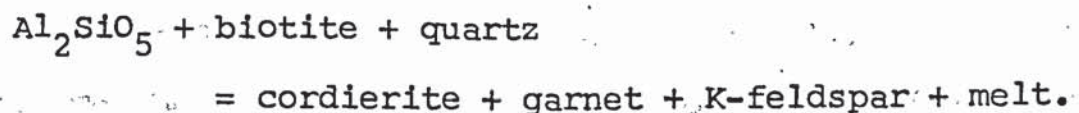
The absence of a hornfelsic texture in the country rocks suggested that they retained much of the heat from the regional metamorphism at the time of intrusion.

The present study is intended to continue the work of Ashworth & Chinner (1978) on the Strontian aureole by identifying the physical conditions prevailing in the thermal aureole and, as far as possible, the preceding regional metamorphism.

2.3 REGIONAL SETTING

2.3.1. Stratigraphy

The aureole of the complex is developed entirely within Moine metasediments. These consist of a dominantly psammitic sequence of deformed schists and gneisses outcropping over much of the North and Central Highlands. They can be separated into two broad stratigraphical and

21

geographical units; the 'older' Moine north of the Great Glen, and the 'young' Moine of the Central Highlands (Johnstone, 1973).

The older Moines extend from the Sound of Mull to the north coast of Sutherland, bounded on the west by the Moine Thrust, and to the east by the Great Glen Fault. Three Divisions are recognised (fig.2.2); the Morar Division, the Glenfinnan Division and the Loch Eil Division (Johnstone et.al., 1969).

The Morar Division forms the most westerly unit and is dominantly psammitic. To the east is the mainly pelitic Glenfinnan Division. Much of the boundary between the two is marked by the Sgurr Beag Slide (Tanner et. al., 1970; Tanner, 1970). To the east the rocks of the Loch Eil Division are again dominantly psammitic. The so called 'Loch Quoich Line' (Leedal, 1952; Clifford, 1957) separates the generally flat-lying Loch Eil from the more steeply dipping Glenfinnan. Sedimentary structures throughout the sequence indicate younging to the east, the Morar being the oldest unit, the Loch Eil the youngest (Johnstone, 1973). Lambert et.al. (1979) suggest that the Loch Eil Division was deposited unconformably onto the already metamorphosed Glenfinnan Division.

The complex itself comes into contact with all three Divisions. (fig. 2.2). To the south of Loch Sunart the contact is against Morar psammites. North of the Loch the more pelitic Glenfinnan Division is found at the contact. Along the eastern contact the rocks are of the Loch Eil Division. At the extreme northern end of the complex the Ardgour granitic gneiss out-crops at the contact.

FIGURE 2.2

Stratigraphy of the Northwest Highlands.

From: Johnstone (1973).

50 km

N

CALEDONIAN THRUST BELT

Sgurr Beag Slide

Quoich Line

GREAT GLEN FAULT

Strontian Complex

	Post-Caledonian Rocks
	Loch Eil Division
	Glenfinnan Division
	Morar Division
	Migmatitic Complex
	Lewisian
	Granitic Gneiss
	Granite Complex

Moinian

24
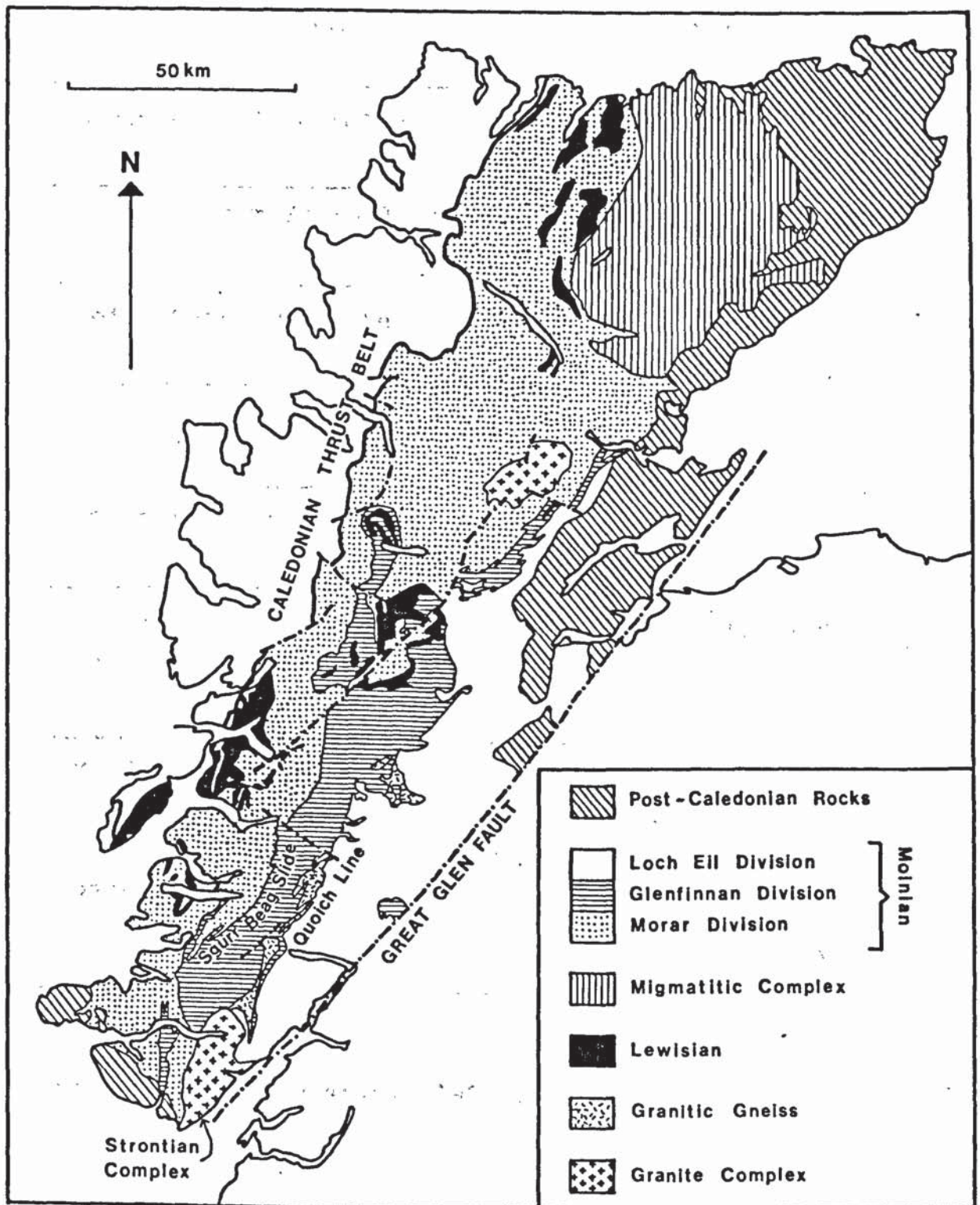
TABLE 2.1

STRATIGRAPHY OF THE MOINES OF ARDGOUR, MOIDART AND SUNART.

Glen Garvan Psammite	LOCH EIL DIVISION
Druim na Saille Pelite	
Beinn a Tuim Striped Schists	GLENFINNAN DIVISION
Beinn Gaire Psammite	
Lochailort (Roshven) Pelite	
Moidart Upper Psammite	
Moidart Striped and Pelitic Schists	MORAR DIVISION
Moidart Lower Psammite base not seen	

taken from Brown et.al (1970).

The aureole is best developed to the northwest within Glenfinnan pelites. Fortunately, Glenfinnan pelites are also found within the vicinity of the complex to both the south-west and northeast, cropping out as the cores of major folds. The detailed stratigraphy of the Moines of Ardgour, Moidart and Sunart, immediately to the north of the complex, is described by Brown et.al. (1970). Their general succession (Table 2.1) can be extended to the rest of the southwest Moine.

2.3.2. Structure

The structure of the Moines to the north of the complex is described by Brown et.al. (1970). Their structural sequence can also be extended to the rest of the southwest Moine. Four deformation episodes are recognised (F_1-F_4), with the majority of major folds belonging to the second and third episodes.

F_1 folds occur as rare, isoclinal, small-scale folds which deform only bedding. The main schistosity in the rocks (S_1) is produced by this deformation, axial planar to the folds and parallel to bedding.

F_2 folds vary in style but generally show a good axial plane schistosity (S_2), well developed in fold hinges and usually defined by crenulation of mica lying in S_1. Axial surfaces of the folds are generally steep and mostly strike NNE-SSW.

F_3 folds are restricted to Sunart and Ardgour. Deformation occurs extensively on all scales. Axial planes are nearly vertical and trend between NNE and NNW. However, a new axial plane cleavage (S_3) is only locally developed.

F_4 structures form rare, open, asymmetrical folds.

Major second and third folds are responsible for the complex outcrop pattern at a distance from the intrusion on Map 1.

2.3.3. Metamorphism

The mapping of metamorphic zones within the Moines has proved difficult due to the scarcity of suitable lithologies. Kennedy (1949) investigated the progressive metamorphism of calc-silicate bands which occur as a common, subordinate lithology. Four zones were identified:-

    (1)   Zoisite-(calcite)-biotite zone

    (2)   Zoisite zone

    (3)   Anorthite-hornblende zone

    (4)   Anorthite-pyroxene zone

corresponding to increasing grade from west to east. These were considered to approximate closely to the pelitic zones found in a Barrovian regional sequence: biotite-garnet-kyanite-sillimanite.

The map presented by Kennedy (1949) has received little mod-ification in later work. Howkins (1961), working in Moidart, reported the occurrence of kyanite and mapped a kyanite/sill-imanite isograd lying 1km west of the calc-silicate anorthite + pyroxene isograd. Staurolite was also reported in the sill-imanite zone. Brown (1964), working immediately to the east reported only sillimanite grade assemblages. However, one occurrence of staurolite is recorded, and reference is made to the co-existence of sillimanite with potash feldspar. The significance of this association was not recognised, no idea being given as to the extent of its occurrence. Winchester (1974) presented a metamorphic map for the Scottish

27

Caledonides in which the calc-silicate assemblages were used in conjunction with index mineral occurrences to delimit pelitic zones. Only minor modifications to the kyanite/sillimanite isograd in the south-west Moine were made. Winchester's isograds, labelled in terms of the calc-silicate assemblages, are used by Fettes (1979) for his more recent metamorphic map of the British Caledonides. Fig. 2.3 is a synthesis of the available information.

Studies concerning the growth of metamorphic minerals and their relationship to deformation in the south-west Moine have been carried out by several authors (Clark, 1961; Howkins, 1961; Dalziel, 1963; Brown, 1964). A synthesis of the earlier work is given by Johnson (1963). Throughout the rocks east of the Sgurr Beag Slide, principally in Glenfinnan pelites, 'foliae' comprising quartz and plagioclase feldspar of oligoclase composition are common. Their distribution has been mapped as a 'regional injection complex' by the Survey, the foliae being regarded as the product of 'lit par lit' injection and permeation of the schists by pegmatitic material (Phemister, 1936). These migmatites are regarded by Johnson (1963) as post-F_1 - pre-F_2 in age. Sillimanite is found associated with the migmatitic foliae and is also deformed by the F_2 folding (Dalziel & Brown, 1965). Garnet grew during this period, fine grained inclusions within it suggesting metamorphism to phyllite grade during the initial F_1 deformation. Garnet growth continued during and after F_2, producing characteristic optical zoning in garnets west of the Sgurr Beag Slide in Morar and Moidart (Clark, 1961; Howkins, 1961; MacQueen & Powell, 1977). To the east of the slide this zoning disappears due to homogenisation of the

28

FIGURE 2.3

Regional metamorphic zones in the southwest Moine.

    After: Howkins (1961) and Winchester (1974), with

            additional information from the present

            study. (See Map 1).
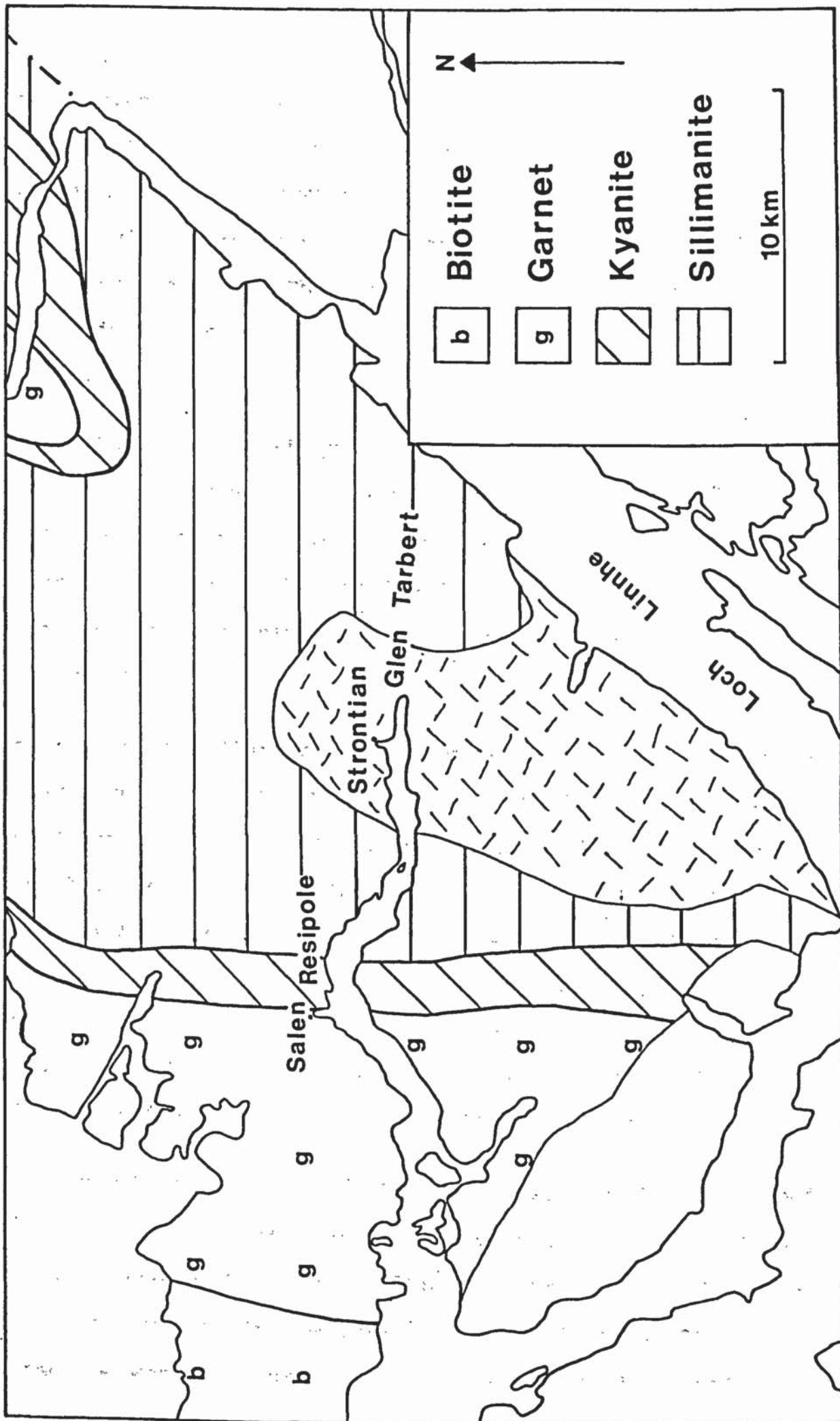
garnet by a later metamorphism (Anderson & Olimpio, 1977).
Large, unorientated muscovite porphyroblasts occur through-
out the kyanite and sillimanite zones (Howkins, 1961; Brown,
1964). These were regarded as the product of a post-F_4 retro-
grade metamorphism. Howkins (1961) regarded this as contemp-
oraneous with retrogression of garnet and biotite to chlorite
further to the west. The porphyroblasts themselves overgrow
sillimanite, kyanite and staurolite and are a replacement of
of them.

2.3.4. Geological History

The events described above were generally regarded as belong-
ing to the Caledonian orogeny (Johnson, 1963). However
evidence is now available indicating the occurrence of at
least one, and possibly two, pre-Caledonian orogenic events
(Johnson et.al., 1979).

Pre-Caledonian radiometric ages for pegmatites from the western
Moines have been given by several authors (Giletti et.al.,1961;
Long & Lambert, 1963; Van Breemen et.al.,1974; Powell, 1974).
These have been taken to indicate an orogenic event at c.750
Ma involving intrusion of pegmatites with attendant amphibolite
facies metamorphism. This was distinct from the Caledonian
Orogeny for which a later set of pegmatites indicate an age
of c.450 Ma (Van Breemen et.al., 1974). Lambert (1969)
referred to the early event as the Morarian Orogeny.

Even older Precambrian ages at 1050^+_-46 Ma, have been obtained
for the Ardgour granitic gneiss (Brook et.al., 1976). This
body was regarded by Dalziel (1966) as the product of large-
scale metasomatism in the core of a major F_2 fold. The
quoted age was therefore taken to date the F_2 deformation

throughout the southwest Moine and was correlated with the Grenville Orogeny of eastern Canada. Similar ages have been obtained from the Morar and Lochailort pelites (Brook et.al., 1977; Brewer et.al., 1979), indicating a minimum age for Grenvillian metamorphism in Morar at 1004 ± 28 Ma (Brewer et.al., 1979). There is some doubt concerning the status of the Morarian event, Brewer et.al. (1979) suggesting that such dates obtained from semi-pelites in Morar and Sunart (Van Breemen et.al., 1978) reflect incomplete resetting of the Grenville isotopic system by Caledonian metamorphism. Dates of c.750 Ma obtained from pegmatites reflect a minimum age for a pre-Caledonian orogeny as they cut across F_2 structures. There is no evidence of a second, pre-Caledonian, amphibolite facies metamorphism. Brewer et.al., (1979) give a minimum age for Caledonian metamorphism in the area at 467 ± 20 Ma.

Johnson et.al (1979) suggest that the non-migmatitic rocks of the Morar Division retain pre-Caledonian structures and mineral assemblages. They are separated from migmatitic gneisses displaying Caledonian structures and assemblages by the Sgurr Beag Slide, itself regarded as an early Caledonian structure. The migmatisation is probably pre-Caledonian, the migmatitic foliae in Ardgour and Sunart being pre-F_2 in age (Dalziel & Brown, 1965). Brewer et.al. (1979) suggest that Grenville metamorphism increased in grade from west to east culminating in upper amphibolite facies conditions, producing anatexis, in the vicinity of the Ardgour granitic gneiss. Remnants of sillimanite + potash feldspar assemblages reported by Brown (1964) reflect this event.

The present outcrop of metamorphic zones is the product of two amphibolite-grade metamorphic events. Movement of some

TABLE 2.2

GEOLOGICAL HISTORY OF THE SOUTHWEST MOINE

		MORAR & MOIDART	SUNART & ARDGOUR
PALAEOZOIC	CALEDONIAN		Intrusion of the Strontian Granite Complex. Growth of muscovite porphyroblasts replacing sillimanite, kyanite and staurolite.
		F_4 fold phase - minor, open folds.	
		Metamorphism to garnet and biotite grade, co-incident with Grenville garnet and biotite zones.	F_3 fold phase, major folding, sillimanite and kyanite zones superimposed on migmatites. Homogenisation of garnet.
		Formation of the Sgurr Beag Slide.	
PROTEROZOIC	MORARIAN	Deposition of Loch Eil Division sediments.	
		Intrusion of pegmetites. (Amphibolite grade metamorphism?)	
	GRENVILLIAN	Optically zoned garnet	
		F_2 fold phase, major folding, metamorphism at high grade continues during and after deformation. Formation of Ardgour Granite Gneiss in the core of F_2 fold.	
		Metamorphism to biotite and garnet grade.	Metamorphism to sillimanite + K-feldspar grade producing anatexis.
		F_1 fold phase, isoclinal folding, development of main schistosity, metamorphism to phyllite grade.	
		Deposition of Morar and Glenfinnan Division sediments.	

See Section 2.3.4 for sources.

33

25km on the Sgurr Beag Slide has resulted in considerable shortening of the sequence of Grenville metamorphic zones (Lambert et.al., 1979), upper amphibolite grade being juxtaposed against garnet grade. Superimposed onto this pattern has been the later Caledonian metamorphism, probably occurring contemporaneously with the F_3 deformation. Garnet- and biotite-grade conditions coincided with the Grenville zones already present, while kyanite and sillimanite zones were superimposed onto the pre-Caledonian migmatites, giving rise to the homogenisation of garnet described by Anderson & Olimpio (1977).

A summary of the geological history of the southwest Moine is given in Table 2.2.

2.4. PETROGRAPHY

2.4.1. Introduction

Some two hundred standard thin sections and thirty polished thin sections have been examined from samples collected around the Strontian complex. Assemblages are listed in Tables 2.3 and 2.4. Particular attention has been paid to the northwestern part of the aureole where pelitic lithologies are common. To the northeast of the area mapped, the lithologies are quartzofeldspathic and hence unsuitable (Ardgour Granite Gneiss and Loch Eil psammites). Information used to define metamorphic zones is summarized in Map 1. Three zones have been identified; an inner cordierite + K-feldspar zone; a sillimanite + K-feldspar zone; and a muscovite + sillimanite + K-feldspar zone. Beyond the muscovite + sillimanite + K-feldspar zone the assemblages represent a regional sillimanite zone.

34

TABLE 2.3

	CRD	GAR	SILL	AND	MUS	KSP	MYR	HBD	MAP REFERENCE
A1	X	X	X		(X)		X		793638
A2	X	X	X		(X)	X	X		791634
A3		X	X		(X)	X	X		787633
A4			X		(X)	X	X		781630
A5	X	X	X		(X)	X	X		781626
A6		X	X		(X)	X	X		782623
A7	X			X	(X)	X	X		778609
A8	X	X	X	X	(X)	X	X		778609
A9					(X)	X		X	770608
A10		X	X		(X)	X	X		764608
A11						X	X		760610
A12		X			(X)	X	X		768619
A13		X				X	X		768622
A14		X	X		(X)	X	X		775615
A15	X		X		(X)	X	X		780615
A16	X	X	X		(X)				778625
A17		X			(X)				777628
A18		X			(X)				783633
A19		X	X		(X)	X	X		783638
A20					(X)	X	X		746431
A21						X		X	743431
A22						X	X		741432
A23						X	X		738432
A24						X			734432
A25						X			732434
A26		X			(X)	X	X		790644
A27					(X)	X			786643
A28						X	X		789646
A29			X		X	X			785649
A30			X		X	X	X		784652
A31		X	X		X	X	X		781649
A32		X	X		X				777646
A33		X	X		(X)	X	X		765612
A34						X		X	779640
A35		X	X		X				776640
A36		X	X		X	X			772631
A37		X							771628
A38		X	X		X	X			767628

35

2.3 (continued)

	CRD	GAR	SILL	AND	MUS	KSP	MYR	HBD	MAP REFERENCE
A39					X	X	X		766655
A40		X			X	X	X		769655
A41		X			X				773654
A42		X			X				780656
A43		X			X	X	X		783656
A44					(X)				804648
A45	X	X	X		(X)	X			806652
A46			X		(X)	X	X		811658
A47					(X)	X	X		834659
A48			X		(X)	X	X		830661
A49			X		(X)	X			827664
A50		X	X		(X)	X	X		823664
A51			X		(X)	X	X		819664
A52		X	X		(X)	X			815665
A53		X							812664
A54			X		(X)	X	X		809663
A55		X	X		(X)	X			806659
A56		X			(X)	X			804664
A57					X	X	X		803669
A58						X	X		780671
A59			X		(X)				798660
A60					X	X			788660
A61		X			X	X	X		788663
A62		X				X	X		790668
A63		X				X	X		790668
A64		X				X	X		794668
A65		X	X		X				793665
A66		X	X		X	X	X		790659
A67						X	X		842658
A68			X		(X)	X	X		845662
A69		X				X	X		847664
A70		X	X		(X)	X	X		841675
A71		X				X			845676
A72		X	X		(X)	X			836674
A73		X	X		(X)				835659
A74		X			(X)	X			885670
A75					X	X		X	887670
A76					(X)	X			868607

2.3 (continued)

	CRD	GAR	SILL	AND	MUS	KSP	MYR	HBD	MAP REFERENCE
A77					(X)	X	X		868605
A78					(X)	X	X		870605
A79			X		(X)	X		X	871605
A80	X	X	X		(X)	X	X		874606
A81	X	X			(X)	X	X		877606
A82						X			882605
A83	X	X	X		(X)	X	X		885605
A84						X	X		740503
A85						X	X		735503
A86						X	X		729503
A87						X	X		722505
A88		X				X			719505
A89						X			715505
A90					(X)	X	X		710505
A91		X			X				702503
A92	X	X		X	(X)	X			773599
A93						X		X	790598
A94		X	X		(X)	X	X		759598
A95			X		X	X	X		753599
A96	X	X	X		(X)	X			883615
A97	X	X	X		(X)	X	X		887614
A98						X	X		890618
A99		X	X		(X)	X	X		906617
A100		X				X	X		920599
A101		X	X		(X)	X	X		894604
22C		X	X		X	X	X		925598
193C	X		X		(X)	X	X		777606
195C	X	X	X		(X)	X	X		777606
197C	X	X	X		(X)	X	X		777606
198C	X		X		(X)	X	X		777606
199C	X		X		(X)	X	X		777606
201C		X	X		(X)	X	X		777606
203C						X			754617
204C						X	X		737636
205C		X	X		X				722639
251C		X	X		(X)	X	X		773607
257C		X	X		(X)	X			766608
259C	X	X	X		(X)	X			834657

2.3 (continued)

	CRD	GAR	SILL	AND	MUS	KSP	MYR	HBD	MAP REFERENCE
267C	X		X		(X)	X	X		838663
270C	X	X	X		(X)	X			837663
271C		X	X		(X)	X			763607
279C		X	X		X				760618
280C		X			X				762617
281C		X	X		X				763619
282C		X	X		X	X			763619
283C					X	X			763622
284C		X				X	X		764623
285C						X	X		764623
288C	X	X	X		(X)	X	X		859655
290C			X		(X)	X	X		859649
291C		X	X		(X)	X	X		831669
294C			X		(X)	X	X		820670
296C			X		(X)	X	X		817672
298C		X	X		X				778682
299C			X		X				798678
300C		X	X		X	X	X		807675
303C	X	X	X		(X)	X	X		777620
304C		X	X		(X)	X	X		777620
307C	X	X	X		(X)	X	X		784630
309C	X	X	X		(X)	X	X		795640
310C		X	X		(X)	X	X		822663
311C		X	X		(X)	X	X		808657
314C			X		X	X			788657
317C			X		(X)	X	X		789658
321C			X		(X)	X	X		790654
323C			X		(X)	X	X		861685
328C			X		(X)	X	X		845684
332C					X				853703
336C			X		(X)	X			842688
337C					(X)	X	X		803675
339C		X	X			X			835669
342C		X	X		(X)	X	X		837671
347C		X	X		(X)	X			770615
349C		X	X			X	X		772621
352C		X	X		(X)	X	X		770626
354C		X	X		(X)	X			768628

38

	CRD	GAR	SILL	AND	MUS	KSP	MYR	HBD	MAP REFERENCE
355C		X	X		(X)	X			770629
356C		X	X		(X)				770629
357C		X			(X)				769632
358C		X	X		X	X			768633
359C		X	X		X				769634
360C		X	X		(X)				773634
361C			X		X				792679
362C		X			X	X			794674
364C					X				797667
365C		X	X		X	X			797667
366C			X		(X)	X			798662
371C			X		(X)	X			795645
375C					X	X			765642
378C					X	X			766646
382C			X		X	X			779651
384C			X		(X)	X	X		786638
386C			X		X				792688
387C	X				X	X			799687
392C					X	X	X		811685
393C			X		X				814684
400C			X		X				829689
402C	X	X			X	X			828683
404C			X		X	X			860696
406C					X	X	X		852698
407C					X	X			860704
411C	X				X	X	X		814693
569C	X				X	X	X		780694
570C					X				786700
572C	X	X			X				791706
573C					X				796711
586C					X	X			785678
588C					X				778677
589C					X				769677
593C	X	X			X				763669
594C					X				766673
595C	X				X				752644
596C	X				X	X			751637
597C	X				X				754627

2.3 (continued)

	CRD	GAR	SILL	AND	MUS	KSP	MYR	HBD	MAP REFERENCE
614C		X	X		X				749617
615C		X			X	X	X		737626

(X) Mineral regarded as secondary

Biotite, plagioclase and quartz are present in all specimens.

TABLE 2.4

OPAQUE ASSEMBLAGES

ZONE	SAMPLE	GRAPHITE	ILMENITE	PYRRHOTITE
Cordierite + K-feldspar	A1	X	X	
	A2		X	X
	A5	X	X	
	A8		X	X
	A45	X	X	X
	A73		X	X
	A83			X
	270C		X	X
Sillimanite + K-feldspar	A10		X	
	A19	X		
	A28		X	
	A33	X	X	
	A52	X	X	X
	A55	X	X	X
	A72	X	X	
	A88		X	
	356C	X	X	
Muscovite + Sillimanite + K-feldspar	A32	X		
	402C		X	X
Regional Sillimanite	A41	X	X	
	A65	—	X	
	A91		X	X
	205C	X	X	
	298C	X	X	
	387C	X	X	
	399C		X	X
	572C		X	X
	595C	X	X	X
	614C	X	X	

41

FIGURE 2.4

a. & b.   'Breccia' structure in contact schists near

Woodend,west of Strontian.

43

Rocks within the aureole do not show a hornfelsic texture. Even at the contact a strong schistose fabric is prominent, although it is distinctively 'braided', forming the 'breccia' structure described by MacGregor & Kennedy (1932) (fig. 2.4). This is restricted to a narrow zone at the contact where shearing is developed in psammitic and other quartzo-feldspathic lithologies. The pelites here are migmatitic, with coarse stromatic leucosomes developed parallel to the schistosity. (See Section 2.4.5.).

Further away from the contact, regional fabrics and structures are preserved. Migmatites are still found. Folding on all scales is common and frequently affects leucosomes. However, stromatic leucosomes do still occur.

In the field the outer limit of discernible contact metamorphism is marked by the appearance of coarse muscovite porphyroblasts.

2.4.2. Regional Assemblages

Pelites sampled from the Glenfinnan and Morar Divisions to the north and west of the aureole (Table 2.3) show two major assemblages: muscovite + biotite + plagioclase + quartz + ilmenite $\pm$ sillimanite $\pm$ garnet $\pm$ graphite $\pm$ pyrrhotite; and muscovite + biotite + plagioclase + K-feldspar + quartz + ilmenite $\pm$ garnet $\pm$ graphite $\pm$ pyrrhotite. Sillimanite is not found where potash feldspar is present. Apatite, zircon and tourmaline are common accessories. Chlorite and myrmekite occur as secondary products.

The rocks are typically coarse-grained, gneissose fabrics being dominated by a strong foliation which may show local crenulation. Small scale folding, on the scale of a single

44

hand specimen, may affect the foliation and segregations of quartz and feldspar developed parallel to it. Groundmass crystals range up to 1mm across and porphyroblasts of garnet and muscovite are common.

Sillimanite is fibrolitic, occurring as small felts of needles generally included by the muscovite porphyroblasts (fig 2.5a). Felts are also found within quartzo-feldspathic segregations.

Muscovite and biotite mica show a strong preferred orientation which defines foliation in the rocks. Muscovite porphyro-blasts however, are unorientated, overgrowing and including biotite which forms the foliation (fig. 2.5a). Biotite may show secondary alteration to chlorite.

Garnet porphyroblasts are xenoblastic, overgrowing the foliation and including grains of quartz, feldspar and mica. Rare 'textural' zoning, similar to that described for garnets from the kyanite zone in south Morar by Anderson & Olimpio (1977, fig. 5), may be seen in 593C (fig. 2.5b). This takes the form of an outer zone heavily sieved by quartz inclusions surrounding a core containing less frequent and finer grained inclusions. The zoning may be incomplete, the garnet grains being broken by a later deformation. Zoning with fine inclusions at the core of the garnet may be seen in 298C (fig. 2.6a). 614C, sampled from a Morar Division pelite, shows the foliation 'flowing around' garnets (fig. 2.6b). This suggests a pre-foliation age for the garnet in the sample.

Feldspar is commonly plagioclase. Compositions are in the oligoclase - andesine range, being between An_{16} and An_{37}.

45

FIGURE 2.5

a. Muscovite porphyroblasts including sillimanite.
    Specimen 593C.

b. Texturally zoned garnet porphyroblast.
    Specimen 593C.

a
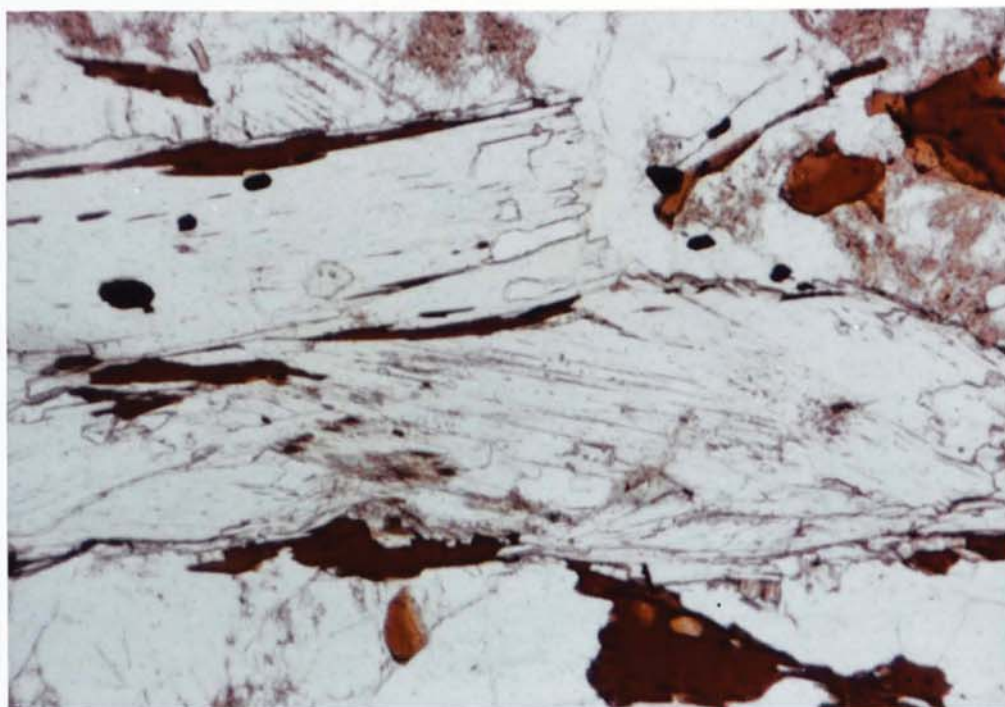
1mm

scale bar is 1mm unless
shown otherwise

b
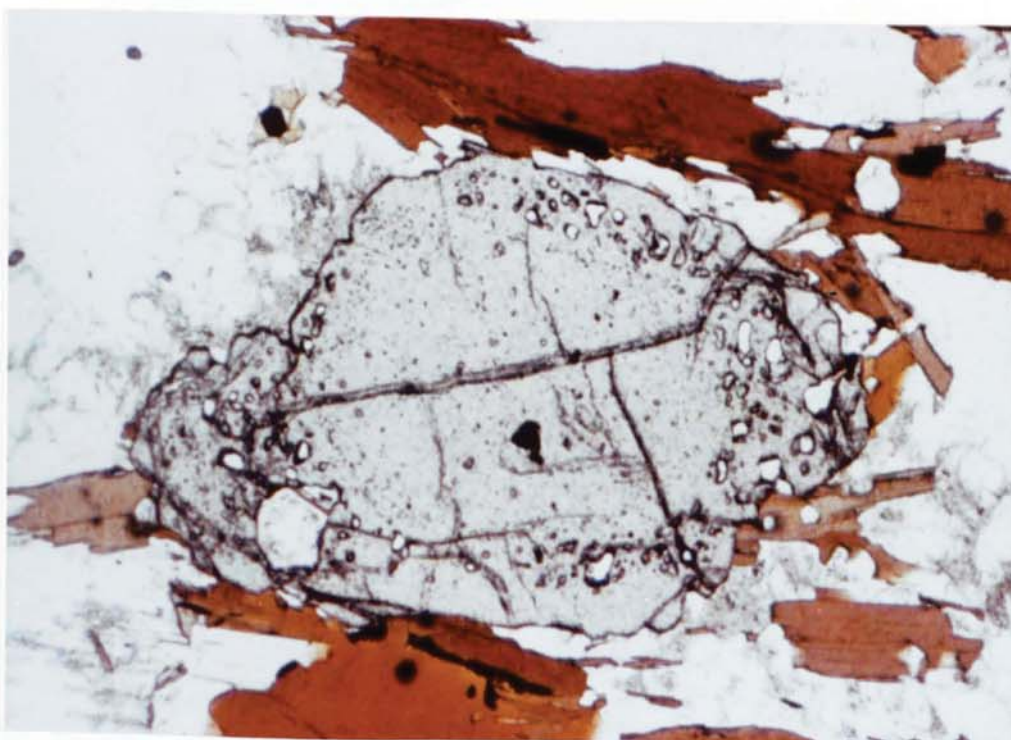
FIGURE 2.6

a. Garnet with fine inclusions. Specimen 298C.

b. Foliation 'flowing around' garnet. Specimen 614C.

a
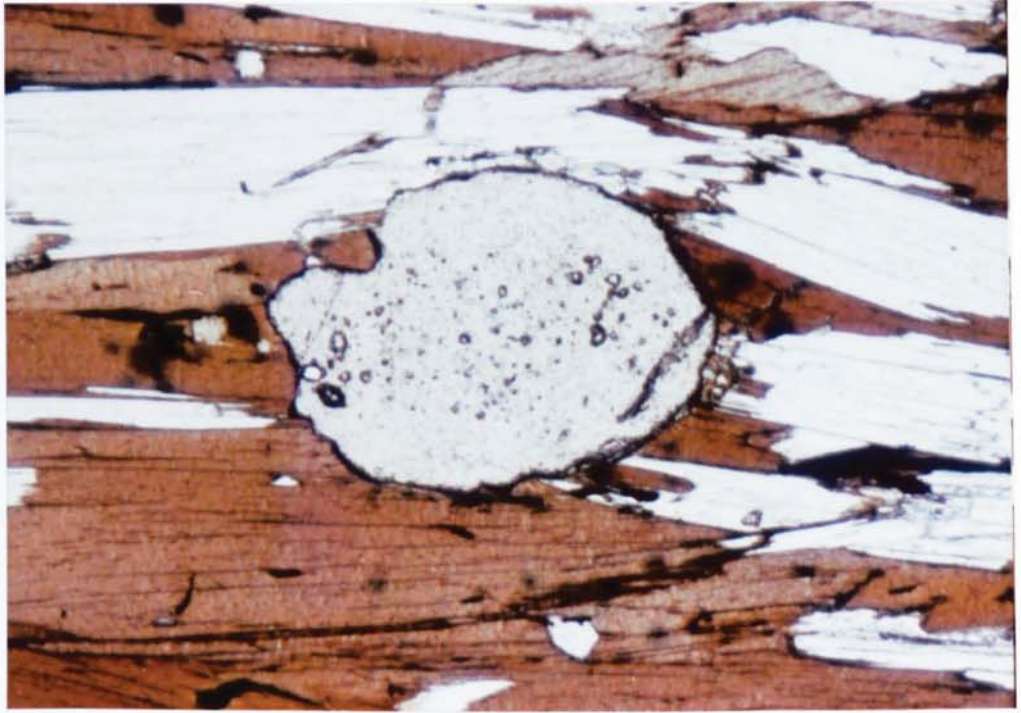
b
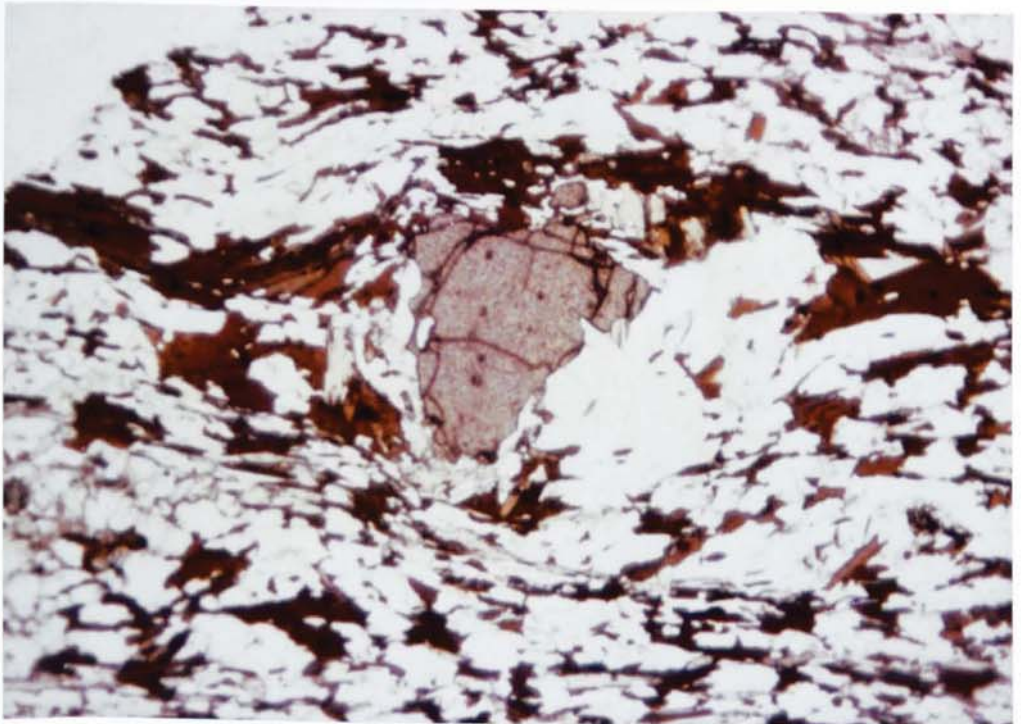
FIGURE 2.7

a. Regional sillimanite + K-feldspar assemblage.
    Sillimanite is included by later muscovite.
    K-feldspar is perthitic.   Specimen 22C.

b. Cordierite porphyroblast.   Specimen A2.
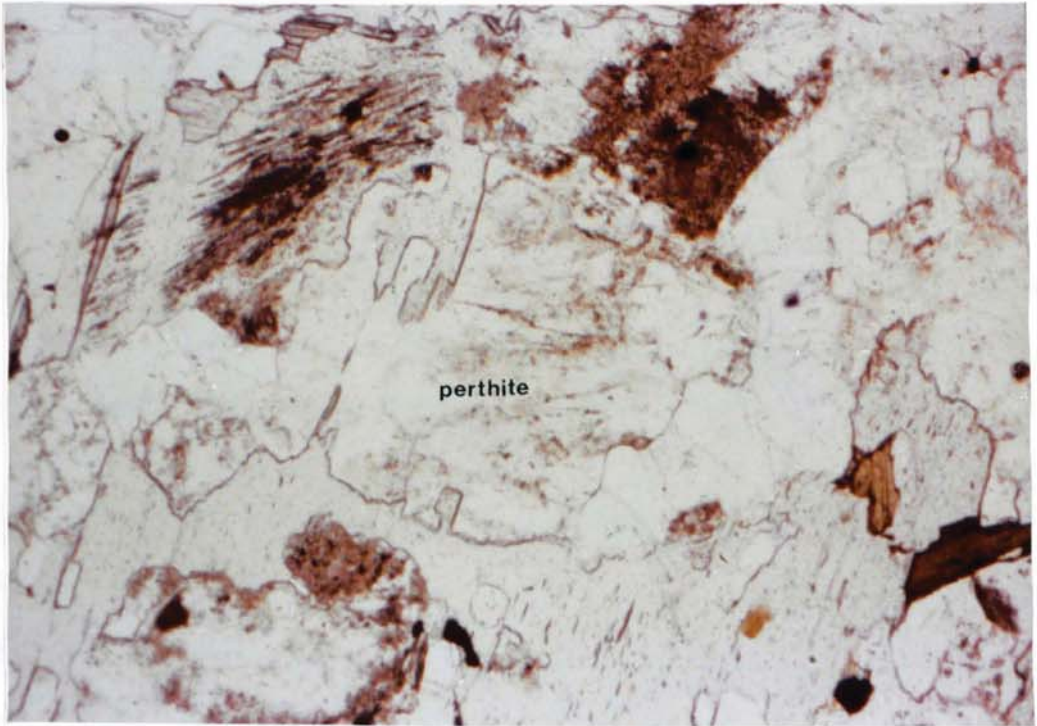
Potash feldspar is not common, occurring as groundmass crystals where sillimanite is absent. Myrmekite is frequently associated with it. Occasionally perthitic porphyroblasts may be present.

Quartz is a ubiquitous constituent of the groundmass.

Ilmenite is always present as part of the opaque assemblage (Table 2.4). Graphite usually occurs intergrown with biotite. Pyrrhotite may also be present.

Samples collected from migmatitic Loch Eil Division semi-pelites at the eastern end of Glen Tarbert may also represent regional assemblages. Here sillimanite and potash feldspar are found in association. Sillimanite felts are included within large, ragged crystals of muscovite which are very different in outline from the porphyroblasts to the west of the complex (fig. 2.7a). Garnet porphyroblasts show replacement by chlorite and green biotite. The rocks are in close proximity to the Great Glen Fault and this feature is probably the result of hydrothermal alteration associated with it.

2.4.3. Aureole Assemblages

2.4.3.(i) Cordierite + K-feldspar zone

This zone is developed adjacent to the margin of the pluton. It varies considerably in width, widening from 500 metres at the western contact on Loch Sunart, to 2.5km in Glen Tarbert to the east. One cordierite locality is found on the southern shore of Loch Sunart (A92). No evidence of cordierite has been found further to the south where rocks at the contact are from the Morar Division (Table 2.3, A20-A26, A84-A90).

The reconnaissance of the Morar Division in the aureole, south of Loch Sunart, showed no sillimanite either. The rocks are feldspathic and do not develop zone-defining assemblages; the westward entry of muscovite is lithologically controlled by the western boundary of the Morar against Glenfinnan rocks.

The general assemblage is: biotite + plagioclase + quartz $\pm$ cordierite $\pm$ K-feldspar $\pm$ sillimanite $\pm$ andalusite $\pm$ garnet $\pm$ muscovite $\pm$ ilmenite $\pm$ graphite $\pm$ pyrrhotite (Tables 2.3, 2.4). Apatite, zircon and tourmaline occur as accessories. Chlorite and myrmekite are present as secondary products. Sillimanite and potash feldspar are found together, as are garnet and cordierite.

The rocks are coarse grained, a prominent gneissose foliation being overgrown by porphyroblasts of cordierite, garnet and feldspar. Coarse segregations of quartz and feldspar are developed parallel to the foliation (Section 2.4.5.).

Cordierite porphyroblasts show extensive alteration to pinite, a symplectic intergrowth of chlorite, green biotite and muscovite. The pinite can become coarse, individual crystals ranging up to 0.5mm across. Alternatively, the cordierite may be altered to a distinctive orange clay. Individual grains can reach 4mm in length and these can preserve unaltered cores (fig. 2.7b).

Xenoblastic garnet porphyroblasts, up to 3mm in diameter, overgrow the foliation and include grains of quartz, biotite and feldspar (fig. 2.8a).

Sillimanite usually takes the form of fibrolitic felts of

53

FIGURE 2.8

a. Garnet porphyroblast. Specimen A45.

b. Coarse sillimanite. Specimen A8.
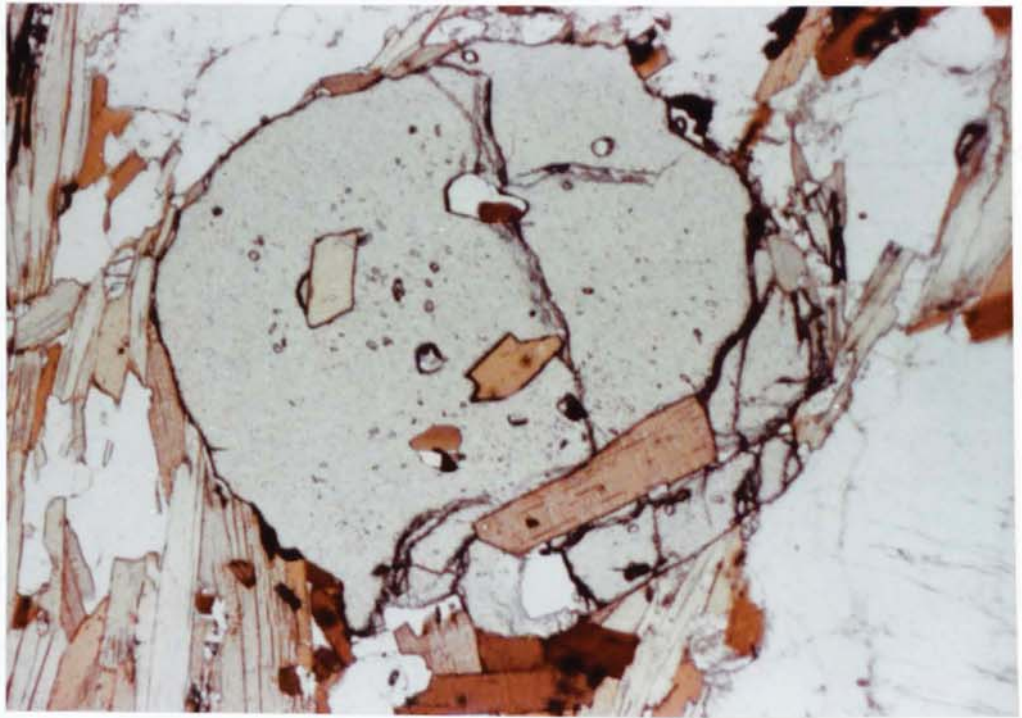
fine needles which may be included by muscovite. Large, well formed crystals can also occur. Strings of needles are found closely associated with biotite which shows a strong preferred orientation, defining the foliation.

Muscovite forms unorientated and often ragged crystals, growing across biotite and including sillimanite.

Andalusite is found in three specimens collected on, or near, the shores of Loch Sunart (fig. 2.9 a&b). In A8 it forms isolated and somewhat ragged crystals surrounded by quartz and feldspar. Coarse sillimanite is also present in this specimen. In A7 and A92 crystals are in contact with biotite and cordierite. No sillimanite is found in either sample.

Plagioclase and potash feldspar are both common and may become porphyroblastic. Plagioclase composition is oligoclase ranging between An_{22} and An_{29}. Zoning is slight with anorthite content dropping by two or three percent between core and rim. Porphyroblasts are commonly anti-perthitic.

Potash feldspar porphyroblasts are perthitic. As a constituent of the groundmass, however, it forms irregular, interstitial crystals. Myrmekitic intergrowths are common and are usually accompanied by fine, and often ragged, muscovite.

Quartz occurs as groundmass crystals in all sections.

The usual opaque assemblage is ilmenite, graphite and pyrrhotite. Graphite is usually intergrown with biotite. Ilmenite and pyrrhotite can form crystals up to 0.5mm across. Rutile may be present as an alteration product of ilmenite.

56

FIGURE 2.9

a. Remnant basal section of andalusite. Specimen A8.

b. Andalusite. Specimen A92.
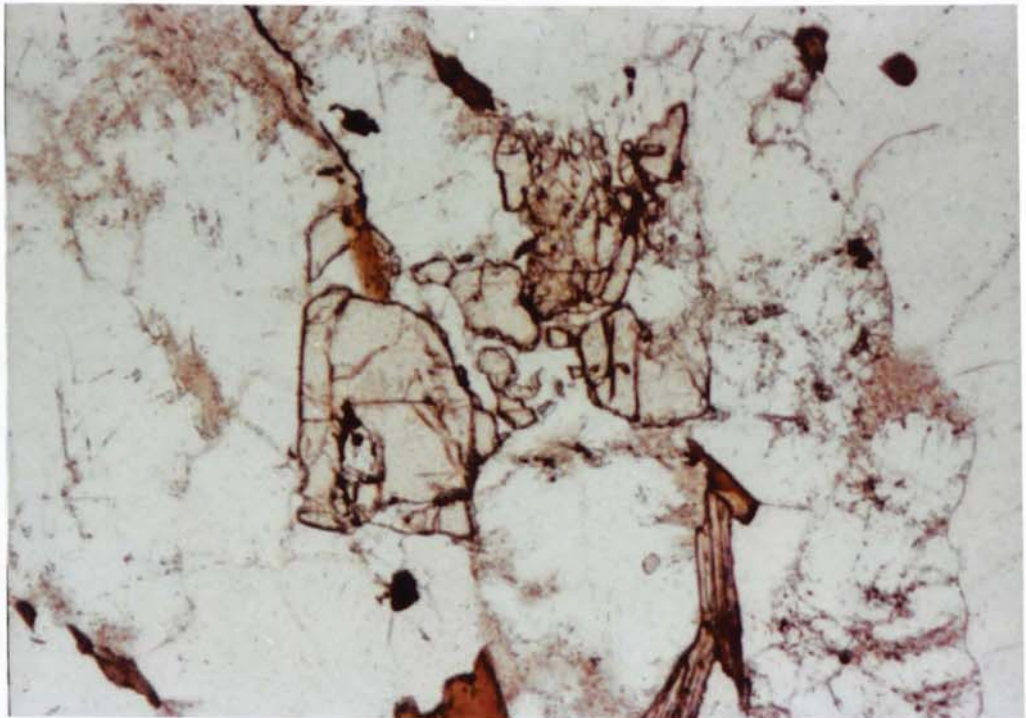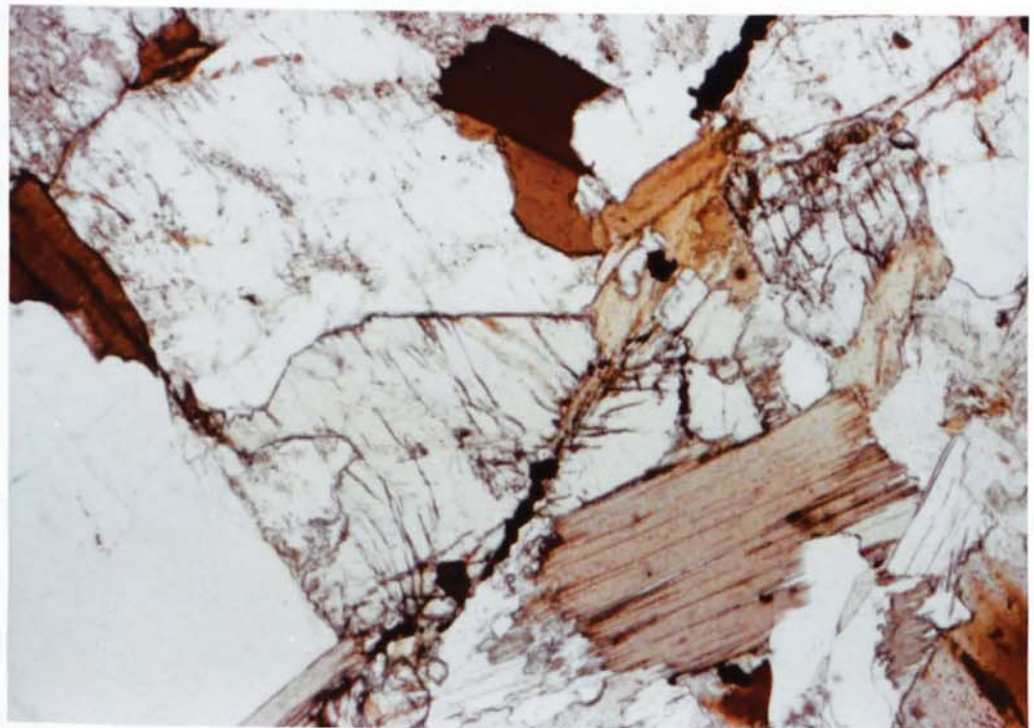
2.4.3.(ii) Sillimanite + K-feldspar zone

The sillimanite + K-feldspar zone surrounds the cordierite + K-feldspar zone. It also becomes wider from west to east, increasing from 1.5km on the north shore of Loch Sunart, to some 4km north of the complex. No sillimanite + K-feldspar assemblages are found in Morar Division rocks south of Loch Sunart.

The rocks have a similar assemblage to the cordierite zone apart from the absence of cordierite and andalusite: biotite + plagioclase + quartz $\pm$ sillimanite $\pm$ garnet $\pm$ muscovite $\pm$ K-feldspar $\pm$ ilmenite $\pm$ graphite $\pm$ pyrrhotite. Rocks from this zone containing sillimanite and muscovite but no K-feldspar or myrmekite are not plotted on Map 1; the muscovite is all regarded as secondary (Section 2.4.3.) and K-feldspar is absent as a consequence of rock composition. Apatite, zircon and tourmaline are common accessories with chlorite and myrmekite representing secondary minerals. Sillimanite and potash feldspar are often found in close association.

The appearance of the rocks in hand specimen is similar to the regional gneisses, with small-scale folding common. The most noticeable difference is the absence of muscovite porphyroblasts. Garnet forms the only significant porphyroblastic mineral species.

Sillimanite is relatively common, and felts are surrounded by fine, generally ragged muscovite (fig. 2.10). The foliation continues to be defined by the preferred orientation of biotite. Garnet is porphyroblastic, overgrowing the foliation. However it is smaller and less frequent in occurrence than in the cordierite + K-feldspar zone. Sample A99

59

FIGURE 2.10

a. & b.   Aureole sillimanite + K-feldspar assemblage.
          In cross polarised light secondary muscovite
          is seen to surround sillimanite. Myrmekite
          is also seen replacing K-feldspar.
          Specimen A14.

a

b

myr
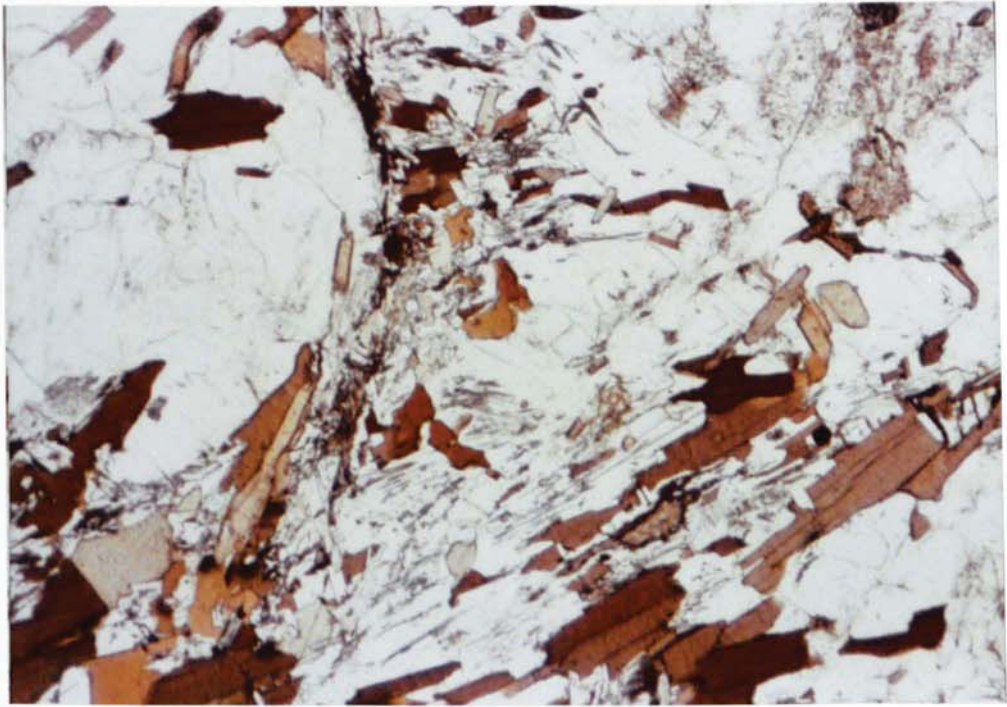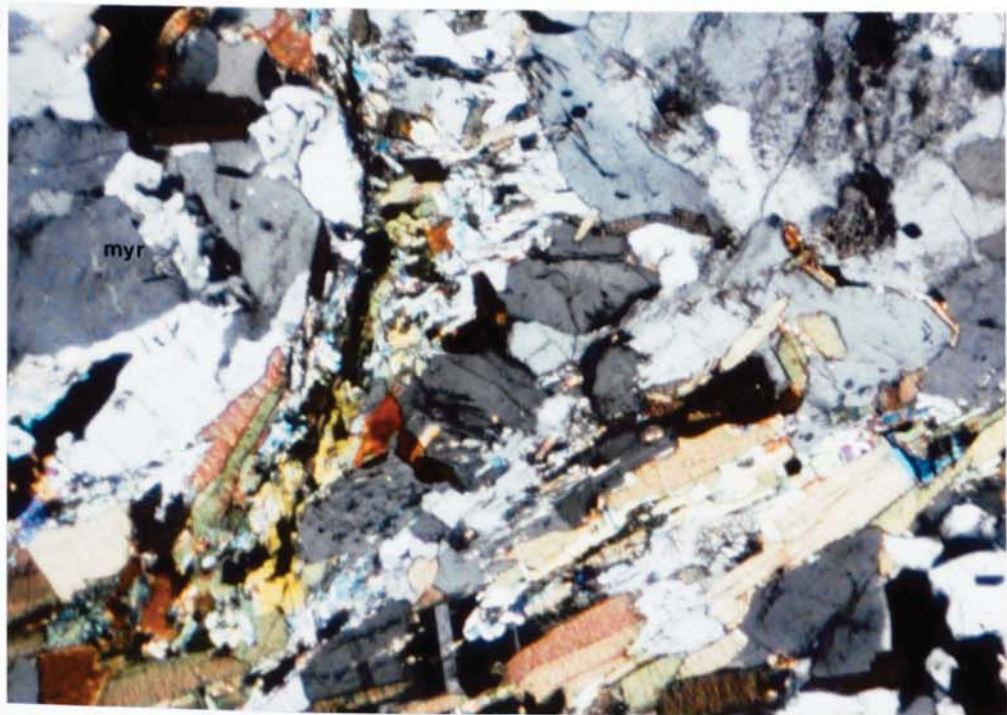
FIGURE 2.11

a. & b. Regional muscovite porphyroblast being replaced
by sillimanite + K-feldspar. Fine secondary
muscovite replaces sillimanite. Myrmekite
is also seen. Specimen A66.
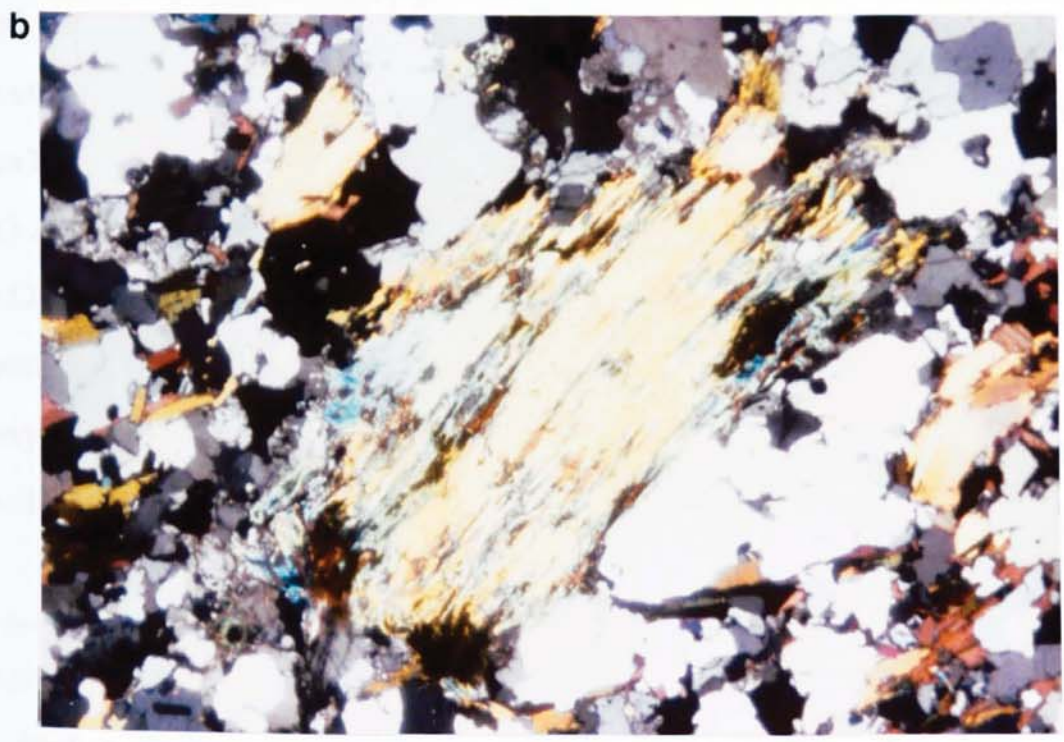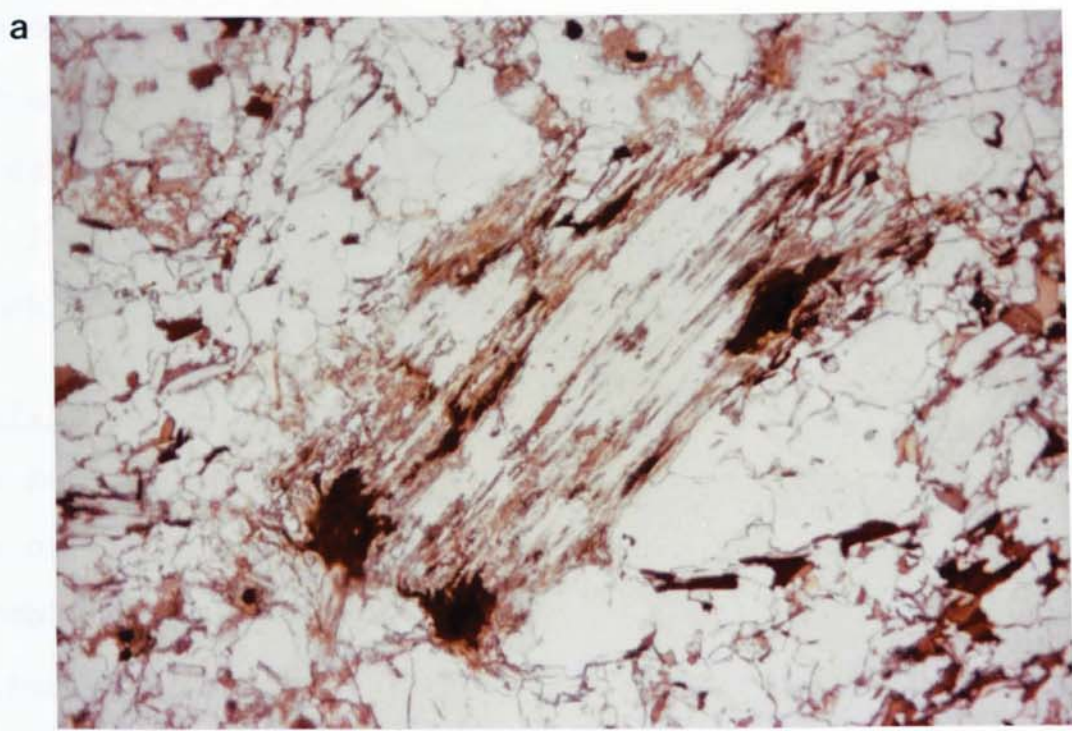
contains symplectic intergrowths of sillimanite, biotite, feldspar and quartz, apparently replacing garnet.

Plagioclase is oligoclase - andesine, composition ranging from An_{25} to An_{38}. Zoning is usually slight, but An may increase by up to six percent from core to rim. Potash feldspar forms irregular interstitial crystals associated with myrmekite. It may also form rare porphyroblasts.

2.4.3.(iii) Muscovite + sillimanite + K-feldspar zone

This zone is identified as a 300-400 metre strip at the outer edge of the sillimanite + K-feldspar zone. The general assemblage is: muscovite + biotite + plagioclase + quartz $\pm$ sillimanite $\pm$ K-feldspar $\pm$ garnet $\pm$ graphite $\pm$ ilmenite $\pm$ pyrrhotite. Apatite, zircon and tourmaline are accessories. Secondary chlorite and myrmekite occur.

The rocks closely resemble the regional gneisses, and muscovite and garnet porphyroblasts are common. The zone is characterised by the occurrence of muscovite of similar appearance to that in regional assemblages. Specimens show muscovite crystals surrounded by sillimanite and potash feldspar (fig. 2.11a). Sillimanite is also found along cleavage traces. The sillimanite and potash feldspar may themselves be surrounded by ragged muscovite and myrmekite (fig. 2.11b). In many cases the turbid cores of these muscovites provides the only evidence for the former presence of sillimanite.

2.4.4. Mineral Parageneses

The outer edge of the muscovite + sillimanite + K-feldspar zone, which represents the limit of detectable contact metamorphism, is defined by a sillimanite + K-feldspar isograd

64

(Map 1)   (cf. Evans & Guidotti, 1966). The isograd is

produced by operation of the dehydration reaction

muscovite + quartz = sillimanite + K-feldspar + H_2O (1)
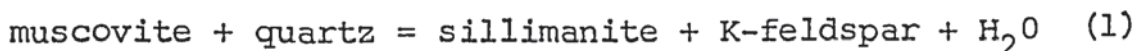
allowing sillimanite and potash feldspar to co-exist (fig. 2.12)

The reaction does not go to completion immediately and mus-

covite persists over the width of the muscovite + sillimanite

+ K-feldspar zone. The inner limit of the zone is marked by

the disappearance of muscovite which can be regarded as

regional in origin. Consequently the zone is not found to

the east where regional assemblages are already at silliman-

ite + K-feldspar grade (see 2.4.1).

The ragged muscovite found within the aureole zones is

identified as secondary, as are small disorientated muscovite

flakes (small primary muscovites being parallel to the biotite

foliation). Ragged muscovite frequently includes sillimanite

and is associated with myrmekite, as a replacement of

K-feldspar (cf. Ashworth, 1972). This muscovite was produced

by reaction (1) operating in reverse.

The retrograde reaction is recognised throughout the aureole

and is illustrated by the modal analysis of 38 pelites to

the north and west of the complex (fig. 2.13a). The results,

and details of counting methods, are set out in Appendix I.

Using the circular grid shown in fig. 2.13b, a trend surface

illustrating the changing nature of muscovite across the

aureole was calculated (fig. 2.13c). Outside the aureole

primary muscovite is dominant. Secondary muscovite may be

present as alteration of feldspar, or from the localised

breakdown of biotite to intergrowths of chlorite and muscovite.

Within the aureole there is a rapid loss of inherited,

FIGURE 2.12

A'FK Diagrams

a. Regional Sillimanite Zone.

b.   Sillimanite + K-Feldspar Zone.

a. REGIONAL SILLIMANITE ZONE

A'
sillimanite
muscovite
garnet
biotite
F
K-feldspar
K

b. SILLIMANITE + K-FELDSPAR ZONE

A'
sillimanite
garnet
biotite
F
K-feldspar
K
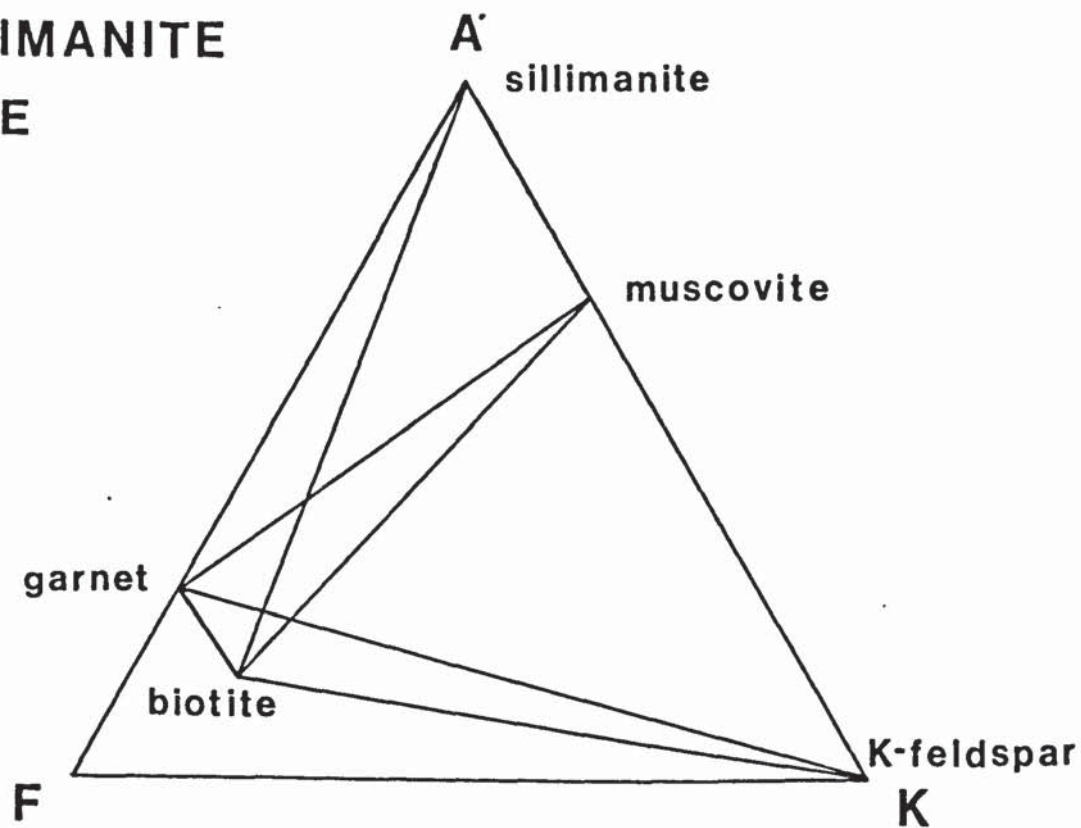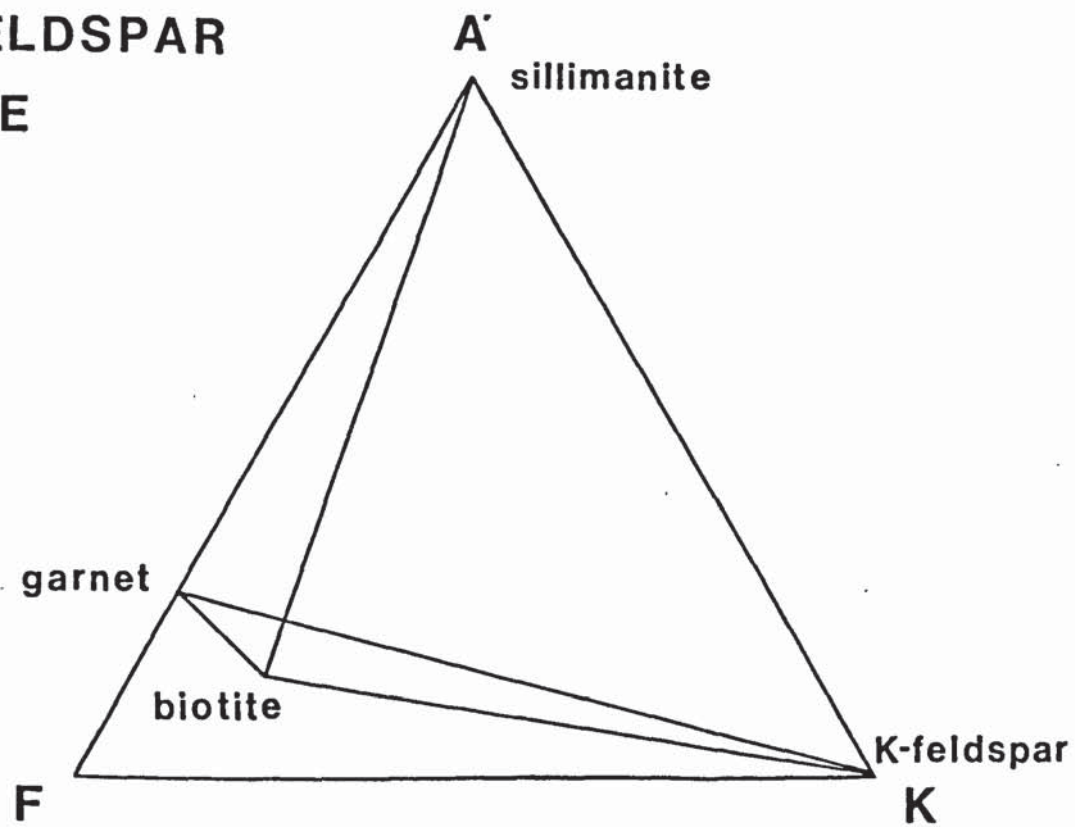
FIGURE 2.13

a. Location of specimens used for modal analysis.

b. Co-ordinates for trend surface analysis are taken
    from a circular grid.

c. Second order trend surface for percentage of
    primary muscovite. (Primary muscovite + secondary
    muscovite = 100%). The trend surface, has completely smoothed out the
    variation and does not reveal the isograds.

d. Third order trend surface for percentage sillimanite
    + K-feldspar. (Muscovite + sillimanite + K-feldspar
    = 100%). The trend lines to the N.W. (with no data points) have
    no significance.

Trend surfaces are calculated using a computer programme
modified after that given by Davis (1973).

a.

3 km

N

•411C
•387C
•402C   •328C
•299C
•362C •300C
•364C
•A61   •A56   A51
•310C   •270C
•A41   •314C   •291C
•321C •311C
•A30
•A29   •A45
•A32
•375C
•A19 •384C •309C
•359C   •A2
•A36 •A4
•A5
•A16
•279C •303C
203C   •A14
257C •A7

b.

0
1
2
3
4
5
6   7   8   9

20 18 16 14 12 10

69
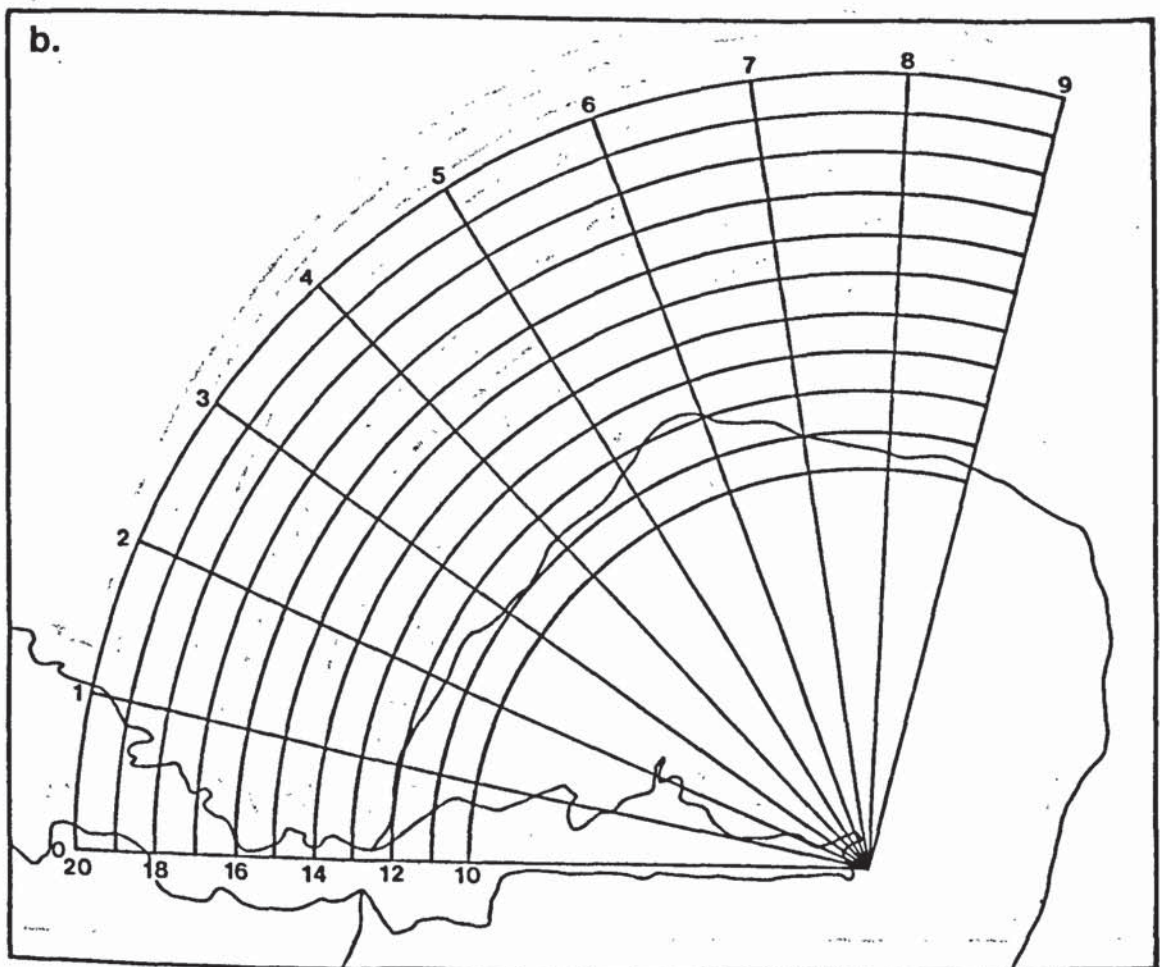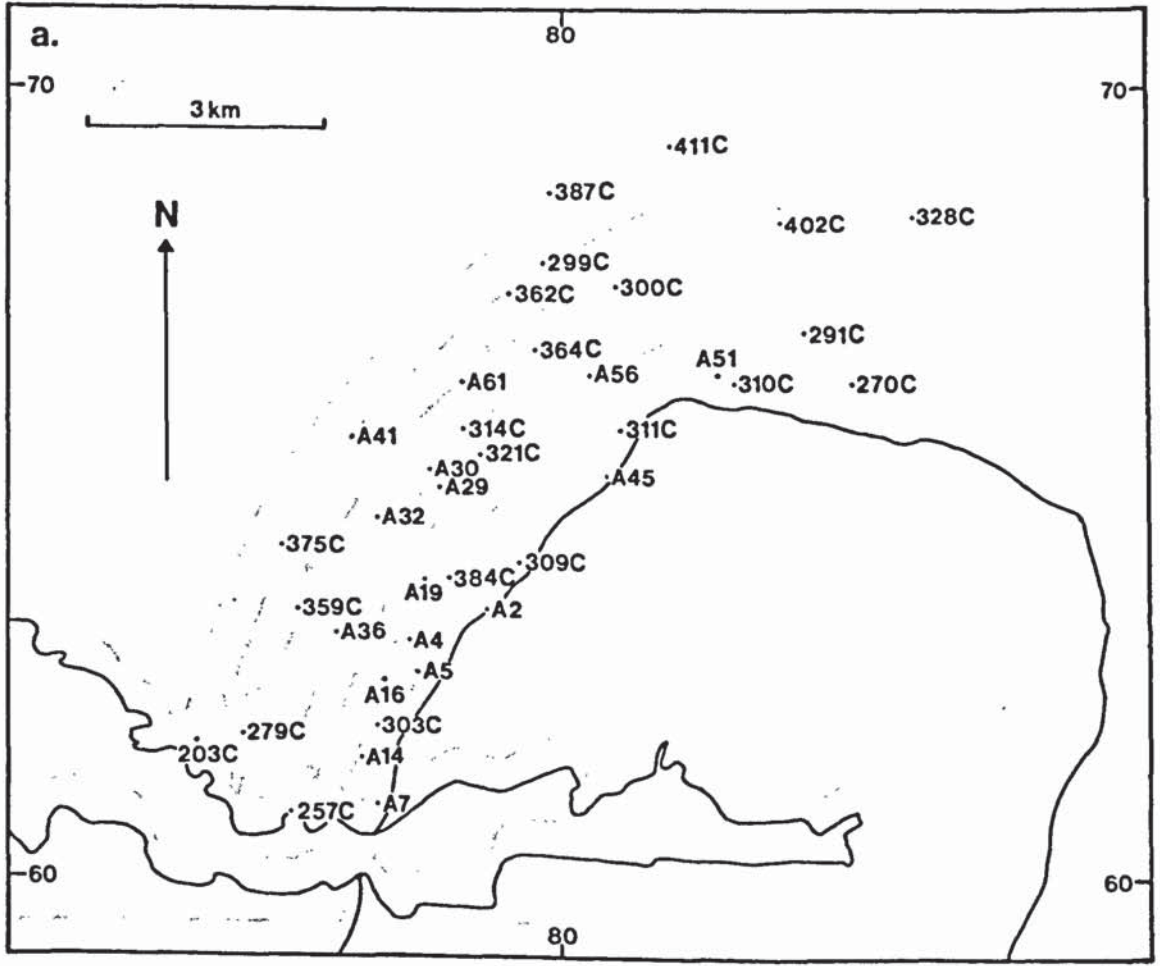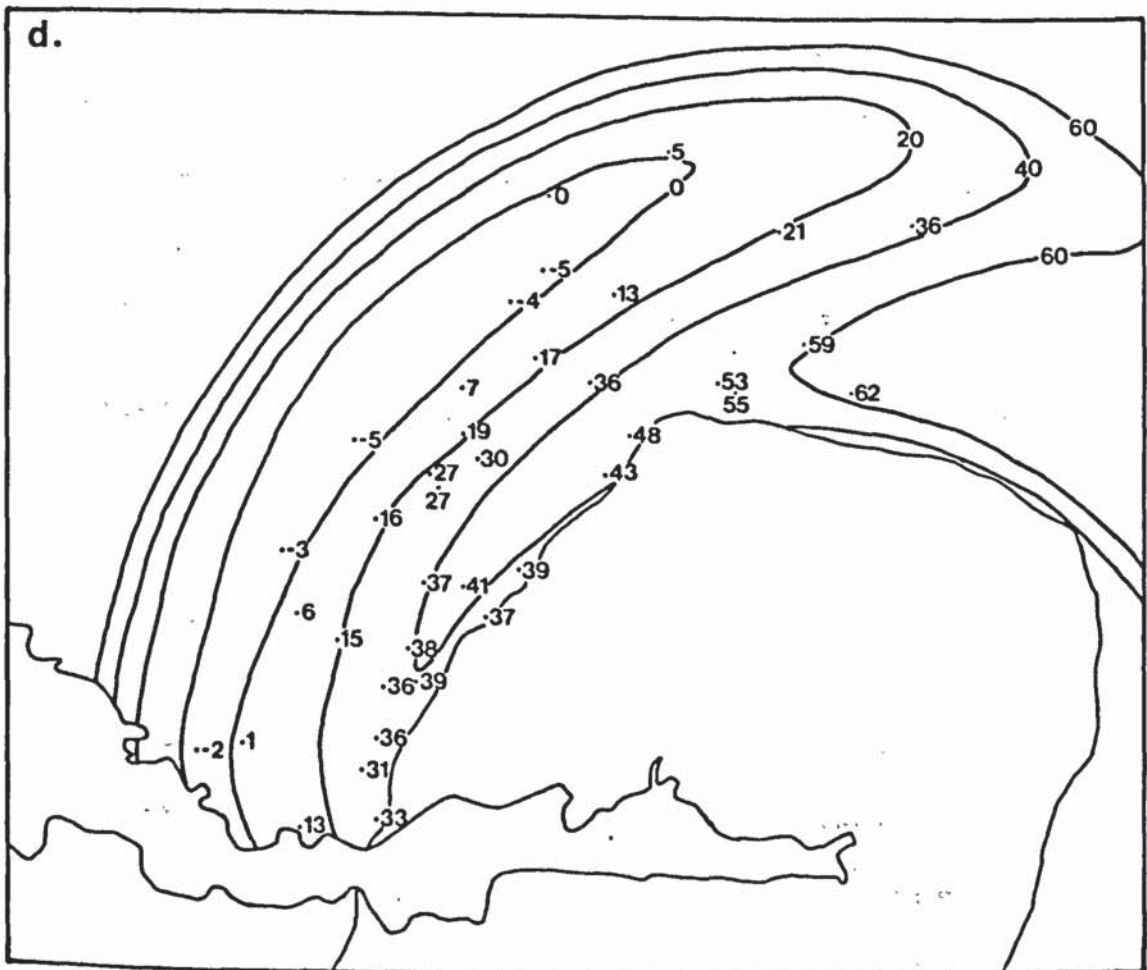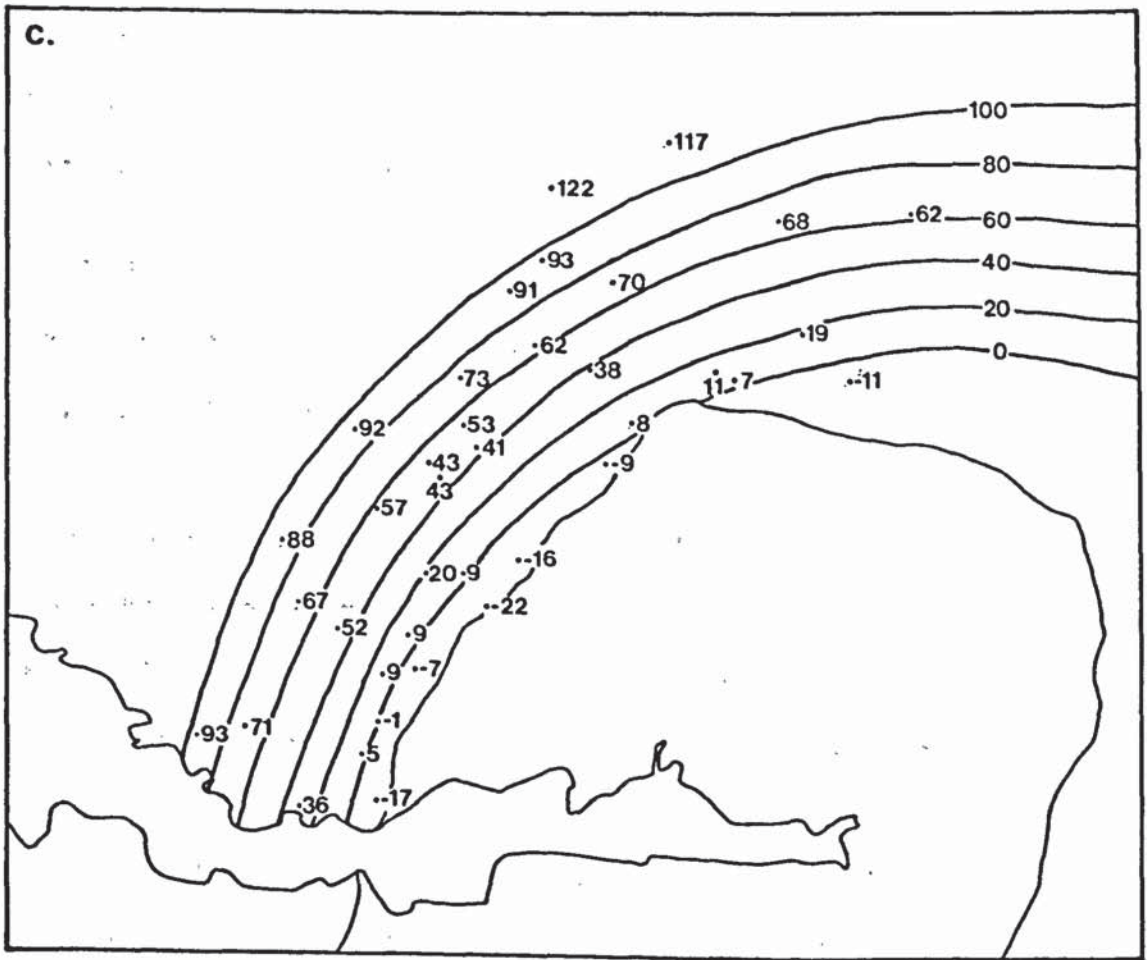
regional muscovite over the width of the muscovite + sill-
imanite + K-feldspar zone. No primary muscovite is found in
the sillimanite + K-feldspar or cordierite + K-feldspar zones.

Fig. 2.13d illustrates the occurrence of sillimanite + K-feld-
spar assemblages. From molar volume data given by Robie et.al.
(1978), sillimanite and K-feldspar produced from muscovite and
quartz by reaction (1) would be expected to have an approximate
modal ratio of 1:2. Any samples which exceed this ratio are
presumed to have contained one or other of the minerals before
reaction (1) operated. Corrected sillimanite + K-feldspar
totals are calculated as a percentage of muscovite + silliman-
ite + K-feldspar. Outside the sillimanite + K-feldspar iso-
grad, rocks where muscovite occurs with sillimanite or K-feld-
spar only, are regarded as containing 0% sillimanite + K-feld-
spar, representing conditions below those at which reaction (1)
operated. Within the aureole, rocks without K-feldspar or
myrmekite are neglected since the muscovite present is secon-
dary and may be due to late alteration of plagioclase. Fig.
2.13d represents a trend surface calculated from the corrected
data. An increase in the amount of retrogression of reaction
(1) is indicated as the contact is approached.

The cordierite + K-feldspar isograd represents operation of
the reaction

      sillimanite + biotite + quartz

        = cordierite + garnet + K-feldspar + H_2O (2)
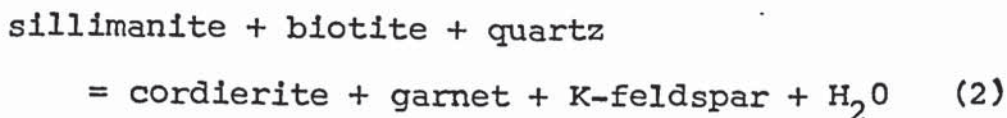
(Ashworth & Chinner, 1978). The mineral parageneses
observed across the isograd are illustrated in fig. 2.14.
Reaction (2), although theoretically discontinuous in the
system $K_2O - Al_2O_3 - MgO - FeO - SiO_2 - H_2O$ (Thompson, 1976a;
Holdaway & Lee, 1977), is continuous in the presence of a

71

FIGURE 2.14

AFM Diagrams

a.   Sillimanite + K-Feldspar Zone.

b.   Cordierite + K-Feldspar Zone.

a. SILLIMANITE + K-FELDSPAR ZONE

A
sillimanite

+ K-feldspar
+ quartz

garnet

biotite

F

M

b. CORDIERITE + K-FELDSPAR ZONE

A
sillimanite

+ K-feldspar
+ quartz

cordierite

garnet

biotite

F

M
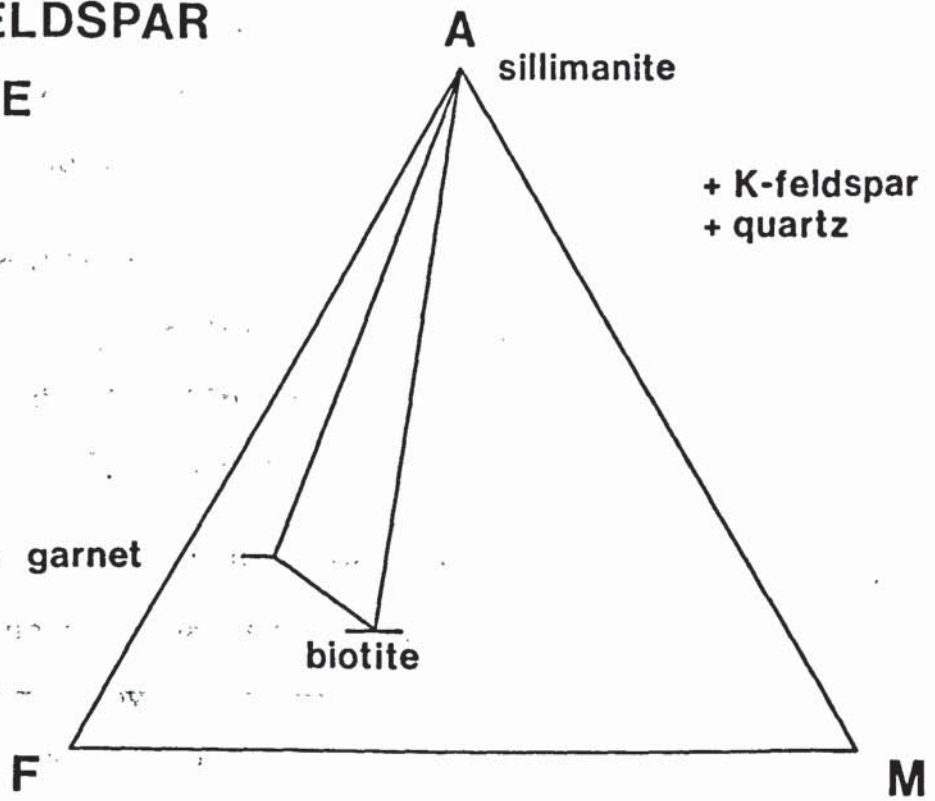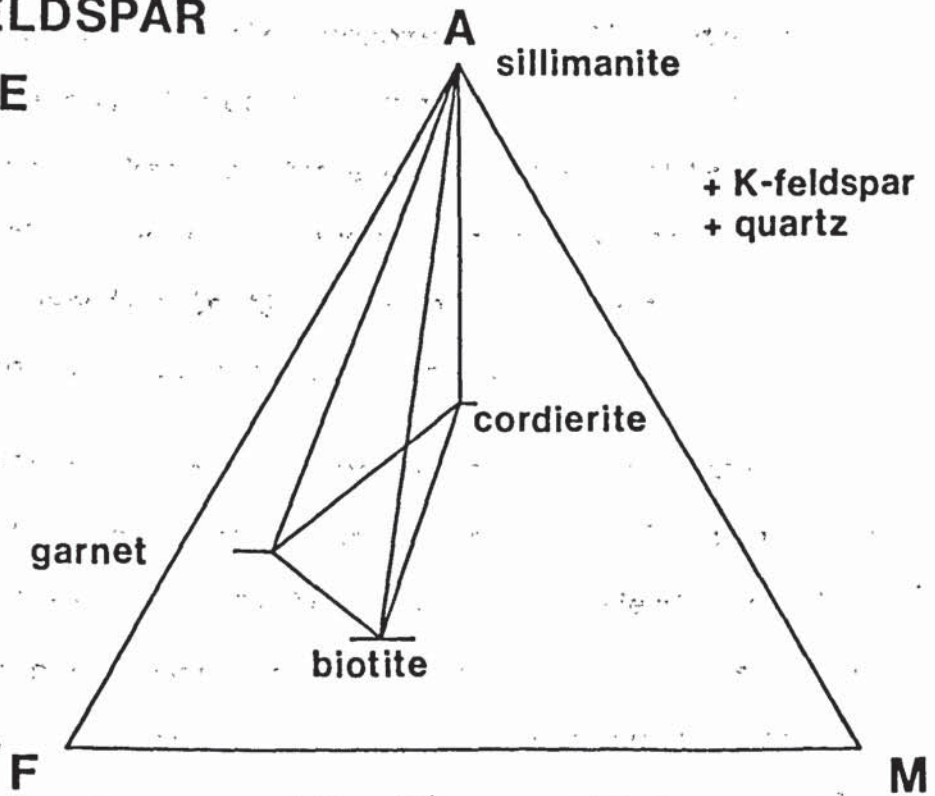
multivariant melt phase (section 2.7.2). Where the four phase assemblage sillimanite + biotite + cordierite + garnet occurs the continuous reaction

$$cordierite = garnet + sillimanite + quartz + H_2O \quad (3)$$
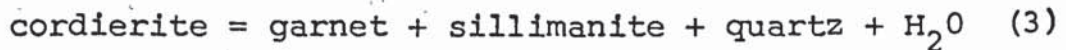
is taking place.

2.4.5 Migmatites

2.4.5 (i) Introduction and Nomenclature

Throughout the Glenfinnan and Loch Eil Divisions of the Moine, migmatitic pelites and semi-pelites are found.

Migmatites can be divided into two components; the palaeosome, representing the unaltered country rock; and the neosome, the portion formed by the migmatisation process. The neosome may itself be subdivided into the leucosome, formed predominantly of leucocratic minerals, and the melanosome, containing mainly dark minerals. The nomenclature used is that established by Mehnert (1968).

In the Moine, migmatitic neosomes form discrete and separate pods and lenses. Leucosomes have clearly defined margins which may be picked out by a melanosome. This distinguishes them from the frequent leucocratic bands which reflect com- positional banding in the original sediment. These grade into adjacent, melanocratic, bands.

The migmatities examined may be divided into two types according to the classification used by Ashworth (1976) based on their mineralogy (Table 2.5). Trondhjemitoid migmatites have the basic assemblage: biotite + plagioclase + quartz. Muscovite, sillimanite and garnet may also be present. Gran- itoid migmatites are distinguished by the additional occurrence of potash feldspar, cordierite - trondjhemitoid and

74

cordierite - granitoid migmatites may be found within the cordierite + K-feldspar zone of the aureole.

2.4.5 (ii) Trondhjemitoid - migmatites

Trondhjemitoid migmatites are most typical of the regional assemblages. Leucosomes are usually stromatic with lensoid bodies, up to 30mm in width and 300mm in length, lying parallel to the foliation (fig. 2.15). Typically, they are folded by the foliation.

Palaeosomes have the mineralogy described in section 2.4.2. Leucosomes are coarse grained with quartz and plagioclase crystals ranging up to 4mm across (fig. 2.16a). Biotite and primary muscovite form minor constituents, up to 1mm across. Secondary muscovite may occur, associated with chlorite as a replacement of biotite, or as metasomatic alteration of feldspar. Sillimanite may be present. Garnet is only found in palaeosomes.

In the aureole, trondhjemitoid migmatites are generally restricted to the muscovite + sillimanite + K-feldspar, and the sillimanite + K-feldspar zones. Leucosomes are stromatic and may be folded. One cordierite - trondhjemitoid migmatite has been recognised (A16, fig. 2.17). The leucosome consists of discontinuous, apparently disrupted, knots, up to 2mm in diameter, which themselves show evidence of pinch and swell. Small scale folding is also apparent. Both sillimanite and cordierite are present in the leucosome. A melanosome, consisting of biotite + cordierite + sillimanite + plagioclase + quartz, surrounds the leucosome and is deformed and disrupted with it.

FIGURE 2.15

Regional Migmatites

a. Trondhjemitoid. Specimen 595C.

b. Granitoid. Specimen 204C.

a

5 cm

b

5 cm
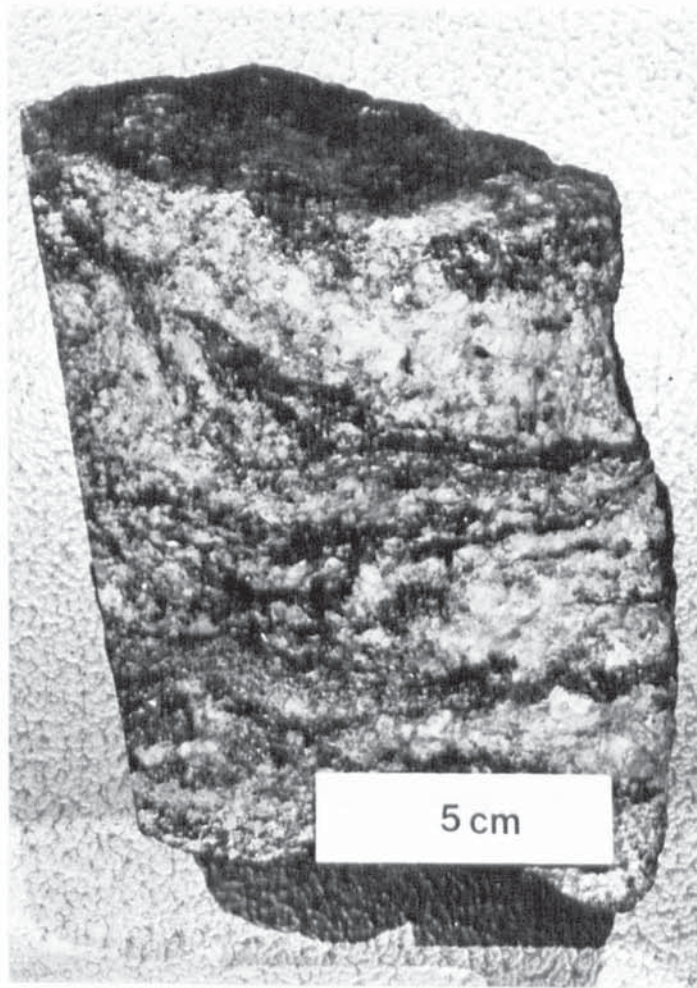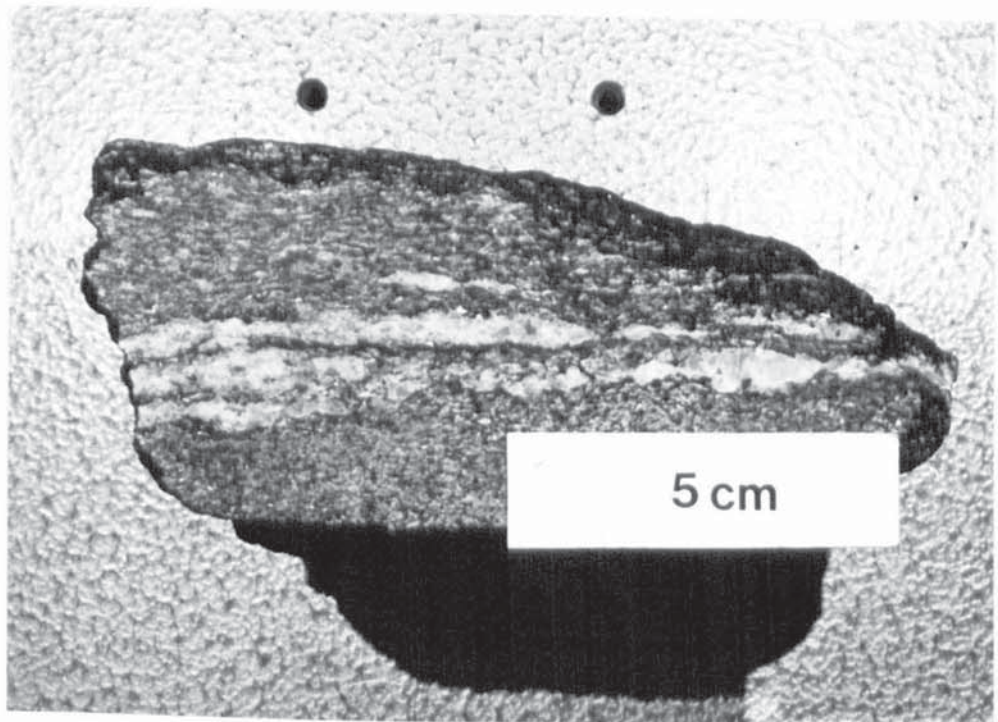
FIGURE 2.16

a. Regional trondhjemitoid leucosome. Specimen 593C.

b. Regional granitoid leucosome. Specimen 204C.
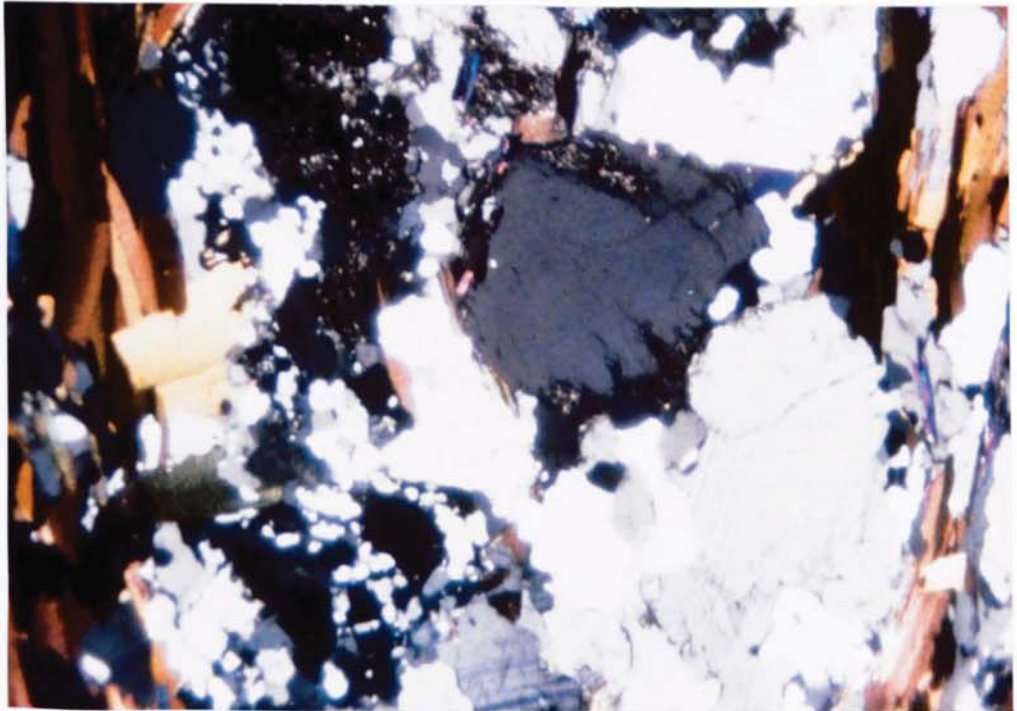
FIGURE 2.17

Disrupted migmatite, cordierite + K-feldspar zone.

a.   Hand specimen, A16.

b.   Thin section, A16.
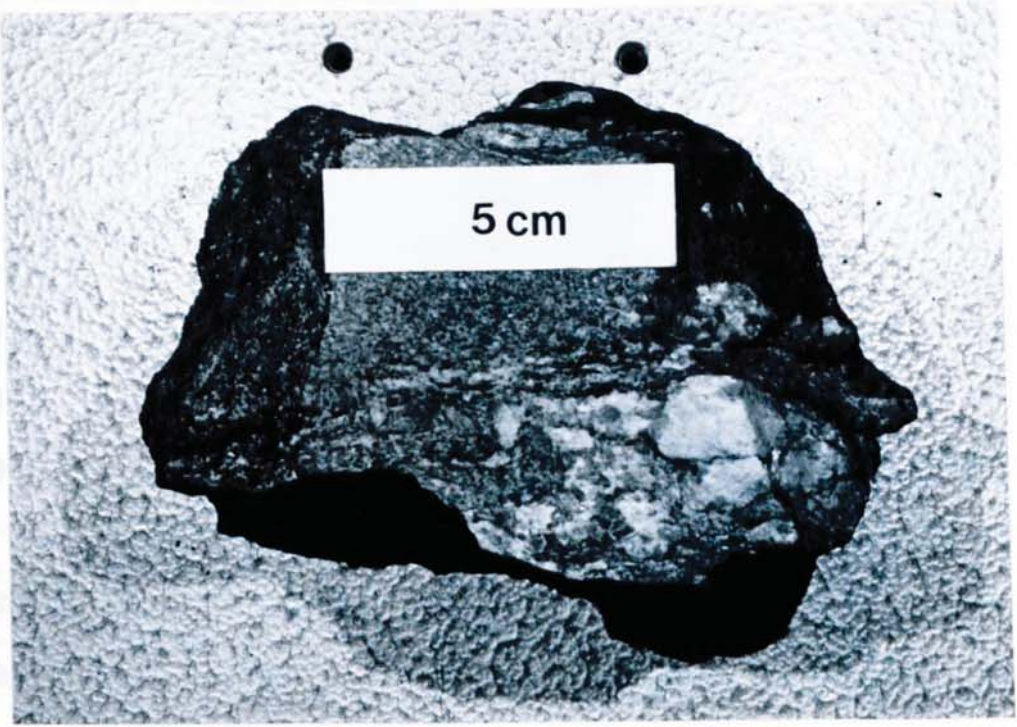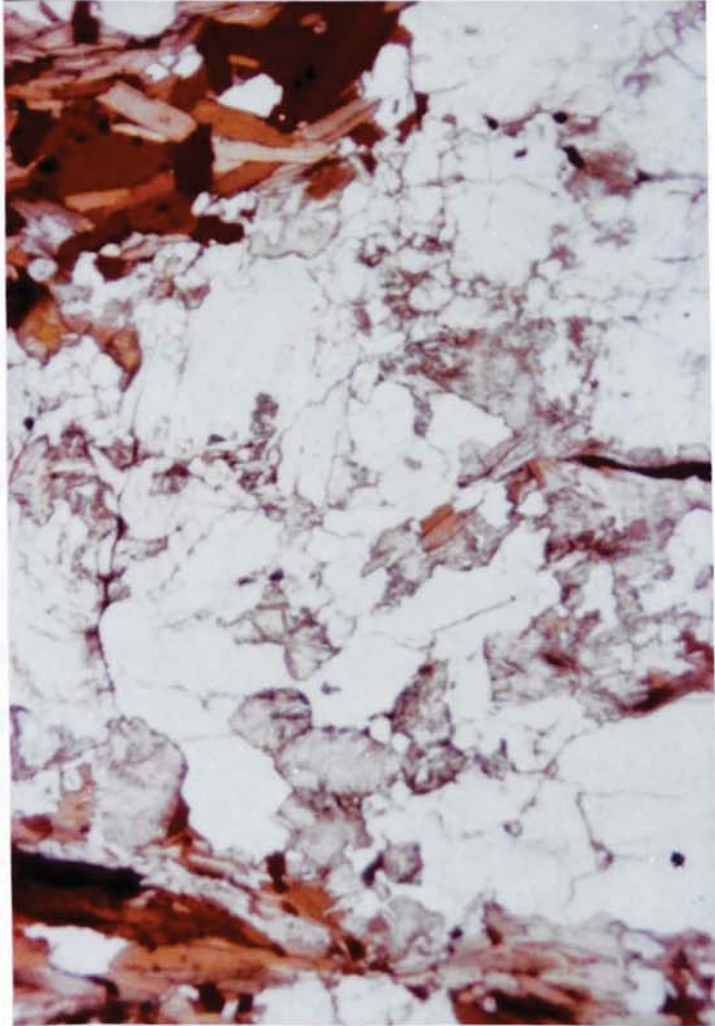
Similar, disrupted, leucosomal knots are a common feature of the zone of intense shearing recognised adjacent to the contact by Munro (1965) (Fig. 2.18a).

2.4.5 (iii) Granitoid migmatites

Granitoid migmatites are usually found within the aureole and two distinct types have been recognised.

The first type is distinguished by the occurrence of large crystals. These are found in both palaeosome and neosome, reaching 20mm in diameter in some leucosomes. In the western aureole these leucosomes are stromatic, and may become very coarse grained. They are not folded, although pinch and swell phenomena are common with extension occurring parallel to the pluton margin (fig. 2.18b, fig. 2.19). Palaeosome assemblages are those described in 2.4.3(i) and 2.4.3(ii). Leucosomes consist of quartz + plagioclase + microperthite + biotite. Sillimanite is usually present as is myrmekite and secondary muscovite. Cordierite is common in the cordierite + K-feldspar zone. Migmatites of this type and morphology are particularly common in the cordierite + K-feldspar zone, although they do occur more rarely in the sillimanite + K-feldspar zone. No migmatites of this type are recognised in regional assemblages west of the aureole.

At the eastern end of Glen Tarbert microperthite - granitoid migmatites are recognised in regional sillimanite + K-feldspar zone rocks. Within the aureole disrupted and deformed leuco-somes of similar appearance to A16 (e.g. A83, fig. 2.20a) have a cordierite - microperthite or microperthite - granitoid composition.

The second type of granitoid - migmatite is distinguished by

FIGURE 2.18

a.   Disrupted leucosomes in contact schists adjacent to
     contact.

b.   Contact migmatites in schists adjacent to contact
     near Woodend.

FIGURE 2.19

<u>Microperthite granitoid migmatite</u>

a. Hand specimen, A8.

b. Thin section, A8.

a

5 cm

b
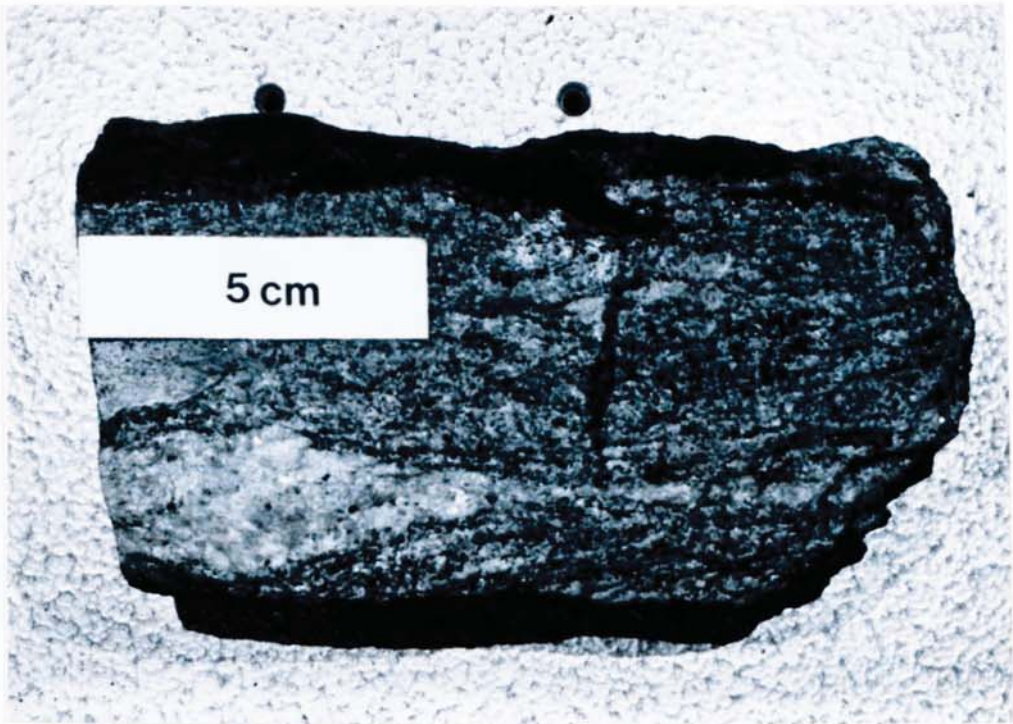
perthite

FIGURE 2.20

a. Disrupted microperthite granitoid leucosome.
   Specimen A83.

b. Aureole granitoid leucosome.   Specimen A28.
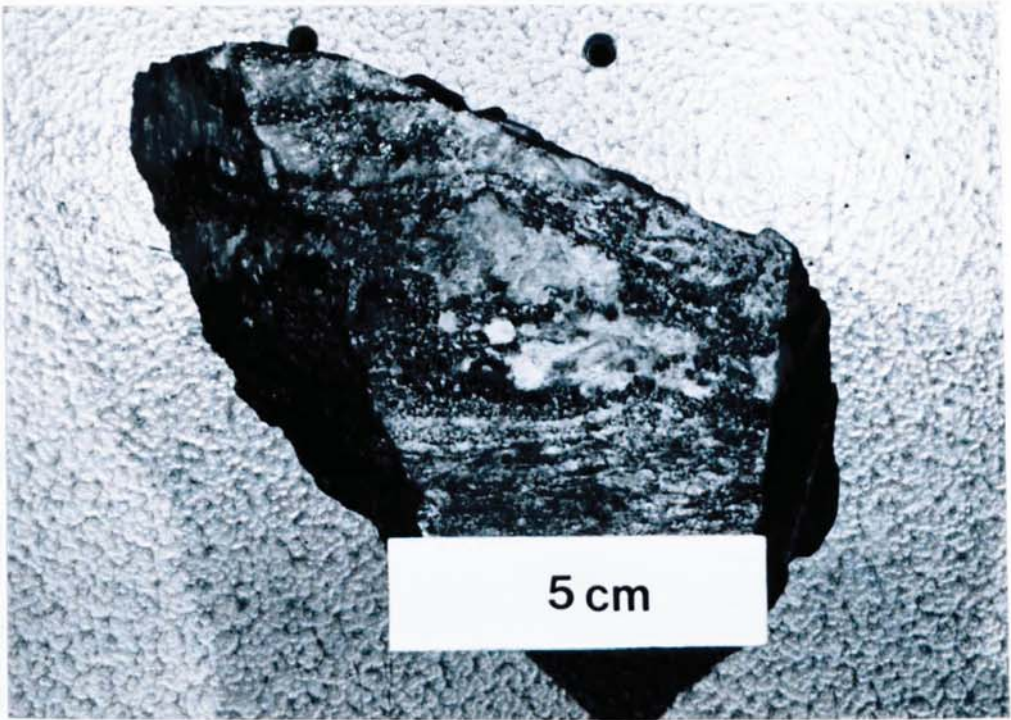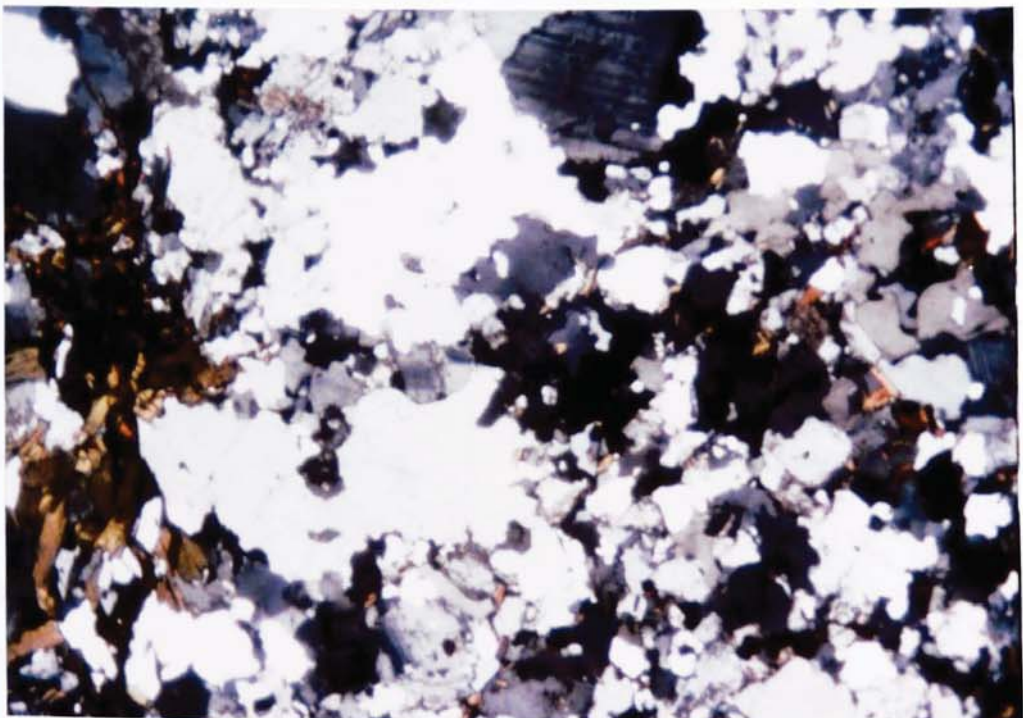
the occurrence of small, irregular and interstitial potash
feldspar crystals which may show replacement by myrmekite.
They are found in all of the aureole zones, but only one
(204C, fig. 2.16b) occurs in a regional sample. Their
general mineralogy is similar to that of the trondhjemitoid
migmatites. Again leucosomes are stromatic but generally show
evidence of deformation. A28 (fig. 2.20b) in particular has
a high modal content of potash feldspar, but the leucosome is
tightly folded. Compared with perthite - granitoid migmatites
the leucosome is fine grained, crystals rarely exceeding 1mm
in diameter.

The petrographic and morphological features of the migmatites
examined is summarised in Table 2.5.

Trondhjemitoid, and the second type of granitoid - migmatites
are both regarded as being of regional origin. To the west
of the aureole migmatites are trondhjemitoid, containing
primary muscovite. If these assemblages are metamorphosed to
aureole sillimanite + K-feldspar and cordierite + K-feldspar
zone conditions, the muscovite will break down according to
reaction (1), producing a sillimanite + K-feldspar assemblage.
If primary muscovite was absent from the regional assemblage,
reaction (1) cannot operate, allowing the migmatite to persist
in the aureole in its unmodified condition. As the contact is
approached, the degree of deformation and shearing increases
(Munro, 1965) and regional migmatites are disrupted, fragments
of leucosome being separated are drawn out along the foliation
in the sheared rocks.

In regional assemblages to the east of the aureole, microperth-
ite - granitoid migmatites are present, and it is these that

TABLE 2.5

MIGMATITE TYPE

| METAMORPHIC ZONE | TRONDHJEMITOID | | GRANITOID | | | |
| | | | MICROPERTHITIC | | RECRYSTALLISED REGIONAL | |
	UNDIS-RUPTED	DIS-RUPTED	UNDIS-RUPTED	DIS-RUPTED	UNDIS-RUPTED	DIS-RUPTED
Regional Sillimanite and Sillimanite + K-feldspar	298C 359C 570C 573C 588C 593C 595C		22C		204C	
Muscovite + Sillimanite + K-feldspar					A31 358C 365C 402C	
Sillimanite + K-feldspar	A17 A18		A10 A12	A99 A101	A28 294C 328C 342C 352C 384C	A4
Cordierite + K-feldspar	A82	A16	A8 A46 A80 201C	A83	A97 195C	270C

are disrupted by the intrusion in the eastern aureole.

Undisrupted microperthite - granitoid and cordierite - micro-
perthite - granitoid migmatites are regarded as the products
of contact metamorphism. The nature of their formation will
be discussed in Section 2.72.

2.5 GARNET ZONING AND RE-EQUILIBRATION

2.5.1 Zoning Models: a review

Complex internal zoning of garnet, not seen by normal optical
microscopy, has for some time been known from electron
microprobe studies (Atherton & Edmunds, 1966; Harte & Henley,
1966; Hollister, 1966). A 'normal' pattern of zoning was
recognised with the amount of Fe and Mg present increasing
from core to rim while the amount of Mn and Ca decreased.
The Mn zoning displayed a pronounced bell-shaped profile.
Garnet crystals were considered to be closed with respect to
the other minerals in the rock due to the high activation
energy for diffusion within them. Only the surface of the
crystals was in equilibrium contact with the matrix. Hollister
(1969) referred to this as 'refractory' behaviour. Sturt (1962)
and Atherton (1965) recognised an increase in the overall FeO
and MgO content of garnet with increasing grade, at the
expense of MnO and CaO. The observed profiles reflect this
trend and were presumed to result from the prograde growth
of the crystals.

Hollister (1966) attempted to explain the Mn zoning by means
of a fractionation model. Garnet is the main Mn-phase found
in pelitic schists. At low grade, early formed garnets are
rich in Mn. As growth continues the surrounding volume of
reservoir rock, the 'reservoir' from which the crystal draws

91

its constituent elements, is depleted in Mn and thus the outer, newly formed, rim of the crystal becomes correspondingly poor in Mn.

Further microprobe studies of garnet zoning from widely differing metamorphic environments, revealed that the 'normal' zoning pattern was not always the rule. Profiles in which Mn increased at the rim while Mg and, more rarely, Fe decreased were recognised, e.g. Grant & Weiblen (1971). A gradual flattening of curves, with a corresponding decrease in their complexity, was also recognised with increasing grade.

Anderson & Buckley (1973) investigated the theoretical zoning profiles which would be produced if diffusion took place within initially homogeneous garnets. Using reasonable coefficients for diffusion in garnet, and for intergranular and grain boundary diffusion within the reservoir, they modelled each of the profiles recognised in natural garnets with increasing grade. A flattening of profiles with time was also predicted.

In order to test these models of garnet growth, several studies investigated the effect on zoning profiles of increasing metamorphic grade (Tracy et.al., 1976; Anderson & Olimpio, 1977; Woodsworth, 1977; Yardley, 1977). In each case 'normally' zoned garnets, with characteristically bell-shaped Mn profiles, were recognised in lower grade assemblages. As grade increased, profiles flattened out until a homogeneous profile, or one in which Mn increases sharply at the edge of the grain, is produced.

Tracy et.al. (1976) explained the changing garnet compositions

in pelitic schists from Central Massachusetts by the various
Fe - Mg - Mn continuous reactions which took place. Rim
compositions were regarded as retrograde in origin where they
showed a sharp change from the profile within the body of the
garnet grain. This was supported by temperature estimates
using Fe - Mg partition data between garnet and biotite or
cordierite. The rims generally showed a low temperature
compared with the core. In the lowest, staurolite grade
garnets, which showed strong 'normal' zoning, temperature
increased towards the rim. Zoning at the extreme edge of the
grains, seen as a slight drop in Mg which had otherwise
increased from the core, revealed a drop in temperature from
the maxima recorded in near rim compositions. As grade
increased to sillimanite + K-feldspar zone conditions, this
type of profile was replaced by one showing a virtually homo-
geneous core with a rapid increase in Mn and to some extent,
Fe, towards the rim. Mg decreased as a result. This was
attributed to late, retrograde, operation of the continuous
reaction

$$bio + sill + qtz = gar + ksp + H_2O \qquad (4)$$
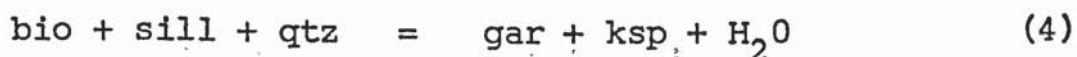
which results in the depletion of Mg in garnet relative to Fe
and Mn. At the highest grade, profiles became virtually
homogeneous. Zoning which did take place was found adjacent
to biotite grains in contact with the garnet, and was attri-
buted to a diffusional cation exchange between the two
minerals.

Anderson & Olimpio (1977) investigated a series of garnets
from Morar. In the lowest grade zone, large, idioblastic
garnets exhibited as many as three, concentric, optical
zones. These were shown to correspond to abrupt changes in

the chemical zoning profiles, particularly of Fe and Ca. Mn
profiles were bell-shaped but were found to vary in magnitude
with the size of the garnet. The largest crystals, growing
for a longer period of time, had a lower Mn content, and
flatter profile in the core, than the smaller crystals. This
progressive flattening of Mn profile with size, and therefore
with time was taken as evidence that diffusion could take
place in low grade garnet, where profiles had previously been
attributed solely to prograde growth.

In Morar a second metamorphic episode has been superimposed on
to rocks already metamorphosed to high grade (Section 2.3.3).
In both cases the grade of metamorphism increased from west
to east. Garnet profiles also show a progressive flattening
and homogenisation in this direction. This trend was inter-
preted as the result of volume diffusion at high grade during
the second metamorphism, destroying complex zoning produced
by the first metamorphism. Intermediate profiles in which
flattened profiles show zoning between Fe and Ca in the core
of the garnet only, were interpreted as representing incom-
plete re-homogenisation of the early profiles.

It was concluded that there was good evidence for the oper-
ation of volume diffusion in garnet at high grade, and that
the efficiency of diffusion improved with increasing grade.
Zoning at the edge of high grade garnets was considered to be
the result of retrograde reaction.

Woodsworth (1977) studied the progressive homogenisation of
garnets from British Columbia. In the lower grade garnet and
staurolite zones 'normal' zoning was found. At high grade,
in the cordierite zone, garnets were homogeneous. Zoning

94

involving increased Mn at the rim, with decreased Mg, was also seen. Using Mn/Fe partition data between garnet and ilmenite, homogeneous garnets were shown to have originally had 'normal', low grade zoning. As the garnet grew, equilibrium was maintained between it and ilmenite grains in the matrix. Ilmenites engulfed by the growing crystal were removed from this system and preserved a Mn/Fe ratio reflecting conditions at that time. Preservation of this ratio also suggests that volume diffusion was not operating in garnets during this period of growth. The growth zoning profiles of homogeneous garnets were reconstructed from the compositions of ilmenite inclusions and revealed a close resemblance to profiles seen in the garnet and staurolite zone. It was concluded that volume diffusion acts at high grade to produce homogeneous profiles, obliterating growth zoning profiles produced at lower grade where diffusion was not effective. Zoning at the rims of homogeneous, high grade garnet was interpreted as a retrograde effect.

Yardley (1977) described a series of garnets from Connemara. An abrupt change in zoning, from 'normal' to homogeneous, was found within the staurolite - sillimanite tranistion zone. The change takes place over a range of about 50° starting at $600^{\circ}C$. It was suggested that this change, interpreted as marking the onset of volume diffusion in garnet, may be used as an isograd in pelitic schists. Again an increase in the Mn content at the rim of high grade garnet was attributed to retrograde effects.

In each of the above studies zoning at the edge of high grade (that is, sillimanite, sillimanite + K-feldspar and cordierite + K-feldspar zone) garnets has been interpreted as a retrograde effect. It may be the result of retrograde

95

operation of a continuous Fe - Mg - Mn reaction involving
garnet, such as reaction (4); or of a cation exchange reaction
involving exchange of Fe and Mg between garnet and cordierite
or biotite (Tracy et.al., 1976; Yardley 1977). Such retrograde
reactions will produce a low Mg/(Mg + Fe) value at the rim
compared with the core. This trend occurs in each of the
above studies. At lower grade the trend is for an increase in
Mg/(Mg + Fe) to the rim, interpreted as the result of prograde
growth. Tracy et.al. (1976) do give evidence that retrograde
reactions can also affect the extreme edge of low grade garnet.
Reactions such as (4) result in the resorption of garnet with
a consequent reduction in the volume of each crystal's outer
shell. As Mg and to a lesser extent Fe, are removed from the
garnet by the reaction, Mn increases in proportion as it is
preferentially retained in the garnet due to its low mobility
(Loomis, 1978).

The general pattern of zoning in garnet with increasing grade
is one in which growth zoning is dominant at low grade.
Diffusion only begins to operate effectively at high grade,
usually at temperatures in excess of $600^{o}C$ (Woodsworth, 1977;
Yardley 1977). Homogeneous zoning profiles result, obliterat-
ing the former growth profiles, and an equilibrium composition
will become established throughout the whole grain, assuming
that peak metamorphic conditions are maintained for a long
enough period. As cooling takes place, retrograde reactions
will affect the rim compositions. Generally, the time period
over which retrograde reactions operate is not long enough to
establish a new homogeneous composition and penetration of
new, lower grade compositions is restricted to the edge of
the grain. In small grains however, the retrograde

composition may become established throughout.

In order to obtain meaningful results from the various geothermometers and geobarometers which involve garnet (see Section 2.6) it is necessary to establish which part of the garnet profile represents peak metamorphic conditions. From the above discussion it seems that the homogeneous core of a large, high grade garnet will correspond most closely to peak conditions. The rim composition represents lower, retrograde conditions. Tracy et.al. (1976) and Ashworth & Chinner (1978) have both followed this course. The Fe - Mg exchange geothermometers of Thompson (1976b), Ferry & Spear (1978) and Holdaway & Lee (1977) for garnet - biotite and garnet - cordierite all indicate higher temperatures for high grade garnet cores than for the rims, exemplified by the observed decrease in Mg/(Mg + Fe). At lower grade Mg/(Mg + Fe) increases to the rim and it is these compositions which are taken to indicate peak conditions (Tracy et.al, 1976).

Hollister (1977) describes textures found in pelites from the Khtada Lake complex, British Columbia, where garnet is seen to be resorbed in favour of cordierite by the prograde reaction

garnet + sillimanite + biotite + quartz

= cordierite + K-feldspar + Ca-plagioclase + H$_2$0   (5)
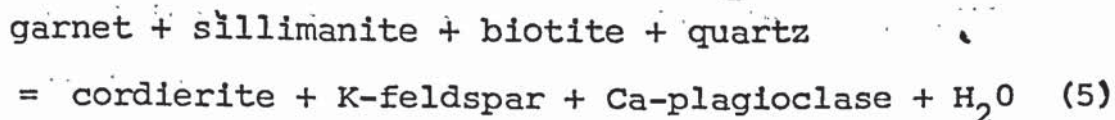
As in the studies already described, the garnet profiles show a decrease in Mg/(Mg + Fe) to the rim while Mn increases. However, in this case, rapid uplift has taken place immediately after peak metamorphism. As a result, zoning profiles in garnet are unaffected by any later diffusion and peak conditions are represented by rim compositions of both garnet and cordierite.

2.5.2 Garnet Zoning in the Strontian Area

Zoning profiles of garnets from sixteen specimens located on fig. 2.23 are presented in fig. 2.21 a-ρ.

Garnets from within the aureole show a decrease from core to rim of Fe and Mg while Mn increases. Ca is usually almost unzoned. In smaller garnets (A2, A73 from the cordierite zone, 402C from the muscovite + sillimanite + K-feldspar zone) this profile type is well developed, showing smooth curves with the inflexion points occurring at, or very near to, the centre of the crystal. As the size of the grain increases, a more homogeneous core is established (A19). In the largest garnets (A8, A45 and A72) this homogeneous core may show minor variations in composition. The Mg/(Mg + Fe) profiles however, are generally smooth. A8 shows a markedly asymmetrical profile, with a high Mg core developed at one end. This is attributed to differing diffusion rates within the surrounding rock matrix. At the high Mg end the grain is in contact with biotite, while the opposite end is against a well developed leucosome. A45 apparently shows a low Mg core, surrounded by a high Mg outer core. This results from the influence of a biotite inclusion lying near to the line of profile in the low Mg/Fe area.

270C has well developed zoning in both Fe and Ca profiles. Ca content drops near the rim while Fe rises from a relatively homogeneous core. As with other garnets in the aureole, Mn increases at the rim, while Mg decreases. The Mg/(Mg + Fe) profile shows an overall drop in Mg from core to rim. A10 and A45 also show a drop in Ca content near the rim.

In A83, sampled from the Loch Eil Division in Glen Tarbert,

FIGURE 2.21

Garnet Zoning Profiles

a. A8; b. A45; c. A2; d. A83; e. A73; f. 270C; g. A10;
h. A72; i. A19; j. 402C; k. A41; l. A91; m. 205C;
n. 298C; o. 614C; p. 572C.

Solid circles - Fe; Triangles - Mg; Squares - Mn; Open
circles - Ca; Solid line - Mg/(Mg+Fe).

Mg, Fe, Ca and Mn are plotted in atomic percentages
(Mg + Fe + Ca + Mn = 100%).

Mg/(Mg+Fe) is plotted in atomic proportions.

Profiles a. to f. - cordierite + K-feldspar zone;
g. to i. - sillimanite + K-feldspar zone; j. - muscovite
+ sillimanite + K-feldspar zone; k. to p. - regional
sillimanite zone.

100

A45

b.

c.   d.

A2   A83

105

g.

A72

k.

l.

qtz inclusion

A91

A41

205C

109

572C
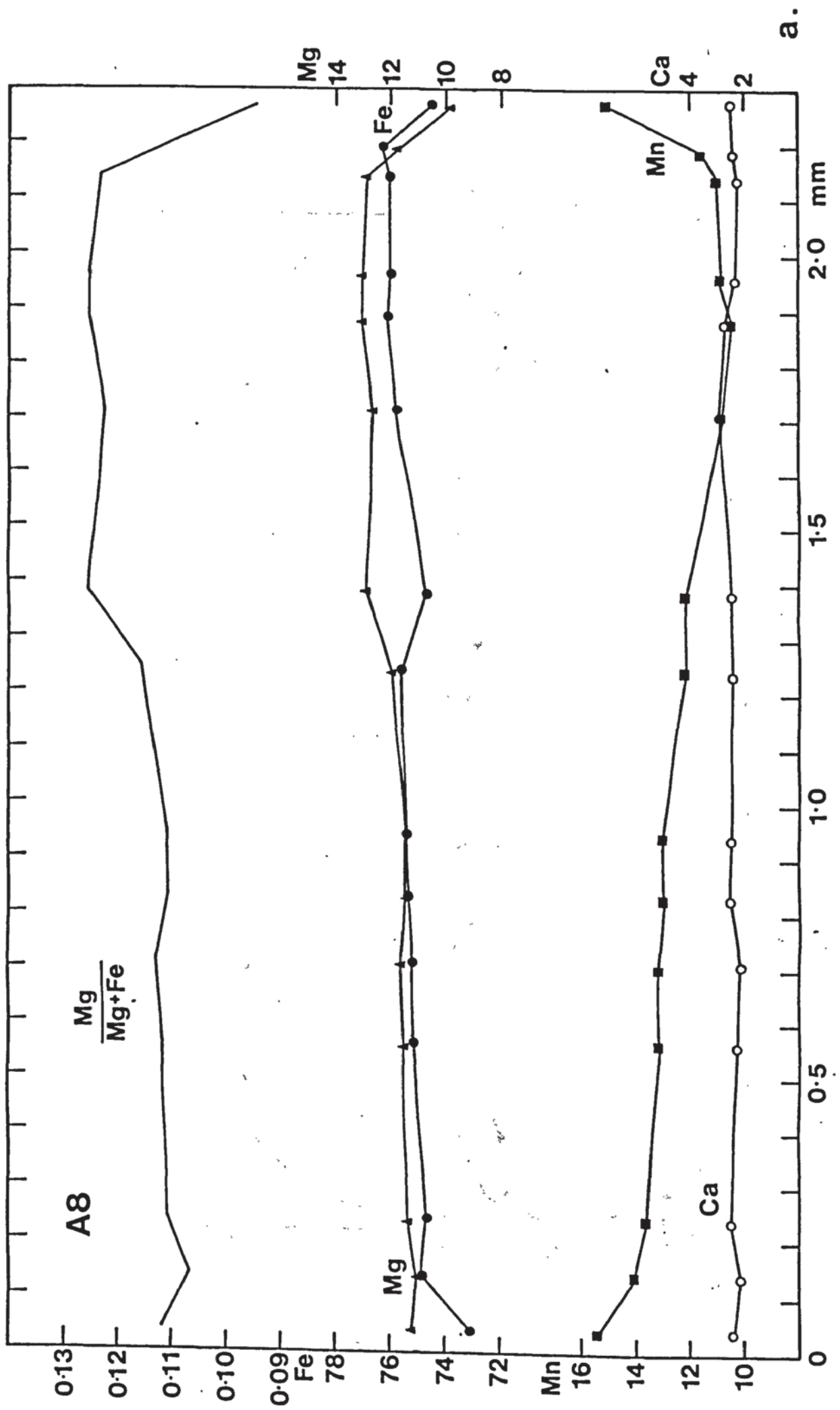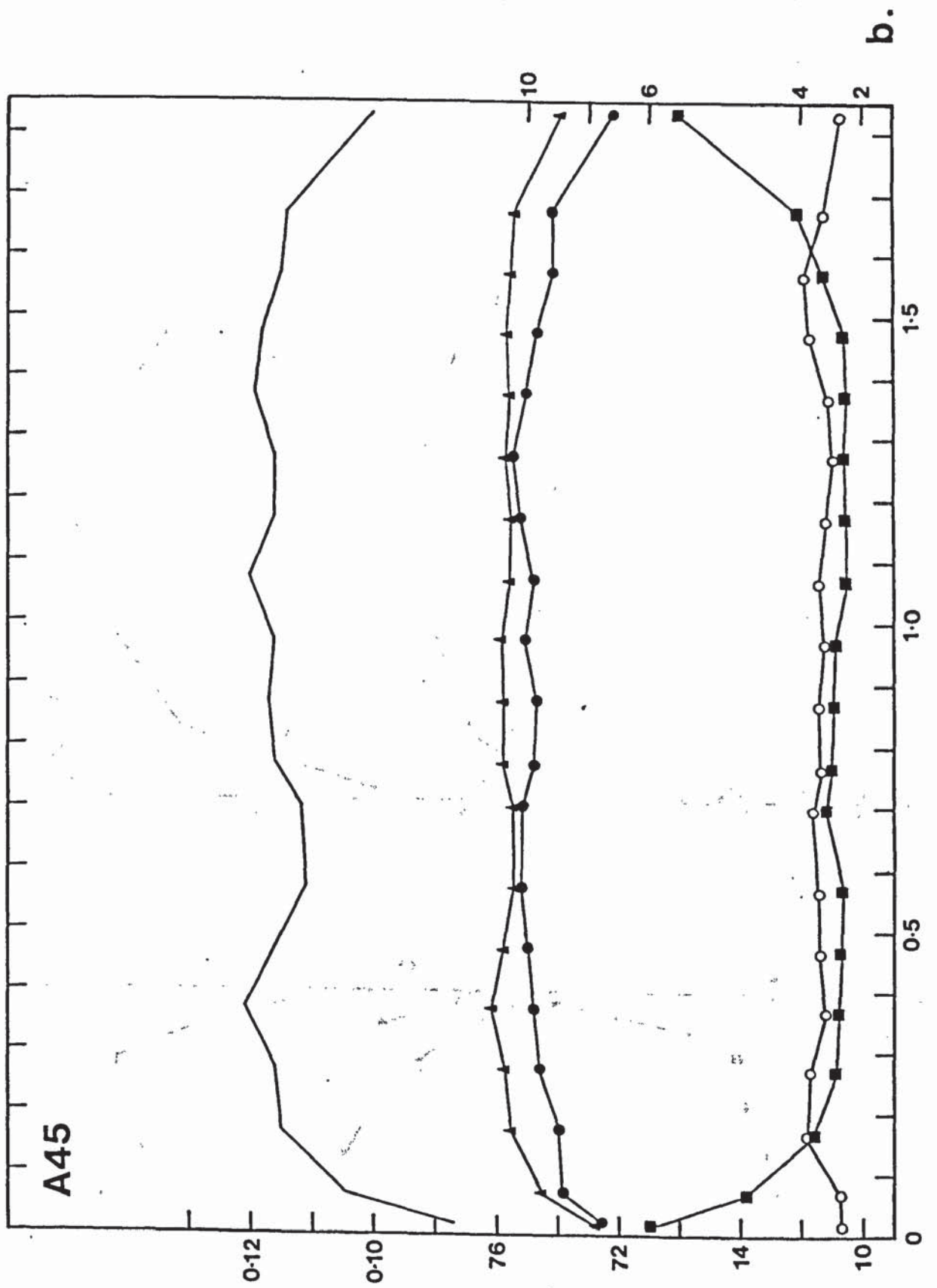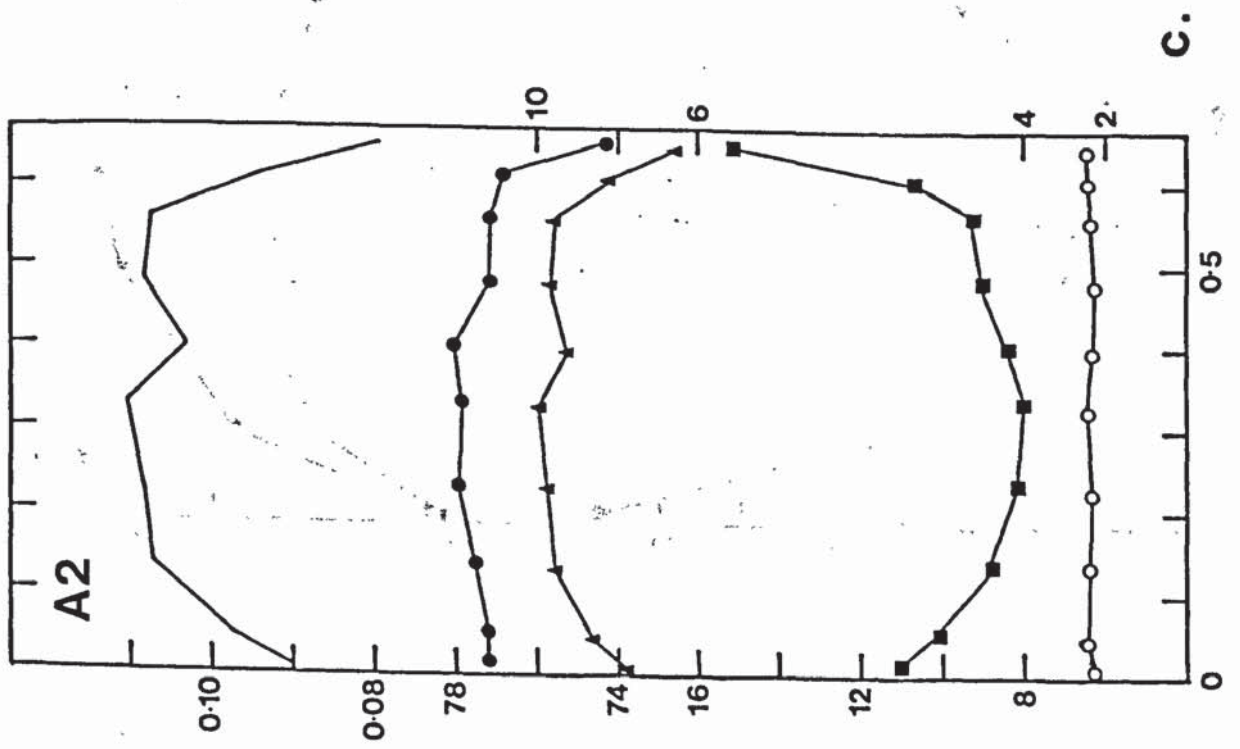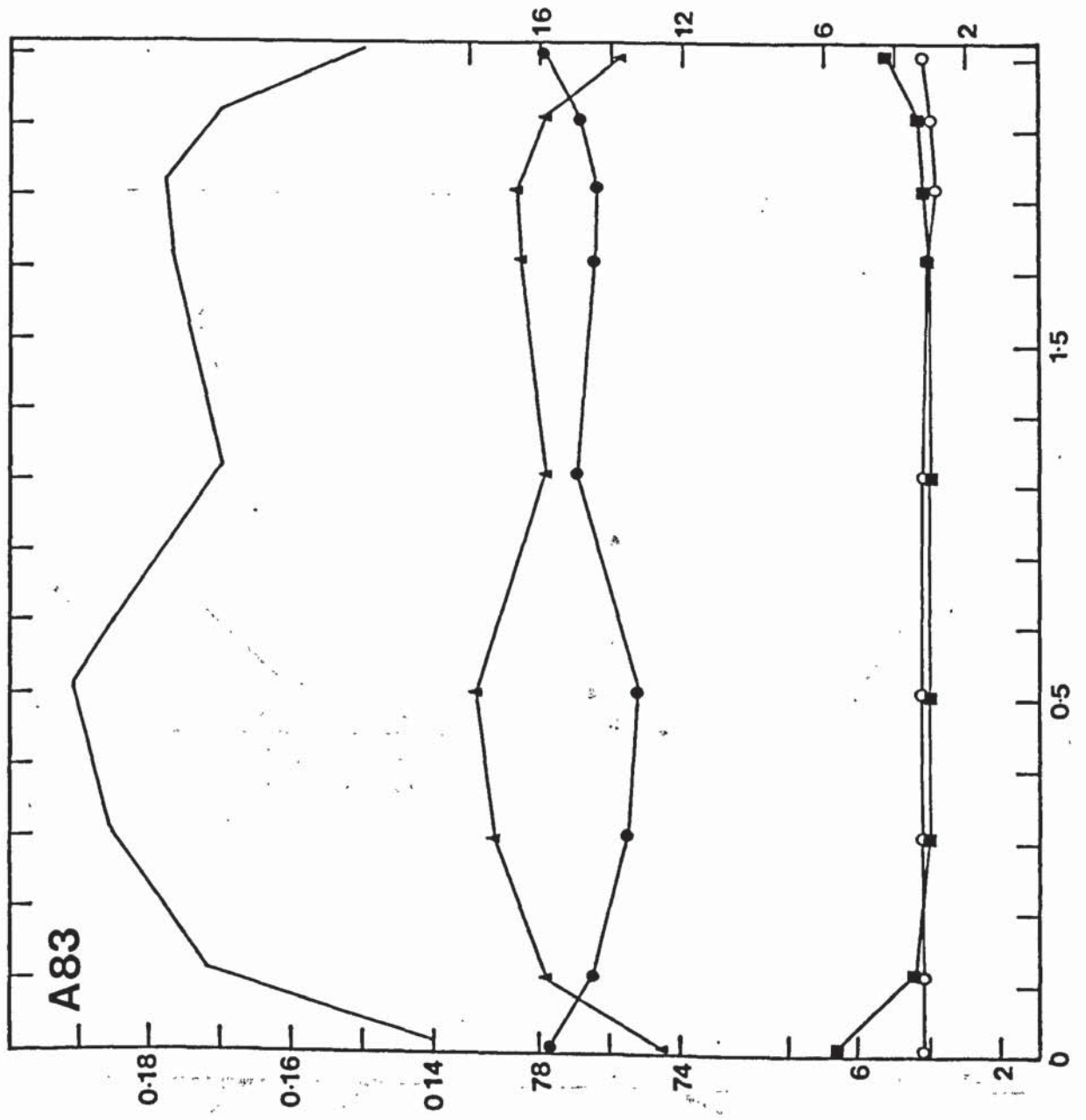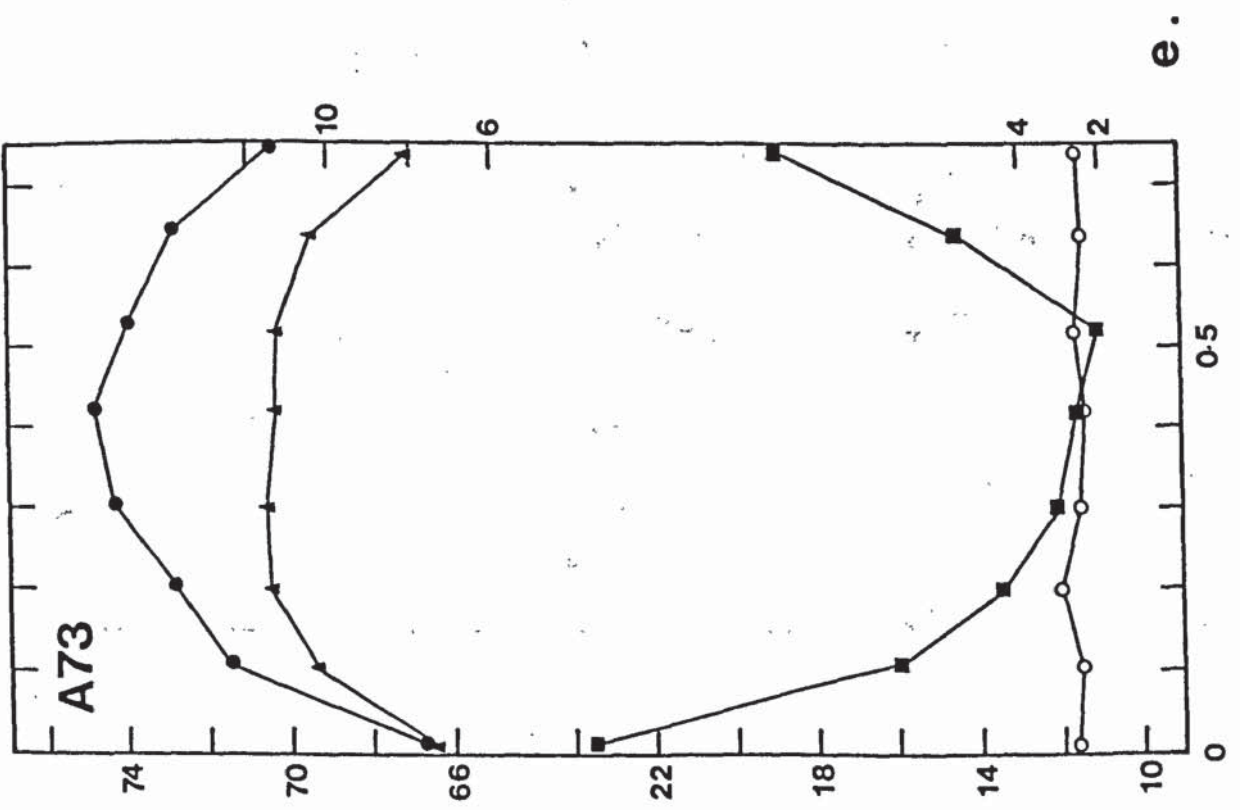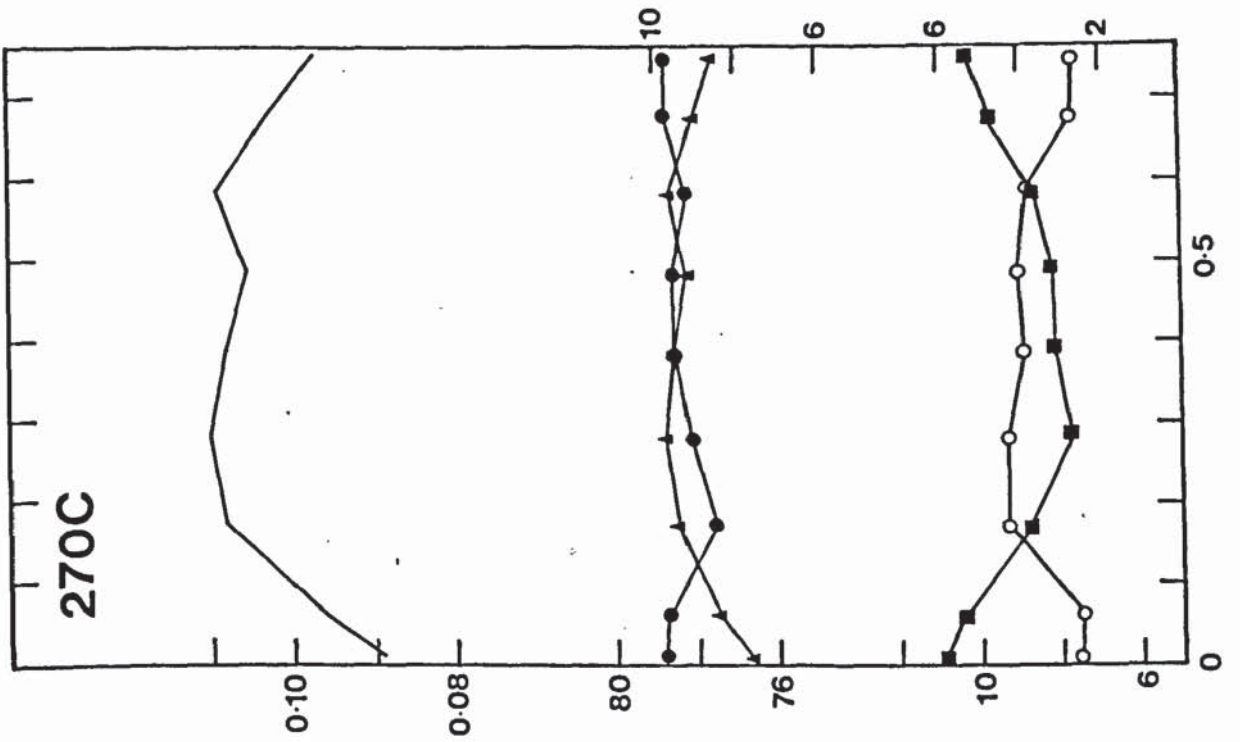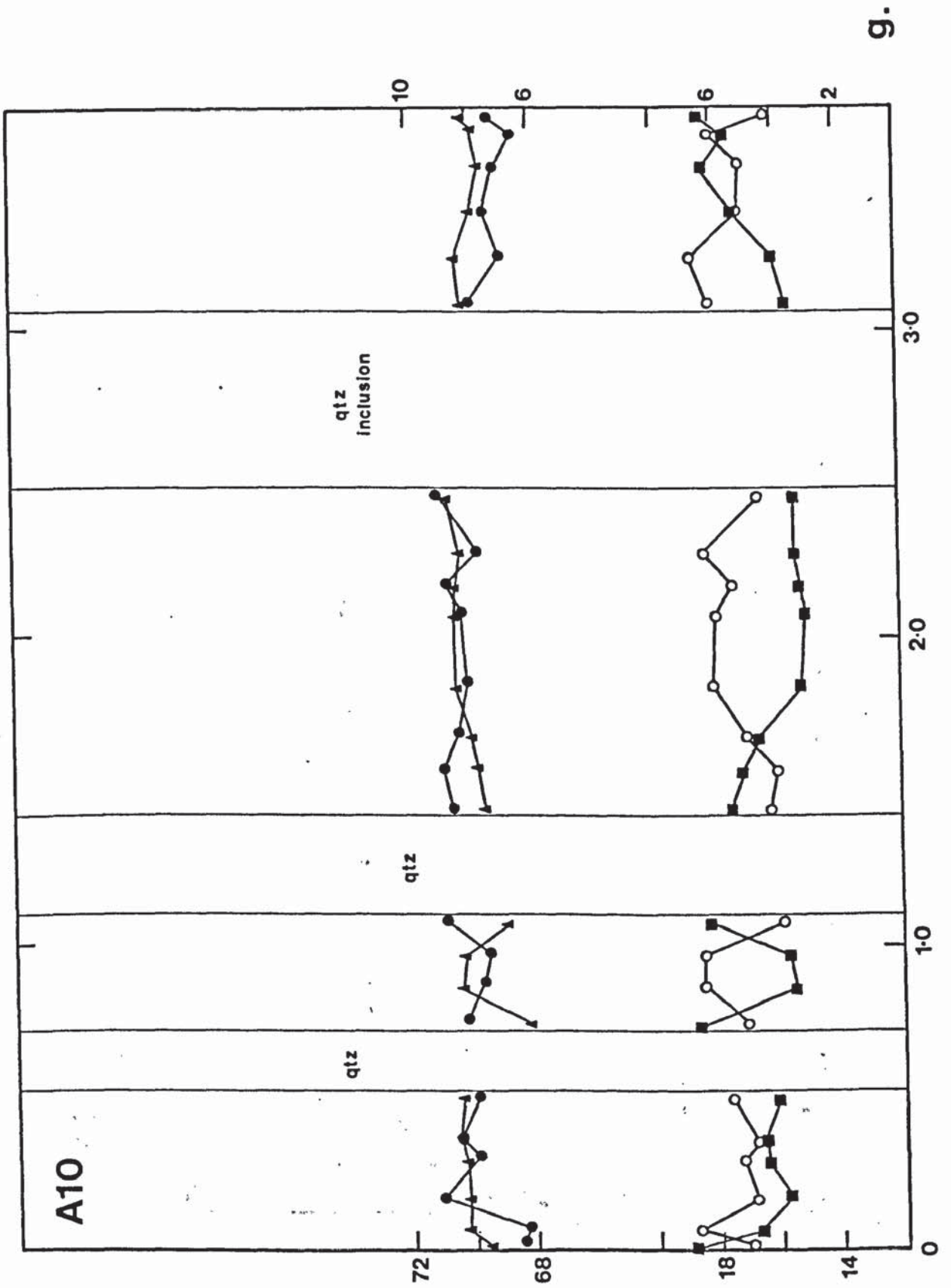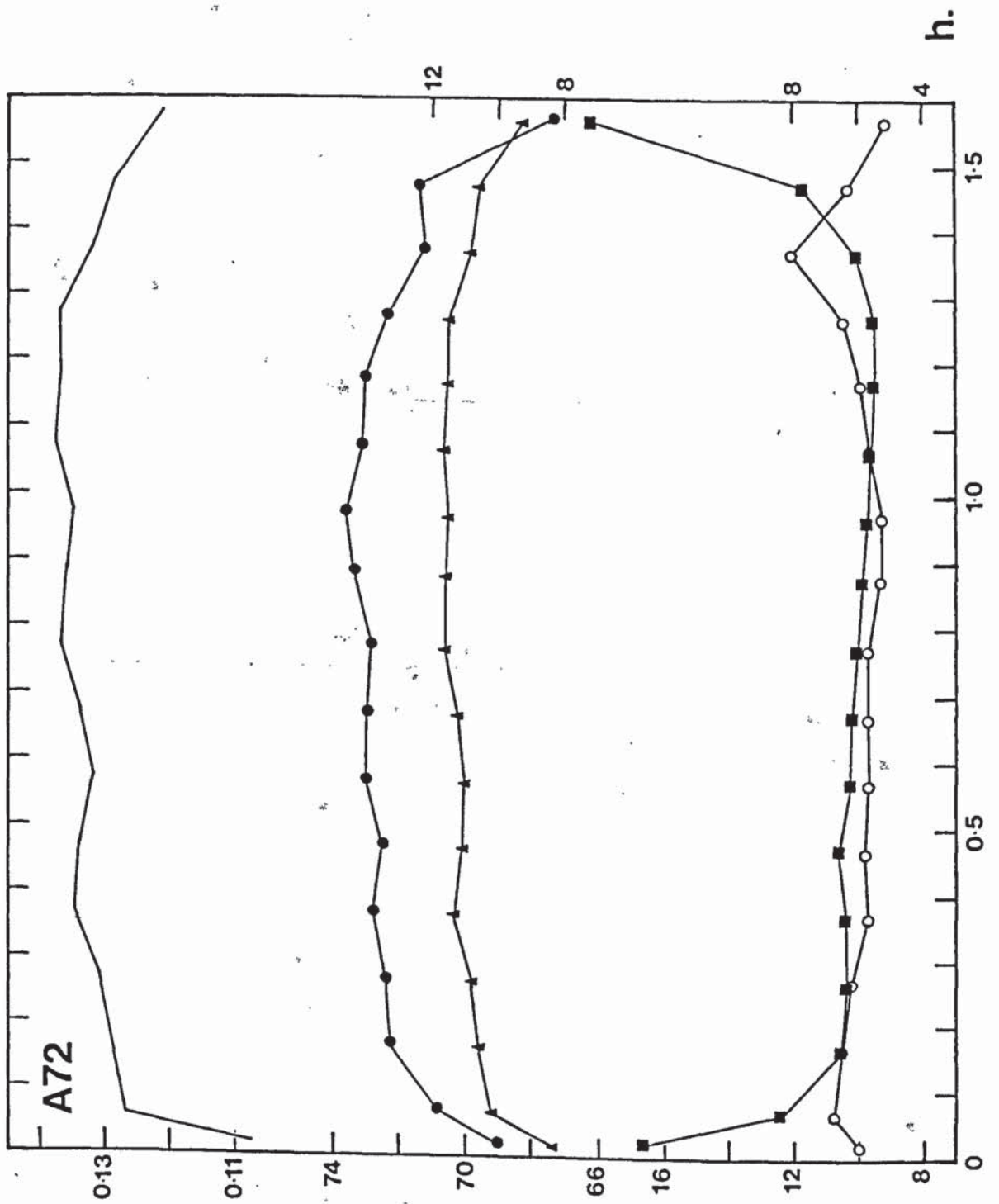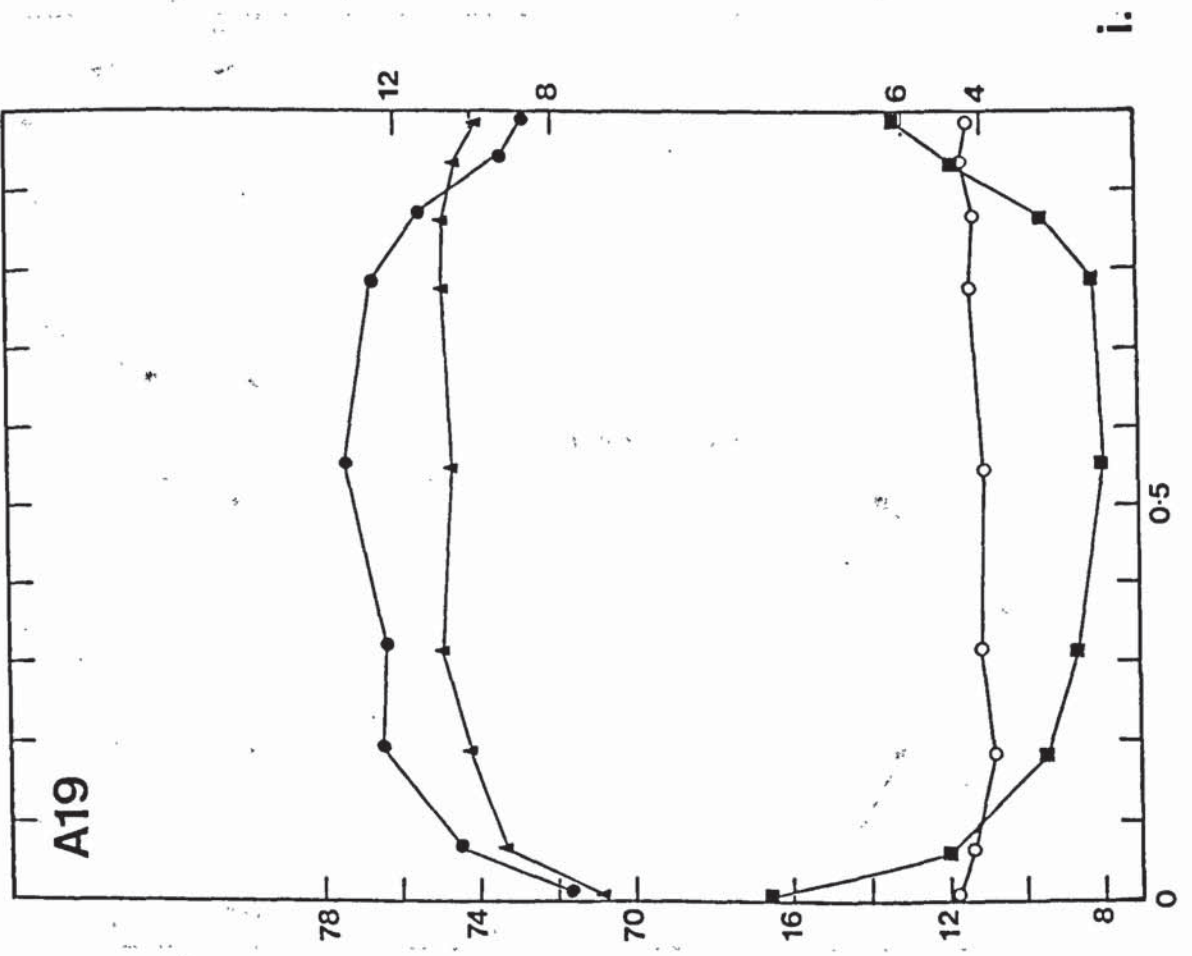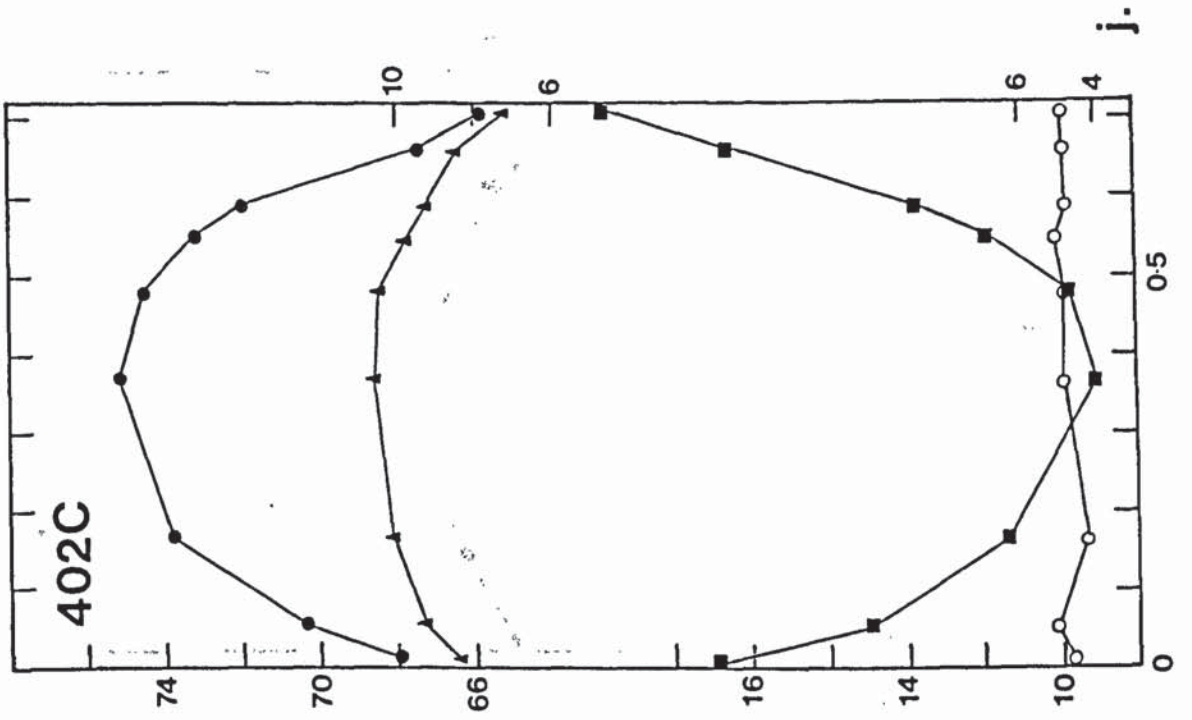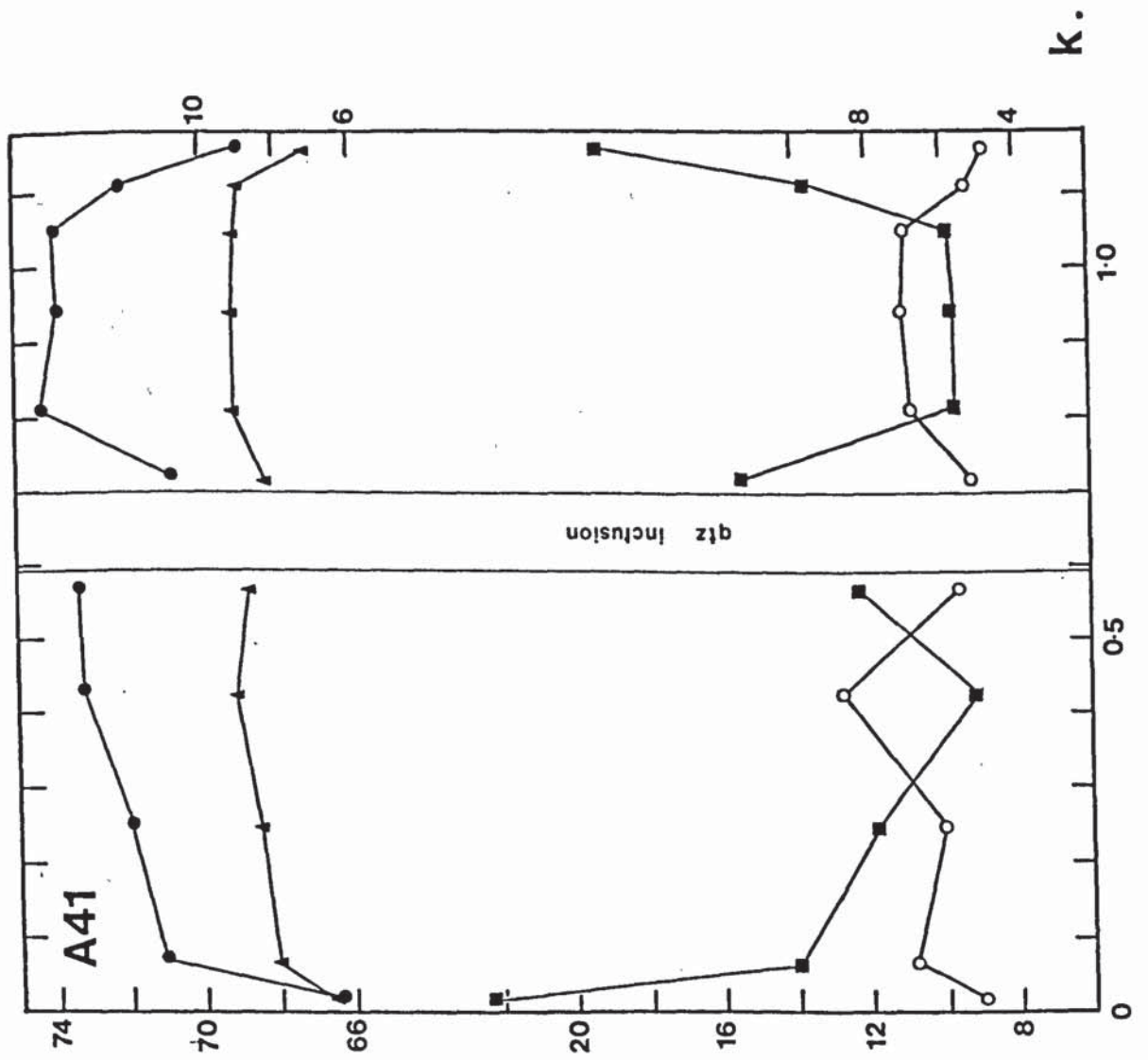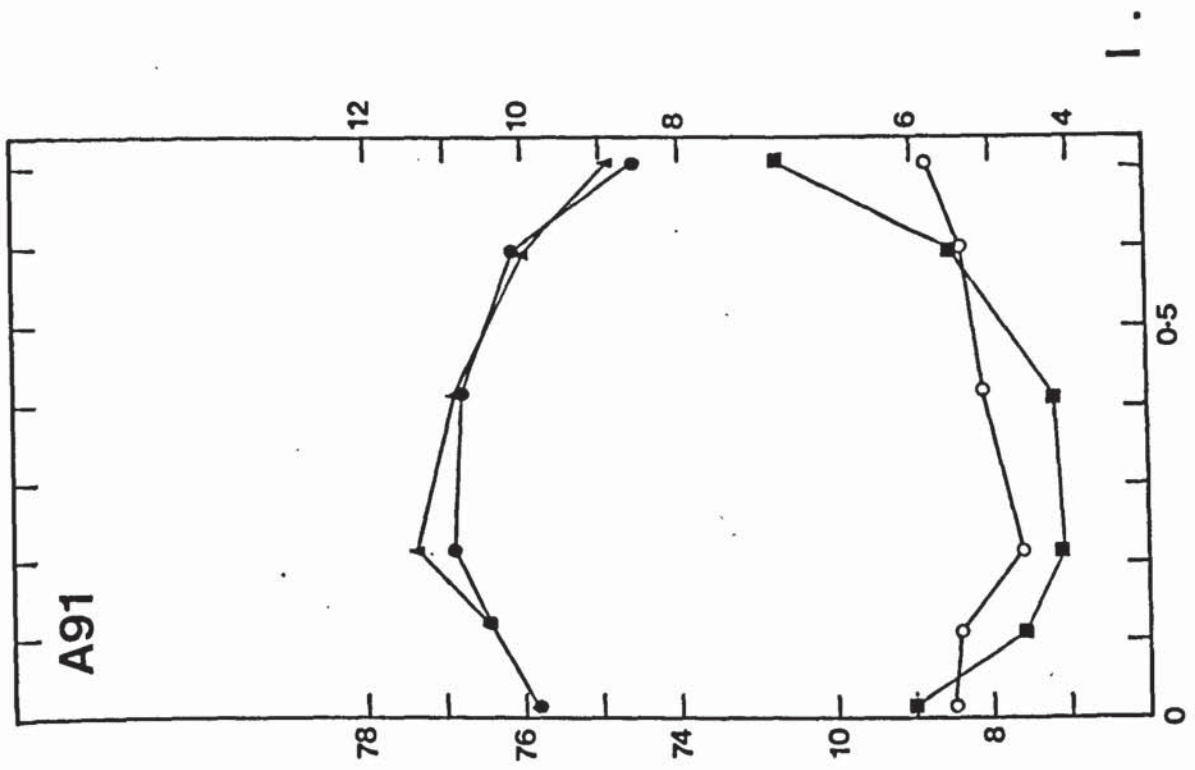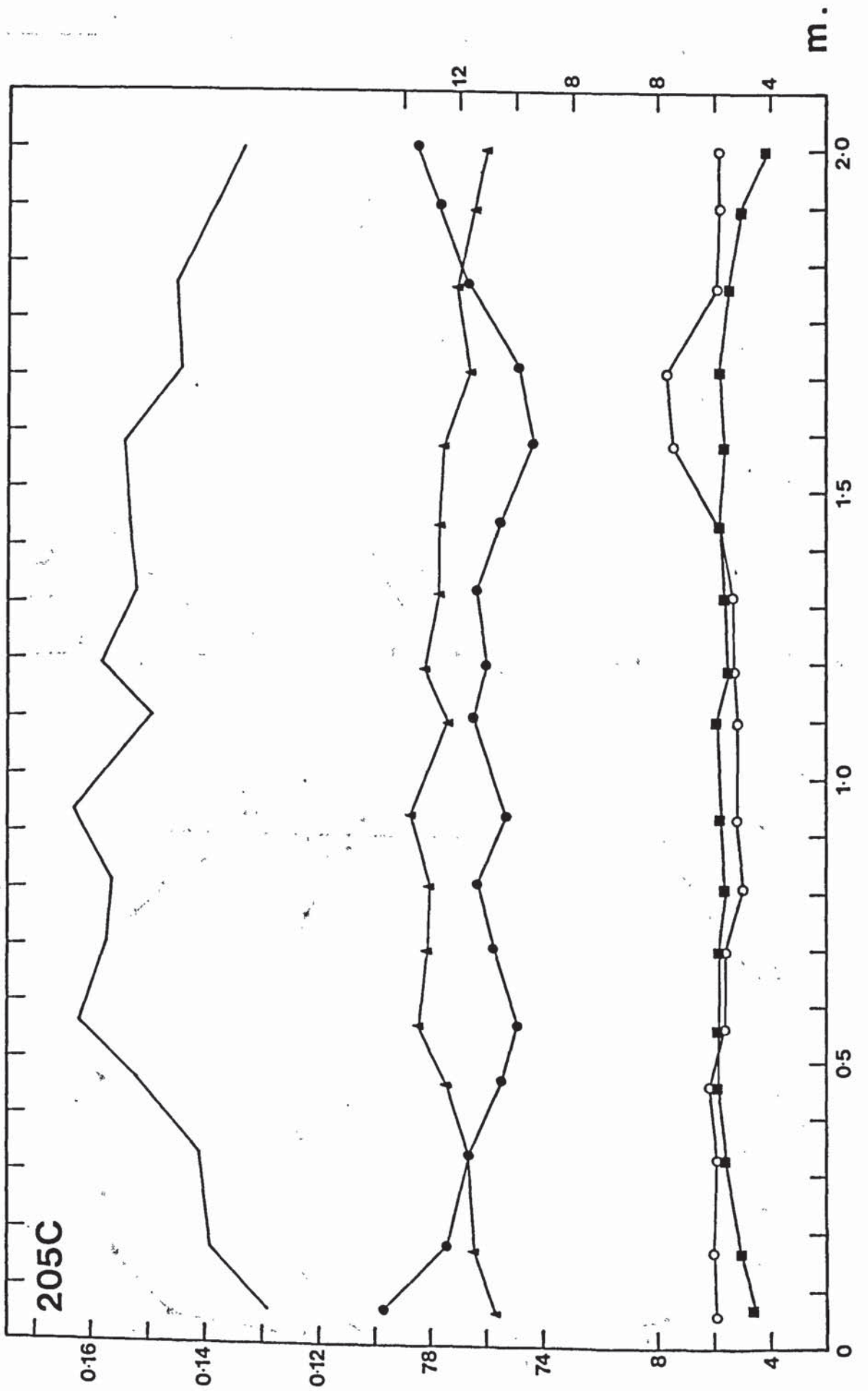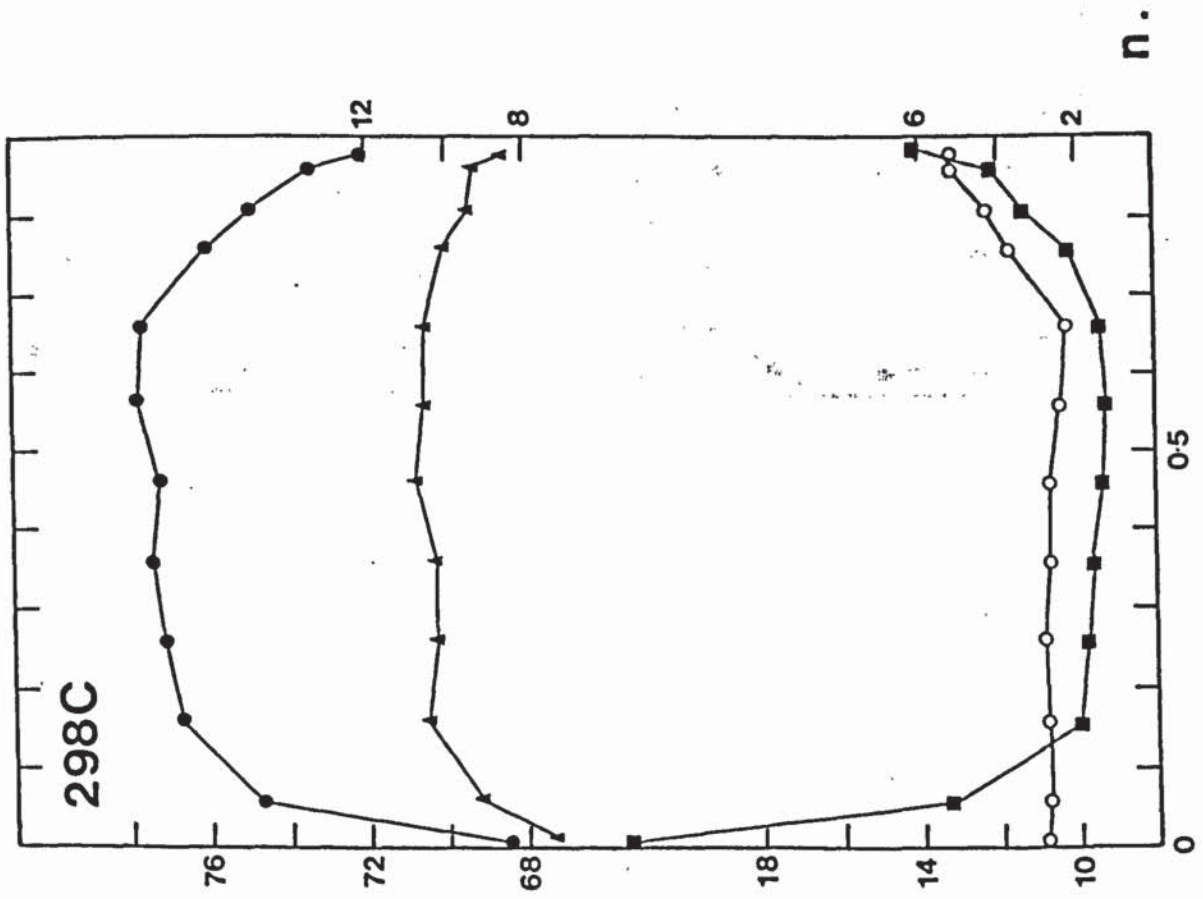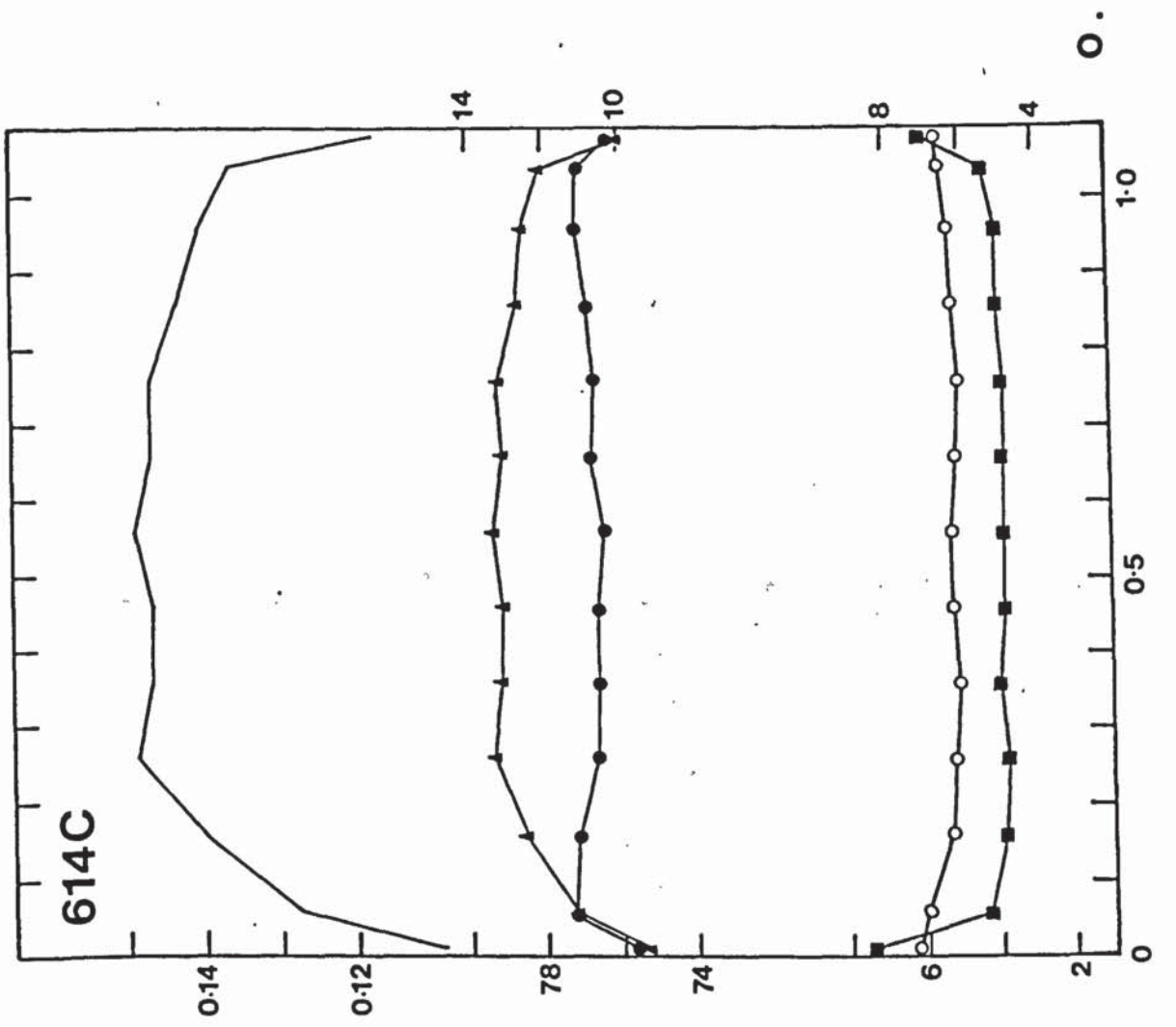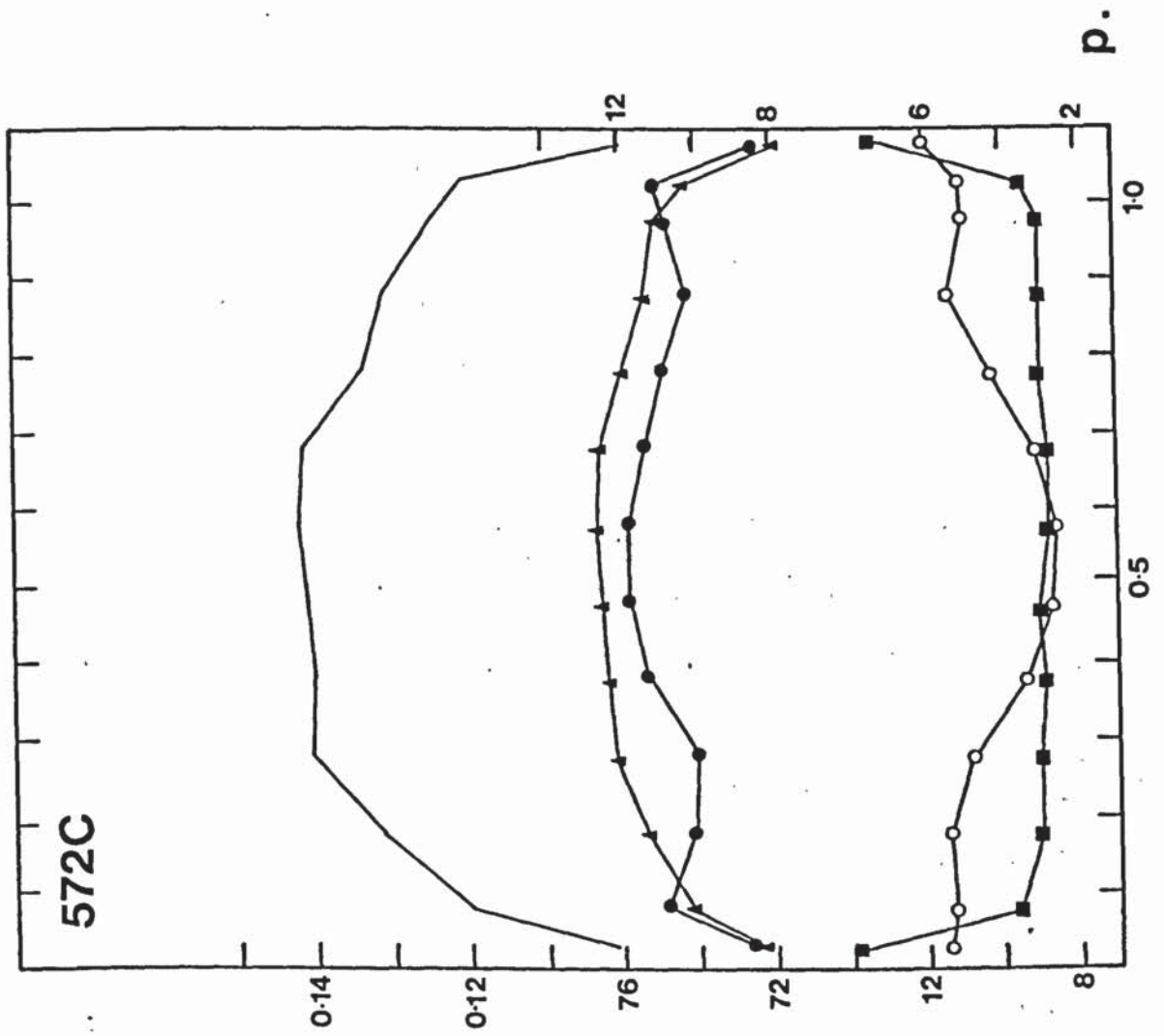
Fe increases from core to rim while Mg decreases. This is due to the low overall Mn content of this garnet and similar profiles have been described by Grant & Weiblen (1971), Loomis (1975) and Hollister (1977) from high-grade, Mn-poor garnets. The Mg/(Mg + Fe) profile is similar to those seen in garnets sampled from the Glenfinnan Division.

Garnets from the regional sillimanite zone show a variety of profiles. A41, A91 and 298C all show similar profiles to those described in the aureole. However, there is some variation in the Ca profiles. In A41 Ca drops near the rim. In A91 and, to a greater extent, 298C, it increases. 614C has a similar profile to 298C with Ca again increasing, along with Mn, at the rim. Fe differs slightly, increasing from the core to a point near the rim, before decreasing at the rim itself.

572C shows a distinctive profile. Mg decreases from core to rim while Mn increases. Fe decreases from an inner core to a distinct outer core, increasing slightly towards the rim. It decreases at the rim itself. Ca has a mirror image of the Fe profile. Overall, it bears a striking resemblance to a profile figured by Anderson & Olimpio (1977, Fig. 5) from a garnet in the kyanite zone, east of Lochailort.

205C differs from the other profiles illustrated in that Mn decreases from core to rim. Fe increases as a result. However, as in all the garnets investigated, the Mg/(Mg + Fe) ratio decreases to the rim.

2.5.3 Interpretation

The garnet profiles illustrated display zoning which is consistent with homogenisation by volume diffusion at high grade.

Zoning at the edge of grains is regarded as retrograde, superimposed on to homogenised, prograde profiles. Lower temperatures are indicated by Fe - Mg cation exchange geothermometers (Section 2.6.2) for garnet edges than for cores. As there is no petrographic evidence for a prograde reaction in which garnet is resorbed in favour of a more magnesium-rich phase (Hollister, 1977), marginal zoning affects garnet outside as well as inside the cordierite + K-feldspar zone and there is no obvious retrograde resorption reaction, such as replacement by chlorite (cf. de Bethune et.al., 1975), it is possible that retrograde concentration of Mn at garnet edges, as well as the decrease in Mg/(Mg + Fe), is due principally to ion exchange reactions (Yardley, 1977).

205C represents a locality distant from the granodiorite. Although the profile does not show an increase in Mn at the rim, Mg/(Mg + Fe) does decrease from core to rim. The sample lies just above the regional kyanite isograd, in the transition zone between low grade growth zoning profiles and high grade diffusion profiles reported by Anderson & Olimpio (1977), and represents a profile in which Mn, due to its low mobility, has not fully readjusted to high grade conditions. Fe and Mg however, are more mobile and retrograde exchange reactions have modified their rim compositions.

Core compositions from twenty analysed specimens (fig. 2.23) together with matrix biotite and plagioclase compositions, have been used to define the distribution measures $\ln K_D$ (gar-bio) and $\ln K$(gar-plag) where

$$K_D \text{ (gar-bio)} = (X_{Mg}^{gar}/X_{Fe}^{gar})/(X_{Mg}^{bio}/X_{Fe}^{bio})$$

and

$$K(gar\text{-}plag) = (X_{Ca}^{gar}/X_{Ca}^{plag})^3$$

(Table 2.5). Each of the samples contains the basic assemblage sillimanite + garnet + biotite + plagioclase + quartz (Table 2.3). Biotite and plagioclase compositions are based on the analysis of several grains, chosen at random, from within each sample section. Anorthite content of plagioclase was determined by optical methods or by electron probe partial analysis for Ca, Na and K. Little variation of either the Fe/Mg ratio of biotite or of the Ca content of plagioclase was found. In the regional garnet 572C, the Ca-rich outer core was used in the calculation.

In the cordierite + K-feldspar zone, K_D(gar-bio) values are closely grouped, though K(gar-plag) shows more scatter. Below the cordierite + K-feldspar zone there is scatter in both variables. The data, taken as a whole, define a trend in which the two K measures are correlated (fig. 2.22). The correlation (r = 0.560, n = 20) is significant at the 99% level.

The isotherms and isobars plotted on fig. 2.22 are not to be regarded as accurate (see sections 2.6.2 and 2.6.3).

The consistent values of lnK_D(gar-bio) from the cordierite + K-feldspar zone, at the high temperature end of the observed range, are interpreted as indicating that garnet cores, and matrix biotite, in this zone were homogenised with respect to Fe and Mg at high temperatures in the thermal event.

The observed, correlated trend in K_D(gar-bio) and K(gar-plag) can be interpreted in terms of two effects; incomplete prograde

TABLE 2.6

GARNET - BIOTITE AND GARNET - PLAGIOCLASE DISTRIBUTION MEASURES.

SAMPLE	ln K_D(gar-bio)	Plagioclase Composition	ln K(gar-plag)
A1	-1.269	0.29*	-6.19
A2	-1.337	0.23*	-6.89
A5	-1.318	0.25*	-5.75
A8	-1.306	0.24*	-6.56
A45	-1.309	0.25+	-6.20
A73	-1.320	0.24+	-6.70
A83	-1.209	0.25+	-6.23
270C	-1.292	0.25+	-5.28
A10	-1.394	0.25*	-4.37
A19	-1.330	0.29*	-5.88
A52	-1.413	0.26*	-6.15
A55	-1.246	0.25+	-6.48
A72	-1.320	0.25+	-4.52
A32	-1.279	0.19*	-5.95
402C	-1.416	0.26+	-4.96
A65	-1.501	0.23*	-4.84
205C	-1.440	0.30*	-5.26
298C	-1.347	0.24+	-6.60
572C	-1.533	0.28*	-4.93
614C	-1.327	0.37*	-5.32

[+] estimated by optical means

[*] electron microprobe partial analysis of Na, Ca and K.

FIGURE 2.22

Distribution of Fe/Mg with biotite and Ca with plagioclase for garnets in sillimanite-bearing assemblages.·

● - cordierite + K-feldspar zone;

+ - sillimanite + K-feldspar zone;

* - muscovite + sillimanite + K-feldspar zone;

x - regional sillimanite zone.

Estimated equilibrium isotherms and isobars are calculated from the work of Thompson (1976, Fig. 1B, assuming pressure - independence), and Schmid et.al. (1978) using activity coefficients of 1.276 for An in plagioclase (Orville, 1972) and 0.8 for grossular in garnet (Cressey et. al., 1978).

Heavy line is least - squares best fit to the data.
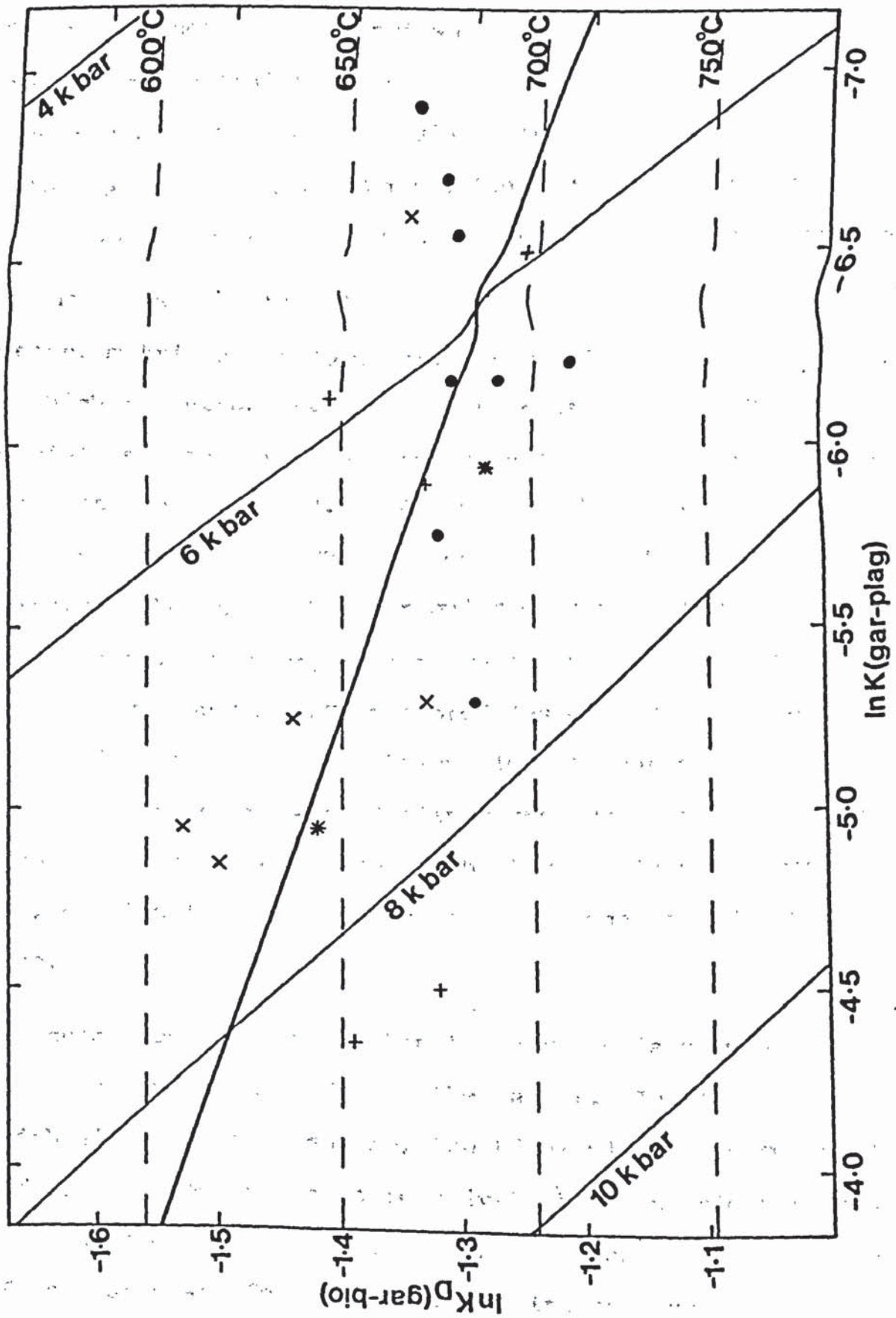
reaction, and temperature dependence of the activity coeff-
icients in the garnet-plagioclase equilibrium (Yardley et.al.,
1980; Section 2.6.3). Incomplete reaction would be expected
in samples taken at some distance from the granodiorite.
Clear evidence that garnet was not homogenised even by the
preceding regional metamorphism is provided by 572C. The
residual effect of early regional compositions can be
illustrated by considering the inner core of this garnet.
Calculations of K values from it are physically meaningless,
in that it was certainly not in reaction contact with the
present matrix assemblage, but gives a lower apparent pressure
and higher apparent temperature than using the outer core.
Partial reaction of such garnets undoubtedly contributes to
the trend in fig. 2.22. 614C and 298C both show high temp-
erature cores with lower apparent pressure than other regional
garnets. They also show irregular Ca zoning with Ca increasing
at the edge. This may well represent partial development of
the zoning seen in 572C, the profiles of 298C and 614C being
relict from the earliest, Grenville, metamorphism in the area.
The influence of pre-Caledonian garnet compositions may persist
into the aureole resulting in the low $\ln K_D$ (gar-bio) value for
A32, sampled from the muscovite + sillimanite + K-feldspar
zone.

Irregular zoning of Ca within the aureole is seen as a decrease
in Ca content at the edge of the garnet. In A10, A45 and 270C,
which all show this feature, the K(gar-plag) measure, taken
from core compositions, is relatively high and plots towards
the high pressure end of the trend in fig. 2.22. Calculation
of lnK(gar-plag) for the rim compositions gives lower apparent
pressure values. The Ca profiles do not appear to be the

product of retrograde reaction although they often coincide
with features in the Fe, Mg and Mn profiles which are certainly
retrograde in origin, as Ca does not take part in any of the
retrograde exchange reactions involving these cations. In
270C Fe zoning mirrors the Ca profile, however the $\ln K_D$ (gar-
bio) value is consistent with other cordierite + K-feldspar
zone samples, and the Mg/(Mg + Fe) profile reveals a smooth
curve, dropping to the rim. It is apparent that, although
re-equilibration of Fe, Mg and Mn profiles is complete in the
cordierite + K-feldspar zone, Ca compositions characteristic
of regional assemblages may persist in garnet cores. Full
equilibration, and therefore low $\ln K$ (gar-plag) values for
garnet cores, has occurred where no zoning of Ca is seen.

2.6 P-T-X RELATIONS

2.6.1 Introduction

The composition of minerals in twenty three samples from both
aureole and regional assemblages have been investigated using
an electron microprobe (fig. 2.23 and Appendix II). In each
sample garnet and biotite were analysed (Appendix II, Tables
1 & 2). Muscovite analyses are presented from seventeen
samples, as well as cordierite analyses from two samples.
(Appendix II, Tables 3 & 4). Plagioclase compositions were
estimated by optical means (Table 2.6) or by partial electron
probe analysis for Na, Ca and K. (Appendix II, Table 5).
K-feldspar compositions in four samples were estimated from
partial analyses for Na, Ca, K and Ba. (Appendix II, Table 6).

The physical conditions of metamorphism have been estimated
using these analyses in conjunction with published calibrations,
both experimental and theoretical, of observed equilibria in

118

Location of specimens used for electron microprobe
analysis.

the rocks. Such calibrations are based on the equation whereby for a reaction at equilibrium

$$(\Delta G^O)_{P,T} = 0 = -RT\ln K = \Delta H_{1,T} - T\Delta S^O_T + (P-1)\Delta V^O_S \qquad (5)$$

(Wood & Fraser, 1977, p.91 & 92). The standard states of components are taken to be the pure phases at the pressure and temperature of interest.

The following notation is used throughout.

A. Phases

gar	garnet
bio	biotite
crd	cordierite
musc	muscovite
plag	plagioclase
ksp	K-feldspar
qtz	quartz

B. Thermodynamic Parameters

T	temperature (K unless otherwise specified)
P, P_{TOTAL}	lithostatic pressure (bars)
P_{H_2O}, P_{CO_2} etc.	partial fluid pressures (bars)
f_{H_2O}, f_{CO_2} etc.	fugacities (bars)
x^j_i	mole fraction of component i in phase j
γ^j_i	activity coefficient of component i in phase j
a^j_i	activity of component $i (=x^j_i \gamma^j_i)$
K	equilibrium constant a(products)/a(reactants)
K_D	distribution coefficient

With the standard states at the P and T of interest.

$(\Delta G)_{P,T}$	change in Gibbs free energy of reaction
$\Delta H_{1,T}$	change in enthalpy of reaction
ΔS^O_T	change in entropy of reaction
ΔV^O_S	change in volume (solids) of reaction

121

$$\Delta V_{H_2O} \qquad \text{change in volume } (H_2O) \text{ of reaction}$$

$$R \qquad \text{universal gas constant.}$$

2.6.2 Geothermometry

The cation exchange reactions

$$\tfrac{1}{3}Fe_3Al_2Si_3O_{12} + \tfrac{1}{2}Mg_2Al_4Si_5O_{18} = \tfrac{1}{3}Mg_3Al_2Si_3O_{12} + \tfrac{1}{2}Fe_2Al_4Si_5O_{18} \quad (6)$$

Fe-garnet   Mg-cordierite Mg-garnet   Fe-cordierite

and

$$\tfrac{1}{3}Fe_3Al_2Si_3O_{12} + \tfrac{1}{3}KMg_3AlSi_3O_{10}(OH)_2$$

Fe-garnet   Mg-biotite

$$= \tfrac{1}{3}Mg_3Al_2Si_3O_{12} + \tfrac{1}{3}KFe_3AlSi_3O_{10}(OH)_2 \quad (7)$$

Mg-garnet   Fe-biotite
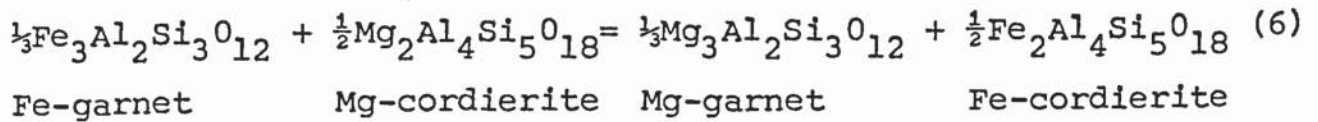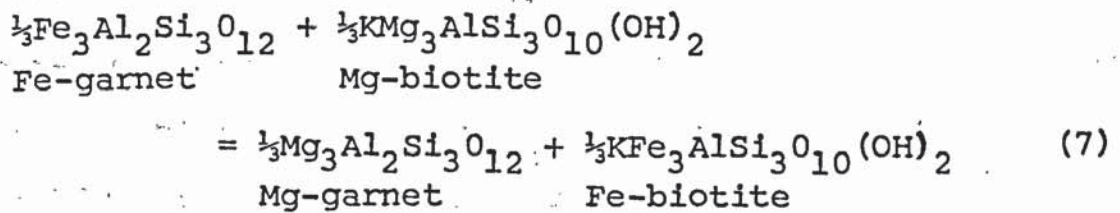
involve only small changes in volume. As a result their
univariant reaction boundaries in P and T space lie almost
parallel to the pressure axis, making them excellent potential
geothermometers (Wood & Fraser, 1977). The distribution
coefficients, K_D(gar-crd) and K_D(gar-bio), are defined by

$$K_D(\text{gar-crd}) = (X_{Mg}^{gar}/X_{Fe}^{gar})/(X_{Mg}^{crd}/X_{Fe}^{crd})$$

and

$$K_D(\text{gar-bio}) = (X_{Mg}^{gar}/X_{Fe}^{gar})/(X_{Mg}^{bio}/X_{Fe}^{bio})$$

They may be related to temperature by rearranging equation (5)
so that

$$T = \frac{\Delta H_{1,T} + (P-1)\Delta V_S^o}{\Delta S_T^o - R\ln K_D}$$

An ideal solid solution model is assumed for each of the
phases.

Reaction (6) has been calibrated by Currie(1971) using K_D
data obtained from experimental investigation of reaction (3).

122

A decrease in K_D was indicated with increasing T. This is at variance with later calibrations and has been attributed to errors in the determination of the composition of the experimental run products, and also to very short run times with equilibrium not being achieved as a consequence (Holdaway & Lee, 1977).

Both reactions have been calibrated by Thompson (1976b) using an essentially empirical method. Values of $\ln K_D$ (gar-crd) and $\ln K_D$ (gar-bio) were obtained from adjacent garnet - cordierite and garnet - biotite pairs in natural assemblages from various metamorphic terrains where the equilibrium temperature had been estimated independently. Garnet and cordierite rim compositions were used at low temperatures. At higher temperatures, above 600°C, core compositions were used. The calibrations shown in fig. 1 of Thompson (1976b, p.429) are each based on four data points and calculated temperatures have an error of $\pm$ 50°C. Relative differences in temperature may be regarded as reasonably accurate. The equilibria are defined by

$$T = \frac{-2690}{\ln K_D - 0.87} \qquad (9)$$

for garnet - cordierite, and

$$T = \frac{-2880}{\ln K_D - 1.72} \qquad (10)$$

for garnet - biotite. Both are assumed to be independent of pressure.

The thermometers have received some adjustment to the low temperature end of the calibrations. Holdaway & Lee (1977) prefer an equilibrium temperature of 530°C for the data of Osberg (1971), estimated at 500°C by Thompson (1976b). The revised geothermometers, which may be derived from

123

equation (7) and Table (7) of Holdaway & Lee (1977, p.190),
also contain a correction for pressure. The adjusted curves
are defined by

$$T = \frac{-3095-0.0152(P-1)}{\ln K_D - 1.35} \qquad (11)$$

for garnet - cordierite, and

$$T = \frac{-3095-0.0124(P-1)}{\ln K_D - 1.98} \qquad (12)$$

for garnet - biotite.

The garnet - biotite geothermometer has been calibrated
experimentally by Ferry & Spear (1978). Again a correction
for pressure has been included, and the reaction is defined by

$$T = \frac{-2089-0.01(P-1)}{\ln K_D - 0.782} \qquad (13)$$

Table 2.7 sets out the results for the anlysed garnet - cord-
ierite and garnet - biotite pairs. One garnet - biotite pair
and two garnet - cordierite pairs are taken from analyses given
by Ashworth & Chinner (1978). Core compositions were used for
garnet and cordierite. The averaged composition of several
matrix grains was used for biotite. Where a pressure correc-
tion is included, the preferred aureole pressure of 4.1 kbars
is used. For rocks lying outside the aureole, an approximate
estimate of 6.0 kbars is used (Section 2.6.3).

The calibrations of Thompson (1976b) and Holdaway & Lee (1977)
give similar results at high grade. In the cordierite + K-feld-
spar zone temperatures range from $676^{\circ}C$ to $710^{\circ}C$ for Holdaway
& Lee's(1977) calibrations, averaging $686^{\circ}C$ ($\sigma=10$) for nine
garnet - biotite pairs, and $691^{\circ}C$ ($\sigma=8$) for four garnet -
cordierite pairs.

124

TABLE 2.7

TEMPERATURE ESTIMATES (^{O}C)

CORDIERITE + K-FELDSPAR ZONE

SAMPLE	Garnet - biotite				Garnet - cordierite		
	lnK_D	(a)	(b)	(c)	lnK_D	(a)	(b)
A1	-1.269	690	694	794			
A2	-1.337	669	676	731	-1.957	678	682
A5	-1.318	675	681	740			
A8	-1.306	679	684	746			
A45	-1.309	678	683	744			
A73	-1.320	674	681	739			
A83	-1.209	710	710	795			
270C	-1.292	683	688	753	-1.984	670	681
193C (d)	-1.320	674	681	740	-1.810	690	692
196C (d)					-1.812	701	701
Average		681	686	750		685	691
σ		12	10	19		14	8

SILLIMANITE + K-FELDSPAR ZONE

SAMPLE	Garnet - biotite			
	lnK_D	(a)	(b)	(c)
A10	-1.394	652	662	704
A19	-1.330	671	678	734
A52	-1.413	646	657	696
A55	-1.246	698	700	776
A72	-1.320	674	681	739
356C	-1.388	654	663	707
Average		666	674	726
σ		19	16	30

2.7 (continued).

MUSCOVITE + SILLIMANITE + K-FELDSPAR ZONE

SAMPLE	Garnet - biotite $\ln K_D$	(a)	(b)	(c)
A32	-1.279	687	693	759
402C	-1.416	645	654	707

REGIONAL SILLIMANITE ZONE

SAMPLE	Garnet - biotite $\ln K_D$	(a)	(b)	(c)
A41	-1.506	620	634	657
A65	-1.501	621	636	659
A91	-1.437	639	651	686
205C	-1.440	638	650	684
298C	-1.347	666	674	726
572C	-1.533	612	628	646
614C	-1.327	672	671	736
Average (e)		626	640	666
σ		12	10	18

(a) Thompson (1976b)

(b) Holdaway & Lee (1977)

(c) Ferry & Spear (1978)

(d) Analyses from Ashworth & Chinner (1978)

(e) Does not include 298C or 614C.

126

The garnet - biotite thermometer should be expected to give slightly lower temperatures than garnet - cordierite, as biotite, which does not preserve earlier compositions as internal zones, has been involved in retrograde exchange reactions. However, as biotite usually makes up some 20 - 30 modal percent of the rocks analysed, and garnet is relatively scarce (1%), it tends to act as an almost infinite reservoir so that a substantial increase in the Fe/Mg ratio due to retrograde reaction with garnet is unlikely (Tracy et.al., 1976).

In the sillimanite + K-feldspar zone, the garnet - biotite thermometers start to diverge. The Thompson (1976b) temperatures range from $646^{\circ}C$ to $698^{\circ}C$, averaging $666^{\circ}C$ (σ=19). The range for Holdaway & Lee (1977) is narrower, $657^{\circ}C$ to $700^{\circ}C$, averaging $674^{\circ}C$ (σ=16). The larger values of standard deviation in this zone than in the cordierite + K-feldspar zone are a further illustration of the re-equilibration trend recognised in fig. 2.22.

Two garnet - biotite pairs were analysed in the muscovite + sillimanite + K-feldspar zone. 402C gives a temperature of $656^{\circ}C$ (Holdaway & Lee, 1977) while A32, by contrast, gives an anomalously high temperature of $691^{\circ}C$ considering its position just above the sillimanite + K-feldspar isograd. It may well represent, as suggested in Section 2.5.3, partial re-equilibration of a garnet core composition relict from Precambrian rather than Caledonian, metamorphism of these rocks.

In the regional sillimanite zone estimates for 298C and 614C are anomalously high compared with the others, and are also regarded as representing early, Precambrian, garnet core compositions. The five remaining garnet - biotite pairs range

127

from 628°C to 651°C, averaging 640°C (σ=10) estimated from the Holdaway & Lee (1977) calibration. The estimate for 572C is taken from its outer core (fig. 2.21).

Estimates obtained from the Thompson (1975b) thermometers are lower than those obtained from Holdaway & Lee (1977). As may be expected these differences become greater at lower temperatures. In the regional sillimanite zone it may be as much as 15°C, whereas results for the cordierite + K-feldspar zone show only minor differences. The preferred calibration is that of Holdaway & Lee (1977), particularly in view of the pressure correction which can increase estimates by some 10° - 20°C.

Estimates obtained from the calibration of Ferry & Spear (1978) are considerably higher than those obtained from Holdaway & Lee (1977). The difference increases with increasing grade. This is probably due to the compositional complexities of natural biotites compared with the Al and Fe^{3+} poor synthetic biotites used (Grew, 1981; Yardley et.al., 1980). It should be noted that the $(Al^{vi} + Ti)/(Al^{iv} + Ti + Fe + Mg)$ ratios of the biotites analysed in this study are in excess of the limit of 0.15 set by Ferry & Spear (1978) for which their calibration may be used without correction for components other than Fe and Mg.

The temperatures of about 690°C, estimated from Holdaway & Lee (1977), for the cordierite + K-feldspar zone are regarded as more realistic than the average of 750°C (σ=19) estimated from Ferry & Spear (1978), particularly as the granodiorite magma was a partially crystalline mush at the time of its intrusion (Munro, 1965). The lower temperatures are also

consistent with the observed dehydration equilibria (Section 2.6.4)). However it should not be forgotten that, as pointed out by Yardley et.al. (1980), by its very nature the empirical calibration of Thompson (1976b) is bound to reinforce pre-existing predjudices about probable metamorphic temperatures.

2.6.3   Geobarometry

2.6.3   (i)   Garnet - cordierite equilibria

Garnet - cordierite coexistence within the aureole is signif-icant as the reaction

$$3 \text{ cordierite} = 2 \text{ garnet} + 4 \text{ sillimanite} + 5 \text{ quartz} \qquad (3)$$
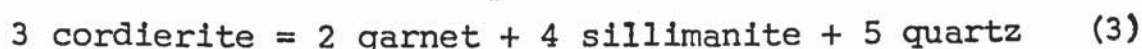
has received considerable attention as a potential geobarometer. In contrast to reactions (6) and (7) this reaction has a rela-tively large ΔV_s^o and may therefore provide a good geobarometer with the reaction boundary lying nearly parallel to the temp-erature axis. There has been disagreement over the slopes of the Fe and Mg end member reactions.

Currie's (1971) results indicated a negative slope for the Fe - end member reaction, occurring at lower pressure than the metastable Mg - end member, which had a positive slope. Doubt has been cast on this calibration in view of the decrease in K_D(gar-crd) with increasing T, which it indicates.

The experimental calibration of Hensen & Green (1973) indicated negative slopes for both end - member reactions. Results for the four garnet - cordierite pairs give pressures of about 7 kbars at 700^oC, too high for an aureole in which andalusite grew at an early stage. The attitude of the lines of equal garnet composition result in an increase in K_D(gar-crd) with T, in line with the preferred calibrations of reaction (6).

Hutcheon et. al. (1974) calibrated the reaction using available thermodynamic data. Positive slopes for each end - member reaction were obtained. Estimated temperatures and pressures are low, with conditions of 550°C at about 4 kbars indicated.

The theoretical calibration of Thompson (1976b) combines thermodynamic data with K_D(gar-crd) values obtained from his own calibration of exchange reaction (7). Calculated temperatures are therefore in the range 680°C-700°C at pressures of about 4.9 kbars. Tracy et.al. (1976) give a correction for the Mn content of garnet, resulting in pressures of about 4.7 kbars (Table 2.8).

All of the above calibrations have assumed cordierite to be anhydrous. However cordierite does contain water within its structure and variations in P_{H_2O} may have a considerable influence on values of K_D(gar-crd) (Wood, 1973). Holdaway & Lee (1977) have attempted to calibrate K_D(gar-crd) in terms not just of T and P, but also in terms of P_{H_2O}.

Two Fe end - member reactions were investigated experimentally.

1.26 Fe-cordierite + 0.84 K-feldspar + $(1-1.26n)H_2O$

= 1 Fe biotite + 2.08 sillimanite + 4 quartz   (14)

and

3 Fe-cordierite

= 2 Fe-garnet + 4 sillimanite + 5 quartz + $3nH_2O$ (15)
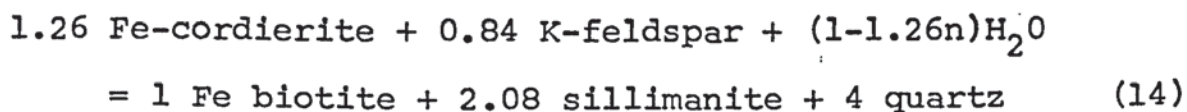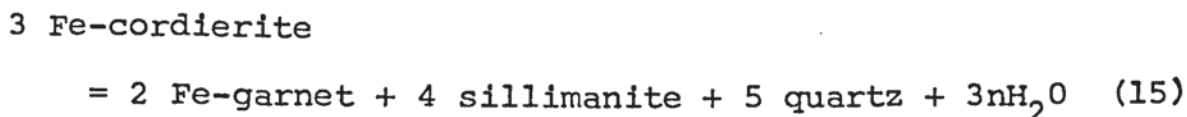
n is the molar water content of cordierite. The biotite composition was synthesised to correspond to that found by Guidotti et.al. (1975), so as to minimise the effect of Al content on the Fe-Mg ratio.

Compositions of coexisting cordierite - biotite and cordierite - garnet from available experimental data for reactions (14)

130

TABLE 2.8

PRESSURE ESTIMATES (bars)

SAMPLE	(a)	(b)	X_{H_2O} (b)
A2	4810	4040	0.46
270C	4600	4080	0.58
193C	4700	4135	0.46
196C	4700	4190	0.60

(a) Tracy et. al (1976)

(b) Holdaway & Lee (1977).

and (15), together with K_D data from natural assemblages were calibrated against P and T using the reaction.

$$\Delta P \Delta V = -RT \ln \frac{X^a_{Fe} \text{ (products)}}{X^a_{Fe} \text{ (reactants)}} \qquad (16)$$

given by Thompson (1976b). Again an ideal solid solution model has been assumed. ΔP is the change in pressure from the Fe end - member reaction to the P indicated by the K_D value, at the T of interest. The ΔV term is a combination of ΔV^o_s and ΔV_{H_2O}. The exponents a and b refer to the site occupancy of the cations. V_{H_2O} was calculated using n estimated from fig. 5 of Holdaway & Lee (1977, p.187) at the T of interest with f_{H_2O} and V_{H_2O} data taken from Burnham et.al. (1969), and averaged over the approximate P involved. P - T diagrams were constructed for the Fe-Mg divariant fields for both reactions at $P_{H_2O} = P_{TOTAL}$ (Holdaway & Lee, 1977; fig.6, p.192 & fig. 7A, p.194). The intersection of these fields define reaction (2).

Diagrams similar to 7A (Holdaway & Lee, 1977, p.194) may be constructed for reduced values of P_{H_2O}, for dilution of almandine - pyrope garnet by grossular and spessartine, and for dilution of K-feldspar by albite using the reactions

$$(Pf-Pi) \Delta V^o_s + (X_{H_2O}Pf - Pi) \Delta \bar{V}_{H_2O} = 0.84RT\ln X^{ksp}_K \qquad (17)$$

for reaction (14), and

$$(Pf-Pi) \Delta V^o_s + (X_{H_2O}Pf - Pi) \Delta \bar{V}_{H_2O} = -6RT\ln X^{gar}_{Fe-Mg} \qquad (18)$$

for reaction (15). Pi is the pressure indicated by the K_D values at the T of interest when $P_{H_2O} = P_{TOTAL}$; Pf is the total pressure at the reduced water pressure. $\Delta \bar{V}_{H_2O}$

is the averaged V_{H_2O} over the ΔP from Pi to an approximate Pf. Calculated P - T diagrams for $X_{H_2O} = 0.8$, $X_{H_2O} = 0.6$ and $X_{H_2O} = 0.4$ are given in Lee & Holdaway (1977, p.86-87).

Pf and X_{H_2O} have been estimated from the four analysed garnet - cordierite pairs, using temperatures from the garnet - cordierite thermometer. Results give pressures between 4.04 kbars and 4.19 kbars, averaging 4.1 kbars. X_{H_2O} ranges between 0.46 and 0.60, averaging 0.53. The results given by Ashworth & Chinner (1978) contained a numerical error giving slightly high values for P and X_{H_2O}; they have been corrected in the present study (Table 2.8).

Newton & Wood (1979) have also investigated the effects of water in cordierite on reaction (3). Whereas Holdaway & Lee (1977) considered only the effect on ΔV of the reaction, the effect on ΔS has also been allowed for and the resulting Fe-Mg divariant field modelled. In a completely dry system ($P_{H_2O}=0$) both the Fe and Mg end - member reactions show positive slopes. Mg-poor compositions show negative slopes at high temperature with increasing P_{H_2O}. Lines of equal Mg content for both phases are parallel and, as a result, K_D(gar-crd) is interpreted as being virtually independent of T, P, and P_{H_2O}. These results are significantly different from those of Thompson (1976b) and Holdaway & Lee (1977) based on natural assemblages, and are in much better agreement with the curves predicted by Hutcheon et.al. (1974). However, there are considerable differences between values of K_D(gar-crd) found in natural assemblages, and those predicted by Newton & Wood (1979). This is suggested to be the result of non-ideal solid solution behaviour in both garnet and cordierite.

Using activity coefficients calculated with the regular solution parameter, W, of 1.7 kcals recommended by Newton & Wood (1979), a pressure of 4.0 kbars from Hutcheon et.al. (1974) and a temperature of 690°C, an estimated P_{H_2O} of 3.5 kbars was obtained. A version of equation (10) of Newton & Wood (1979) for the Fe end - member reaction, and their equation (3) for the hydration state of cordierite were used to make this estimate.

Until there is more accurate information concerning solid solution models for garnet and cordierite, the calibration of Holdaway & Lee (1977), using natural K_D(gar-crd) values, must be regarded as the best available. Therefore a P of 4.1 kbars with X_{H_2O} at 0.53 is the preferred estimate.

2.6.3 (ii) Garnet - plagioclase Equilibria

The equilibrium distribution of Ca between garnet and plagioclase is controlled by the reaction

$$3CaAl_2Si_2O_8 = Ca_3Al_2Si_3O_{12} + 2Al_2SiO_5 + SiO_2 \qquad (19)$$
in plagioclase   in garnet   sillimanite   quartz.
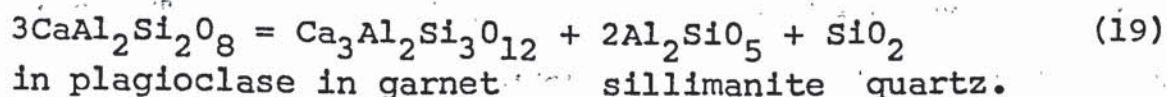
If temperature is estimated independently, this equilibrium may be used as a geobarometer (Ghent, 1976). The equilibrium constant K(gar-plag) has been defined in Section 2.5.3 and values from twenty specimens containing the assemblage plagioclase - garnet - sillimanite - quartz are given in Table 2.6. The reaction

Anorthite = grossular + kyanite + quartz   (20)

has been investigated experimentally by Schmid et.al. (1978). Yardley et.al. (1980) have combined this with data for sillimanite from Holdaway (1971) to obtain an equation for reaction (19) such that

134

$$\ln K_D(\text{gar-plag}) = -15.10 + \frac{3061}{T} + \frac{0.6565(P-1)}{T} + 3\ln \frac{\gamma_{Ca}^{plag}}{\gamma_{Ca}^{gar}} \quad (21)$$

The isobars shown of fig. 2.22 are calculated from equation (21) using γ_{Ca}^{plag} of 1.276, taken from Orville (1972), and γ_{Ca}^{gar} of 0.8, taken from Cressey et.al. (1978). A non-ideal solid solution model is assumed for both phases due to their restricted Ca end - member contents.

The trend identified in fig. 2.22 has been interpreted as indicating an approach to equilibrium in the aureole with increasing T, at a nearly constant P. The apparently poly-baric trend indicated by the isobars does not contradict this since it may result from changes in the activity coefficients of the grossular and anorthite components with temperature. Yardley et.al. (1980) suggest that these solid solutions may deviate strongly from ideality with decreasing T, causing true isobars on a diagram such as fig. 2.22 to be convex upwards. The P - T grid on fig. 2.22 is therefore not a rel-iable indicator of P and the observed trend is determined by an approach to equilibrium dependent almost wholly on T. The pressures calculated using the simple solution model with equation (21) are certainly wrong for the aureole, being too high compared with pressures based on garnet - cordierite compositions, interpreted as fully equilibrated to cordierite + K-feldspar zone conditions. The activity coefficient ratio $\gamma_{Ca}^{plag}/\gamma_{Ca}^{gar}$ may be calculated using preferred Fe - Mg estim-ates: P = 4.1 kbars and T = 690°C for the cordierite + K-feld-spar zone and T = 630°C for the sillimanite + K-feldspar iso-grad. These give values of 2.5 and 3.4, similar to those used by Yardley et.al. (1980) to reconcile their data with the Al_2SiO_5 phase diagram.

2.6.3 (iii) Regional Pressures

Estimation of pressures from regional assemblages is hampered by the lack of suitable equilibria. Until data are available concerning activity coefficients for grossular in garnet and anorthite in plagioclase at temperatures below 700°C, garnet - plagioclase barometry is unreliable.

An estimate of pressure can be made if an equilibrium tempearature for the reaction

$$kyanite = sillimanite \qquad (22)$$
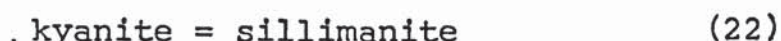
is known. Fig. 2.3 shows the position of the regional kyanite - sillimanite isograd in Moidart and Sunart; based on Al_2SiO_5 occurrences from Howkins (1961), and from the present study. As mentioned in Section 2.3.3 this lies 1km to the west of the calc-silicate anorthite + pyroxene isograd in Moidart. Kennedy (1949) and Winchester (1974) both indicate that this isograd then trends southeastwards, towards the granodiorite. Sillimanite occurrences noted during the present study and by Marsh (pers. comm.) indicate that the kyanite - sillimanite isograd continues southwards, reaching the shores of Loch Sunart immediately west of Resipole.

No temperature estimates are available for the kyanite zone. However 205C lies immediately to the east of the isograd and may give a maximum temperature for reaction (22). This temperature estimate must be regarded with a degree of uncertainty in view of the trend illustrated in fig. 2.22, indicating some modification of the Fe - Mg composition by the Strontian aureole.

Anderson & Olimpio (1977) have shown that Caledonian re-homogenisation of garnet begins to take place in the kyanite zone

136

in Morar. Temperature estimates from the outer core of 572C
suggests a starting temperature of approximately 630°C for
this process. If it can be regarded as pressure independent,
the temperature will give a minimum pressure for the kyanite
zone in Morar of 6.3 kbars, calculated from the data of
Holdaway (1971) for reaction (22), such that

$$P = \frac{2.807T - 1650}{0.139} + 1 \qquad (23)$$

The temperature estimate of 630°C for 572C, which lies well
within the sillimanite zone, suggests lower pressures for
Caledonian metamorphism in Sunart than in Morar, allowing
reaction (22) to take place at lower T. The minimum P
estimate for the kyanite zone in Morar of 6.3 kbars therefore
represents a maximum estimate for the Sunart Moines.

2.6.4 Muscovite - Feldspar Equilibria

2.6.4 (i) Muscovite - plagioclase

The paragonite content of muscovite is largely dependent on
temperature (Guidotti & Sassi, 1976). The reaction

K,Na-muscovite+quartz = sillimanite+albite+K-muscovite+H_2O, (24)
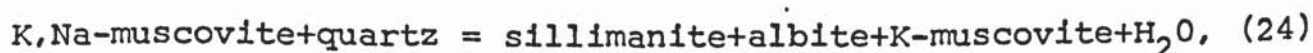
results in muscovite enriched in K, combined with an increase
in the Na content of plagioclase with increasing T. This
trend may be used as a qualitative geothermometer (Guidotti
& Sassi, 1976, fig.7 p.118).

In the Strontian aureole, $Na/(Na + K)$ ratios from adjacent
zones show considerable overlap as may be seen from the
seventeen muscovite analyses presented in Appendix II (Table
3). Of these, three were obtained from samples which do not
contain sillimanite. Table 2.9 sets out the ratios from the
remaining 14 samples. Those within the aureole give values
indicating sillimanite + K-feldspar conditions. The five

137

TABLE 2.9

MUSCOVITE - PLAGIOCLASE COMPOSITIONS

ZONE	SAMPLE	X_{Na}^{mus}	X_{Na}^{plag}	K-FELDSPAR
CRD+KSP	A2	0.069	0.77	X
	A5	0.067	0.75	X
	A8	0.089	0.76	X
	A83	0.065	0.75	X
SILL+KSP	A10	0.038	0.74	X
	A19	0.084	0.71	X
	A55	0.068	0.75	X
MUS+SILL+KSP	A32	0.073	0.81	
	402C	0.086	0.74	X
REG. SILL	A65	0.058	0.63	
	205C	0.121	0.77	
	298C	0.065	0.70	
	572C	0.104	0.76	
	614C	0.078	0.72	

analyses from the regional sillimanite zone are consistent with sillimanite grade conditions, those with low Na/(Na + K) coexist with calcic plagioclase. This is reflected in the trend recognised for the five sillimanite zone samples (r=0.85, n=5), significant at the 99% level in fig. 2.24. No relationship is seen for samples within the aureole.

The trend recognised at low grade results from partitioning of Na between muscovite and plagioclase, controlled by reaction (24). Fig. 3 of Cheney & Guidotti (1979, p.425) shows a similar relationship for the sillimanite zone at Puzzle Mountain, northwest Maine. The lack of correlation for samples within the aureole may be due to several factors. Firstly, all muscovite analysed in the sillimanite + K-feldspar zone and cordierite + K-feldspar zones is regarded as secondary in origin, produced by retrogression of reaction (1). As these muscovites have high grade Na/(Na +K) ratios, the retrograde reaction is presumed to have occurred at high grade. This phenomenon has also been reported by Ashworth (1975) for the Huntly-Portsoy aureole. Data used by Cheney & Guidotti (1979), which includes analyses from Evans & Guidotti (1966), were all obtained from primary muscovites in assemblages similar to those found in the muscovite + sillimanite + K-feldspar zone at Strontian. Secondly, the reaction recognised by Evans & Guidotti (1966) and Cheney & Guidotti (1979) as controlling the sillimanite + K-feldspar isograd is

muscovite + plagioclase + quartz

$$= \text{sillimanite} + \text{alkali feldspar} + H_2O \qquad (25)$$
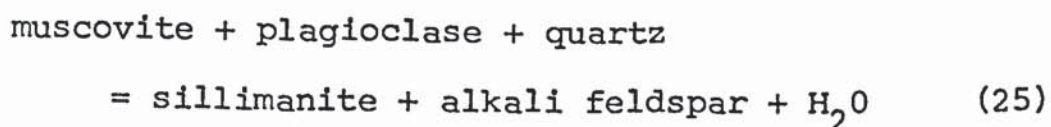
which differs from the approximation in use at Strontian. Reaction (1) is preferred due to the almost identical Na/(Na + K) ratios of muscovite and K-feldspar in equilibrium in

Plot of X_{Na}^{mus} against X_{Na}^{plag} for sillimanite-bearing assemblages.

● - cordierite + K-feldspar zone;

+ - sillimanite + K-feldspar zone;

* - muscovite + sillimanite + K-feldspar zone;

x - regional sillimanite zone.

Solid line: least - squares best fit to the five regional sillimanite zone specimens.
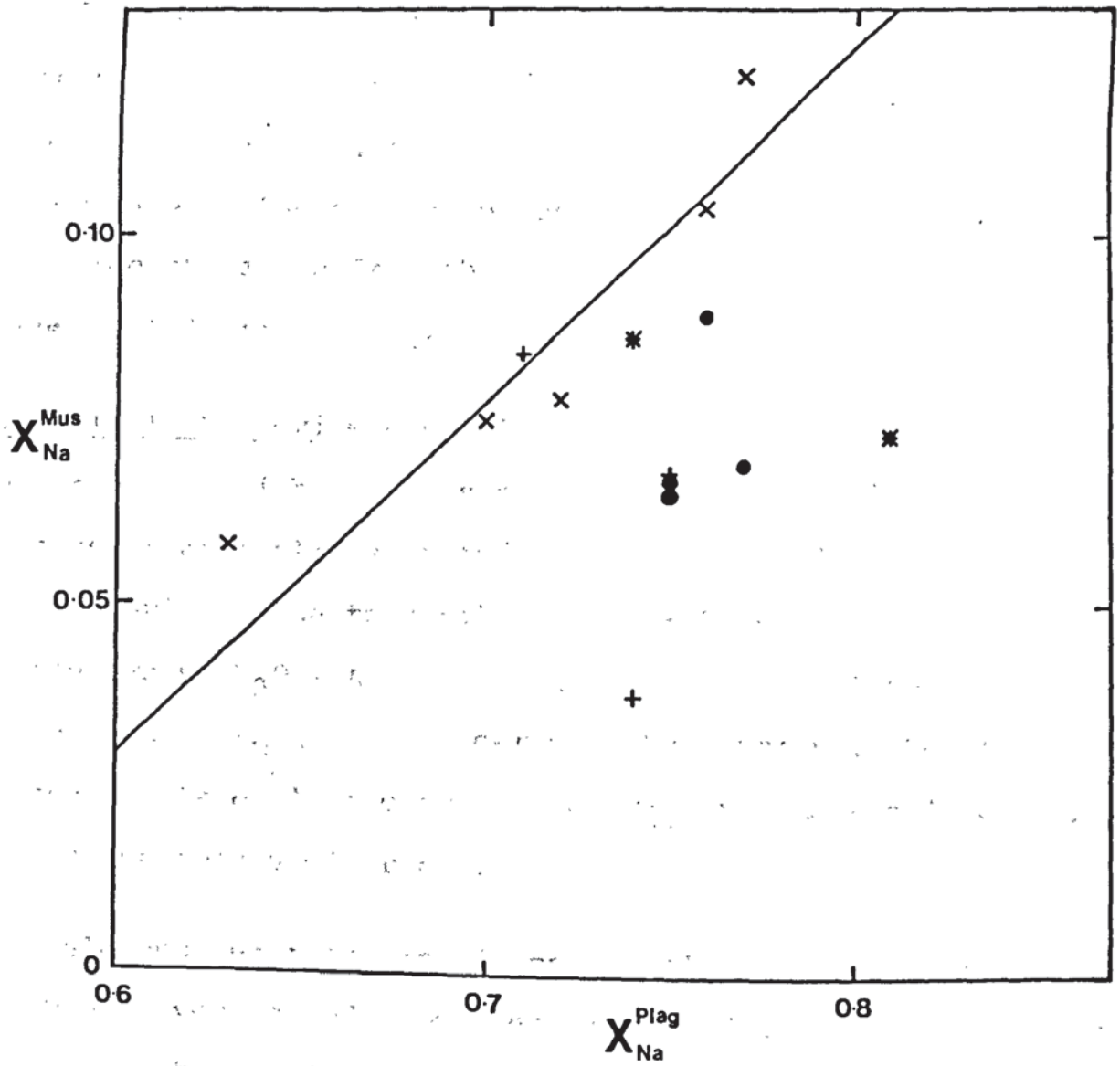
the aureole. This results in divariance due to the presence of a Na component being small. Any divariance that may be recognised for reaction (1) is more likely to be the result of variation in a_{H_2O} than from the influence of Na (Evans & Guidotti, 1966). Plagioclase does not therefore play an essential part in muscovite - feldspar relations in the aureole. Only where K-feldspar is absent in the muscovite + sillimanite + K-feldspar zone is Na enrichment of albite, by reaction (24), seen. A32 plots away from the sillimanite zone trend in fig. 2.24, reflecting its higher grade position. Muscovite and plagioclase compositions are similar to K-feldspar free specimens from the sillimanite + K-feldspar zone of Cheney & Guidotti (1979).

2.6.4 (ii) Muscovite - K-feldspar

The reaction which controls the appearance of sillimanite + K-feldspar assemblages in the aureole is modelled as

muscovite + quartz = sillimanite + K-feldspar + H_2O. (1)
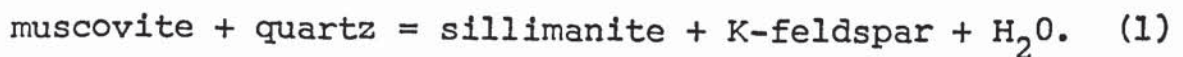
In the system K_2O - Al_2O_3 - SiO_2 - H_2O the reaction is univariant if a_{H_2O} is considered to be constant. Reaction (1) is seen to take place over a zone up to 500 metres in width, and is apparently divariant.

An analagous reaction, involving sanidine as the K-feldspar, has been investigated experimentally by Chatterjee & Johannes (1974). Substituting thermodynamic data from Helgeson et.al. (1978) and Hovis (1972) for a more ordered K-feldspar, an equation for reaction (1) can be derived such that

$$\ln K = 21.36 - \frac{12823}{T} + \frac{0.055 \ (P-1)}{T} \qquad (26)$$

where K is the equilibrium constant, defined by

FIGURE 2.25

T - X_{H_2O} section for muscovite + quartz stability

Curve is calculated from equation 26, using f_{H_2O} data from Burnham et.al. (1969).

Granite minimum curve is taken from Kerrick (1972).

Maximum X_{H_2O} curve is taken from Figure 3 of Ohmoto & Kerrick (1977).
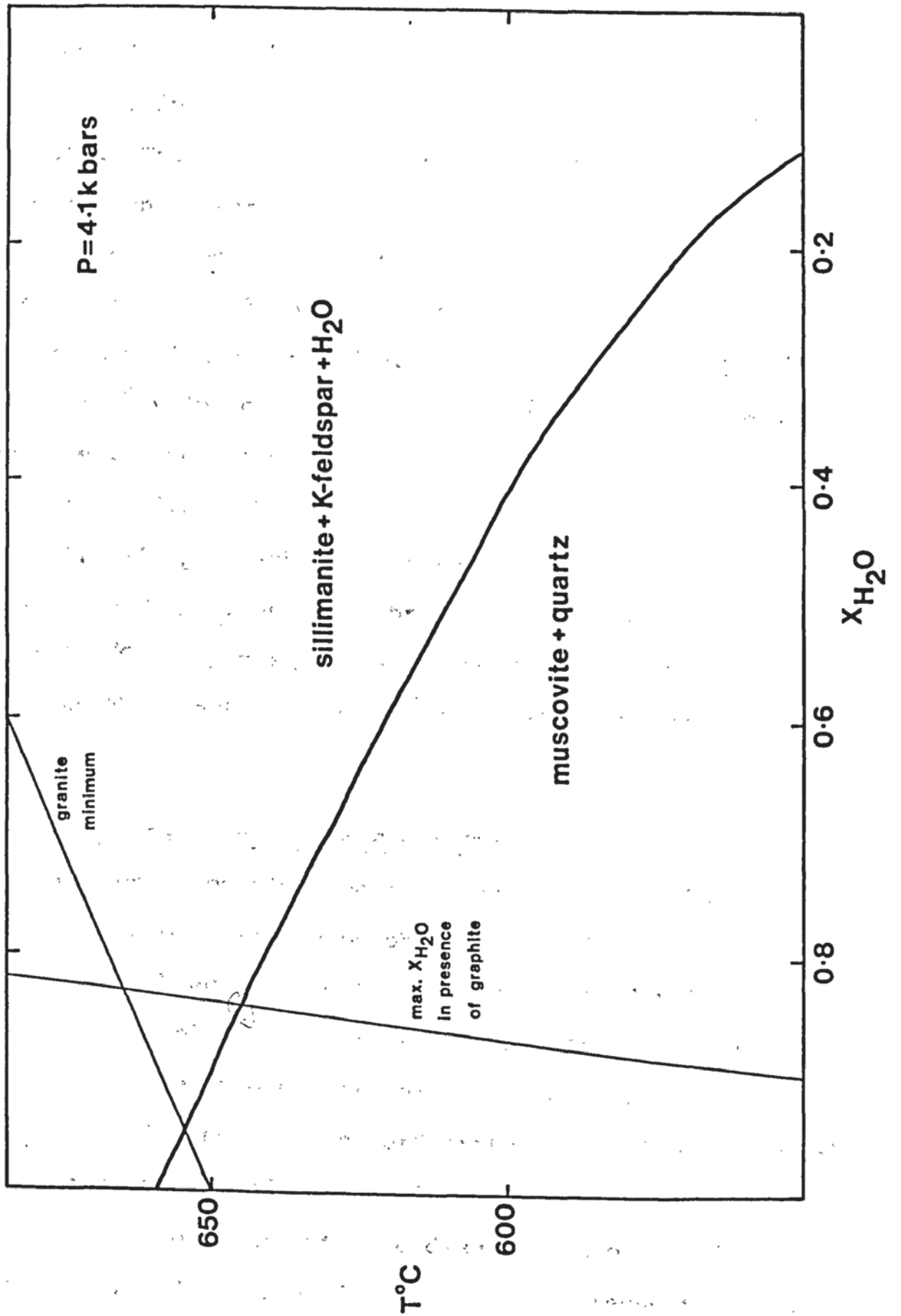
$$K = \frac{a_K^{Ksp} \cdot f_{H_2O}}{a_K^{mus}}$$

A $T - X_{H_2O}$ section has been constructed from equation (26) at the preferred aureole pressure of 4.1 kbars (fig. 2.25). The activity of muscovite may be estimated using the X_K^{mus} from 402C, in the muscovite + sillimanite + K-feldspar zone, of 0.91. The activity coefficient for the K-end - member composition is estimated as 1.0 using an equation analagous to (12) of Cheney & Guidotti (1979, p.427) together with data from their Table 3 (p.428). For K-feldspar a γ_K^{Ksp} of 1.03 has been estimated from fig. 3 of Waldbaum & Thompson (1969) at an X_K^{Ksp} value of 0.86, averaged from the four samples analysed. The activity of the K-feldspar component is calculated as 0.89. Data for f_{H_2O} is taken from Burnham et.al. (1969). If P_{H_2O} within the aureole rocks can be shown to be less than P_{TOTAL}, an equilibrium temperature considerably less than $659^{\circ}C$ ($P_{H_2O} = P_{TOTAL}$), is indicated. Any increase in P_{H_2O} as the reaction proceeds will extend muscovite - quartz stability.

2.6.5 Composition of the Fluid Phase

Information concerning the composition of the fluid phase during metamorphism may be obtained by identification of the opaque assemblages present. Thirty polished thin sections, prepared for electron microprobe analysis, were investigated. The assemblages present are given in Table 2.4. Pyrrhotite is most commonly seen in the cordierite + K-feldspar zone, where estimates by eye indicate an increase in its modal abundance and grain size, attributed to desulphidation of biotite (Guidotti, 1970). Graphite occurs less frequently in the cordierite + K-feldspar zone than in the outer part of the

145

aureole, but there is no obvious decrease in its modal abundance, again estimated by eye, where it is present.

The assemblage graphite + ilmenite + pyrrhotite indicates the presence of a C - O - H - S fluid. Ohmoto & Kerrick (1977) have investigated the proportions of the various fluid species present in such a fluid in equilibrium with the assemblage graphite + pyrite + pyrrhotite over a range of P, T, and f_{O_2}. Under typical metamorphic conditions, CO_2, H_2O and CH_4 are the main species present. Values of X_{H_2O} and X_{CO} exceed 0.1 only at very high temperatures ($> 800^{O}$C) and low pressures (< 2 kbars). Sulphur species do not usually exceed a mole fraction of 0.01. Where pyrrhotite, rather than the assemblage pyrite + pyrrhotite, is present, values for sulphur species will be even lower. X_{H_2O} estimated from Ohmoto & Kerrick (1977) for the aureole are therefore minimum values. As the correction to X_{H_2O} would be small (< 0.01) there would be little effect on estimated equilibrium temperatures.

At any particular P and T, X_{H_2O} will reach a maximum value at the f_{O_2} where X_{CO_2} and X_{CH_4} are equal. This is due to the reaction

$$2C + 2H_2O = CO_2 + CH_4. \qquad (27)$$
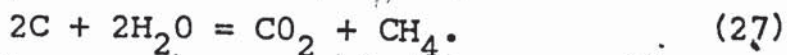
Operation of this reaction will tend to decrease the amount of graphite present in the rock, as well as decreasing maximum X_{H_2O}, as temperature increases. Values of maximum X_{H_2O} for fluids in equilibrium with graphite + pyrite + pyrrhotite are given in fig. 3 of Ohmoto & Kerrick (1977). As argued above these will differ only slightly from those in equilibrium with graphite + pyrrhotite.

Ohmoto & Kerrick (1977, fig. 8, p.1026-1027) present a series

of $T - f_{O_2}$ sections for carbonate free pelites at 2, 4, 6, and 8 kbars. Fig. 2.26 is a similar section estimated from these at the aureole pressure of 4.1 kbars. The actual prograde $T - f_{O_2}$ path taken during metamorphism is dependent on whether the fluid composition is buffered internally or externally. Internal buffering is controlled by the various dehydration equilibria which take place (Greenwood, 1975). External buffering involves control of the fluid phase composition by introduction of fluid from an external source. In the Strontian area there is no evidence of external buffering and the fluid phase is internally buffered.

The well-defined nature of the sillimanite + K-feldspar isograd suggests a constant X_{H_2O} for the regional sillimanite zone just below it. At this grade the $T - f_{O_2}$ path will parallel the maximum X_{H_2O} trace at the X_{H_2O} value found in the rocks. When the equilibrium temperature for reaction (1), at the regional X_{H_2O}, is reached, the assemblage muscovite + sillimanite + K-feldspar will be stable. As reaction (1) is a dehydration reaction its prograde operation will tend to increase X_{H_2O}, extending muscovite + quartz stability. The $T - f_{O_2}$ path will follow the $T - X_{H_2O}$ reaction boundary as X_{H_2O} and T increases, until the maximum X_{H_2O} trace is intersected. At this point X_{H_2O} can no longer increase and the upper limit of muscovite stability is reached. The $T - f_{O_2}$ path then follows the maximum X_{H_2O} trace, fluid phase composition being controlled by reaction (27).

An estimate for the equilibrium temperature of reaction (1), when X_{H_2O} is at a maximum, can be made by combining data from fig. 3 of Ohmoto & Kerrick (1977) for maximum X_{H_2O} at

147

FIGURE 2.26

T - fO$_2$ section

Section is based on the 4 kbars section in Figure 8
of Ohmoto & Kerrick (1977) interpolated at the aureole
pressure of 4.1 kbars. Muscovite + quartz stability
is calculated from equation 26. Biotite dehydration
is idealised from data given by Holdaway & Lee (1977)
and Lee & Holdaway (1977).

149
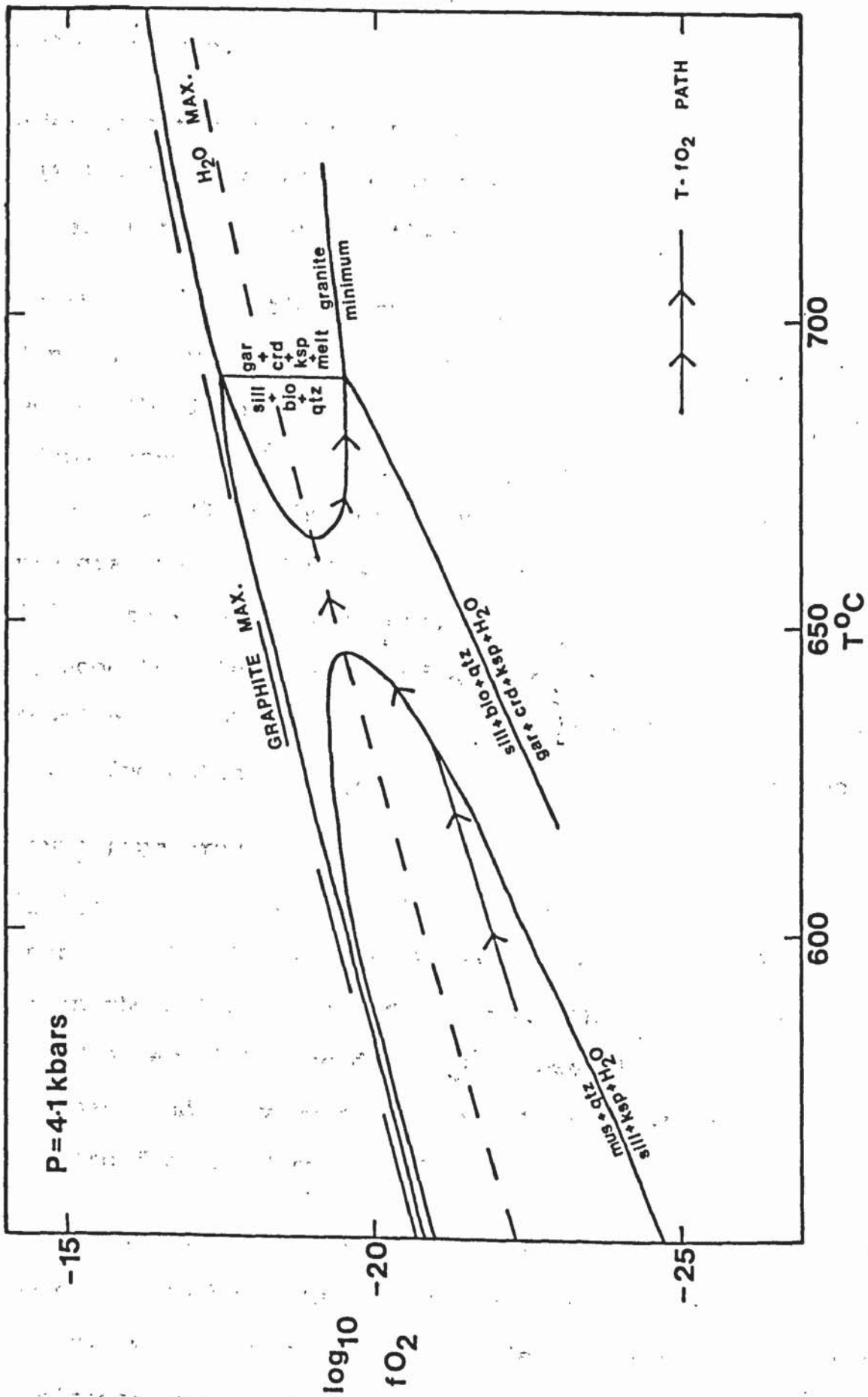
P_{TOTAL} = 4.1 kbars, with the calculated $T - X_{H_2O}$ section for reaction (1) (fig. 2.25). Intersection of the two curves indicates a temperature of 645°C at an X_{H_2O} of 0.84. This corresponds to the inner limit of the muscovite + sillimanite + K-feldspar zone.

In order to establish the temperature and X_{H_2O} conditions at the sillimanite + K-feldspar isograd, one or other of the variables must be independently estimated.

Making the approximation that aureole temperature gradients are linear, they may be estimated using the temperatures iden- tified for the inner limit of the muscovite + sillimanite + K-feldspar zone (645°C) and the cordierite + K-feldspar iso- grad (690°C). Along the north shore of Loch Sunart the temp- erature gradient is 30°/km. Applying this to the muscovite + sillimanite + K-feldspar zone, 500 metres wide at this point, suggests a temperature of approximately 630°C for the sillimanite + K-feldspar isograd. Applying the temperature to fig. 2.25 indicates an X_{H_2O} of 0.69 for regional assemblages.

2.7 INTERPRETATION

2.7.1 The Sillimanite + K-feldspar Isograd

Sillimanite + K-feldspar assemblages provide an important marker in the metamorphism of pelites. Their occurrence is used by Winkler (1976) to define the lower limit of high grade metamorphism and they correspond to the highest grade of the amphibolite facies (Turner, 1968).

The occurrence of sillimanite with K-feldspar in western Maine has been studied by Evans & Guidotti (1966). Three major assemblages were recognised in a series of graphitic schists and gneisses; one was defined by the presence of K-feldspar;

one by sillimanite, and the third by sillimanite and K-feld-
spar together. Quartz, biotite, plagioclase, muscovite and
garnet were common to all three. A sillimanite + K-feldspar
isograd was drawn at the first appearance of that assemblage.
At high grade, the sillimanite bearing, K-feldspar free assem-
blage was still recognised.

The coexistence of sillimanite and K-feldspar was attributed
to the reaction

$$\text{muscovite} + \text{plagioclase} + \text{quartz}$$

$$= \text{sillimanite} + \text{alkali feldspar} + H_2O. \qquad (25)$$
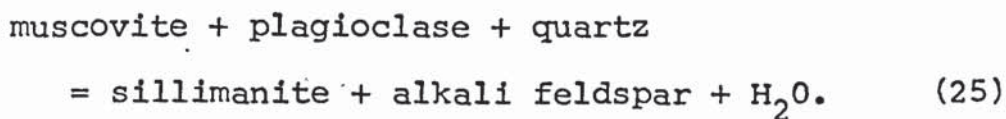
The continued stability of the assemblage muscovite + sill-
imanite + K-feldspar above the isograd resulted from divariance
produced by the effect of Na in muscovite and K-feldspar, and,
more importantly, variation in a_{H_2O}. It was recognised that
the presence of graphite indicated P_{H_2O} to be less than P_{TOTAL}.
The operation of a dehydration reaction such as (25) would
increase the X_{H_2O} value in the fluid phase and therefore
extend the equilibrium indicated by (25), over a range of T.
As muscovite is stable throughout the area, its upper stability
limit in terms of both T and X_{H_2O} was not reached. The stab-
ility of muscovite + sillimanite + K-feldspar over a distance
of at least 11km implies a large temperature range, which in
turn implies that X_{H_2O} must have been low when reaction (25)
began to operate. The widespread occurrence of muscovite +
sillimanite assemblages above the isograd indicates that X_{H_2O}
was not uniformly low, operation of reaction (25) being
retarded by locally high values. This has been confirmed by
more recent work from an adjacent area (Cheney & Guidotti, 1979).

In a study of sillimanite + K-feldspar assemblages in south-

east Connecticut, Lundgren (1966) defined an isograd above which muscovite was unstable in the presence of sillimanite + K-feldspar. The area differed from that described by Evan & Guidotti (1966) in that graphite bearing lithologies were rare. Muscovite + sillimanite + K-feldspar assemblages did occur below the isograd but were restricted to the one stratigraphic unit where graphite was present. The three phase assemblage was found up to 5km below the isograd and has been interpreted by Ohmoto & Kerrick (1977) in terms of variation in a_{H_2O}.

As in western Maine the presence of graphite was taken to indicate $P_{H_2O} < P_{TOTAL}$. The wide geographical range of the muscovite + sillimanite + K-feldspar assemblage suggested a wide temperature range for reaction (25) in the graphitic lithologies. Low initial X_{H_2O} values were therefore inferred where the assemblage was present. In graphite free rocks, muscovite + sillimanite and muscovite + K-feldspar assemblages were widespread. Sillimanite with K-feldspar was only found above the isograd when muscovite was no longer present. The occurrence of muscovite + sillimanite + K-feldspar zones associated with muscovite dehydration is not restricted to graphite bearing rocks. Ashworth (1975) described a poorly exposed example from the Huntly-Portsoy aureole. Graphite was rare or absent, but nearby calcareous assemblages may have been the cause of a low initial X_{H_2O} (Ashworth & Chinner, 1978). Yardley et.al. (1980) also recognised muscovite + sillimanite + K-feldspar assemblages at high grade in graphite free pelites from Connemara. Investigation of fluid inclusions indicated a fluid phase consisting of CO_2 and H_2O, with H_2O dominant at $X_{H_2O}=0.8$. In both cases $P_{H_2O} < P_{TOTAL}$ allowed buffering of the fluid phase by a muscovite dehydration reaction to produce

a divariant muscovite + sillimanite + K-feldspar zone, despite the absence of graphite.

In the Strontian aureole muscovite + sillimanite + K-feldspar assemblages occur in a narrow and well defined zone (Map 1). The upper limit of this zone is marked by a 'muscovite out' isograd. This corresponds to the isograd recognised by Lund-gren (1966).

The 'muscovite out' isograd would be expected to provide a well defined boundary. Where initial P_{H_2O} is less than P_{TOTAL} the isograd reaction is divariant, occurring over a range of T. In the presence of graphite, the limit of muscovite stab-ility in such a divariant field is reached when X_{H_2O} in the fluid phase reaches its maximum possible value (Ohmoto & Kerrick, 1977, fig.3). This value will be the same for all graphite bearing rocks at a particular T and P_{TOTAL}.

By contrast the first appearance of sillimanite + K-feldspar assemblages, marked by the sillimanite + K-feldspar isograd, is controlled by initial P_{H_2O}. Where there is considerable variation in P_{H_2O} in low grade assemblages, a sharp isograd will not be expected. This is the case in southeast Connecti-cut, where low X_{H_2O} values are expected only in the rare graphite bearing pelites. In the non-graphitic rocks, it appears that X_{H_2O} was almost 1, so that the dehydration reaction is univariant, sillimanite + K-feldspar appearing at the 'muscovite out' isograd.

The sharp sillimanite + K-feldspar isograd at Strontian would therefore seem to imply a relatively uniform value for X_{H_2O} in assemblages below the isograd. This also appears to be

the case in western Maine where the isograd is sharp (Evans & Guidotti, 1966). In both cases graphite-bearing lithologies are common.

Thermal metamorphism in the Strontian area took place soon after regional metamorphism to sillimanite and sillimanite + K-feldspar grade. The aureole sillimanite + K-feldspar isograd is best developed to the west (Map 1), superimposed on to the regional sillimanite zone. To the east it merges into the regional sillimanite + K-feldspar assemblages described by Stoker (1980). Bearing in mind the long, high-grade metamorphic history to which the southwest Moines have been subjected, and the relatively widespread occurrence of graphite-bearing pelites, the fluid phase composition would be expected to have been driven to a fairly uniform value by Caledonian regional metamorphism. Where muscovite + sillimanite assemblages are found in the muscovite + sillimanite + K-feldspar zone, a locally high X_{H_2O} must be assumed (Cheney & Guidotti, 1979).

Movement of H_2O within the aureole can control X_{H_2O} and may take place as a result of dehydration reactions, and also convectively as a direct result of the emplacement of the intrusion. Such circulation is not ruled out by the occurrence of a sequence of buffer assemblages (Ferry, 1978). At distances up to 5km from the contact, in rocks displaying no noticeable evidence of contact metamorphism, and where the fluid phase has not been buffered by reactions such as (1), it is unlikely that fluid movement driven by the intrusion could control X_{H_2O}.

Circulation of fluid within the Strontian aureole is likely to

have been impeded by the low porosity and permeability of the country rocks, which have suffered at least two regional meta-morphisms. There are also no obvious reactions which may be attributed to an influx of fluid. Secondary muscovite and myrmekite can be attributed to retrograde reactions resulting from anatexis (see Section 2.7.2).

2.7.2 Migmatisation

The Moinian metasediments into which the granodiorite has been intruded, are highly migmatitic. As has already been described, they can be divided into three mineralogical types; trondhjem-itoid, granitoid, and microperthite - granitoid (Section 2.4.5).

Trondhjemitoid migmatites have been interpreted as regional in origin, the products of Grenvillian metamorphism re-equil-ibrated at lower grade conditions by subsolidus reaction during Caledonian metamorphism.

Granitoid migmatites occur within the aureole and represent modification of regional muscovite bearing trondhjemitoid assemblages by subsolidus operation of reaction (1). If trond-hjemitoid migmatites were muscovite-free at regional grades they would be unaffected by reaction (1), and persist unmod-ified into the aureole.

Microperthite - granitoid migmatites are restricted to the sillimanite + K-feldspar and cordierite + K-feldspar zones. They are not obviously the product of subsolidus recrystallis-ation by reaction (1), which produces characteristically inter-stitial, non-perthitic K-feldspar. This type of migmatite is also found in regional assemblages to the east, but within the aureole they are affected by disruption caused by the intrusion of the pluton. Undisrupted microperthite-granitoid migmatites,

155

best developed in the western aureole are presumed to be products of thermal metamorphism.

The sillimanite + K-feldspar isograd at medium and high pressure is commonly associated with the appearance of anatectic migmatites (Winkler, 1976). This results from the intersection of a muscovite dehydration reaction with the minimum melting curves for the granitic components in pelites (e.g. Kerrick, 1972; Thompson & Algor, 1977; Thompson & Tracy, 1979). The temperature and pressure of this intersection can vary significantly according to the nature of the dehydration and melting reactions operating. The positions of the minimum melting reactions, as with dehydration reactions, may be affected by variations in fluid phase composition.

The muscovite dehydration reaction identified at Strontian is

$$\text{muscovite} + \text{quartz} = \text{sillimanite} + \text{K-feldspar} + H_2O. \quad (1)$$

Intersection of this reaction with the granite minimum curve of Kerrick (1972) takes place at about 3.8 kbars when $P_{H_2O} = P_{TOTAL}$. In the presence of graphite P_{H_2O} will be less than P_{TOTAL} and the intersection occurs at 4.5 kbars for the maximum X_{H_2O} value (Ohmoto & Kerrick, 1977, p. 1029). Consideration of fig. 2.25 and fig. 2.26 illustrates the effect this has on melting reactions in the Strontian aureole.

At the estimated aureole pressure of 4.1 kbars partial melting of pelites would not be expected associated with reaction (1). Melting governed by the reaction

$$\text{albite} + \text{K-feldspar} + \text{quartz} + H_2O = \text{melt} \quad (28)$$
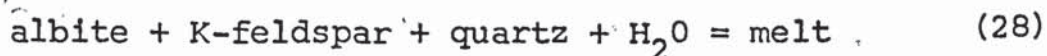
takes place at temperatures above the stability limit of muscovite. In this region the fluid phase composition is controlled by reaction (27). Intersection of the maximum X_{H_2O}

curve (Ohmoto & Kerrick, 1977, fig. 3), with the granite minimum $T - X_{H_2O}$ curve from Kerrick, (1972) at 4.1 kbars gives a temperature of $664^{\circ}C$ at $X_{H_2O} = 0.83$. The plagioclase at Strontian is not pure albite but oligoclase, generally about An_{25}. Thus the onset of melting,

$$oligoclase + K\text{-}feldspar + quartz + H_2O = melt \qquad (29)$$
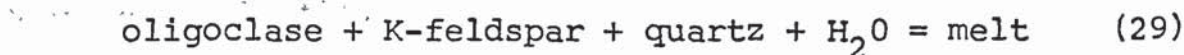
is expected at temperatures some $20^{\circ}C$ higher than in the Ca-free system (Winkler, 1976). The actual melting reaction, bearing in mind assemblages in the sillimanite + K-feldspar zone, will probably be

$$oligoclase + K\text{-}feldspar + sillimanite + quartz + H_2O = melt \qquad (30)$$
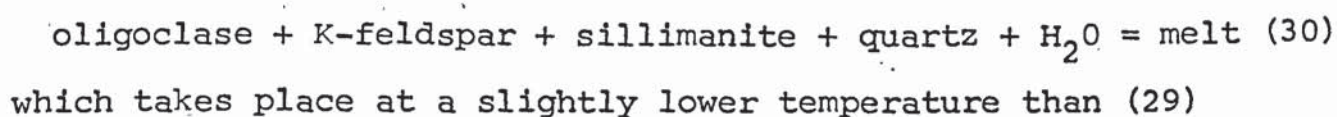
which takes place at a slightly lower temperature than (29) (Thompson & Algor, 1977). The general onset of partial melting would therefore be expected between 660° and 680° ($X_{H_2O} = 0.83$). The possible 'fluxing' role of minor components, such as halogens, is difficult to assess but probably not important (Winkler, 1976, p. 294-295). Continual melting at higher temperatures will consume water and lower X_{H_2O} of the fluid phase. In fig. 2.26 the $T - f_{O_2}$ path leaves the maximum X_{H_2O} trace, and follows the granite minimum curve. At this stage, the amount of melt produced will be restricted by low availability of pore water. It was argued above that fluid movement in this aureole had relatively minor effects. Thus it is reasonable to suppose that the progress of reaction (30) to the right would usually be halted by shortage of H_2O. Intersection of the granite mimimum curve with reaction (2) should take place at $690^{\circ}C$ and $X_{H_2O} = 0.53$ (Sections 2.6.2 & 2.6.3). Lee & Holdaway (1977, fig. 4, p.89) predict melting of the five phase assemblage sillimanite + biotite + K-feldspar + quartz at this point, and the cordierite + K-feldspar isograd reaction will be

157

sillimanite + biotite + quartz

= cordierite + garnet + K-feldspar + melt   (31)
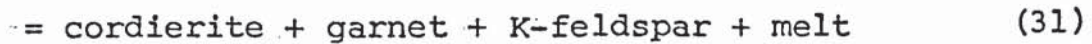
(Ashworth & Chinner, 1978). X_{H_2O} in the cordierite + K-feldspar zone will remain buffered by this reaction. The observed coexistence of sillimanite and biotite above the isograd (Section 2.4.3, fig. 2.14) will result from the multivariant nature of the melt phase. Fig. 2.26 is very crude in this region and substantial variations in X_{H_2O} are possible between rocks with the same assemblage. The major dehydration - melting reaction (31) would be expected to mark the production of large quantities of melt.

The occurrence of microperthite - granitoid migmatites (Table 2.5) indicates that they are not associated with the muscovite + sillimanite + K-feldspar zone. They first appear in the sillimanite + K-feldspar zone. If the migmatization is attributable to anatexis, this pattern is consistent with, and tends to confirm, the cordierite - garnet geobarometry. At $p > 4.5$ kbar anatexis would be expected in the muscovite + sillimanite + K-feldspar zone, while at lower P it would be suppressed to ever higher T. Two specimens (A10, A12) occur some 500 metres east of the 'muscovite out' isograd. From the thermal gradient along the north shore of Loch Sunart, estimated in Section 2.6.5, this corresponds approximately to the position of the $660^{\circ}C$ isotherm, which should represent the minimum temperature for the onset of partial melting. Four other microperthite-granitoid migmatites have been recognised, all from within the cordierite + K-feldspar zone. From the above discussion it would be expected that anatectic migmatites are common in this zone. In the road cut exposures immediately north of Sròn na Saobhaidh this is certainly the case, with

frequent, closely spaced leucosomes dominant (fig. 2.18b). Over much of the zone, and in the sillimanite + K-feldspar zone, however, these migmatites are apparently rare. In order to explain this, it is first necessary to establish their mode of origin.

Available whole rock analyses for pelites within the aureole show little evidence to suggest external metasomatism (Gould, 1966; Butler, 1969). Some metasomatism by the granodiorite was recognised by Sabine (1963), but this was limited to within a few metres of the contact. Injection by magma from the granodiorite has also been discounted by Ashworth & Chinner (1978), due to the presence of sillimanite, rather than hornblende in the migmatites.

Yardley (1978, Table 2, p.944) has tabulated criteria which may be used to distinguish between the various mechanisms of migmatite formation. Plagioclase compositions in leucosomes are expected to be significantly more sodic than in palaeosomes if anatexis has taken place. If this is not the case a metamorphic segregation process is preferred. Ashworth (1979) has pointed out that the differentiation of plagioclase composition may only be pronounced if the leucosome crystallises as a closed system. Where the leucosome remains in direct contact with the palaeosome, and cooling is slow, homogeneous plagioclase will be expected in both palaeosome and leucosome. At Strontian migmatites of all three types show relatively uniform feldspar compositions. This is also the case in various studies of migmatites concluded to have an anatectic origin (e.g. Mehnert, 1968; Ashworth, 1976).

It has proved difficult to obtain modal analysis data for the migmatites, owing to their coarse grain size, and small

159

relative volume. It is not therefore known whether their compositions correspond to expected minimum melting compositions (cf. Ashworth, 1976).

In the absence of such information, an anatectic origin is preferred for the microperthite - granitoid migmatites despite their limited occurrence.

The occurrence of microperthite in the anatectic migmatites, rather than orthoclase cannot be attributed to its crystallisation temperature, as this must have been similar to that at which non-anatectic granitoid migmatites were produced.

Rocks which have undergone partial melting may be relatively Na-rich. Certainly low An content in plagioclase would allow melting to occur at lower temperatures. A high subsequent content of Na in K-feldspar would be likely to promote exsolution.

More important may be the relatively high P_{H_2O} at which anatectic melts crystallise, compared to the P_{H_2O} in rocks where K-feldspar grew as the result of subsolidus reaction. Complete miscibility of Na- and K-feldspar occurs at low P_{H_2O}, while high P_{H_2O} will promote exsolution (Mehnert, 1968, p.104). Exsolution can also be promoted by shearing stress (Mehnert, 1968, p.102) and this may be important in rocks deformed by the emplacement of the granodiorite.

The microperthite granitoid migmatites are therefore consistent with the predicted process of anatexis. Further circumstantial evidence for partial melting is provided by the difference between X_{H_2O} values at the 'muscovite out' and cordierite + K-feldspar isograds. A non-anatectic model would

require the influx of a carbon-rich fluid from an external source. The observed trend of increasing retrograde replacement of sillimanite + K-feldspar assemblages is also well explained by an anatectic model, with water being released from the melts as they cooled and crystallised. There is good evidence of an increase in secondary muscovite towards the contact, replacing sillimanite + K-feldspar assemblages (Section 2.4.3, fig. 2.13 c & d). Ashworth (1976, 1979) suggests that as crystallisation of a leucosome proceeds, sillimanite + K-feldspar will tend to be rehydrated by water released from the melt, the former presence of K-feldspar should be revealed by myrmekitic intergrowths (Ashworth, 1972), usually associated with secondary muscovite. These textures are recognised in microperthite-granitoid migmatites. They also occur extensively throughout the cordierite + K-feldspar zone, and may be found in rocks showing a high degree of disruption by the intrusion.

The apparent scarcity of migmatites may be the result of several factors. Firstly, the recognition of the different migmatite types in the field is uncertain and, due to the very common occurrence of regional leucosomes, random sampling will mostly reveal those types.

Secondly, the composition of the migmatites may have been altered by retrograde reaction. Subsolidus re-equilibration of rocks containing muscovite and myrmekite will produce a trondhjemitoid assemblage.

Thirdly, the cordierite + K-feldspar zone rocks have been subjected to extensive deformation during intrusion of the pluton. Disruption of regional leucosomes has been recognised and contact leucosomes may also be affected. It might be expected that melts formed during deformation would be expelled from

161

the rock. The results of Van der Molen & Paterson (1979) suggests that at low melt fractions, the deforming rock will actually tend to take up externally available melt by a mechanism of dilatancy pumping. Shearing will spread melt through the rock along grain boundaries. Early-formed migmatites, which may have contained molten, or partially crystallised melt during the intrusion period would not therefore be expected to survive as discrete leucosomes. Partially melted rocks subjected to shearing should display considerable grain coarsening, particularly of leucocratic components, in the absence of typical migmatite structures. This is certainly the case at Strontian where rocks become coarse grained, and feldspar porphyroblastic, in the cordierite + K-feldspar zone. In view of the coincidence of this with the zone of deformation produced by forceful intrusion of the granodiorite (Munro, 1965), the lack of contact leucosomes is regarded principally as the effect of shearing on partially molten rocks.

At melt fractions of between 20% and 30% the strength of the rock is drastically reduced (Arzi, 1978; Van der Molen & Paterson, 1979). This will promote plastic flow in rocks containing melt which are subjected to stress. In the cordierite + K-feldspar zone at Strontian, where general melting of pelites is expected, plastic flow in pelites has been recognised, with more rigid psammites and amphibolites preserved as dismembered blocks (the 'breccia structure' of Mac-Grego & Kennedy, 1932). The intrusion of the granodiorite takes place over a relatively long time period, with the associated deformation increasing as the volume of magma increases. The quantity of partial melt in the country rock will also increase with time and the critical melt fraction will be

FIGURE 2.27

Aureole P - T Model

Numbers refer to equations in the text.

Arrow from regional conditions to line defining the
sillimanite + K-feldspar isograd represents a difference
in time as well as P - T space.

163

REGIONAL T&P
(RESIPOLE)

ONSET OF
ANATEXIS

MUS + SILL + KSP ZONE

SILL + KSP
ZONE

CRD + KSP
ISOGRAD

P kbars

$X_{H_2O} = 0.69$

$X_{H_2O} = 0.84$

$X_{H_2O} = 0.53$

$X_{H_2O} = 0.83$

$X_{H_2O} = 0.53$

600   650   700

$T^{o}C$
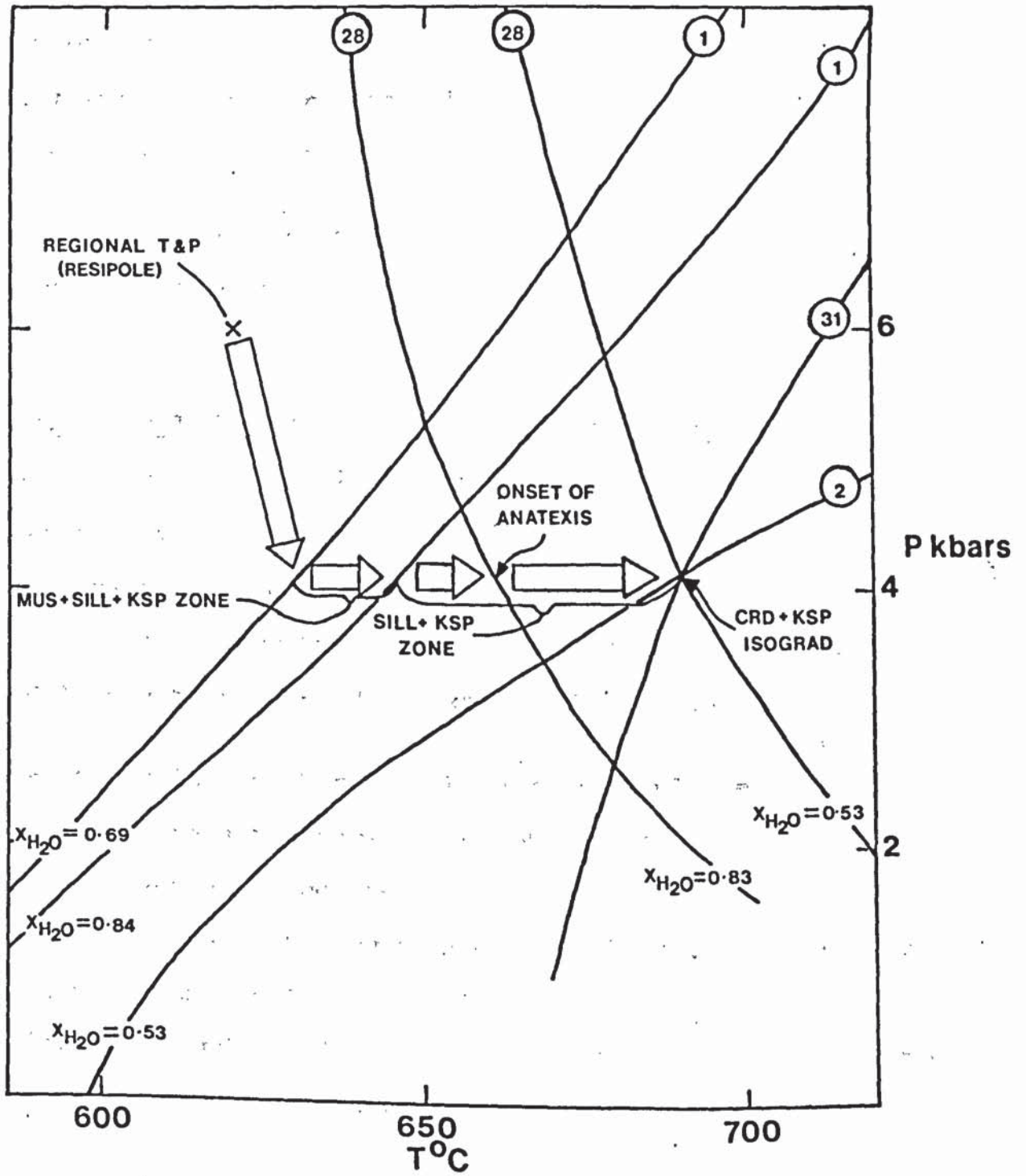
approached as deformation becomes more intense. The plastic behaviour of pelites can therefore be attributed to lubrication from melt dispersed along grain boundaries by deformation associated with forceful emplacement of the granodiorite.

Well developed contact migmatites north of Sron na Saobhaidh show some evidence of extension parellel to the contact and may represent later formed leucosomes. Areas which do not show any shearing are not pelitic, and are therefore mica-poor and non-migmatitic.

Fig. 2.27 summarises the positions of the observed aureole isograd reactions, and the inferred melt reactions, in P - T space.

2.7.3   The Influence of Regional Metamorphic Conditions

One of the most striking features of the aureole is the pronounced asymmetry of the cordierite + K-feldspar zone which displays a five fold increase in width from 500 metres, on the shores of Loch Sunart, to 2.5km, in Glen Tarbert. Several models may be presented to explain this feature.

Variations in the shape of the aureole could be attributed to the immediate subsurface topography of the intrusion. This does not appear to be the case considering the shape of the intrusion interpreted by Munro (1965, 1973). The gravity data presented by Blythe (1975), supports a harpolithic shape (fig. 2.28) and provides no evidence for a major subsurface extension of the pluton to the north and east.

The observed divergence of the isograds from the contact could alternatively be attributed to a steep pressure gradient, decreasing from west to east, across the area. At high pressures

FIGURE 2.28

Shape of the granodiorite intrusion

From: Munro (1973).

the isograd reactions will occur at higher temperatures, and will therefore be close to the granodiorite. At low pressures, they will occur at lower T and will be seen at correspondingly greater distances from the contact. It would be necessary to invoke extensive tilting of the intrusion and its aureole after emplacement. Again, bearing in mind the intrusion's harpolithic shape, this is unlikely particularly with regard to the vertical, stock-like form of its southern portion.

Intrusion of the granodiorite into a regional temperature gradient increasing from west to east is probably the best explanation. The existence of such a gradient is suggested by the observed regional assemblages (see Section 2.3). The orientation of the regional isograds is relatively steep as they are little affected by topography, and this will be reflected by regional isotherms. It is likely that the regional gradient was approximately horizontal during the major period of Caledonian metamorphism, grade increasing eastwards. A vertical gradient, in which temperature increased simply with depth, would require uplift of the Loch Eil Division from a structurally deep position in the orogen. As the Loch Eil is the youngest of the stratigraphic Divisions in the Moine this is unlikely.

An estimate can be made for the size and orientation of the temperature gradient from the extent to which it has modified the aureole.

A temperature produced by thermal metamorphism at a point within the aureole (T_{therm}) can be regarded as a function of the initial regional temperature at that point (T_{reg}), the temperature of the intrusion (T_{intr}), its distance from the contact (x) and the conduction properties of the rocks. If the heat

168

flow around the intrusion and the conduction properties are
taken as constant, they may be related by an equation such
that

$$T_{(therm)} - T_{(reg)} = f(x).(T_{(intr)} - T_{(reg)}). \quad (32)$$

This may be rearranged so that

$$T_{(therm)} = f(x).T_{(intr)} + (1 - f(x)) T_{(reg)}. \quad (33)$$

At distances from the contact in the order of the radius of
the pluton, where aureole temperatures tend towards the back-
ground regional temperatures, f(x) will become small. If two
points at an equal distance from the contact are considered,
heating by the intrusion can be assumed to be constant and any
differences in temperature will reflect differences in initial
regional temperatures, so that

$$\Delta T \approx \Delta T_{(therm)} \approx \Delta T_{(reg)}. \quad (34)$$

A linear regional temperature gradient has been assumed. A
line drawn between two points of known temperature, each the
same distance from the contact, will be orientated at some
angle   to the regional gradient (fig. 2.29a). Taking the
distance between the points as l, and the distance for the
same temperature change along the regional gradient as r, then

$$r = l.\cos\theta \quad (35)$$

The regional temperature gradient, g, in degrees per kilometre,
is defined by

$$g = \frac{\Delta T}{r} \quad (36)$$

therefore

$$g = \frac{\Delta T}{l.\cos\theta} \quad (37)$$

If two vectors l_1 and l_2, one either side of r, with the same
value of   T, are considered then

169

FIGURE 2.29

a. Model for estimating regional T gradient.

b. Thermal model of aureole and background regional
    T gradient. Vectors used to estimate gradient are
    indicated.

a.

b.

171
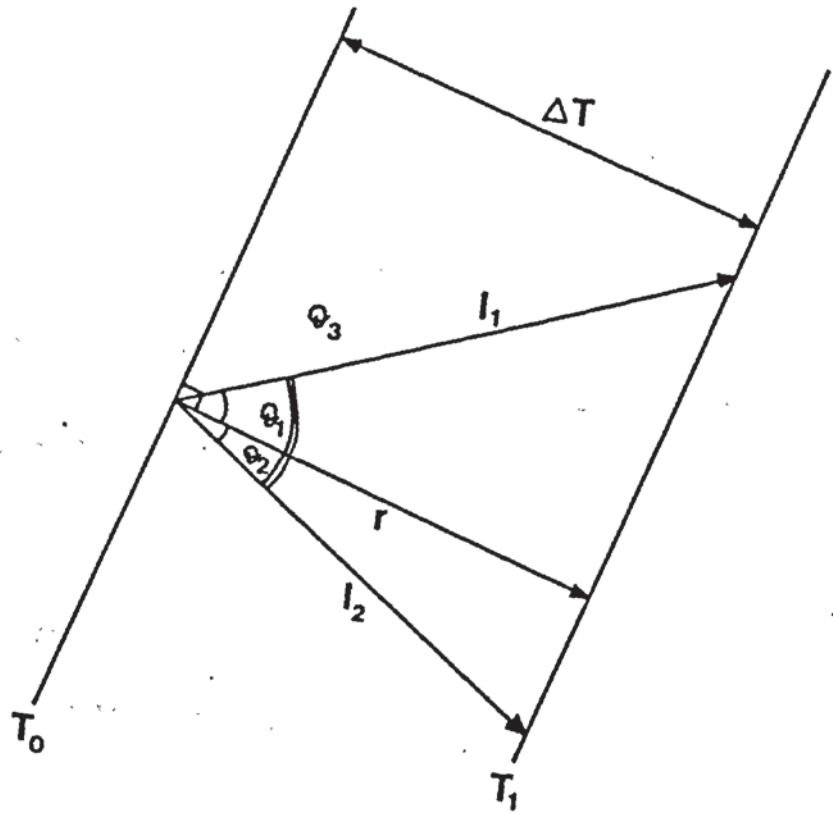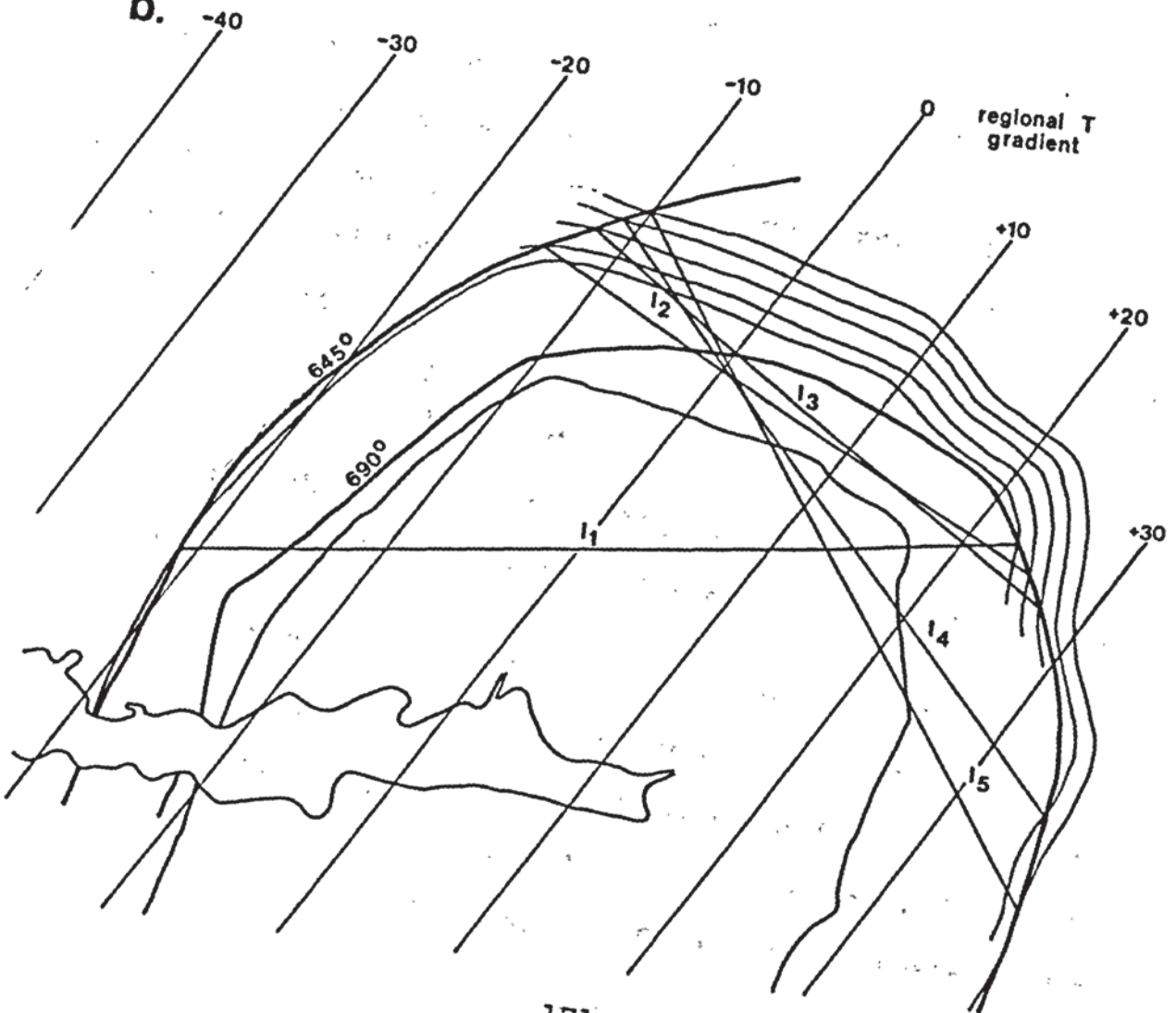
$$\frac{\Delta T}{g} = l_1 \cdot \cos \theta_1 = l_2 \cdot \cos \theta_2 \qquad (38)$$

Let $\theta_1 + \theta_2 = \theta_3$, the measurable angle between the two vectors. Then

$$\cos \theta_2 = \cos(\theta_3 - \theta_1) = \cos \theta_3 \cdot \cos \theta_1 + \sin \theta_3 \cdot \sin \theta_1 \qquad (39)$$

$$l_2(\cos \theta_3 \cdot \cos \theta_1 + \sin \theta_3 \cdot \sin \theta_1) = l_1 \cos \theta_1 \qquad (40)$$

$$(l_2 \cdot \cos \theta_3 - l_1) \cos \theta_1 = -l_2 \cdot \sin \theta_3 \cdot \sin \theta_1 \qquad (41)$$

$$\tan \theta_1 = \frac{l_1 - l_2 \cdot \cos \theta_3}{l_2 \cdot \sin \theta_3} \qquad (42)$$

In fig. 2.29b two of the aureole isograds are taken as lines of equal temperature ('muscovite out' = $645°C$, cordierite + K-feldspar = $690°C$). Five vectors, l_1 - l_5, may be drawn, with ΔT of $45°$, connecting pairs of points at 1.5, 1.75, 2.0, 2.25 and 2.5km from the contact. If the regional gradient is assumed to trend to the east, θ_3 can be measured as the angle between l_1 and any of the other four vectors. This allows θ_1 to be calculated from (42). The regional gradient, g, can then be estimated from

$$g = \frac{\Delta T}{l_1 \cdot \cos \theta_1} \qquad (43)$$

Results are set out in Table 2.10. An average regional gradient of $5.24°$/km is estimated trending towards $122.5°$.

From Map 1 it can be seen that the apparent position of the aureole sillimanite + K-feldspar isograd in Glen Tarbert, not known accurately but inferred from the first occurrence of regional sillimanite + K-feldspar assemblages, does not correspond to that implied by the five fold increase in the

172

TABLE 2.10

ESTIMATION OF REGIONAL TEMPERATURE GRADIENT

l_1 11.2km
l_2 8.0km
l_3 7.9km
l_4 10.1km
l_5 10.7km

Vector pair	ΔT	θ_3	θ_1	$g(^o/km)$	Isotherm orientation
$l_1 - l_2$	45°	35°	45.36	5.57	038°
$l_1 - l_3$	45°	42°	45.23	5.71	038°
$l_1 - l_4$	45°	57°	33.93	4.84	027°
$l_1 - l_5$	45°	64°	34.09	4.85	027°
Average	45°	49.5^o	39.65	5.24	032.5^o

width of the cordierite + K-feldspar zone. It occurs at approximately 7km from the contact, rather than the expected 10km.

The discrepancy could be interpreted in terms of a change in the regional temperature gradient in the eastern part of Glen Tarbert. It is more likely to reflect a regional change in the composition of the fluid phase.

At higher values of X_{H_2O}, muscovite dehydration takes place at higher temperatures (fig. 2.25). The aureole temperature gradient in Glen Tarbert may be estimated as $6°/km$, suggesting a T of approximately $660°C$ at the observed position of the isograd. This is consistent with $X_{H_2O} = 1$, at the aureole pressure of 4.1 kbar. High X_{H_2O} may be caused by a lack of graphite in Loch Eil Division metasediments. In any case a general increase in X_{H_2O} would be expected at grades above a regional sillimanite + K-feldspar isograd.

In view of this, only the western aureole sillimanite + K-feldspar isograd, where it occurs in graphite pelites replacing regional sillimanite grade assemblages, may be regarded as isothermal. Where the isograd occurs against rocks metamorphosed to regional sillimanite + K-feldspar grade, variations in equilibrium temperature may be expected depending on regional fluid phase X_{H_2O}.

The observed shape of the aureole is therefore taken to indicate relatively high temperatures to the north and east of the intrusion at the time of its emplacement. That high temperatures were present during peak regional metamorphism has already been inferred from regional assemblages. A Caledonian age for

these is supported by the age relations of a suite of deformed amphibolite minor intrusions described by Smith (1979). These are concentrated into a narrow band running northeast from the Strontian complex, and are seen to cut across the Carn Chuinneag granite, dated at c560 Ma. They themselves are cut across by the late Caledonian pegmatite suite dated at c450 Ma, and are deformed by the last phase of folding. Amphibolite grade conditions are known to have occurred after 455 Ma, from the deformation and metamorphism of the Glen Dessary syenite (Van Breeman et.al., 1979). The maintenence of relatively hot conditions in the orogen up to the intrusion of the granodiorite is indicated by amphibolite grade assemblages in a suite of microdiorite minor intrusions (Smith, 1979, fig.3). These bodies were intruded after the Cluanie granite, but are cut across by veins extending from the granodiorite, as well as forming inclusions within it. The amphibolite grade assemblages do not in themselves imply that country rock temperatures were at amphibolite grade, rather they reflect the degree to which the cooling rate of the minor intrusions was controlled by the regional temperature gradients. Regional temperatures were probably below amphibolite grade. It was felt (Smith, 1979, p.696) that the region of amphibolite grade microdiorite assemblages represents a residual Caledonian thermal high consistent with the conclusions of Watson (1964). From its effect on the Strontian aureole, the highest temperature part of this residual high must lie just to the north of Glen Tarbert, rather than coinciding with the area of highest concentration of intrusions. The distribution of intrusions is probably controlled structurally by the 'Loch Quoich line' and is not neccessarily related to the thermal structure in the country rocks.

175

2.7.4 The Time Scale of Thermal Metamorphism

It is possible to obtain an estimate for the timescale of the thermal event (t_2), relative to the regional event (t_1), by assuming that complete homogenisation of garnet took place only in the cordierite + K-feldspar zone (Section 2.5.3). The ratio of diffusion coefficients for garnet, D_2/D_1, at two temperatures, T_2 and T_1, is given by

$$D_2/D_1 = \exp\left[(-Q/R)(1/T_1 - 1/T_2)\right] \qquad (44)$$

where Q is the activation energy of diffusion, and R is the gas constant. Times required for isothermal homogenisation in garnets of the same size, with the same initial compositional variations to provide the driving force for diffusion, are given by

$$D_1 t_1 = D_2 t_2 \qquad (45)$$

(cf. Yardley, 1977). The outer core of 572C is taken to indicate a lower limit for the temperature at which homogenisation was effective in the regional event. It is reasonable to assume the same driving force since the amount of compositional change is similar in the two cases. This approach gives $T_1 \approx 890^\circ K$, $T_2 \approx 960^\circ K$ and $1/T_1 - 1/T_2 \approx 8 \times 10^{-5}/K$, a difference that is not sensitive to systematic errors of calibration. From the published range of estimates for Q, 24 to 100 kcal/mole (Yardley, 1977; Freer, 1979), an estimate for t_2/t_1 of approximately $10^{-1.1\pm0.7}$ is obtained. The timescale of the thermal event may be estimated if the timescale of the regional event is known. An upper limit of 20 m.y. is indicated from the ages of the Glen Dessary syenite and of the granodiorite. The suite of late pegmatites suggests that amphibolite grade conditions were established by 450 Ma. Therefore a timescale of 15 m.y. is probably reasonable. This suggests a thermal timescale of between 6.0 and 0.54 m.y. The

result is consistent with emplacement of the granodiorite at a relatively early stage of regional cooling and uplift (see Section 2.7.3). The residual heat and depth of burial has contributed to the retention of the heat of intrusion. The aureole of an intrusion emplaced at a later stage, either at shallow depth or at lower residual temperatures, would have cooled more rapidly. If the timescale of the thermal event was much less than 10^{-2} relative to the regional, re-homogenisation of garnet would not be expected even at the temperatures of the cordierite + K-feldspar zone. In such short-lived thermal events aureole garnets will grow with sharp compositional differences from remaining regional garnet (e.g. Edmunds & Atherton, 1971; Okrusch, 1971).

CHAPTER 3

THE FOYERS AUREOLE

3.1 INTRODUCTION

The Foyers granitic complex forms a triangular shaped mass
occupying an area of some 65 square kilometres, to the south
and east of the village of Foyers on Loch Ness in the Central
Highlands. Like the Strontian Complex it is a member of the
Caledonian 'Newer Granite' suite of intrusions.

The igneous petrography of the complex has been described by
Mould (1946) and by Marston (1970). It consists of three
bodies; a tonalite, a granodiorite and an adamellite (fig. 3.1).
The tonalite occupies most of the eastern half of the complex,
as well as fringing the southern contact. The granodiorite
was intruded after the tonalite but is texturally similar,
differing in the amount of K-feldspar, which increases, with
an attendant drop in the mafic and quartz contents. The
adamellite intrudes both the tonalite and the granodiorite,
and forms numerous small intrusions as well as the large bodies
in the eastern part of the complex. A flow fabric can be seen
in all three bodies, and the contacts between them are irregu-
lar and gradational. Inclusions of appinitic and microdioritic
material, as well as xenoliths of country rock, are common.

Moine metasediments are found against the northeastern and
southern contacts. The northwestern contact has been greatly
affected by faulting associated with the Great Glen fault
zone. Here the complex may be faulted against, or overlain
unconformably by, Old Red Sandstone. The Gleann Liath Series,
suggested by Mould (1946) to be of Lewisian age, is also
faulted against this contact.

The complex has been dated at 400 ± 8 Ma by K/Ar methods (Brown
et.al., 1968). A slightly younger age was indicated by U-Pb

178

FIGURE 3.1

Geological map of the Foyers complex and surrounding country rocks.

After: Mould (1946), Marston (1970), Parson (1979) and Piasecki (1980).

Old Red Sandstone

Granitic Complex
- Adamellite
- Granodiorite
- Tonalite

Dalradian

Moinian
- Grampian Division
- Central Highland Division

Loch Ness

Loch Ruthven

Loch Killin

N

5 km
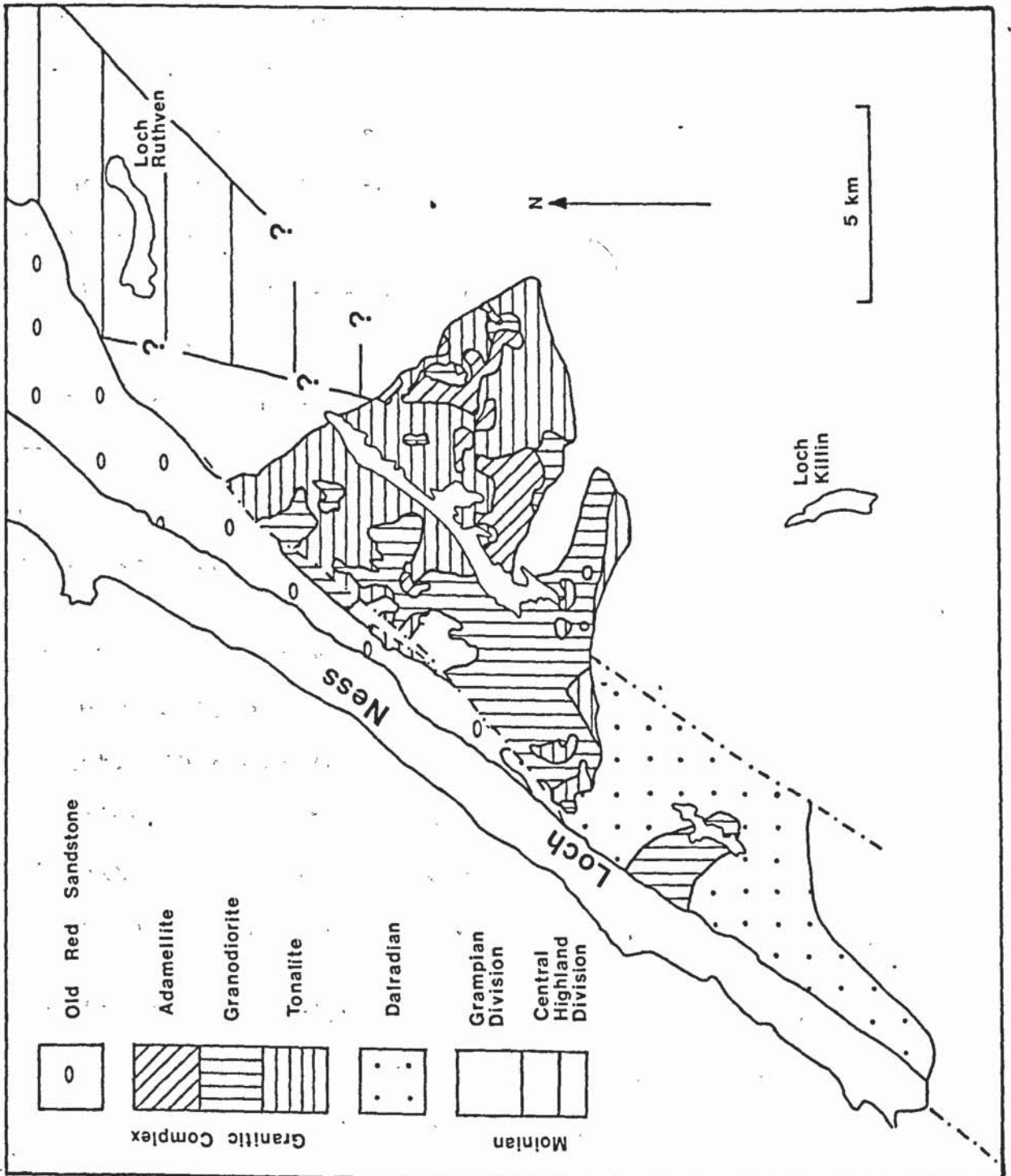
ratios in zircons (Pidgeon & Aftalion, 1978); however it was felt that these had been disturbed by later events.

3.2 PREVIOUS RESEARCH ON THE AUREOLE ROCKS

Mould (1946) described contact metamorphic assemblages developed in semi-pelitic schists adjacent to the contact. Cordierite, with 'foxy' red biotite, was recognised near Loch an Ordain at the northeastern contact, and cordierite with sillimanite and andalusite occurred in muscovite - biotite 'injection gneiss' in Conagleam. To the south the schists became hornfelsic in the vicinity of the contact near Loch Kemp, with development of cordierite, andalusite and sillimanite. Sillimanite occurred both as felted masses of small needles and as larger blades visible in hand specimen. These rocks were graphitic, forming characteristically dark coloured schists and hornfelses.

Thermal metamorphism was also recognised by Marston (1970) in the lobe of metasediments projecting into the complex from the southeast. This was interpreted as lying structurally above the complex. Semi-pelitic hornfelses contained cordierite, sillimanite, andalusite and K-feldspar, and were interpreted as representing pyroxene - hornfels facies metamorphism.

Deflection of the regional strike in the metasediments into approximate parallelism with the contact was recognised along the northeastern and southern margins. This was regarded as evidence of the forceful nature of the intrusion.

Contacts between the complex and metasediments were generally steep, dipping inwards at 70° or more along the northeastern contact. To the south the contact was vertical or dipped steeply outwards. Foliations within all three igneous lithol-

ogies tended to parallel the contacts, and were also steep. Where the foliation was horizontal or gently inclined, it was interpreted as being concordant with the roof. The complex was interpreted from the foliation, and from the orientation of the contacts, as having a wedge-shaped funnel-like structure (fig. 3.2). The foliation itself was interpreted as a distensive feature, produced by lateral expansion of the complex as magma was intruded. Large scale stoping is evident in the southwestern part of the complex, and this was attributed to the close proximity of the present erosion level to the roof of the complex.

The country rocks near to the contact displayed extensive injection by igneous material derived from the complex. Many of the thinner veins had suffered boudinage and small-scale folding indicating continued expansion of the complex during injection. Parts of the contact, particularly to the southwest of Loch Kemp and Carn Gairbhthinn, and on Beinn Dubhcharaidh, were poorly defined with a continuous graduation from igneous material into injected metasediment. In the area between Loch Kemp and Loch Knockie, some 50% of outcrop was igneous, suggesting the presence of the complex at shallow depth beneath it.

Marston (1970) also made some attempt to estimate the physical conditions of contact metamorphism. The presence of andalusite and sillimanite together was taken to indicate a pressure at the time of intrusion, of between 1.5 kbars and 4.0 kbars, based on available experimental data for the reaction

andalusite = sillimanite.

Temperatures of between 600°C and 650°C were estimated for the inner aureole based on a magmatic temperature of

182

FIGURE 3.2

Block diagram and cross section illustrating the
structure of the Foyers complex.

From: Marston (1970).

approximately 800°C.

Wells (1979) attributed the occurrence of fibrolitic silliman-
ite in the vicinity of the 'Newer Granite' bodies to instab-
ility of garnet and muscovite due to the reaction

muscovite + garnet = biotite + sillimanite.
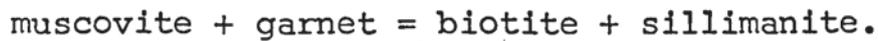
One such occurrence was recognised in pelites near Loch Killin
to the south of the complex. However this occurrence is
within the aureole of Allt Crom Granite bodies (Wells, 1981)
and is not regarded as the product of metamorphism by the
Foyers Complex.

3.3 REGIONAL SETTING

3.3.1 Stratigraphy

To the southeast of the Great Glen fault Moinian rocks out-
crop over much of the Grampian Highlands. They consist of a
dominantly psammitic sequence generally known as the Central
Highland granulites, and pass conformably upwards into the
Dalradian. Two Divisions have been recognised (fig. 3.1);
the Central Highland Division, and the Grampian Division
(Piasecki, 1980).

The Central Highland Division forms a sequence of psammitic
and semi-pelitic gneisses extending northwest from a line
joining Aviemore and Forres, to the Old Red Sandstone in the
Great Glen. Pelites occur as coarse, migmatitic biotite -
gneisses. The Grampian Division occupies the rest of the
Moinian outcrop. It is also psammitic in character, but is
less metamorphosed, finer-grained and less deformed. Sedimen-
tary structures may be preserved. The two units are separated
by a major tectonic break, the Grampian Slide.

Little detailed information has been published concerning the stratigraphy of rocks in the Foyers aureole. To the south and east rocks are predominantly of the Grampian Division (Piasecki, 1980, fig. 1). Possible Dalradian metasediments do outcrop in the vicinity of Loch Killin (Johnstone, 1973, fig. 6), though these may actually be Moinian (Piasecki, 1980), and extend into the aureole along the shore of Loch Ness (Unit A of Parson, 1979). Piasecki (1980, fig.1) indicates that the Central Highland Division extends as far southwest as Loch Ruthven. Along the northeastern contact migmatitic pelites are found (Section 3.4, this study) which probably belong to the Central Highland Division (Piasecki & Van Breeman, 1979, fig. 1). The position of the Grampian Slide is uncertain. Rocks attributed to the Grampian Division do occur between Errogie and Torness (Piasecki & Van Breeman, 1979), and fine-grained psammites are found to the east of Dunmaglass Mains.

3.3.2 Metamorphism

As with the stratigraphy, little detail is available concerning metamorphic mineral assemblages and growth sequences in the Grampian Highlands. Winchester (1974) has mapped the zonal sequence in the area, based on assemblages found in calc-silicate bands (fig. 3.3). A garnet zone was recognised to the south and west. Grade increased eastwards, a kyanite zone being followed by a sillimanite zone at the highest grade. Metamorphism centred on Strathdearn, coinciding with the Central Highland Division.

Fettes (1979) has again used the calc-silicate isograds of Winchester (1974) in the Central Highlands for his metamorphic Map of the Caledonides.

FIGURE 3.3

Metamorphic map of the Central Highlands.

    c - chlorite

    b - biotite

    g - garnet

    k - kyanite

    s - sillimanite

    a - andalusite

G.G.F. - Great Glen Fault; H.B.F. - Highland Boundary
Fault.
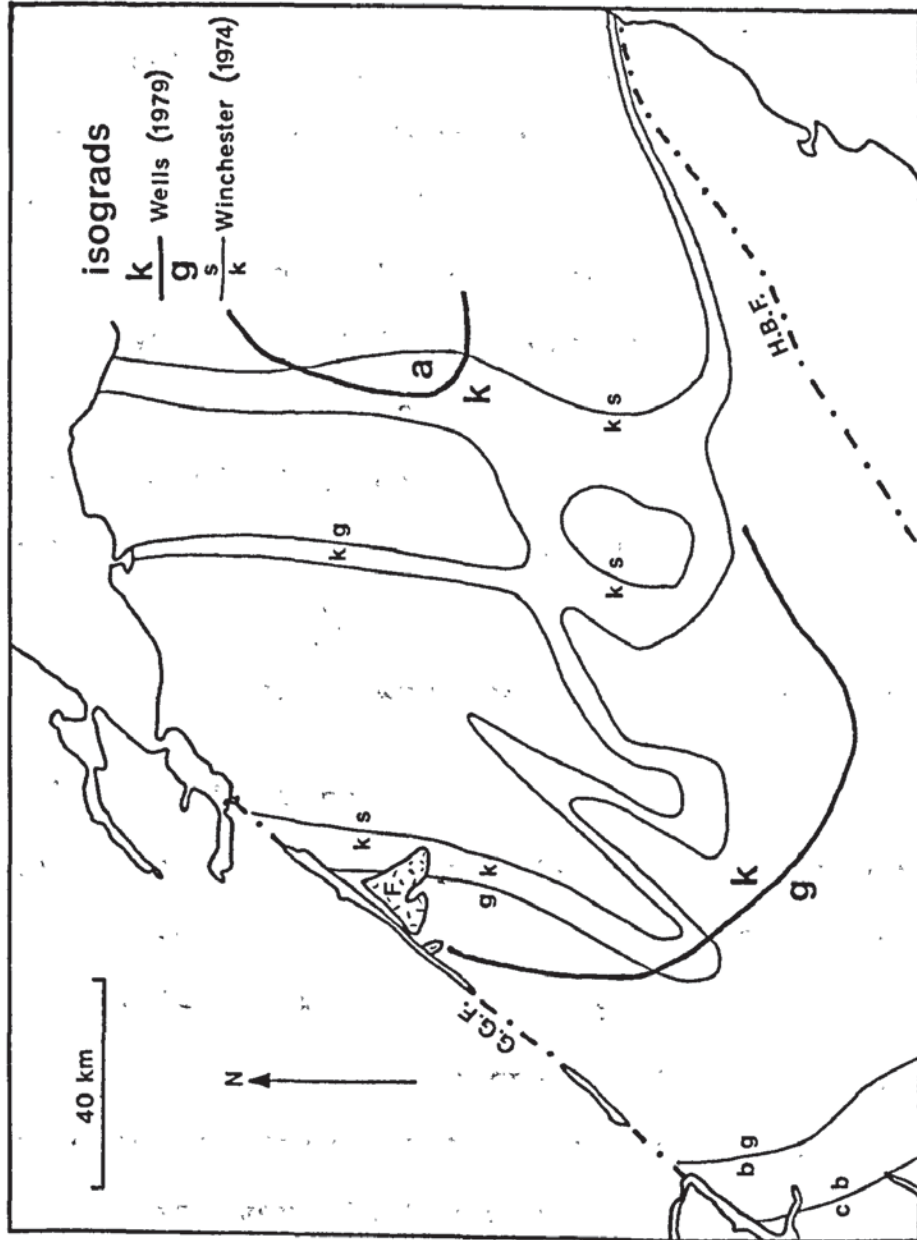
The high grade assemblages found in the Central Highland Division may be attributable to an early, possibly Precambrian, metamorphic event (Fettes, 1979; Piasecki & Van Breeman, 1979). Wells and Richardson (1979) and Wells (1979) have estimated the physical conditions of Caledonian metamorphism for the Central Highlands, using end-member calibrations of various equilibria recognised in pelitic and calc-silicate lithologies. Their results indicate high pressures, ranging from 7 kbars on Loch Laggan to 12 kbars between Loch Rannoch and Braemar. Temperatures ranged between 550°C and 640°C. The general increase in pressure and, to a lesser extent, temperature from west to east was consistent with the P and T estimate of 525°C at 5 kbars by Richardson & Powell (1976) for pelites at Spean Bridge. Conditions of 570°C at 9 kbars were estimated at Loch Killin. From the P and T conditions most of the Central Highlands were interpreted as being at kyanite grade (fig. 3.3). Garnet grade was recognised to the southwest.

3.3.3 Geological History

Precambrian ages of up to 718±19 Ma have been obtained from pegmatites within the Grampian Division, deformed by the Grampian Slide (Piasecki & Van Breeman, 1979). These have been taken to indicate the occurrence of a Precambrian amphibolite grade metamorphic event, correlated by Piasecki (1980) with the Morarian event in the western Moine.

The Central Highland Division has been correlated with the 'older' Moine of the Western Highlands, largely on the basis of lithological similarities (Piasecki, 1980). Characteristics of both the Glenfinnan Division, and the Loch Eil Division are seen. In view of this the Grenvillian event, which affects these rocks, is presumed to have also affected the

189

Central Highland Division, and is held responsible for the early, sillimanite grade migmatisation. The Grampian Division is regarded as younger than the Central Highland Division, deposition of at least part of it taking place between the Grenvillian and Morarian orogenies onto a Grenvillian basement, represented by the Central Highland Division (Piasecki, 1980).

At its top the Grampian Division passes conformably into the Dalradian (Harris et.al., 1978), which is affected only by Palaeozoic orogenic events. Assuming that a separate Morarian event has taken place, and there is some doubt concerning its status in the western Moine, a break must exist within the Grampian Division. As yet this has not been recognised, but deposition of the upper part, equivalent to the Grampian Group of Harris et.al. (1978), must have occurred between the Morarian and Caledonian orogenies.

The major Caledonian metamorphic event in the Grampian Highlands occurred at an earlier date than the comparable event in the Western Highlands (Van Breeman et. al. 1979). Rb-Sr ages of c.480 Ma (Pankhurst & Pidgeon, 1976) have been obtained from the Younger Basic complexes in N.E. Scotland, suggesting that the metamorphic climax took place around 480-490 Ma (Fettes, 1979). In Central Perthshire ages of 514 ± 67 Ma for the pre-metamorphic Ben Vuirich granite, and 491 ± 15 Ma for the Dunfallandy gneiss (Pankhurst & Pidgeon, 1976) constrain it to between 490 Ma and 500 Ma (Bradbury et.al., 1976). Lambert & McKerrow (1976) have assigned this metamorphism, and its attendant tectonism, to a separate 'Grampian Orogeny'. Richardson & Powell (1976) estimate the length of metamorphism as being between 20 and 40 My. The gap between the last peak

190

regional metamorphism and intrusion of the Foyers complex is therefore much longer than that estimated at Strontian.

3.4 PETROGRAPHY

3.4.1 Introduction

Some ninety standard thin sections and twelve polished thin sections, have been examined from samples collected in the vicinity of the Foyers complex. Assemblages are listed in Tables 3.1 and 3.2. As at Strontian particular attention has been paid to pelitic lithologies, which are found mainly in Central Highland Division gneisses to the northeast. Three zones have been identified (Map 2); an inner cordierite + K-feldspar zone; a sillimanite + K-feldspar zone and an outer sillimanite zone. Regional assemblages ranging from garnet to sillimanite grade are recognised.

Rocks within the aureole are often hornfelsic in texture, and this is particularly true of Grampian Division and Dalradian pelites and semi-pelites. Only at localities very close to the contact is the foliation lost in the coarse-grained, migmatitic pelites of the Central Highland Division. Within these rocks regional fabrics and structures are preserved and folding of migmatitic leucosomes is frequent.

Evidence of the forceful nature of the intrusion is provided by the frequent occurrence of shear structures near the contact These are particularly well seen on Beinn Dubhcharaidh (fig. 3.4), and bear a striking similarity to those recognised at Strontian (fig. 2.4). Throughout the inner part of the aureole numerous veins of granitic material are seen, often showing evidence of boudinage (fig. 3.5). Veining may become extensive enough for the rock to be described as a migmatite (fig. 3.5b).

191

TABLE 3.1

TRANSMITTED LIGHT ASSEMBLAGES

	CRD	GAR	SILL	AND	MUS	KSP	MYR	CHL	HBD	ZOI	MAP REFERENCE
B1						X					580274
B2					(X)	X	X				580264
B3					(X)	X					578267
B4					(X)	X	X				578258
B5		X^+	X		(X)						588250
B6		X^+	X		(X)						588256
B7		X^+	X		(X)						591253
B8		X^+	X		(X)		X				591253
B9					(X)	X	X				575248
B10	X	X	X		(X)	X	X				574236
B11					(X)	X	X				574236
B12		X^+			(X)	X	X				565235
B13	X	X			(X)	X	X				561248
B14	X		X		(X)	X	X				558251
B15					(X)	X					557243
B16	X				(X)	X					563236
B17			X		(X)						589243
B18			X		(X)						589238
B19			X		(X)	X					586233
B20			X		(X)	X	X				587228
B21			X			X	X				586224
B22			X		(X)						587241
B23						X	X		X		596239
B24					(X)	X	X				591227
B25			X		(X)	X					588216
B26						X	X				584213
B27	X		X		(X)	X	X				580214
B28						X					581218
B29	X		X		(X)	X					578213
B30	X	X^+	X		(X)	X	X				576205
B31	X		X		(X)	X					579209
B32	X		X		(X)	X	X				577203
B33						X	X				580206
B34					(X)	X	X				582209
B35						X					590210
B36						X	X		X		588209
B37					(X)	X					587203

3.1 (continued)

	CRD	GAR	SILL	AND	MUS	KSP	MYR	CHL	HBD	ZOI	MAP REFERENCE
B38						X	X				584202
B39		x^+			(X)	X					589120
B40					(X)	X	X				586196
B41		x^+			(X)		X				583196
B42						X					585193
B43					(X)						574236
B44		x^+									589242
B45	X				(X)		X				583212
B46	X		X		(X)	X					583212
B47	X	x^+	X	X	(X)	X	X				580214
B48	X		X		(X)	X	X				578206
B49	X		X	X	(X)	X					579202
B50			X			X					583203
B51	X				(X)	X					583203
B52		x^+	X		(X)	X	X				469169
B53		x^+	X	X	(X)	X	X				471175
B54		x^+			(X)	X	X				466167
B55			X	X	(X)	X	X				467163
B56		x^+	X		(X)	X	X				467163
B57		x^+	X		(X)	X	X				471161
B58		X			X			X			430095
B59		X			X			X			389083
B60					(X)						449130
B61		X				X			X	X	532093
B62		X			X						532093
B63		X			X						531101
B64		X			X						502126
B65					(X)	X	X				485152
B66			X		(X)	X	X				495150
B67						X			X		496150
B68					(X)						498149
B69			X		(X)	X	X				497155
B70	X	x^+			(X)	X					596191
B71	X				(X)	X					594190
B72						X			X		594190
B73	X	x^+	X			X					592194
B74	X	x^+	X		(X)						592194
B75		x^+			(X)						592194

193

3.1 (continued)

	CRD	GAR	SILL	AND	MUS	KSP	MYR	CHL	HBD	ZOI	MAP REFERENCE
B76					(X)	X	X				591198
B77	X	X+			(X)	X					594203
B78			X		X	X					598219
B79		X	X		X						633276
B80		X	X		X						630273
B81		X	X		X						623270
B82					X						620263
B83		X			X	X					611268
B84		X			(X)				X		630273
B85					X						466123
B86					(X)	X			X		500198
B87					(X)	X			X		500198
B88			X			X					513197
B89					(X)						502199

(X) Mineral regarded as secondary

+Garnet disequilibrium texture

Biotite, plagioclase and quartz are present in all specimens.

194

TABLE 3.2

OPAQUE ASSEMBLAGES

| ZONE	SAMPLE	GRAPHITE	ILMENITE	PYRRHOTITE
Cordierite + K-feldspar	B10		X	X
	B13			X
	B75		X	X
	B77		X	X
Sillimanite + K-feldspar	B56	X	X	X
	B57	X		X
Sillimanite	B8	X	X	
	B44	X	X	
Regional Garnet	B62	X		
	B64	X		
Regional Sillimanite	B79	X	X	
	B83	X	X	

FIGURE 3.4

a. & b.   Shearing and 'breccia' structures in rocks
         adjacent to the contact on Beinn Dubhcharaidh.

FIGURE 3.5

a. Boudinaged granitic vein, Beinn Dubhcharaidh.

b. Injection migmatite, quarry north of Errogie.

a

b

3.4.2 Regional Assemblages

Pelites are found to the northeast of the complex, outcropping on Craig Ruthven. They have the general assemblage: muscovite + biotite + plagioclase + quartz + ilmenite + graphite ± sillimanite ± garnet. K-feldspar occurs in one sample (B83) where sillimanite is absent. Apatite and zircon occur as frequent accessories. Chlorite may replace biotite.

The rocks are coarse grained and migmatitic, having a strong gneissose fabric which is frequently crenulated. Folding is common on all scales. Groundmass crystals range between 1 and 2mm across and porphyroblasts of garnet and muscovite are common.·

Sillimanite is fibrolitic and occurs as felts of needles included by large muscovite porphyroblasts (fig. 3.6).

Muscovite and biotite crystals up to 2mm long show a strong preferred orientation, and define the foliation. This usually shows evidence of crenulation, but a new penetrative fabric does not develop. Muscovite porphyroblasts range up to 3mm across and usually show some orientation to the foliation.

Garnet porphyroblasts are generally xenoblastic but may rarely be sub-idioblastic, overgrowing the foliation and including grains of quartz, feldspar and mica. Textural zoning is common, and consists of an outer zone heavily sieved by inclusions, while the inner core contains finer inclusions which may show some degree of orientation (fig. 3.6). These garnets are often incomplete being broken up by later deformation (fig. 3.7). They show many features recognised in texturally zoned garnets from the southwest Moine (Anderson & Olimpio, 1977).

200

FIGURE 3.6

a. ·Muscovite porphyroblasts including sillimanite.
Specimen B79.

b. Texturally zoned garnet. Inclusions in inner core
show a preferred orientation. Specimen B79.
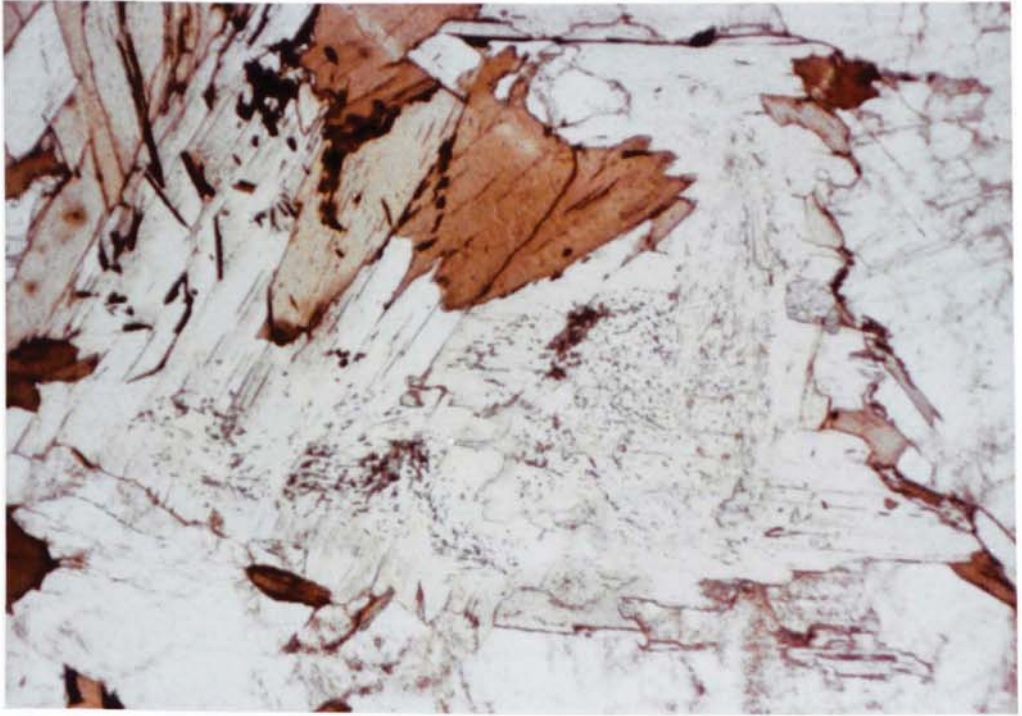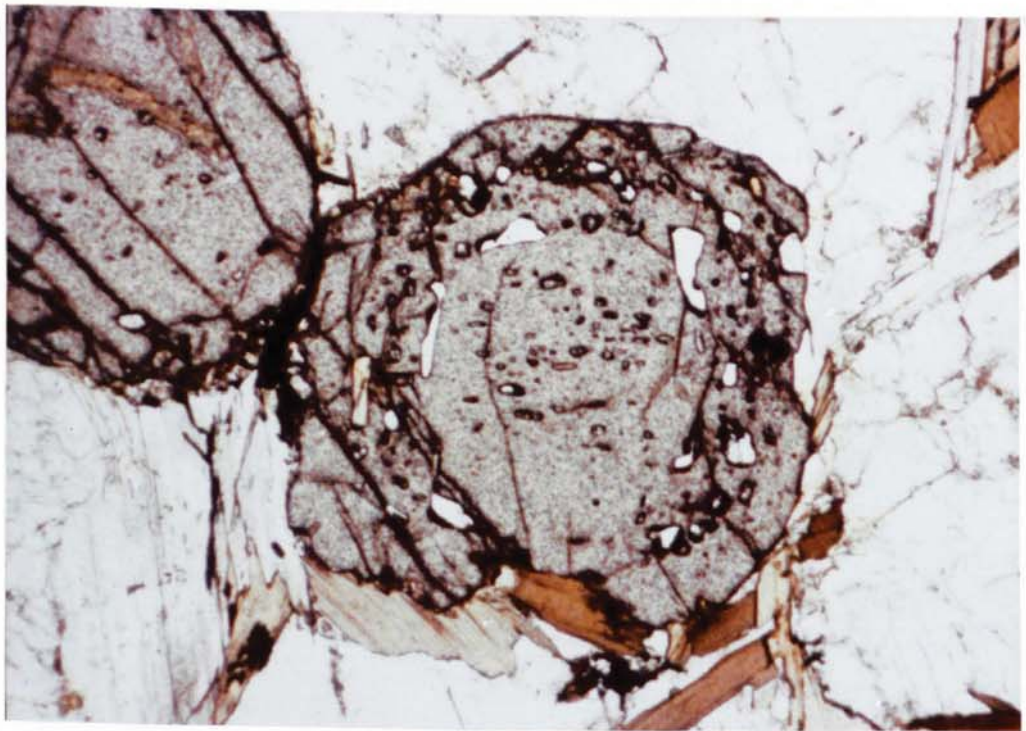
FIGURE 3.7

a. Broken garnet showing incomplete textural zoning.
   Specimen B79.

b. *Heavily sieved garnets.* Specimen B62.

a
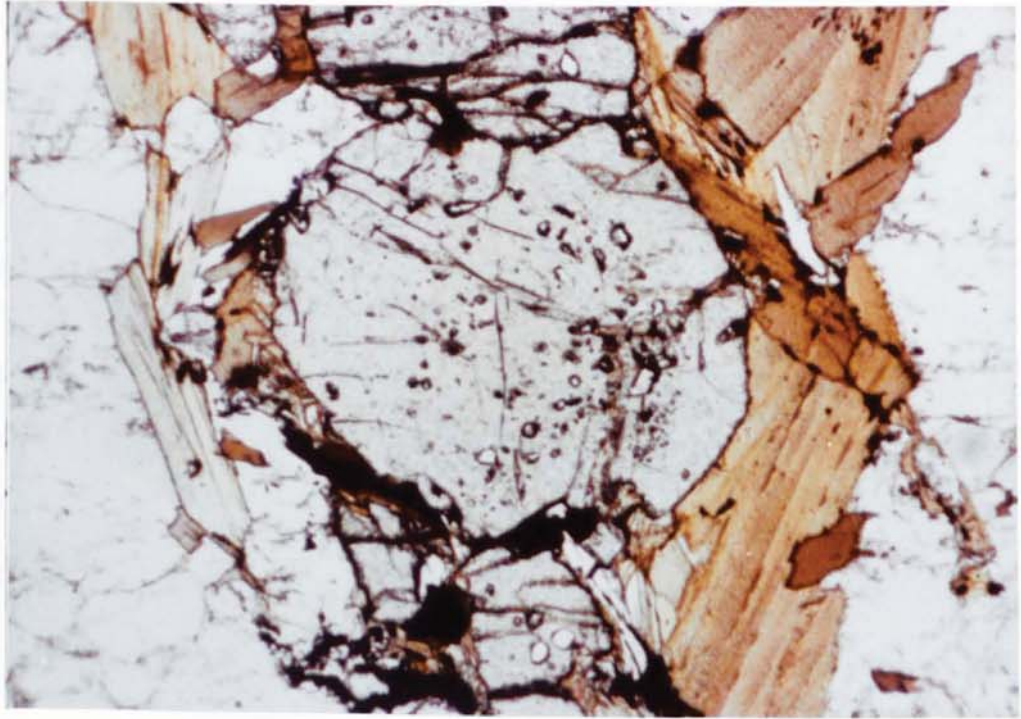
b
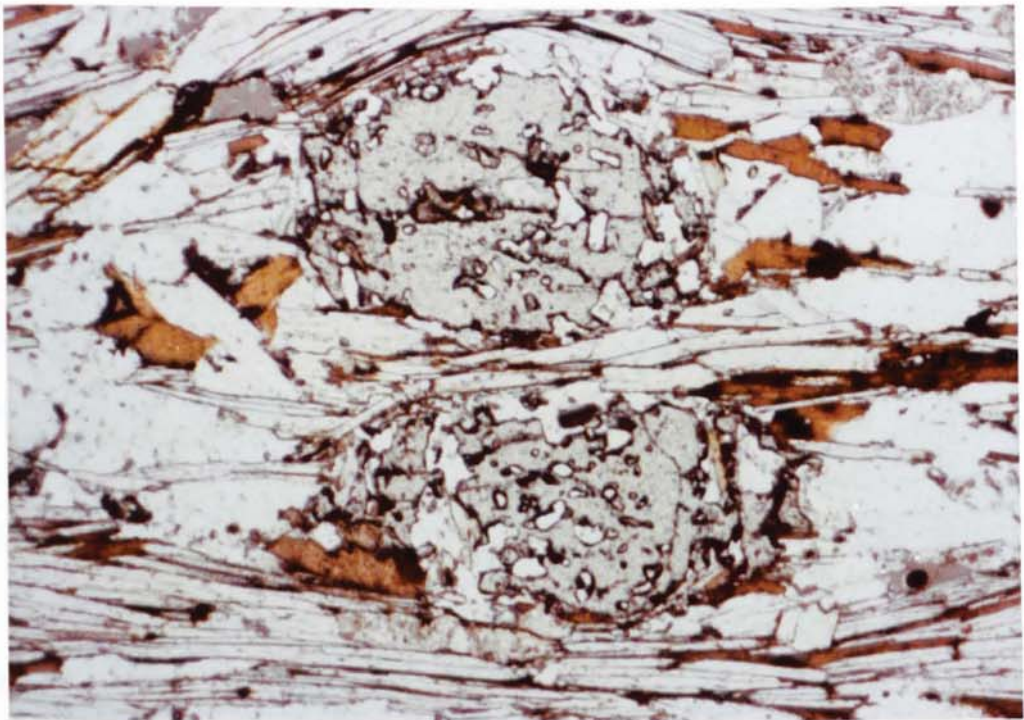
Feldspar is usually plagioclase. K-feldspar occurs as small interstitial crystals in only one sample. Plagioclase compositions range from An_{32} to A_{28} and zoning is slight.

Quartz is found ubiquitously in the groundmass.

Ilmenite and frequent graphite occur in both polished thin sections investigated.

To the south of the complex regional assemblages do not contain sillimanite. The general assemblage is muscovite + biotite + plagioclase + quartz + graphite ± garnet. Again apatite and zircon occur as accessories. Chlorite occurs as a secondary mineral after biotite.

The rocks are typically medium grained and a schistose foliation, which may show extensive crenulation, is well developed. Folding on all scales is common. Porphyroblasts are not usually seen.

In thin section muscovite and biotite pick out the foliation, with crystals up to 1mm in length. Xenoblastic garnets are frequent, and are heavily sieved and embayed by quartz (fig. 3.7b).

Plagioclase and quartz form the leucocratic portion with plagioclase compositions of An_{25} to An_{23}. Zoning is limited.

Graphite is common, being finely disseminated throughout the rock.

Further southwest, near Loch Tarff, Dalradian pelites (Unit A of Parson, 1979) occur. These are fine to medium grained and a strong schistosity is crenulated to give a well developed fold hinge lineation. Chlorite is common in thin section and

muscovite - chlorite clots, pseudomorphing garnet, are seen (fig. 3.8a). Biotite, plagioclase, K-feldspar and quartz also occur. .

3.4.3 Aureole Assemblages

3.4.3 (i) Cordierite + K-feldspar zone

In the present study cordierite has only been identified in samples to the northeast of the complex. However, Mould (1946) and Marston (1970) have recorded its occurrence to the south, and the locations are indicated on Map 2.

Pelites to the northeast have the general assemblage: biotite + plagioclase + quartz + pyrrhotite ± cordierite ± garnet ± K-feldspar ± muscovite ± ilmenite. Graphite is not recognised in those samples for which polished thin sections are available. Zircon and apatite occur as accessory minerals. Chlorite and myrmekite are secondary.

Central Highland Division pelites are coarse-grained and migmatitic, usually preserving a strong gneissose fabric (fig. 3.10b) which is lost only at locations in close proximity to the contact (fig. 3.8b). Grampian Division pelites, which outcrop at the contact between Loch Mhor and the River Farigaig, are finer grained and tend to be hornfelsic (fig. 3.9a).

Cordierite is common, occurring as relatively fine crystals, seldom exceeding 1mm in diameter (figs. 3.8b & 3.9a). Pinitisation is common, usually affecting the rims. Alteration to an orange clay also occurs.

Garnet is also common, associating with cordierite, but crystals are much smaller than those seen in regional

206

FIGURE 3.8

a. Muscovite - chlorite clots pseudomorphing garnet. Specimen B58.

b. Cordierite - biotite hornfels in Central Highland Division pelite near contact. Specimen B30.
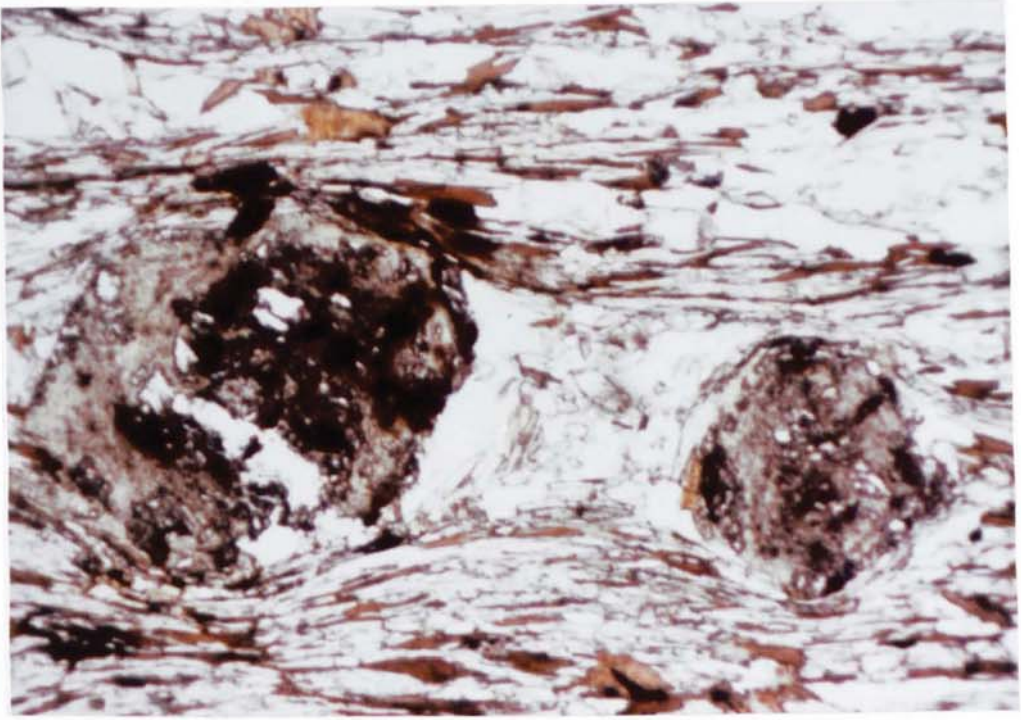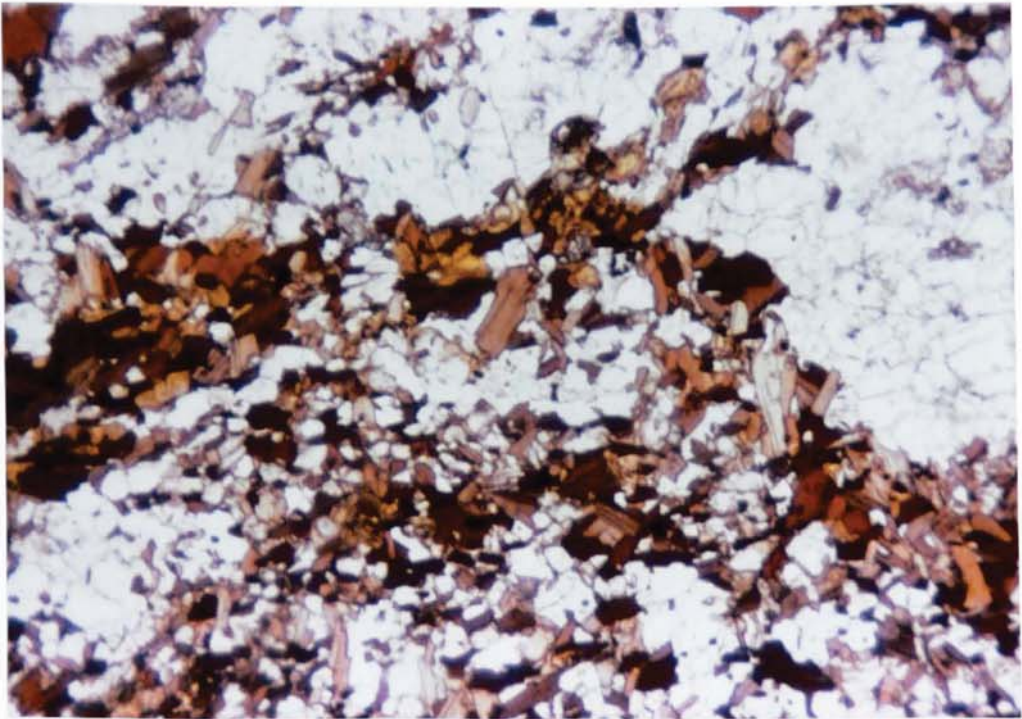
FIGURE 3.9

a. Cordierite - biotite hornfels in Grampian Division
    pelite. Specimen B10.

b. Symplectic intergrowth of garnet, biotite, plagioclase
    and quartz. Specimen B77.
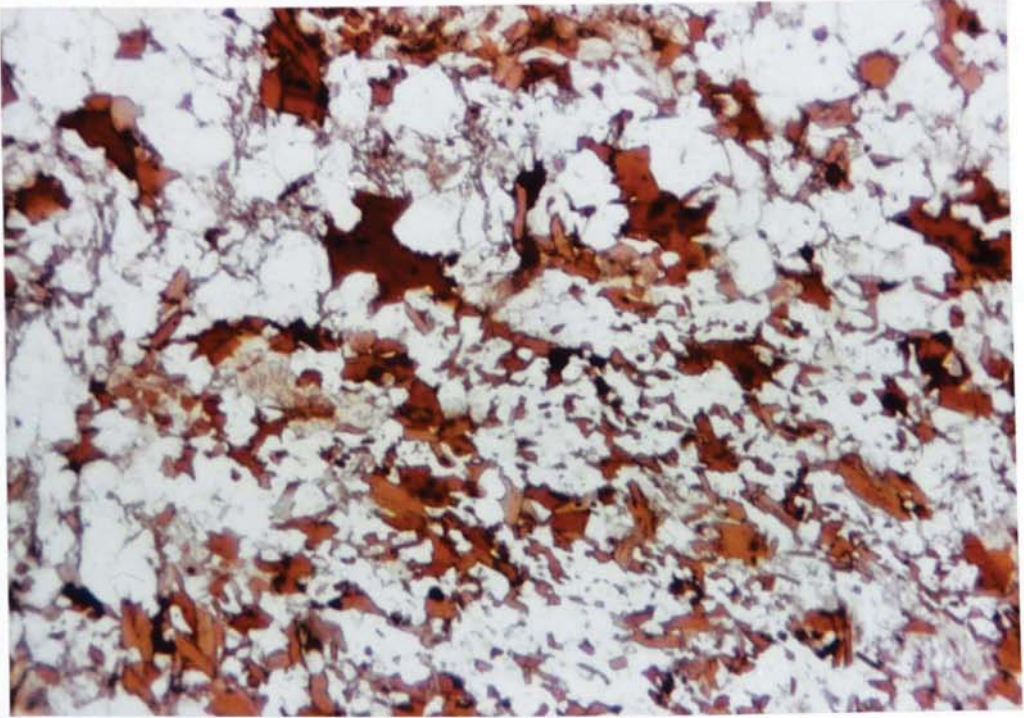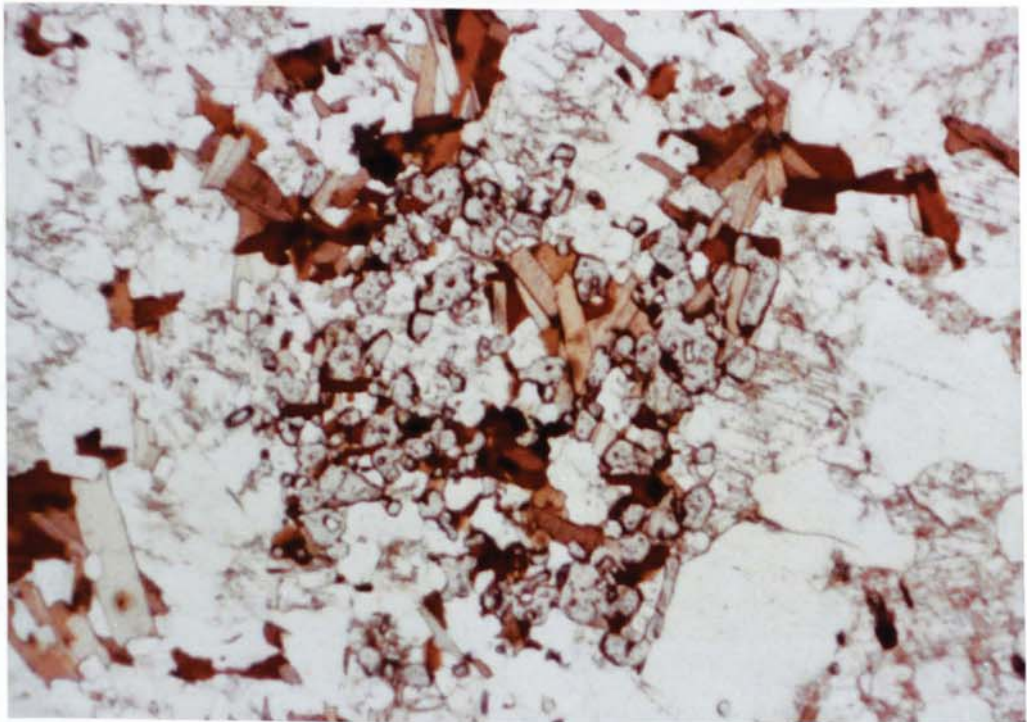
assemblages. Individual grains are usually less than 1mm
across and several grains may be found within a symplectic
intergrowth of biotite, plagioclase and quartz (fig. 3.9b).
Biotite also occurs, aligned to the foliation, as crystals up
to 2mm long.

Both sillimanite and andalusite are found, with sillimanite
occurring more frequently. Andalusite forms large sub-idio-
blastic crystals, 2-3mm across. Sillimanite may also be
coarse-grained with needles reaching 2mm in length. Typically
sillimanite is seen to replace andalusite, with stacks of
crystals orientated parallel to the andalusite z crystallo-
graphic axis (fig. 3.10a). Sillimanite can also occur as
felts of fine needles.

Muscovite occurs as fine and unorientated crystals, surrounding
andalusite and sillimanite.

Plagioclase is the most common feldspar, occurring as crystals
up to 2mm across. Albite twinning is well developed and
crystals may be antiperthitic. Its composition is in the
oligoclase – andesine ranging from An_{24} to An_{31}. Zoning is
common with the anorthite content decreasing to the rim, but
rarely by more than 2-3%.

K-feldspar varies widely in the extent of its occurrence, and
is more common in Grampian Division lithologies. It usually
occurs as small, interstitial grains, less than 1mm across.
However, some samples may contain grains up to 1.5mm, which
can be perthitic. Replacement by myrmekitic intergrowths
is common.

Quartz is again a ubiquitous constituent of the groundmass

FIGURE 3.10

a. Sillimanite replacing andalusite. Specimen B47.

b. Sillimanite surrounded by fine, unorientated
    muscovite. Specimen B19.
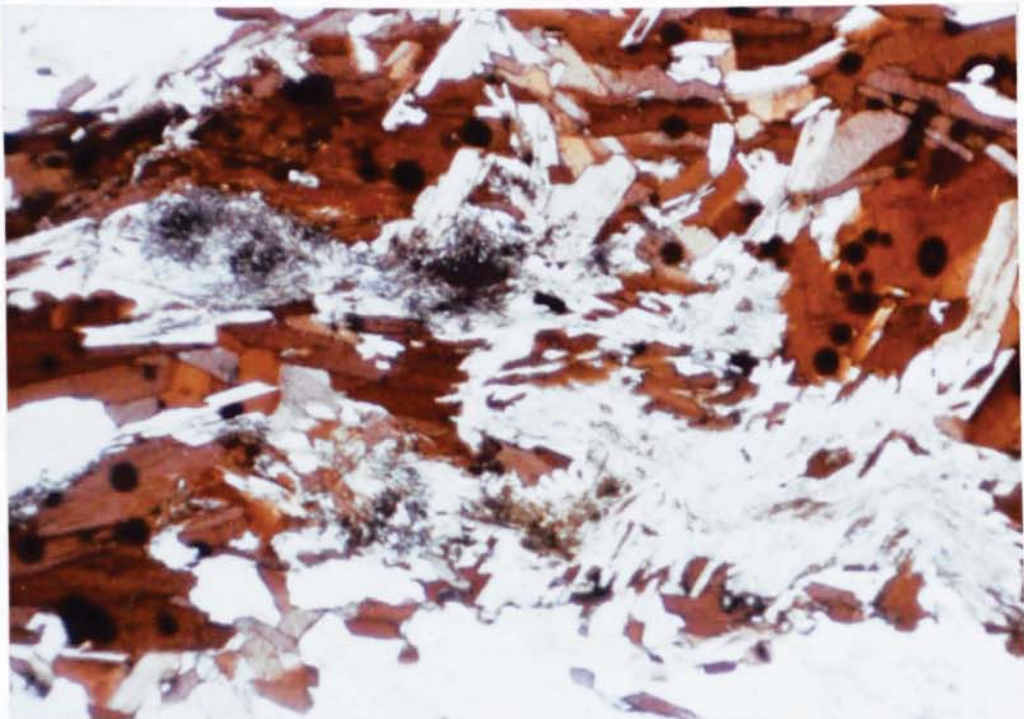
and frequently displays subgraining due to strain.

Pyrrhotite and ilmenite form the opaque assemblage, and may
be quite coarse, reaching 0.5mm across. Some pyrrhotites may
be sub-euhedral.

3.4.3 (ii) Sillimanite + K-feldspar zone

Sillimanite + K-feldspar assemblages have been identified in
both the northeast and southern aureoles. To the northeast
they are developed in Central Highland Division pelites.
These rocks have a similar appearance to those in the cordierite
+ K-feldspar zone being coarse-grained with a well developed
gneissose fabric. A hornfelsic texture does not develop.
They have the assemblage: biotite + plagioclase + quartz $\pm$
sillimanite $\pm$ K-feldspar $\pm$ muscovite. Apatite and zircon occur
as accessories. Alteration of biotite to chlorite, and of
.K-feldspar to myrmekite may be seen. Garnet is not recognised.
Polished thin sections are not available, but opaques are pre-
sent and are presumed to be a combination of pyrrhotite,
ilmenite or graphite.

Andalusite is not seen, and sillimanite occurs as felts of
needles, commonly associated with biotite, which picks out the
foliation (fig. 3.10b). As in the cordierite + K-feldspar zone,
sillimanite is often surrounded by fine and unorientated mus-
covite.

K-feldspar occurs as fine interstitial crystals ranging up to
1mm in diameter.

Plagioclase crystals may be up to 2mm across, and have oligo-
clase compositions ranging from An_{26} to An_{30}. Slight zoning
may be present.

In the southern aureole similar assemblages are seen in the Grampian Division metasediments. The Dalradian metasediments found along the shores of Loch Ness, however, differ considerably. These rocks are dark coloured, with a 'glassy' texture making the foliation difficult to identify. They have the assemblage: muscovite + biotite + plagioclase + K-feldspar + quartz + pyrrhotite + ilmenite ± garnet ± andalusite ± sillimanite ± graphite. Apatite and zircon form accessories. Chlorite may replace biotite and myrmekite replaces K-feldspar.

In thin section garnet porphyroblasts are xenoblastic forming crystals up to 1.5mm across. They may be associated with symplectic intergrowths of biotite, muscovite, plagioclase and quartz. Biotite occurs up to 1mm in length and may show a good perferred orientation. The foliation is seen flowing around garnet (fig. 3.11a).

Andalusite and sillimanite are coarse, with andalusite occurring as porphyroblasts up to 3mm in diameter. Sillimanite forms needles up to 2mm long, and again appears to replace andalusite. They may be orientated to the foliation. Muscovite is common, usually surrounding sillimanite and andalusite.

K-feldspar occurs either as interstitial crystals, or as large perthite crystals which may be porphyroblastic (fig. 3.11b). By contrast plagioclase is relatively rare, forming small and generally untwinned groundmass crystals. Its composition is oligoclase, An_{25}.

Opaques are relatively common in these rocks, with pyrrhotite and ilmenite occurring in both those investigated. Graphite is very common in B56, with fine grains disseminated through-

FIGURE 3.11

a. Foliation 'flowing around' garnet.   Specimen B56.

b. Perthite porphyroblast.   Specimen B56.
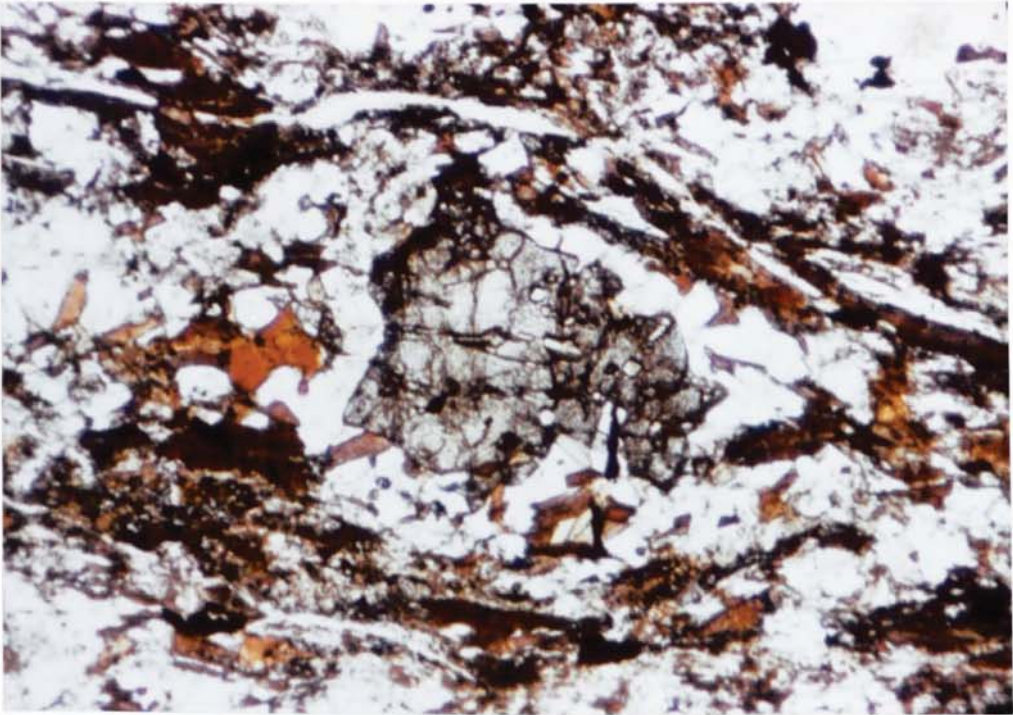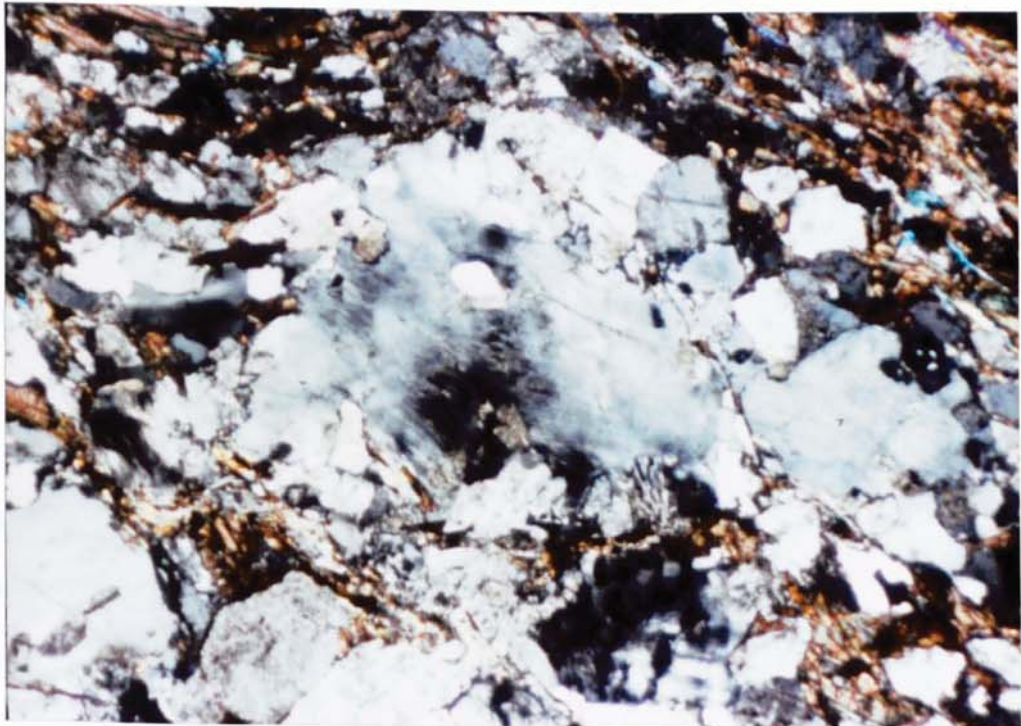
out the rock.

In one sample taken from Grampian Division rocks to the east
of Dunmaglass Lodge (B78), muscovite, of a similar appearance
to that seen in regional assemblages, is recognised coexisting
with sillimanite and K-feldspar. Sillimanite occurs in the
cores of the muscovite. The K-feldspar is microcline (fig.
3.12a).

3.4.3 (iii) Sillimanite Zone

The sillimanite zone is recognised only in pelites from the
northeast aureole. They have the assemblage: biotite + plagio-
clase + quartz + ilmenite + graphite $\pm$ sillimanite $\pm$ muscovite
$\pm$ garnet. Apatite and zircon form accessories. Chlorite may
occur as alteration of chlorite.

Again the rocks are coarse, migmatitic gneisses having a strong
foliation. In thin section this foliation is picked out by
the strong preferred orientation of biotite. Sillimanite
occurs as felts of fine needles, associated with biotite.
Muscovite is fine and unorientated, and usually surrounds
sillimanite felts. Coarse, regional muscovite is not seen in
this zone.

Garnet occurs as irregular and fragmentary crystals up to 2mm
across, associated with intergrowths of fine unorientated
biotite, plagioclase and quartz (fig. 3.12b). These are inter-
preted as a disequilibrium texture and all stages of replace-
ment are seen (fig. 3.13). Where garnet is absent from the
intergrowth they are taken to indicate its former presence.

Plagioclase crystals are up to 2mm across and compositions
range from An_{25} to An_{35}. Ilmenite and finely disseminated
graphite are common.

FIGURE 3.12

a. Muscovite + sillimanite + K-feldspar assemblage. K-feldspar is microcline. Specimen B78.

b. Disequilibrated garnet. Specimen B44.
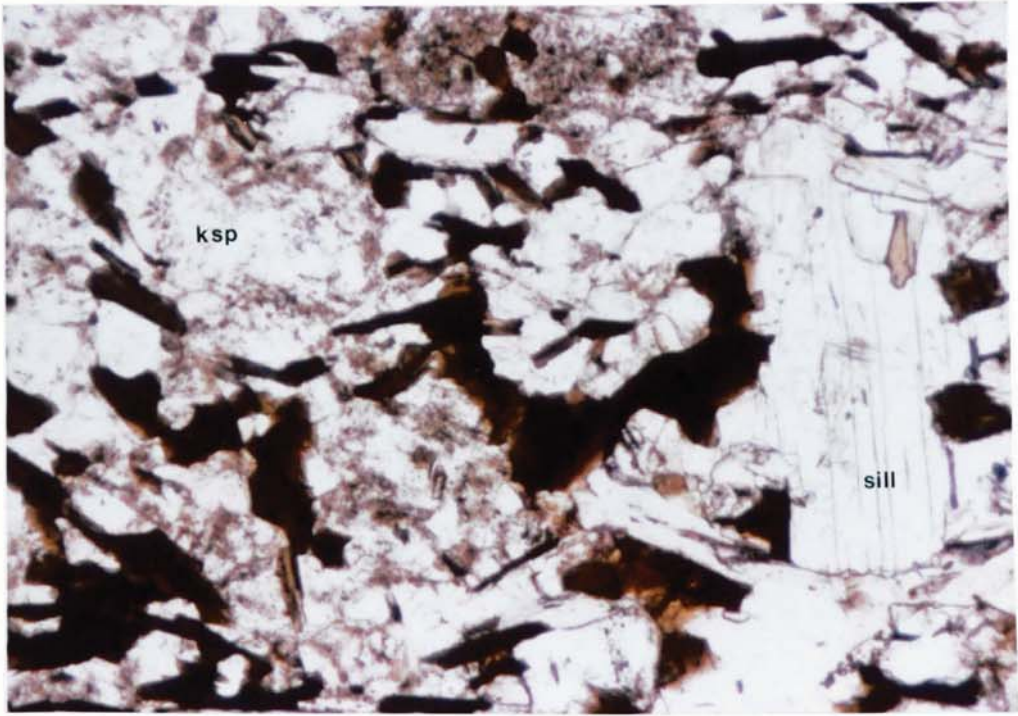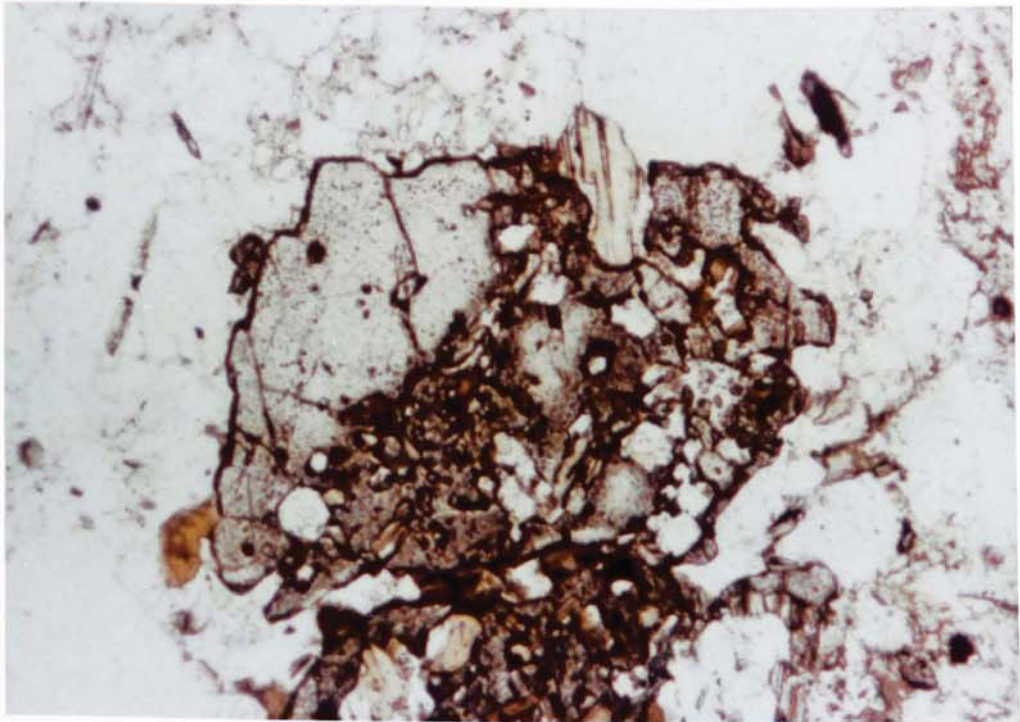
FIGURE 3.13

a. & b. Replacement of garnet by intergrowths of biotite,
plagioclase and quartz. Specimen B8.
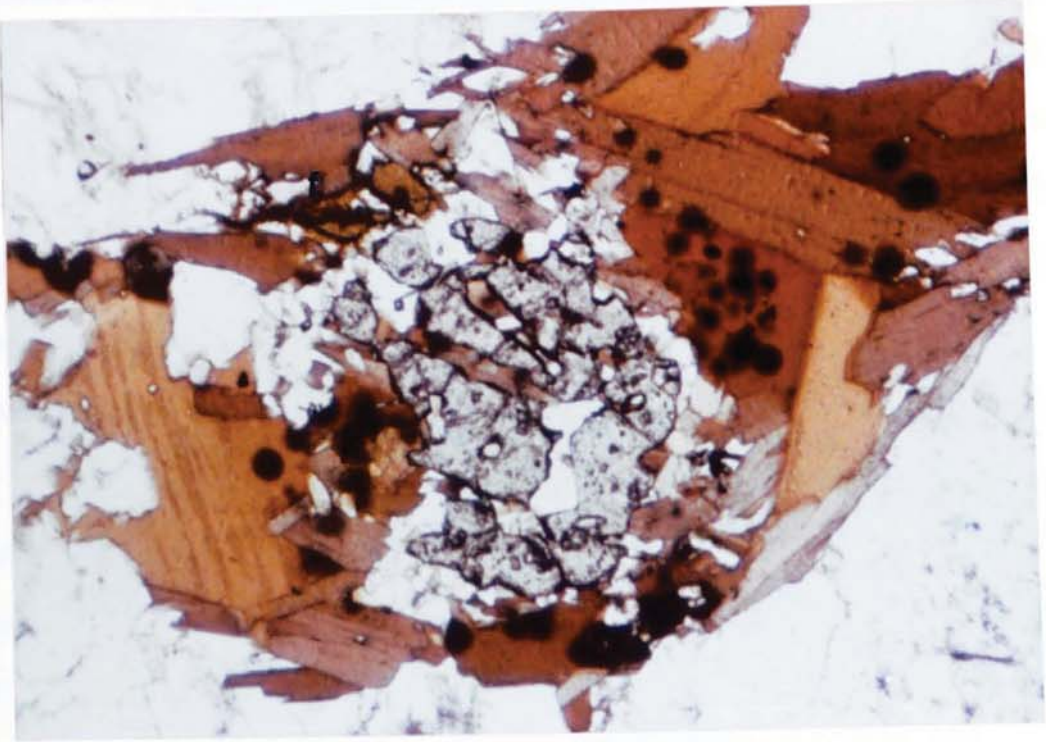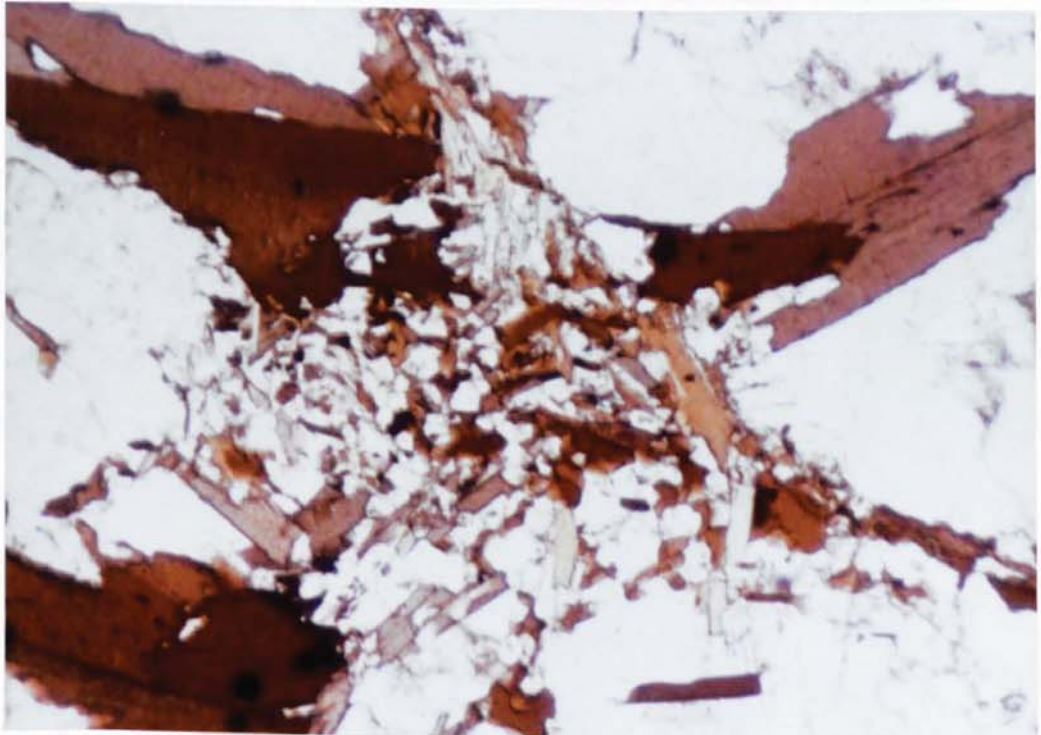
3.4.4 Mineral Parageneses

Regional assemblages to the northeast of the aureole are characterised by the occurrence of large, well equilibrated muscovite and garnet crystals. Aureole assemblages do not contain primary muscovite, and garnets typically display reaction textures. On this evidence a 'muscovite out' isograd, representing the outer limit of contact metamorphism, can be drawn based on the reaction

$$\text{muscovite} + \text{garnet}_1 + \text{biotite}_1$$
$$= \text{garnet}_2 + \text{biotite}_2 + \text{sillimanite} + \text{quartz}. \quad (44)$$
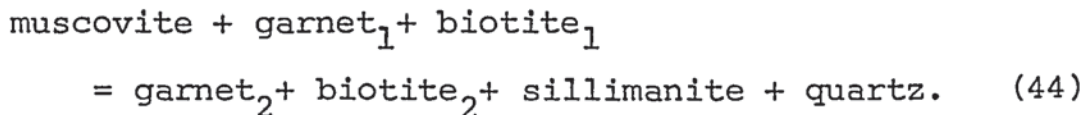
The grossular component of garnet is consumed by the reaction

$$\text{grossular} + 2\ \text{sillimanite} + \text{quartz} = \text{anorthite} \quad (19)$$
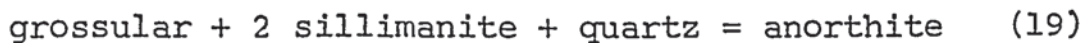
and the combination of the two reactions has produced the observed pseudomorphs of biotite, plagioclase and quartz after garnet. It also accounts for the general scarcity of sillimanite in these pseudomorphs.

The amount of sillimanite present is dependent on the relative amounts of garnet and muscovite present in the original regional assemblage. Where muscovite was scarce, sillimanite will be scarce above the isograd. In this case garnet will be preserved and will display evidence of reaction. Where muscovite was common, sillimanite will be common above the isograd. However, unless the molar occurrence of muscovite and garnet is in the correct ratio so that both will be consumed, primary muscovite would be expected to survive at the expense of garnet. This is not the case, and a third reaction is necessary to account for the disappearance of muscovite.

Large modal amounts of sillimanite generally occur in the sillimanite + K-feldspar zone, associated with K-feldspar.

A reaction of the form

muscovite + quartz = sillimanite + K-feldspar + quartz (1)

is presumed to have occurred. If adjustment of garnet comp-
osition by (44) and (19) was occurring at the same time as
reaction (1), the overall reaction in initially muscovite-
rich rocks would be a combination of (1), (19) and (44), so
that

muscovite + garnet + quartz

= sillimanite + biotite + K-feldspar + plagioclase + H_2O. (45)

The rocks sampled from Carn Ardachy are K-poor. As a result
they plot towards the garnet end of the muscovite + garnet +
biotite field of the KFM diagram in fig. 3.14 (Point A), with
only minor amounts of muscovite available below the isograd.
Operation of reaction (44) results in rock A losing muscovite
and reduces the amount of garnet present. In more K-rich
specimens (Point B) reaction (44) results in the loss of
garnet, assuming equilibration to aureole conditions is com-
plete. This is best seen in the southern aureole, and in the
cordierite + K-feldspar zone, where disequilibrium textures
associated with garnet are seen together with sillimanite and
K-feldspar. In the most K-rich specimens where garnet is
absent from initial regional assemblages, reaction (1) only
will operate. This is the case in sample B78, where a mus-
covite + sillimanite + K-feldspar assemblage is recognised.

The sillimanite zone, which is recognised only in the north-
eastern aureole, is therefore regarded as a product of varia-
tions in bulk rock chemistry within the sillimanite + K-feld-
spar zone. This zone cannot be traced up to regional assem-
blages in the northeast due to poor exposure and unsuitable
lithologies in key areas. There has also been some modific-

FIGURE 3.14

KFM Diagrams

a.   Regional sillimanite zone.

b.   Aureole assemblages.
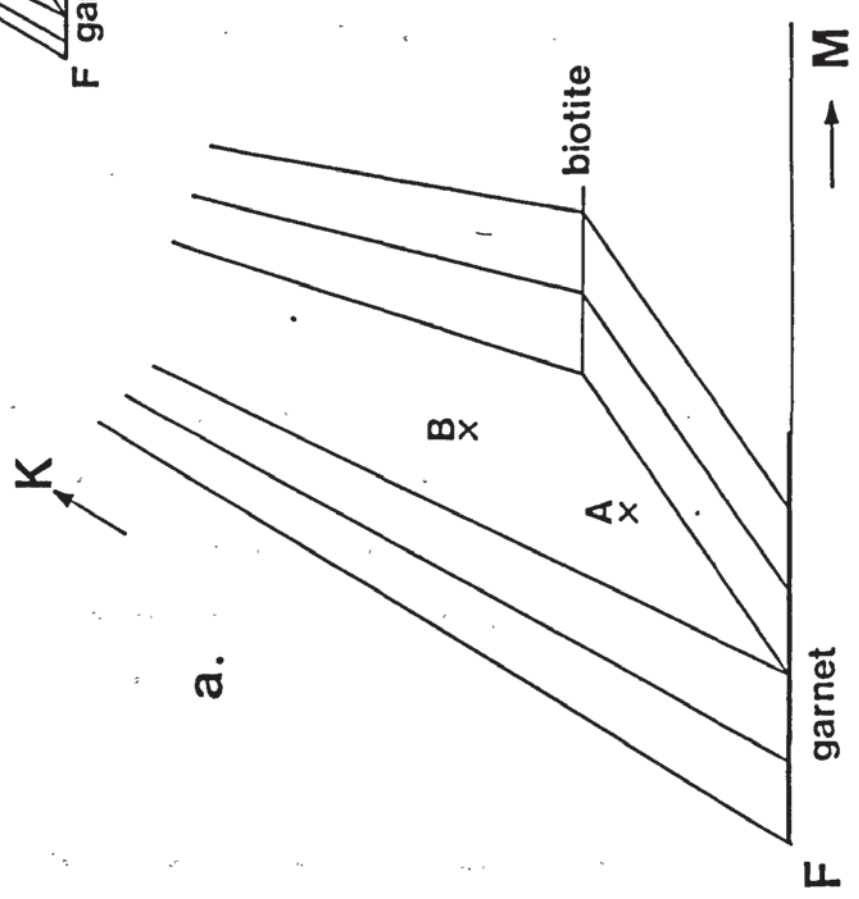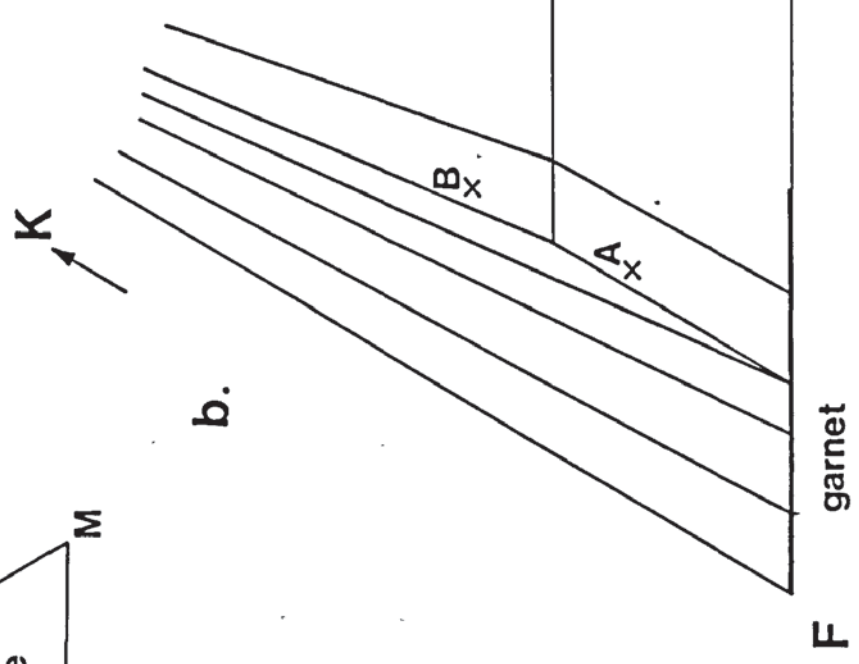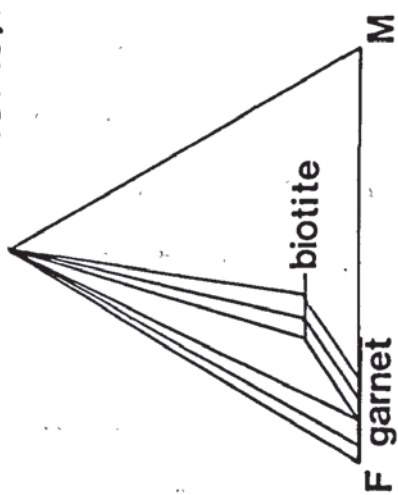
ation of the isograds by movement on the numerous N.E.-S.W. faults which cut the aureole. These are associated with the Great Glen fault and post-date both the igneous complex and the aureole.

As at Strontian the cordierite + K-feldspar isograd is defined by the reaction

sillimanite + biotite + quartz

= cordierite + garnet + K-feldspar + H_2O.   (2)
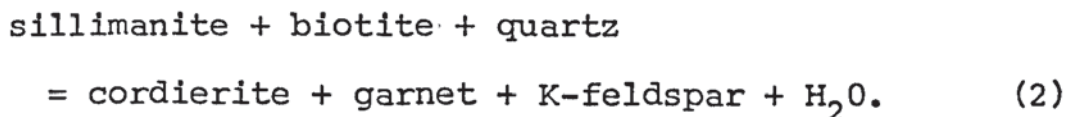
Disequilibrium textures associated with garnet persist. However, new garnet produced by the reaction would be expected to nucleate in the pseudomorphs which replaced regional garnet.

In the southern aureole garnet in the Dalradian metasediments persists in the same sites occupied by regional garnet. The apparent pre-foliation age indicated by the foliation 'flowing around' garnet may therefore be attributed to a relict regional fabric.

The occurrence of andalusite and sillimanite together suggests a close proximity to the reaction.

andalusite = sillimanite,   (46)

and textures indicating the replacement of andalusite by sillimanite are common.

Muscovite is seen throughout the aureole as fine, unorientated crystals closely associated with sillimanite. It is interpreted as secondary produced by retrogression of reactions (1), (44) and (45). Some muscovite may also be attributed to late, hydrothermal alteration.

3.4.5 Migmatites

The Central Highland Division pelites in the northeast aureole

are highly migmatitic (fig. 3.15a). They are trondhjemitoid in composition with leucosomes up to 10mm in width. Plagioclase and quartz crystals occur up to 3mm across and muscovite and biotite may also be present (fig. 3.15b). These migmatites persist into the aureole, and granitoid migmatites, with K-feldspar produced by reaction (45), are also seen (fig. 3.16).

At some locations migmatites occur where the leucosome, which consists of biotite, plagioclase, K-feldspar and quartz, has a distinctively igneous appearance (fig. 3.5). Oscillatory zoning is seen in plagioclase and euhedral apatite crystals are common. They are therefore interpreted as injection migmatites, magma being derived from the pluton.

Associated with this phenomenon minor leucosomes, up to 5mm across and cutting across the foliation are seen in the country rock (fig. 3.17a). These are trondhjemitoid in composition, and a melanosome may be developed at their edge (fig. 3.17b). The absence of K-feldspar and euhedral apatite suggests that they do not have an intrusive igneous origin. As they are discordant to the foliation, they may be interpreted as the product of contact metamorphism. Similar fine leucosomes are associated with the shearing seen on Beinn Dubhcharaidh (fig. 3.4), as well as veins of definite igneous origin.

Microperthite - granitoid leucosomes occur in Dalradian metasediments from the sillimanite + K-feldspar zone in the southern aureole. However, K-feldspar-rich bands of sedimentary origin are seen in regional specimens, and these may provide the basis for such leucosomes in the aureole.

FIGURE 3.15

Regional trondhjemitoid migmatites

a. Hand specimen B80.

b. Thin section B80.
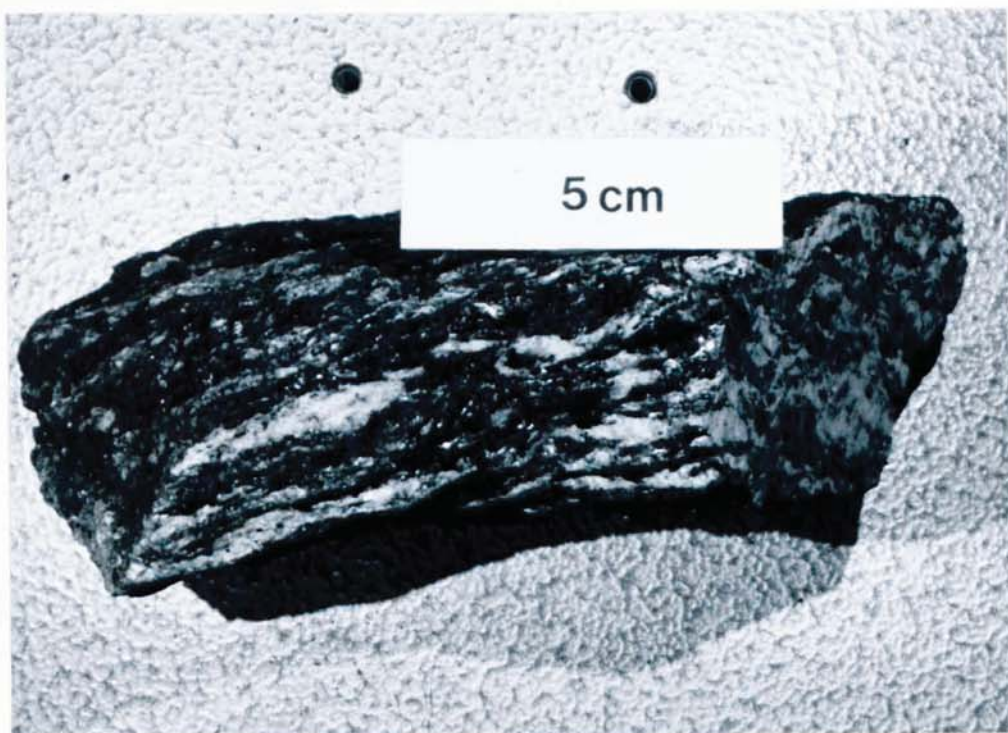
FIGURE 3.16

Aureole granitoid migmatite

a.   Hand specimen,   B47.

B.   Thin section, cross polarised light, B47.
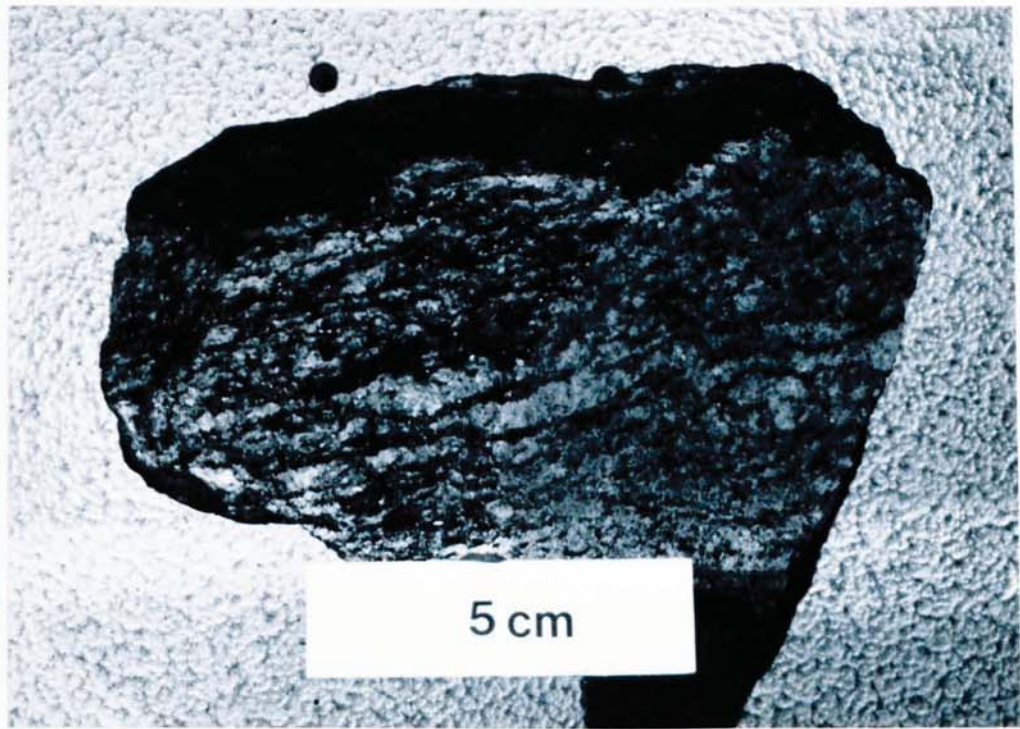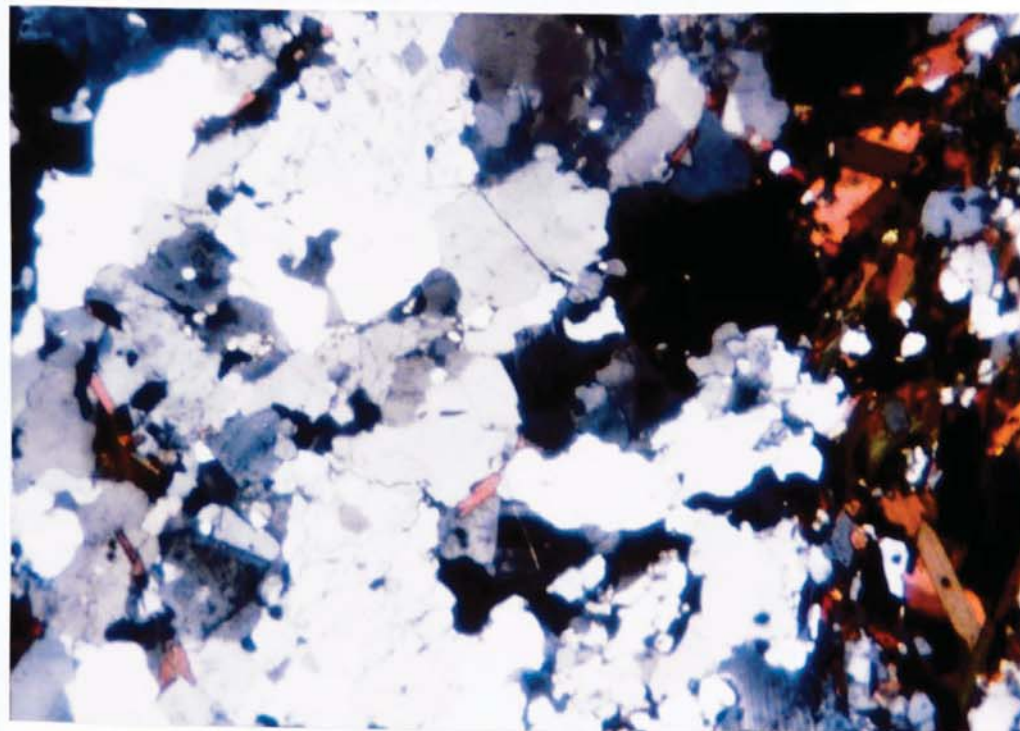
FIGURE 3.17

Anatectic migmatite

a. Hand specimen, B43.

b. Thin section, B43.
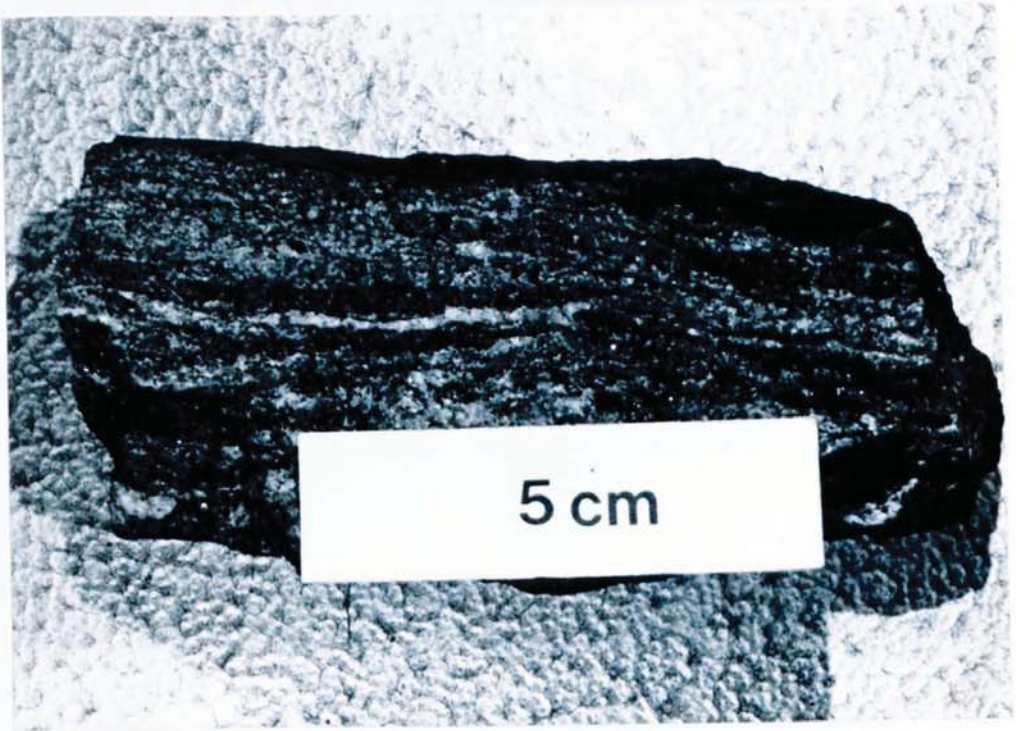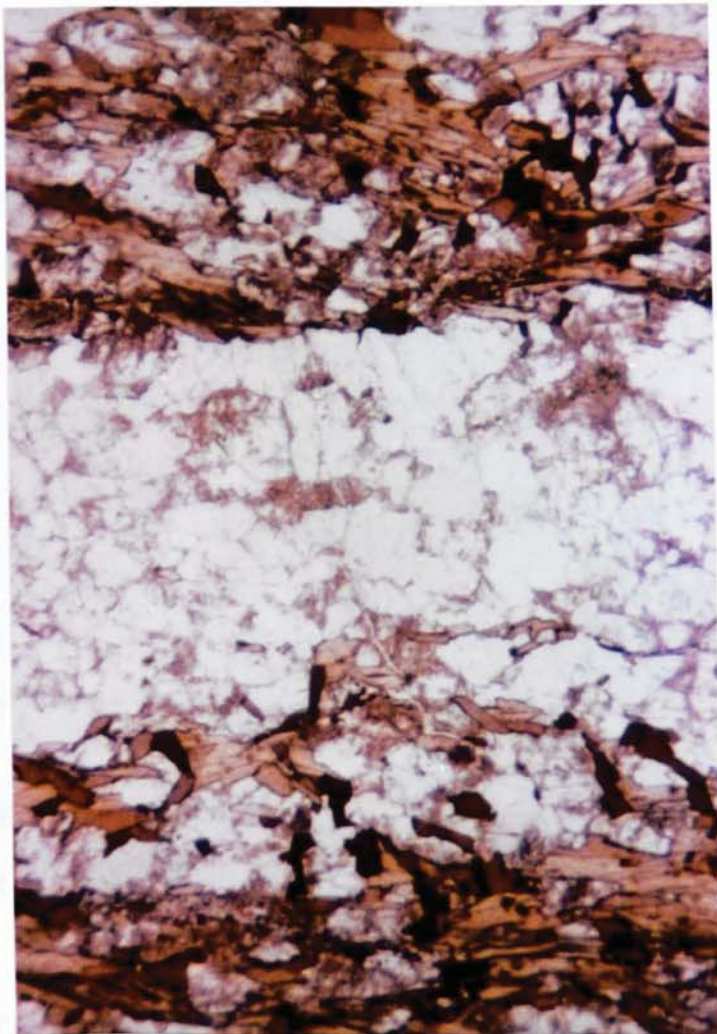
3.5 GARNET ZONING

3.5.1 Description

Zoning profiles from seven garnets, located on fig. 3.19, are presented in fig. 3.18 a-g. Representative analyses are given in Appendix III, Table 1.

Two garnets have been investigated from the cordierite + K-feldspar zone. In B10 the observed profile shows many similarities to those seen in the Strontian aureole. Both Fe and Mg decrease outwards to the rim, while Mn increases. Ca shows no zoning. The Mg/(Fe + Mg) ratio also decreases to the rim.

The profile for B77 was obtained from a small, individual grain within a symplectic intergrowth of garnet, biotite, plagioclase and quartz. Only minor zoning is seen with slight decreases in Fe and Mg, and an increase in Mn, to the rim. Ca is again unzoned.

B57 is sampled from Dalradian metasediments in the sillimanite + K-feldspar zone to the south. Fe, Mg and Mn profiles are similar to those seen in B10. Ca is zoned in this case, decreasing from core to rim.

Two profiles are presented from sillimanite zone rocks. B8, like B77, is from a small grain within a symplectic intergrowth (fig. 3.13). Again Fe and Mg decrease to the rim while Mn increases. Ca also decreases to the rim.

In B44 an unusual profile is seen. Ca and Fe both show strong zoning. The garnet (fig 3.12b) shows evidence of disequilibrium however the core is well preserved. Ca is concentrated into this core, forming some 27% of the cations present

FIGURE 3.18

Garnet Zoning Profiles

a. B10; b. B77; c. B57; d. B8; e. B44; f. B62; g. B79.

Solid circles - Fe; Triangles - Mg; Squares - Mn; Open circles - Ca; Solid line - Mg/(Mg+Fe).

Mg, Fe, Ca and Mn are plotted in atomic percentages (Mg + Fe + Ca + Mn = 100%).

Mg/(Mg+Fe) is plotted in atomic proportions.

Profiles a. & b. - cordierite + K-feldspar zone; c. - sillimanite + K-feldspar zone; d. & e. - sillimanite zone; f. & g. - regional assemblages.

f.

e.

B79

g.
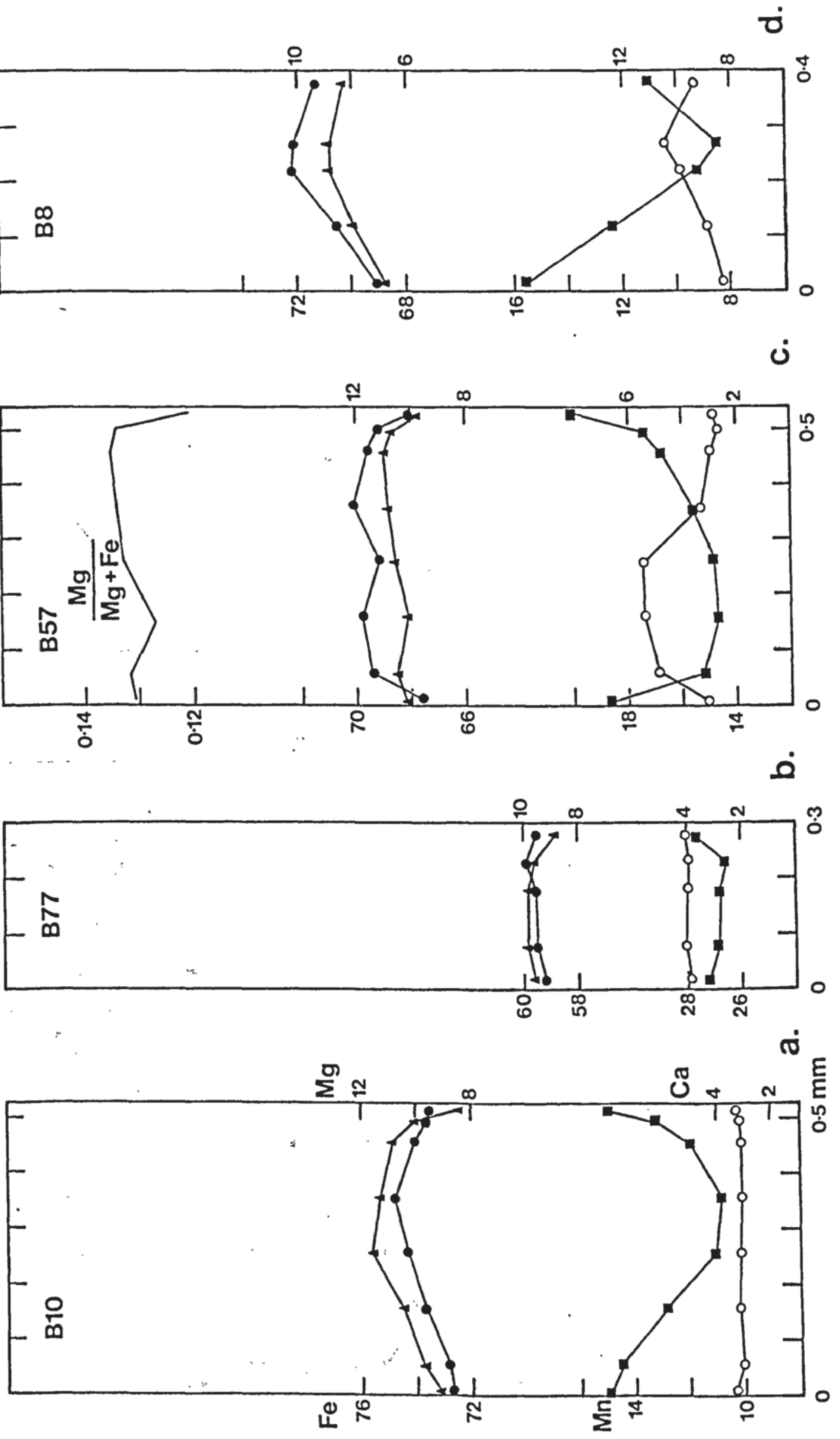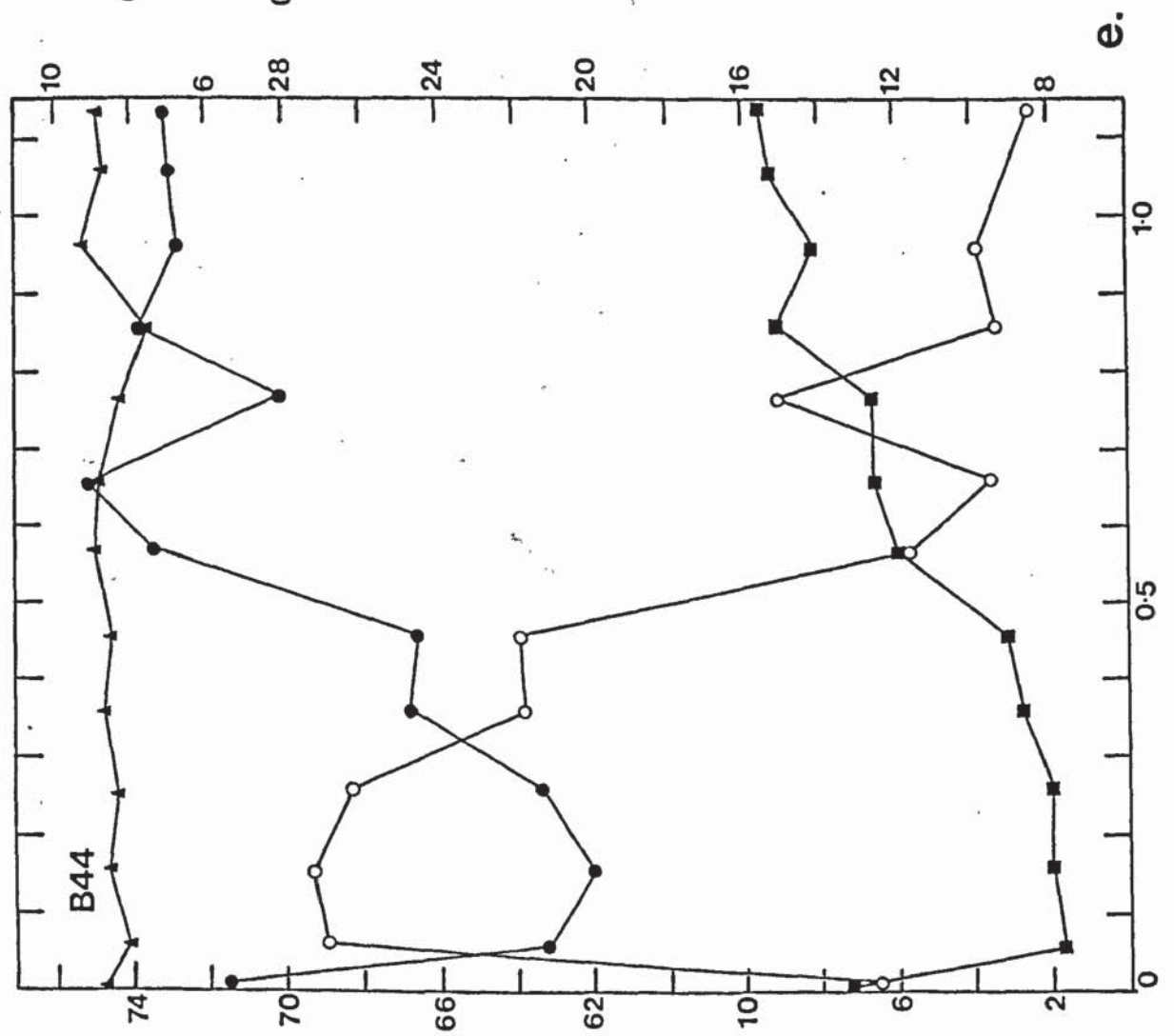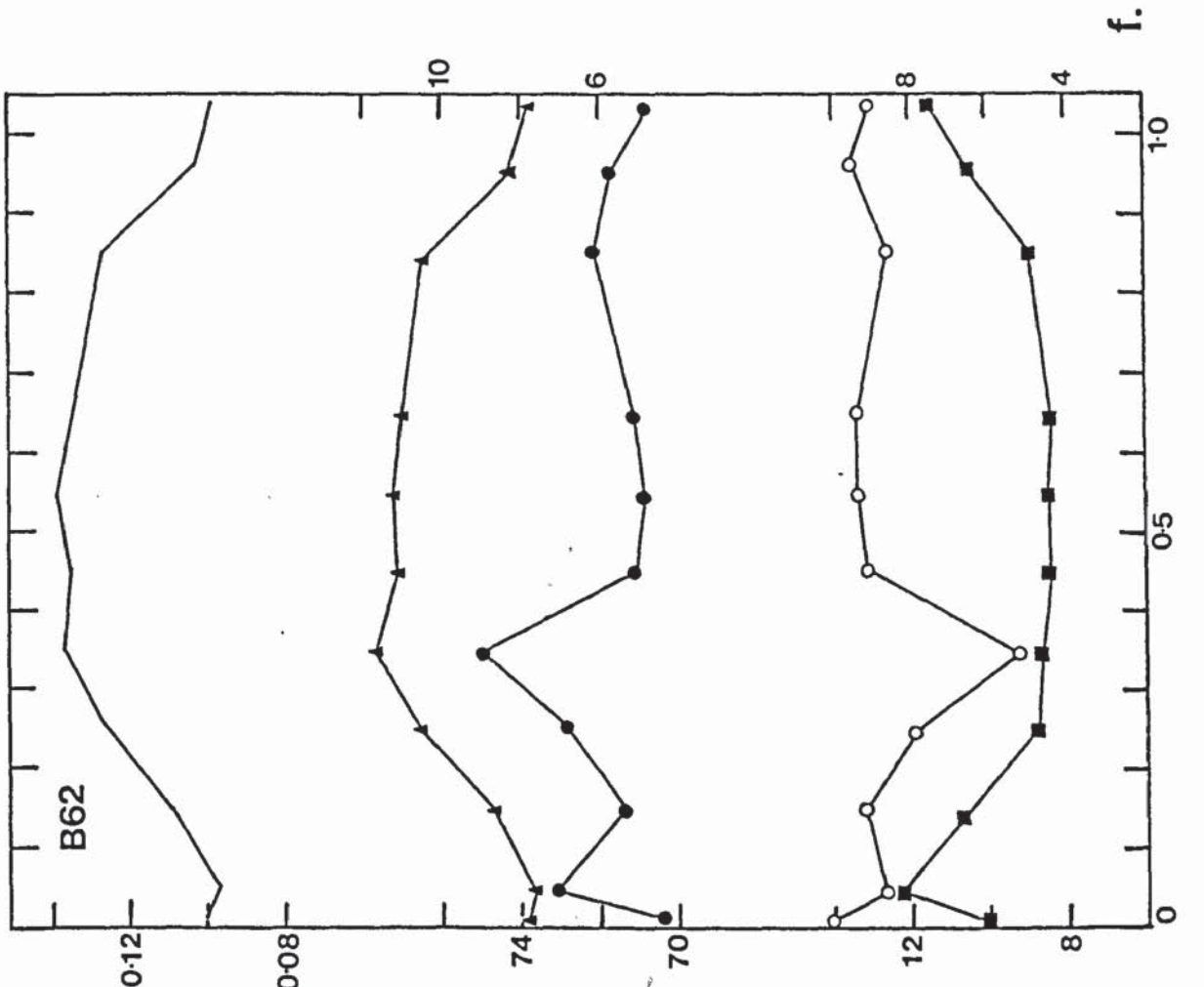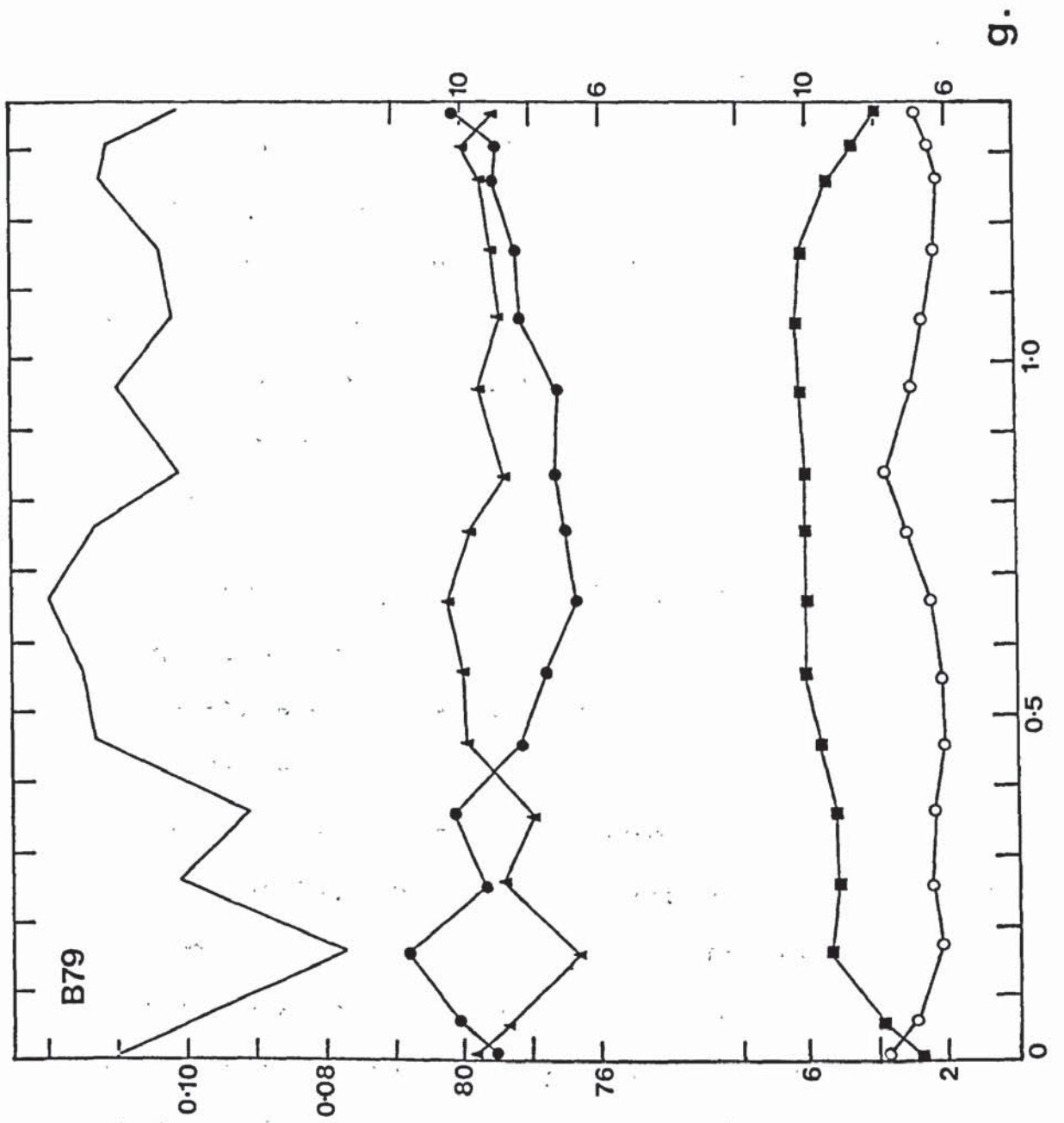
(Fe + Mg + Mn + Ca = 100%). It decreases in importance appreciably in the disequilibrated part of the grain, dropping nearly to 8% at the edge. The Fe profile mirrors this profile. Mn is low in the core, but increases steadily through the disequilibrated part. Mg shows a slight decrease in this direction.

Two profiles are available from regional assemblages. B62 (fig. 3.7b) is taken from a pelitic schist sampled near Loch Killin. Again Fe and Ca profiles are mirror images of each other. The unusual peak and trough effect in these profiles may be due to the presence of an inclusion. Fe increases from core to the right of the peak, before decreasing at the edge. Mn increases from core to rim, while Mg decreases. Mg/(Fe + Mg) increases from core to rim.

The profile from B79 is complex. The grain shows textrual zoning (fig. 3.7a), and is broken by later deformation. Zoning takes place mostly between Fe and Mg. Fe is low in the core, increasing towards the rim. A peak is reached within the outer textural zone, and then decreases to the rim. Mg mirrors this profile. Mn decreases from core to rim, while Ca, apart from a small peak, increases. The Mg/(Fe + Mg) profile which shows a low Mg content in the inner rim, increases from there into the core, and to the adjacent rim. There is also a decrease from the core to the opposite rim.

3.5.2 Interpretation

Zoning profiles are generally not as simple as those recognised at Strontian. Their interpretation is complicated by obvious reaction textures produced by the consumption of garnet in the 'muscovite out' isograd reaction.

Within the inner part of the aureole, in the cordierite + K-feldspar zones, profiles are seen which suggest that some degree of re-equilibration has taken place, with the cores representing peak conditions. This is well seen in B10 and B57. B77 suggests that small grains within symplectic inter-growths are well equilibrated. The profile of B8 indicates that this may also be true at lower grade. The profile from B44, which is a large grain with an apparently well preserved core, illustrates the disequilibrium of regional garnet compositions in the aureole. This rock which does not contain sillimanite, K-feldspar or secondary muscovite, is alkali poor and both garnet and plagioclase (An_{40}) are Ca-rich. The Ca-rich core is therefore the product of regional metamorphism. Operation of reaction (19) combined with (44) would tend to reduce the Ca content of the garnet and the rim composition in this case is interpreted as representing aureole conditions, although complete re-equilibration has probably not been achieved.

The profile from B62 is relatively simple. The Mn and Mg/(Fe + Mg) profiles suggests that volume diffusion has taken place and that peak regional conditions are represented by the core.

In B79 the textural zones are incomplete implying that they were produced during an early metamorphism, before being broken by later tectonism. The correlation of these zones with the complex zoning profile suggests that both the core and the inner rim are the product of this early metamorphism. Diffusion has not modified the profile during Caledonian metamorphism and rim compositions must be taken to represent this event.

241

Table 3.3 gives the $\ln K_D$(gar-bio) and $\ln K$(gar-plag) values interpreted as representing peak Caledonian regional, and peak aureole conditions. It can be seen that there is a general trend with K_D(gar-bio) and K(gar-plag) increasing towards the contact. Howeverm the six specimens which contain the assemblage sillimanite + biotite + garnet + plagioclase + quartz show no correlation of the two distribution measures. This is further illustration of the disequilibrium of garnet within the aureole, and is reflected principally in K(gar-plag).

3.6 P-T-X RELATIONS

3.6.1 Geothermometry

The composition of garnet, cordierite, biotite, muscovite, plagioclase and K-feldspar in ten specimens from the aureole, and surrounding regional, assemblages have been investigated by electron-probe microanalysis. Representative analyses are set out in Appendix III. The location of the specimens is shown on fig. 3.19.

Temperatures have been calculated from the calibrations of Thompson (1976b), Holdaway & Lee (1977) and Ferry & Spear (1978) for ten garnet - biotite pairs, using the $\ln K_D$(gar-bio) values given in Table 3.3. These have been interpreted as representing peak conditions. One garnet - cordierite pair is available (B10). As with the Strontian data, biotite Fe/Mg ratios are averaged from the analyses of several grains in each sample section. The results are set out in Table 3.4.

Holdaway & Lee (1977) and Ferry & Spear (1978) estimates were obtained using the preferred pressure for the aureole of 3.9 kbars (see Section 3.6.2 (i)). For B10 in the cordierite + K-feldspar zone, where garnet shows the greatest equilibration

FIGURE 3.19

Location of specimens used for electron microprobe analysis.
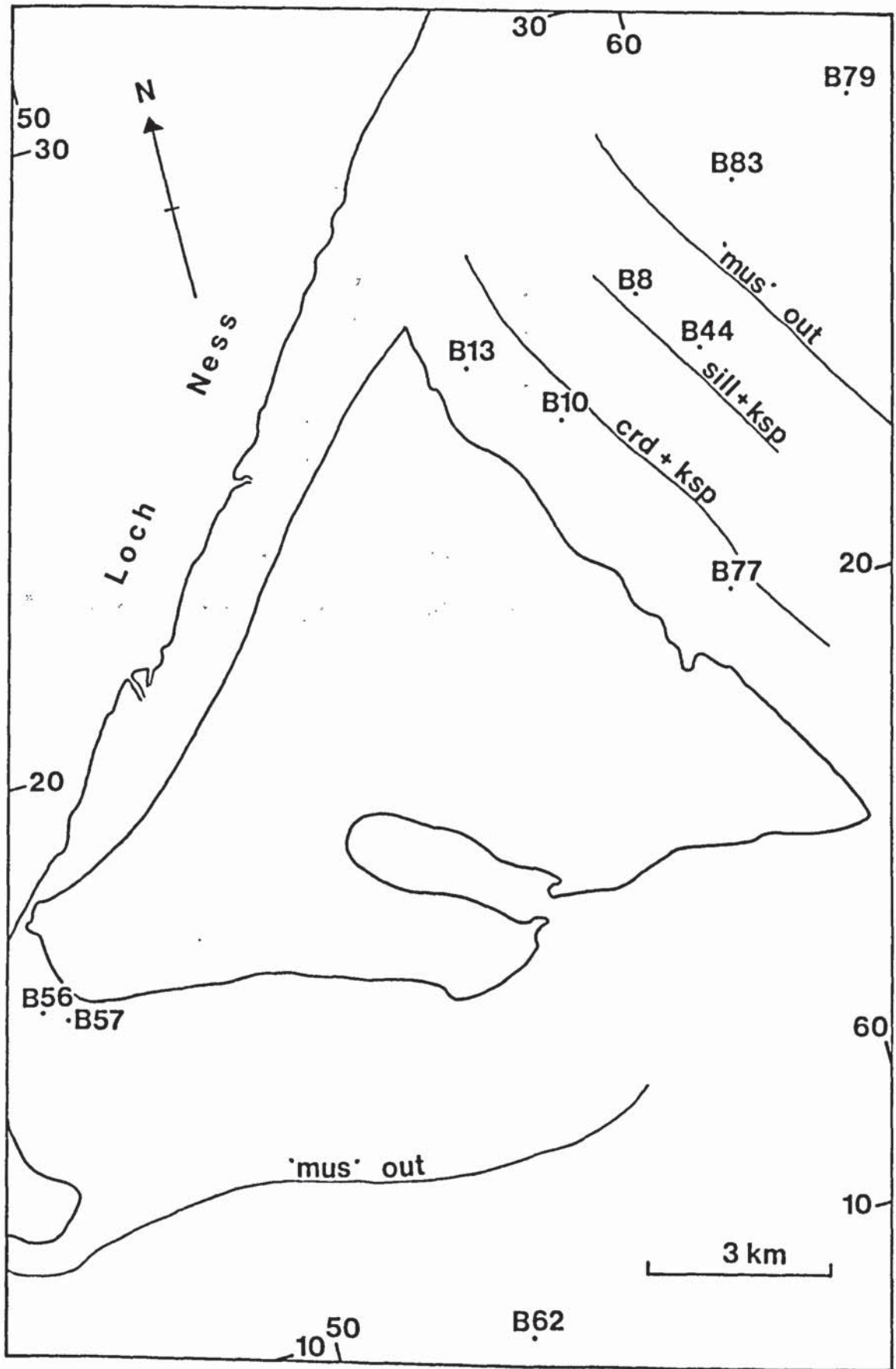
TABLE 3.3

SAMPLE	$\ln K_D$(gar-bio)	Plagioclase	$\ln K$(gar-plag)
[+]B10	-1.350	0.31[*]	-6.908
[+]B13	-1.478	0.28	-6.701
B77	-1.518	0.28	-5.838
[+]B56	-1.511	0.25	-3.906
[+]B57	-1.438	0.25	-6.462
[+]B8	-1.647	0.29[*]	-3.076
B44	-1.664	0.40	-4.219
B62	-1.536	0.24	-2.812
[+]B79	-1.874	0.32	-4.559
B83	-1.772	0.31	-3.677

[+]contains the assemblage sill + bio + gar + plag + qtz

[*]obtained by microprobe analysis

TABLE 3.4

TEMPERATURE ESTIMATES ($^{\circ}$C)

CORDIERITE + K-FELDSPAR ZONE

SAMPLE	Garnet - biotite				Garnet - cordierite		
	lnK_D	(a)	(b)	(c)	lnK_D	(a)	(b)
B10	-1.350	665	671	725	-2.039	652	658
B13	-1.478	616	636	669			
B77	-1.518	606	626	652			

SILLIMANITE + K-FELDSPAR ZONE

SAMPLE	Garnet - biotite			
	lnK_D	(a)	(b)	(c)
B56	-1.511	607	627	655
B57	-1.438	627	647	685

SILLIMANITE ZONE

SAMPLE	Garnet - biotite			
	lnK_D	(a)	(b)	(c)
B8	-1.647	572	594	603
B44 rim	-1.664	568	590	597

REGIONAL ASSEMBLAGES

SAMPLE	Garnet - biotite			
	lnK_D	(a)	(b)	(c)
B62	-1.536	601	632	667
B79 rim	-1.874	519	559	547
B83	-1.772	542	582	580

(a) Thompson (1976b)

(b) Holdaway & Lee (1977)

(c) Ferry & Spear (1978).

to aureole conditions, the Holdaway & Lee (1977) calibrations give 658°C for garnet - cordierite, and 671°C for garnet - biotite. Lower temperatures obtained from B13 and B77, result from retrograde reaction which affects the cores of small grains. This is reflected by the high Mn content.

The profile of B57 suggests good equilibration to aureole conditions of Fe and Mg contents. A temperature of 647°C is obtained and is regarded as a good estimate for the sillimanite + K-feldspar zone.

Estimates of 594°C and 590°C have been obtained from B8 and B44 respectively, in the sillimanite zone. These garnets exhibit considerable disequilibrium, and temperatures are not necessarily accurate.

Regional assemblages vary to the northeast and south of the aureole. B79 and B83 come from Central Highland Division gneisses, and the sillimanite grade assemblages have a Precambrian age (Piasecki, 1980). However the temperatures of 559°C for B79, and 582°C for B83 are regarded as Caledonian. These must be regarded as maximum estimates as a pressure of 9 kbars, taken from Wells (1979), has been used in the calculations. There is some uncertainty in the accuracy of this pressure and the actual figure may be lower, resulting in lower calculated temperatures (see Section 3.6.2 (ii)). These temperature estimates are in good agreement with other Caledonian estimates obtained by Wells (1979) from other Central Highland Division rocks.

B62 is from Grampian Division schists to the south. Wells (1979) has obtained an estimate of 570°C for rocks from the

same area. However garnet rim compositions have apparently been used to calculate this estimate (Wells & Richardson, 1979, p.341). The profile obtained from B62 bears all the features of a garnet which has undergone retrograde reaction at its rims, compositions representing peak conditions being found in the core. Therefore the estimate of $632^{\circ}C$ obtained from the core is preferred in this case.

3.6.2 Geobarometry

3.6.2 (i) Aureole Pressures

A pressure estimate of 3.9 kbars, with an X_{H_2O} of 0.14, has been calculated from the one garnet - cordierite pair available using the method of Holdaway & Lee (1977). The garnet - cordierite temperature of $658^{\circ}C$ obtained from the Holdaway & Lee (1977) calibration, was used for the calculation. This is regarded as the best estimate available. It may, however, be checked using other, less well calibrated, equilibria.

Reaction (44) may be used to estimate temperature and pressure. Holdaway (1980) has estimated that the pure Fe end - member reaction passes through the point $550^{\circ}C$, -770 bars. This is based on a P and T estimate of 4 kbars and $550^{\circ}C$ for a specimen from the Augusta Quadrangle in Maine in which garnet was partly replaced by biotite and sillimanite. The activities of biotite, garnet and muscovite were used to estimate a pressure difference of 4770 bars between the hypothetically pure end - member equilibrium and the equilibrium as it occurred in the natural assemblage. Using ΔV_s^O for the reaction of 0.506 cal/bar, and an average estimate of the equilibrium boundary of 8.5 bars/degree from Thompson (1976b), an equation can be derived for reaction (44) such that

$$-3RT\ln K = 3929 - 4.301T + 0.506(P-1) \qquad (46)$$

where

$$K = \frac{a_{Fe}^{bio}}{a_{Fe}^{gar}}$$

The Na content of biotite and muscovite is neglected. Pressure is calculated, using X_{Fe}^{bio} and X_{Fe}^{gar} values from B8 together with the temperature estimate of 594°C, at 3.7 kbars. This is in reasonable agreement with the garnet - cordierite pressure. However equilibration of garnet and biotite compositions to aureole conditions is not certain. Further errors may result from the use of an ideal solid solution model, and from neglecting Na in biotite. Primary muscovite is absent from this specimen as it lies above the 'muscovite out' isograd. The pressure estimate is therefore a maximum.

The occurrence of textures implying operation of the reaction

$$\text{andalusite} = \text{sillimanite} \qquad (47)$$

has implications for pressure. The abundance of andalusite suggests that the aureole pressure was below the Al_2SiO_5 triple point. The pressure estimate using garnet and cordierite data is inconsistent with Richardson et.al's (1969) Al_2SiO_5 phase diagram. The preferred T estimate of 647°C (from B57) for the sillimanite + K-feldspar zone would lie in the andalusite field of their diagram unless the pressure is in excess of 4.8 kbars. The andalusite - sillimanite transition at T less than 650°C and P at approximately 4 kbars, is consistent with Holdaway's (1971) Al_2SiO_5 diagram. If the pressure estimate using garnet and cordierite compositions is correct then the prominence of andalusite suggests that the andalusite field is quite extensive at 4 kbars so that Holdaway's triple point would be at rather too low P.

249

TABLE 3.5

SAMPLE	MUSCOVITE Na/(Na+K)	PLAGIOCLASE An
B10	0.048	0.31
B13	0.032	0.28
B56	0.063	0.25
B57	0.075	0.25
B79	0.101	0.32

TABLE 3.5

3.6.2 (ii) Regional Pressures

No suitable equilibria are available within regional assemblages for an estimate of regional pressure to be made. Wells (1979) has given values of 9 kbars for rocks in the vicinity of Loch Killin. The equilibria used by Wells (1979), and by Wells & Richardson (1979) all involve plagioclase. In both cases the plagioclase activity coefficient data of Orville (1972) have been used at the relatively low temperature conditions of the Central Highlands. In view of the arguments put forward in Section 2.6.3 (ii), these pressures must be regarded with suspicion, and actual pressures are likely to be lower.

3.6.3 Muscovite - Feldspar Equilibria

Muscovites have been analysed from seven specimens (Appendix III, Table 4). Of these, five contain sillimanite and their $Na/(Na + K)$ ratios, together with coexisting plagioclase compositions, are given in Table 3.5.

Muscovites within the aureole all have a secondary origin; however, their $Na/(Na + K)$ ratios suggest equilibration under high grade conditions. As at Strontian, retrogression of sillimanite to muscovite, in this case by reversal of reactions (44) and (45), has taken place soon after peak metamorphism in the aureole.

The analyses from B79 are of primary, regional muscovites. The $Na/(Na + K)$ ratio, and coexisting plagioclase compositions, are consistent with sillimanite zone conditions (Guidotti & Sassi, 1976; Cheney & Guidotti, 1979).

3.7 INTERPRETATION AND DISCUSSION

3.7.1 The Composition of the Fluid Phase

The low X_{H_2O} value of 0.14, estimated for the cordierite +
K-feldspar zone, cannot be interpreted in terms of lowering
of X_{H_2O} by anatexis. Calculated temperatures and pressures
of 3.9 kbars at approximately $660^{\circ}C$ for this zone are too low
for melting to take place by reactions such as (28) or (31),
particularly as graphite is present.

The opaque assemblage (Table 3.2) is similar to that seen at
Strontian, consisting of graphite, ilmenite and pyrrhotite.
Pyrrhotite is best developed in the cordierite + K-feldspar
zone, and graphite may be very common, particularly in
regional assemblages. The amount of graphite seen would be
consistent with a low X_{H_2O} in regional assemblages.

In the Strontian aureole the composition of the fluid phase
was extensively buffered by muscovite dehyration. At Foyers,
muscovite is removed from aureole assemblages by a combination
of reactions (1) and (44) , or, in K-poor rocks, by reaction
(44).

Reaction (44) does not influence the fluid phase as a net
release of H_2O is not involved. Reaction (1) by contrast,
does release H_2O. However, a zone of muscovite + sillimanite
+ K-feldspar is not seen and this lack of divariance is inter-
preted as reflecting reaction at approximately constant a_{H_2O}.
Muscovite left after partial or complete operation of (44)
was consumed by reaction (1), but buffering of the fluid phase
was not appreciable due to the small amounts involved. Where
muscovite breaks down entirely by reaction (1), due to absence
of regional garnet, the assemblage muscovite + sillimanite +

K-feldspar is seen, implying that a_{H_2O} is buffered in such samples.

The failure of the 'muscovite out' isograd reaction to buffer X_{H_2O} has important implications for higher grade dehydration reactions within the aureole. On a diagram similar to fig. 2.27, drawn at the slightly lower Foyers aureole pressure of 3.9 kbars, (fig. 3.20) the $T-fO_2$ path lies parallel to the maximum X_{H_2O} trace but at the much lower X_{H_2O} present in regional assemblages. It would not be affected by the 'muscovite out' isograd reactions, persisting into the aureole at a value close to its regional value. Buffering of the fluid phase will occur where the $T-fO_2$ path intersects reaction (2). This intersection would be expected to take place somewhere below $T= 660^{\circ}C$, $X_{H_2O}= 0.14$. The cordierite + K-feldspar isograd is therefore defined by reaction (2). Reaction (31) will not take place until the X_{H_2O} has been raised to a suitable value by reaction (2). According to fig. 4 of Lee & Holdaway (1977), this will be approximately 0.6 at $690^{\circ}C$.

This interpretation is consistent with the absence of wholesale migmatisation in the cordierite + K-feldspar zone. Localised contact leucosomes have been recognised associated with injection migmatites. These may be explained in terms of high local temperatures and water pressures produced by close proximity to granodiorite magma injected from the pluton. In the case of B43, conditions were suitable for the production of a trondhjemitoid melt.

The absence of aureole leucosomes on a large scale cannot be attributed to the distribution of the melt along grain boundaries by shearing. Shearing is common near the contact, but

253

FIGURE 3.20

T - fO$_2$ Section

Section is based on the 4 kbars section in Figure 8
of Ohmoto & Kerrick (1977) interpolated at the aureole
pressure of 3.9 kbars. Muscovite + quartz stability is
calculated from equation 26. Biotite dehydration is
idealised from data given by Holdaway & Lee (1977) and
Lee & Holdaway (1977).

P = 3·9 kbars

H₂O MAX.

granite minimum

GRAPHITE MAX.

mus + qtz
sill + ksp + H₂O

sill + bio + ksp + qtz
+ H₂O

gar + crd + ksp + H₂O

T - fO₂ Path

700   650   600   T°C

-15   -20   -25   log₁₀ fO₂
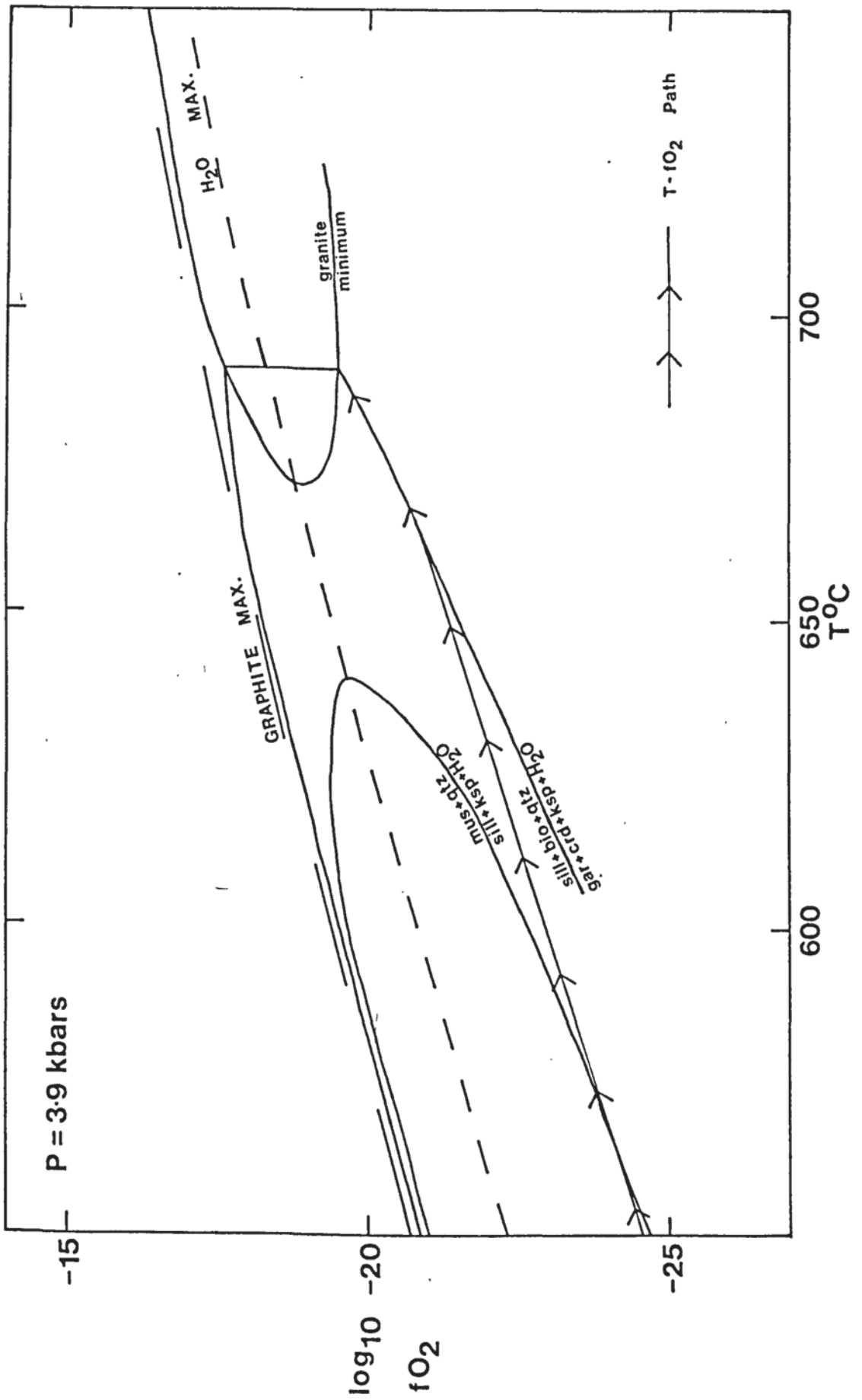
grain coarsening of sheared rocks would be expected if such a process had occurred and this is not seen. Also, undisturbed aureole migmatites would be expected where shearing is absent, and these are also absent.

3.7.2 The Influence of Regional Metamorphic Conditions

The Strontian aureole has been influenced to a considerable extent by its intrusion at an early stage of regional uplift and cooling. This is seen principally in the asymmetry of the metamorphic zones, and in the absence of textures and zoning profiles indicating garnet disequilibrium.

Regional assemblages around the Foyers aureole are lower grade than those around Strontian and suggest a regional temperature gradient increasing from southwest to northeast. This pattern reflects the influence of Precambrian sillimanite grade assemblages. Wells (1979) indicates the presence of a Caledonian thermal high, centred on Newtonmore, 30km to the southeast of Foyers. This is reflected by the regional temperatures estimated in this study. Any residual gradient at the time of the intrusion of the complex would be expected to show a temperature increase in this direction. From Map 2 it can be seen that no asymmetry of the aureole is recognisable.

Peak Caledonian metamorphic conditions in the Central Highlands were achieved 30-40 m.y. before peak metamorphism in the Western Highlands, and tectonism and metamorphism were complete by 460 Ma (Van Breemen et.al., 1979). The K/Ar age for the Foyers complex of 400 Ma indicates that a gap of up to 90 m.y. has occurred between regional and contact metamorphism. In these circumstances residual regional temperatures would be expected to be low when the complex was intruded.

The main result of this low initial regional temperature is seen in the garnet disequilibrium textures. In the Strontian aureole garnet remains stable in the presence of muscovite and Fe, Mg and Mn compositions are equilibrated to aureole conditions gradually by cation exchange reactions such as reaction (7). At Foyers the sharp difference between aureole and residual regional temperatures has not allowed a gradual re-equilibration. In this case the rocks have attempted to re-equilibrate abruptly, resulting in garnets with regional compositions being in disequilibrium within the aureole, despite the fact that a range of garnet compositions is stable under aureole conditions.

A further consequence of the low initial temperatures is the absence of large scale migmatisation. High enough temperatures, at the water pressures present, are only achieved locally in country rocks associated with injection migmatites.

3.7.3 Implications of the Aureole Pressure Estimate

Correlation of the Foyers and Strontian granitic complexes was first suggested by Kennedy (1946), based principally on the petrological similarities of the two bodies. It was used to establish a sinistral movement of some 105 km along the Great Glen fault.

The pressures calculated for the cordierite + K-feldspar zones in the two aureoles, suggest that both bodies were intruded at similar depths. For the Foyers aureole a pressure of 3.9 kbars indicates a depth of 14.5km. At Strontian the pressure estimate of 4.1km suggests a depth of 15km.

If the two bodies are to be regarded as parts of an originally continuous Strontian - Foyers pluton, the above results require

that they represent similar structural levels within it. The structural work of Munro (1965, 1973) suggests that the present erosion level at Strontian lies at some depth within the pluton. By contrast, Marston (1970) has shown that the Foyers complex has only recently been unroofed, and large areas of roofing sediment lie within it.

The regional geology surrounding the two complexes also suggests higher structural levels are found to the east of the Great Great Glen (Marston, 1970). Here rocks are generally younger, with Grampian Division and Dalradian metasediments dominant, and regional metamorphic grades lower. These observations are inconsistent with intrusion of a single pluton before the initiation of the fault, bearing in mind the similarities of calculated depths for the presently exposed aureoles of the complexes. The different structural levels might be explained if intrusion occurred after the fault had already formed, and movement on it had been mainly vertical. At Strontian a late, regional, thermal high is central to the northeast of the complex, and relatively high residual regional temperatures have been estimated. These temperatures are not reflected in the Foyers aureole. This may be explained by relatively cool rocks being juxtaposed against deeper, warmer, rocks by vertical movement on the fault, downthrow to the east, immediately prior to intrusion of the pluton. The main lateral component of movement followed this, with no further vertical movement taking place.

The occurrence of the roof of the Foyers complex at the same level at which the interior of the Strontian complex is exposed, suggests that, if the two bodies are correlated, vertical movement must have taken place after intrusion, with downthrow

258

to the east. In view of this, it is felt that the physical conditions calculated for contact metamorphism around the two complexes, are not consistent with them forming the mechanically separated parts of an originally continuous pluton.

CHAPTER 4

THE DALBEATTIE AUREOLE

4.1 INTRODUCTION

The Dalbeattie granitic complex forms a roughly eliptical body intruded into Silurian sediments to the south and west of Dumfries in the Southern Uplands of Scotland. As with the Strontian and Foyers intrusions, it is a member of the Caledonian 'Newer Granite' suite.

The igneous petrography and geochemistry of the pluton have been described by Phillips (1956) and by Stephens (1972). It consists of two main intrusive bodies (fig. 4.1), an outer granodiorite and an inner porphyritic granodiorite, which grade into each other and are separated by the appearance of alkali feldspar megacrysts. A third, earlier, granodiorite body is recognised at the southwest end of the pluton. The two outer granodiorites display a well developed foliation. Quartz-diorite in the vicinity of Bengairn, at the western margin, and has been interpreted as metasomatic in origin (MacGregor, 1937; Phillips, 1955; Stephens, 1972).

The pluton has a roughly conical cross section with the margins dipp-ing steeply outwards. Phillips et.al. (1981) have concluded that intrusion was achieved principally by stoping. This is based on the extensive occurrence of hornfels xenoliths which show progressive recrystallisation and modification of their external shape away from the margin. Stoping of such xenoliths is seen at the contact, and a flattening schistosity, increasing in intensity towards the contact, is not seen. Also, although tilting of the strata is recognised, there is no evidence of shearing, or of a new penetrative fabric within the hornfelses which might suggest forceful intrusion. The foliation within the outer granodiorite is attributed to

260

FIGURE 4.1

Geological map of the Dalbeattie complex and the surrounding country rocks.

After: Phillips (1956) and Survey Sheet 5.

Carboniferous

porphyrite

porphyritic granodiorite

granodiorite

'early' granodiorite

quartz diorite

Wenlock
Llandovery } Silurian

R.L.   Riccarton Line

Dalbeattie

Rockcliffe

Bengairn

10 km

N
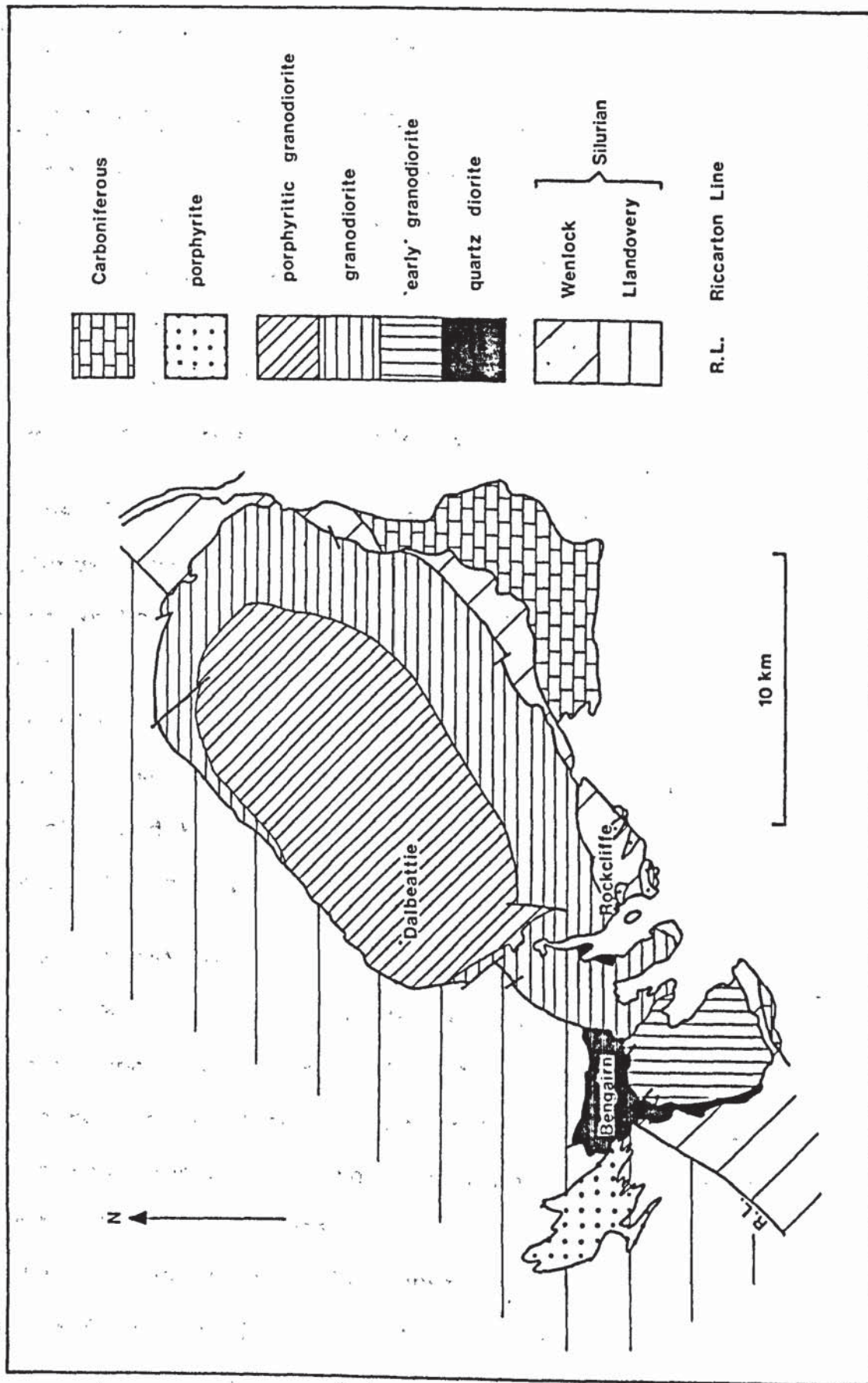
convective flow within the pluton.

Halliday et.al. (1980) have determined the age of the pluton as 397 ± 2 Ma by Rb/Sr methods.

4.2 PREVIOUS RESEARCH ON THE AUREOLE ROCKS

A metamorphic aureole up to 2km wide was recognised by Peach & Horne (1899) during preparation of Sheet 5 of the Scottish Geological Survey. Bands of calc-silicate hornfels were recognised near Southwick on the southern margin, but the extent of the aureole was based principally on the recognition of hornfelsic textures in the field.

Phillips (1955) recognised the occurrence of biotite and hornblende - biotite hornfelses within the aureole. Near the contact at Rockcliffe a transition from hornblende - biotite hornfels to rocks with a quartz - diorite or porphyrite composition, was recognised. This was attributed to metasomatic replacement of the greywacke and shale hornfelses by Na-bearing and K-bearing solutions associated with the adjacent granodiorite magma.

Stephens (1972) carried out a more detailed petrographic study of the hornfelses forming the aureole. A sequence of hornfels types was recognised with biotite - chlorite and biotite hornfelses found furthest from the contact. As the contact was approached hornblende, and then diopside appeared. The outer hornfelses were attributed to albite-epidote hornfels facies conditions, the inner hornfelses to hornblende hornfels facies conditions. The limits of the two facies were not mapped, but the higher grade assemblages generally occurred within 150 metres of the contact. Contact metamorphism was recognised up to 2000 metres from the contact.

263

Pressures within the contact rocks were estimated at between 1 and 2 kbars, with the transition from albite-epidote horn-fels facies to hornblende facies taking place at approximately 535°C.

4.3 REGIONAL SETTING

4.3.1 Stratigraphy

The lower Palaeozoic rocks of the Southern Uplands consists of ten or more Ordovician and Silurian deep water stratigraphic sequences, consisting of basalt, chert and graptolitic shales, below thick greywackes (Legget et.al., 1979). These are sep-arated by a series of major reverse strike faults. They have been interpreted as representing an accretionary prism depos-ited on the northwest margin of the Iapetus Ocean.

The Dalbeattie pluton has been intruded entirely into Silurian sediments. Along the southern margin the rocks are of Wenlock age, forming the Southern Belt of Peach & Horne (1899). They are separated from Llandovery rocks in the Central Belt to the north, by the Riccarton Line (fig. 4.1).

The Wenlock is represented by the Riccarton Beds, which con-sist of greywackes, flaggy siltstones, shales and slates, with thin bands of graptolitic shales. The Raeberry Castle Beds are not seen in this area. Along the northern contact Llan-dovery age rocks comprise the Queensbury Grits and the Hawick Beds of the Gala Group. These consist of a sequence of flags, grits, greywackes and shales (Greig, 1971).

4.3.2 Metamorphism

Caledonian metamorphism has affected the lower Palaeozoic of the Southern Uplands and this is seen locally in the crystall-isation of low-grade micas and more rarely biotite (Fettes, 1979)

264

However, little detailed information is available.

4.4 PETROGRAPHY

4.4.1 Introduction

Some ninety standard thin sections have been examined from rocks sampled in the vicinity of the Dalbeattie complex. Assemblages are listed in Table 4.1. The rocks are generally rather Ca-rich, and genuine pelitic lithologies are rare. Two zones have been recognised; an outer biotite zone and an inner hornblende zone. Diopside is also recognised in the inner zone. The distribution of the zones is shown on Map 3. Regional assemblages are characterised by the occurrence of chlorite, together with sedimentary textures. One cordierite locality is recognised adjacent to the contact.

4.4.2 Regional Assemblages

Rocks lying outside the aureole consist of a sequence of shales, siltstones and greywackes, which are typically green in colour. They have the general assemblage: chlorite + muscovite + biotite + plagioclase + quartz $\pm$ calcite $\pm$ K-feldspar. Opaques are also present.

Chlorite, muscovite and biotite form randomly orientated-flakes, rarely exceeding 0.1mm in length. These often show deformation resulting from compaction and diagenesis of the sediment (fig. 4.2). Feldspar, which may be a combination of plagioclase and K-feldspar of detrital origin, and quartz form larger, angular grains. Calcite is a frequent component, occurring both in the groundmass (fig. 4.2b), and as late, cross cutting veins.

4.4.3 Aureole Assemblages

TABLE 4.1

TRANSMITTED LIGHT ASSEMBLAGES.

	CRD	DIOP	HBD	BIO	MUS	CHL	CALC	MAP REFERENCE
C1				X			-	852533
C2				X	X			852529
C3[+]				X	X	X		855525
C4	X			X				841521
C5				X		(X)		841517
C6				X	X	(X)		828495
C7				X	X			824489
C8[+]				X	X	X		798654
C9[+]				X	X	X		798654
C10[+]				X	X	X		799635
C11				X	X	X		803617
C12				X		X		803612
C13				X				805609
C14				X		X		803604
C15			X	X	X			816608
C17			X	X				808563
C18				X	X	X	X	781590
C19			X	X	X			809595
C21				X				852541
C22			X	X				850540
C23			X	X				850540
C24			X	X				850540
C26[+]				X	X	X		831657
C27				X		X		849659
C28		X	X	X				863660
C29[+]				X		X		885698
C30		X	X	X				884680
C31		X	X	X				872671
C32			X	X				858655
C33				X				858656
C34				X				864542
C35[+]				X	X			878542
C38[+]				X	X	X		869528
C39					X	X		871532
C40				X				899553
C41				X	X			892548

	CRD	DIOP	HBD	BIO	MUS	CHL	CALC	MAP REFERENCE
C42				X	X			885544
C43				X				909558
C44		X	X	X				922568
C46				X		(X)		980642
C47			X	X				979631
C48		X	X	X	X			811486
C49				X	X			779480
C50[+]				X	X	X		759487
C51			X	X				778493
C52			X	X				805562
C53		X	X	X				825582
C54			X	X				940579
C55		X	X	X				948583
C56				X	X			952588
C57		X	X					957591
C58				X				797595
C59			X	X				790558
C60[+]				X	X	X		778578
C61[+]				X	X	X	X	782568
C62			X					794555
C63		X	X	X				795550
C64				X	X	(X)		785549
C65			X	X				779553
C66			X	X				773554
C67[+]				X	X	X		776562
C68						(X)		848537
C69[+]				X	X	X		947710
C70			X	X				945710
C71				X	X	X		940707
C72			X	X				931705
C73				X				941710
C74[+]				X	X		X	941721
C75				X				944719
C76				X	X	X		943715
C77				X				943713
C78[+]				X	X	X		928730
C79[+]				X	X	X	X	919718
C80			X					760533
C81		X	X	X				760535

	CRD	DIOP	HBD	BIO	MUS	CHL	CALC	MAP REFERENCE
C83			X	X	X			756531
C85			X	X				757525
C88			X	X				765521
C89		X	X	X				770518
C90			X	X				773516
C91		·	X	X				777617

[+] denotes regional assemblages

(X) mineral regarded as secondary

Feldspar and quartz are present in all specimens.

4.4.3 (i) Biotite Zone

In the field the limit of contact metamorphism may be recog-
nised by the loss of the green colouration of the sediments,
combined with an increase in hardness. Bedding and associated
sedimentary structures are preserved, despite the rocks becom-
ing increasingly hornfelsic towards the contact. They have
the assemblage: biotite + plagioclase + quartz $\pm$ muscovite $\pm$
chlorite $\pm$ K-feldspar. Opaques form frequent accessories.
Tourmaline may also be present.

In thin section chlorite, biotite and muscovite of regional
origin is lost. The rocks are recrystallised with biotite
dominant. It is intimately intergrown with muscovite and, to
a lesser extent, chlorite. Biotite occurs as well formed
grains up to 0.2mm long (fig. 4.3a). They show no evidence
of deformation and hornfelsic textures are well developed.
Where a preferred orientation is developed, it generally
parallels bedding and is interpreted as mimetic growth of the
metamorphic minerals on pre-existing, sedimentary structures.
Chlorite of apparently contact origin is developed in a few
samples. It is seen only in the outer part of the biotite
zone, but is too-infrequent to define a separate chlorite +
biotite zone as has been done by Cook (1976) for the Cairns-
more of Fleet aureole. Chlorite may also occur as alteration
of biotite.

4.4.3 (ii) Hornblende Zone

Rocks in the hornblende zone become medium grained in places,
but bedding and other sedimentary structures are preserved.
The general assemblage is: biotite + plagioclase + quartz $\pm$
hornblende $\pm$ muscovite $\pm$ diopside $\pm$ K-feldspar. Tourmaline
and opaques occur as accessory minerals.

269

FIGURE 4.2

a. & b.   Regional assemblages. Biotite, chlorite and
         muscovite are common. In b.,mica and chlorite
         grains may be deformed. Calcite is also
         present.
   a. Specimen C18
   b. Specimen C79.

271
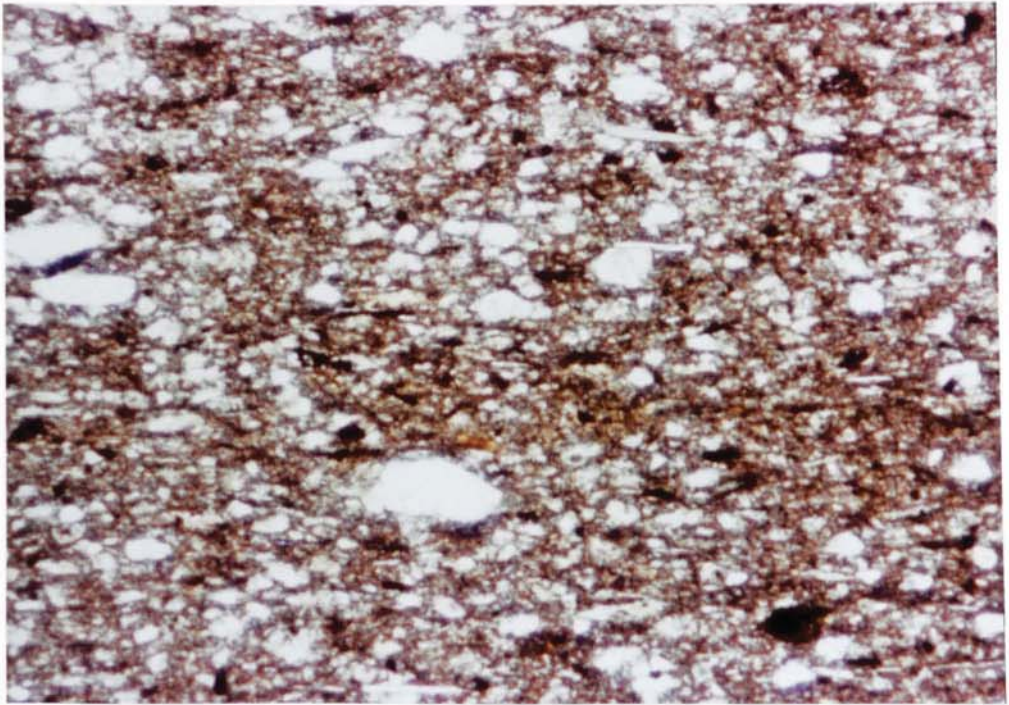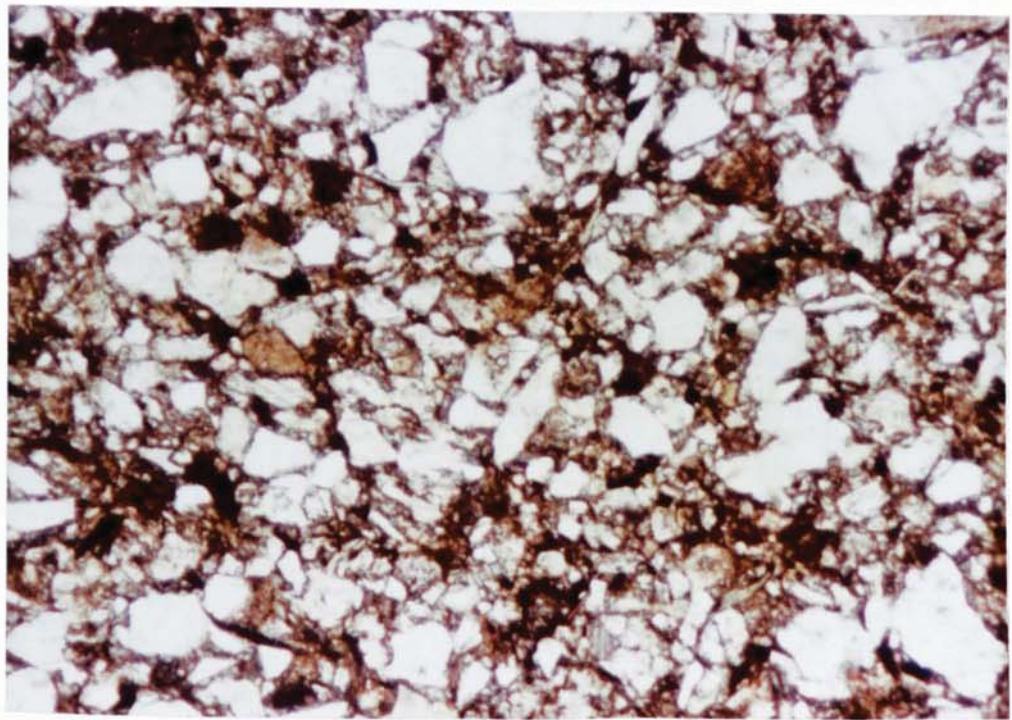
FIGURE 4.3

a. Biotite hornfels, specimen C40.

b. Hornblende - diopside hornfels, specimen C55.

0·5 mm

0·5

273
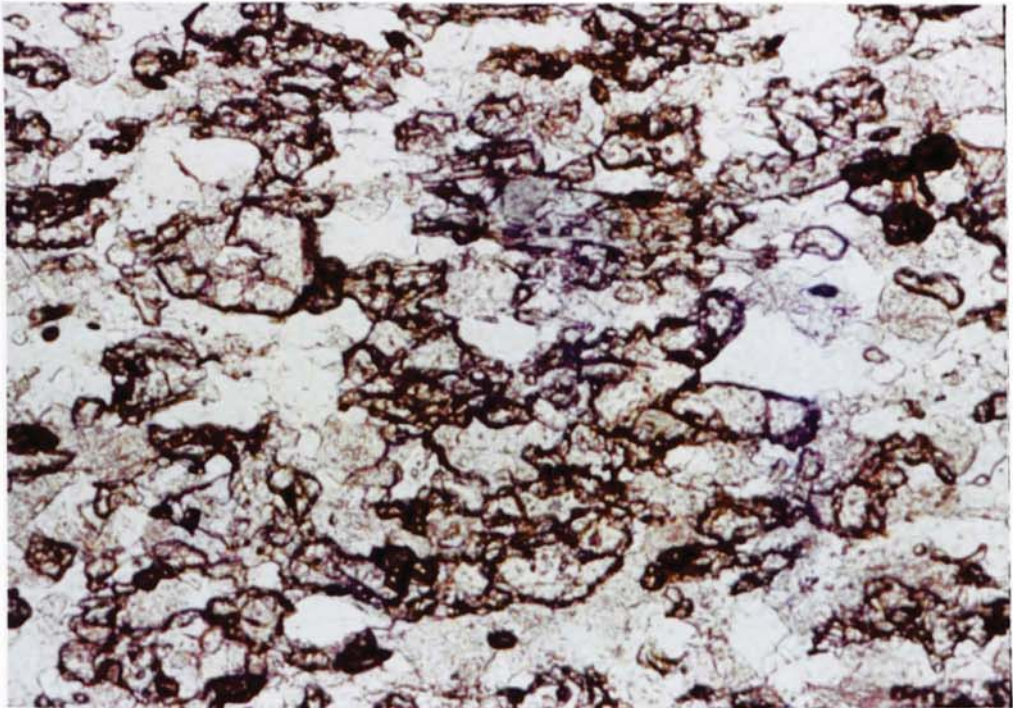
Two distinct types of hornfelses are recognised. The first is characterised by the extensive occurrence of hornblende with biotite. The second has a calc-silicate composition with hornblende and diopside occurring (fig. 4.3b). In some samples bands of hornblende - biotite hornfels are interbedded with bands of hornblende - diopside hornfels. The assemblage hornblende + diopside + biotite may also be seen (fig. 4.4a). Both hornfels types are fine to medium grained, with hornblende, diopside and biotite occurring up to 0.5mm in length. Hornfelsic textures are generally well developed.

Cordierite is recognised in one specimen sampled at the contact. The rock has a well developed hornfelsic texture and cordierite, occurring up to 0.5mm in diameter, is intergrown with biotite (fig. 4.4b). It is a distinctively green colour and shows complete alteration to clay material. Plagioclase, K-feldspar and quartz also occur.

K-feldspar is well developed in the metasomatic rocks described by Phillips (1956b) at the contact near Rockcliffe, occurring with hornblende, biotite, plagioclase and quartz. Rocks throughout the zone may be cut by late calcite veins.

4.4.4 Mineral Parageneses

Mineral parageneses in and around the Dalbeattie aureole show considerable differences from those seen at Strontian and Foyers. This is due to the low grade of regional assemblages, which represent greenschist facies, rather than amphibolite facies, conditions. It also reflects the more calcic nature of the rocks.

The outer limit of the aureole is marked by an increase in

FIGURE 4.4

a. Hornblende - diopside - biotite hornfels, specimen
    C53.

b. Cordierite - biotite hornfels, specimen C4.

0·5
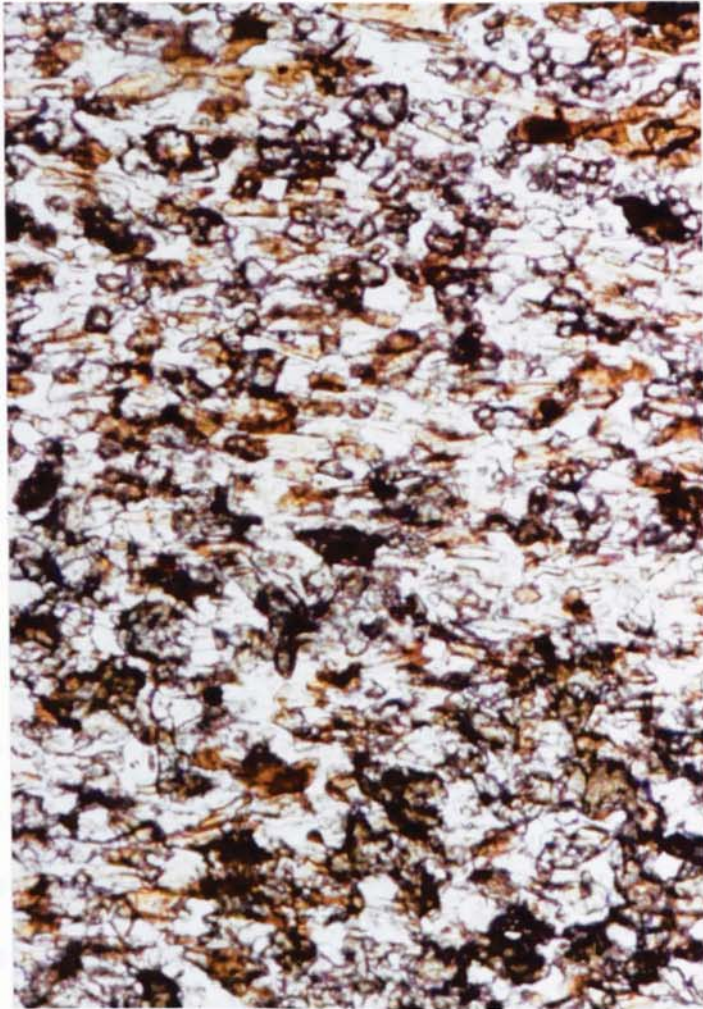
grain size, and by good crystal form in the phyllosilicates. In more Ca-rich lithologies calcite disappears. Overall assemblages are the same as those recognised in regional rocks.

The appearance of hornblende in the hornblende + biotite hornfelses may be attributed to a reaction such as

biotite + plagioclase + quartz = amphibole + K-feldspar. (48)
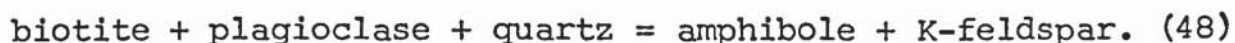
Diopside is produced by a continuous reaction within the hornblende zone, so that

Al-poor hornblende =

Al-richer hornblende + plagioclase + clinopyroxene. (49)
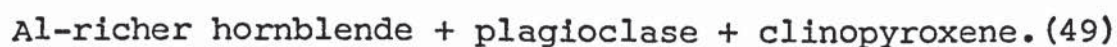
The cordierite occurrence, although it is found at the contact, is characteristic of the biotite zone. The reaction

chlorite + muscovite + quartz = cordierite + biotite + H_2O (50)

occurs at relatively low grade, and if suitable lithologies are available, would be seen operating in the outer part of the biotite zone. The limited occurrence of chlorite in this part of the aureole, and therefore of cordierite, is due to unsuitable bulk rock compositions.

4.5 CONCLUSIONS

Without detailed analyses of the various phases present it is not possible to give accurate estimates of temperatures and pressures developed in the aureole. However, the width of the aureole, and the low-grade reactions which mark its outer limits, are a reflection of the low regional temperatures at the time of intrusion. Relatively low pressures are indicated by intrusion taking place by stoping, rather than by the forceful shouldering aside of country rock. In view of this the estimates of Stephens (1972) of temperatures of approximately $535^{\circ}C$ for the outer part of the aureole, at pressures of

between 1 and 2 kbars are regarded as reasonable. Temperatures were probably in excess of $600^{\circ}C$ in the hornblende zone. The widespread occurrence of calc-silicate lithologies suggests that CO_2 was an important component of the fluid phase, with P_{H_2O} considerably less than P_{TOTAL}.

CHAPTER 5

SUMMARY OF CONCLUSIONS

The Strontian granitic complex has been intruded into Moinian metasediments in the core of the Caledonian Orogen. The aureole consists of three zones; a muscovite + sillimanite + K-feldspar zone, a sillimanite + K-feldspar zone, and an inner cordierite + K-feldspar zone. Regional assemblages are at sillimanite grade to the north and west of the aureole, increasing to sillimanite + K-feldspar grade at the eastern end of Glen Tarbert.

A sillimanite + K-feldspar isograd, marking the outer limit is discernable contact metamorphism, is drawn at the first occurrence of sillimanite and K-feldspar together. The muscovite + sillimanite + K-feldspar zone is transitional between regional and aureole assemblages, muscovite breaking down by the reaction

$$\text{muscovite} + \text{quartz} = \text{sillimanite} + \text{K-feldspar} + H_2O. \quad (1)$$

Muscovite within the inner two zones is all secondary in origin, resulting from retrogression of reaction (1) at high grade. The disappearance of primary, regional muscovite is marked by a 'muscovite out' isograd. The cordierite + K-feldspar isograd represents operation of the reaction

$$\text{sillimanite} + \text{biotite} + \text{quartz}$$
$$= \text{cordierite} + \text{garnet} + \text{K-feldspar} + \text{melt}. \quad (31)$$
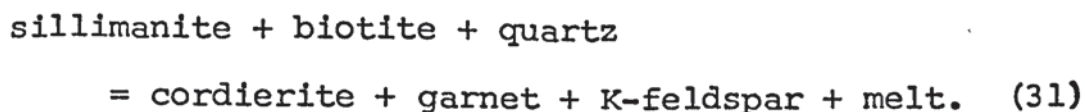
Migmatites are recognised in both aureole and regional assemblages. Regional migmatites generally have a trondhjemitoid composition. These persist unaffected into the aureole if muscovite was absent from the regional assemblage. Where regional muscovite was present, subsolidus operation of reaction (1) results in a granitoid composition. Microperthite - granitoid migmatites are the result of migmatisation during

contact metamorphism.

Zoning profiles of garnets within the aureole are consistant with homogenisation by volume diffusion at high grade. Mn enrichment, due to retrograde ion exchange reactions, is recognised at the rims. Garnets from regional assemblages show similar profiles. One profile shows partial re-homogenisation of a Precambrian garnet by Caledonian metamorphism. Other Precambrian garnet compositions may be recognised by relatively high K_D(gar-bio) values.

A correlation of the distribution measures, K_D(gar-bio) and K(gar-plag), calculated from garnet and plagioclase core compositions, and from matrix biotite, is recognised. It is interpreted as a combination of two effects; incomplete re-equilibration of garnet Fe-Mg compositions, and the temperature dependence of the activity coefficients in garnet-plagioclase equilibria. Consistent values of K_D(gar-bio) in the cordierite + K-feldspar zone suggest that garnet cores and matrix biotite in this zone were equilibrated with respect to Fe and Mg in the thermal event.

Calibrations of the temperature dependent Fe-Mg exchange reactions between garnet-biotite and garnet-cordierite indicate temperatures of approximately 690°C for the cordierite + K-feldspar zone. Estimates of pressure obtained from the assemblage cordierite - garnet - biotite - sillimanite - K-feldspar - quartz, give values of 4.1 kbars, with P_{H_2O} < P_{TOTAL} (X_{H_2O} = 0.53). Regional conditions are estimated as approximately 620°C at 6 kbars in the Resipole area.

The occurrence of a zone of muscovite + sillimanite + K-

feldspar coexistence is interpreted in terms of buffering of the fluid phase by reaction (1). The presence of graphite limits the maximum X_{H_2O} value which the fluid phase may achieve. This controls the upper stability limit of muscovite and, at the aureole pressure of 4.1 kbars, the 'muscovite out' isograd occurs at 645^OC $(X_{H_2O} = 0.84)$.

From calculated temperature gradients within the aureole, the sillimanite + K-feldspar isograd is estimated at 630^OC $(X_{H_2O} = 0.69)$. The sharpness of this isograd reflects the relatively uniform X_{H_2O} values produced in regional assemblages by Caledonian metamorphism.

Contact migmatisation, resulting from anatexis, has taken place within the inner part of the aureole. Within the sillimanite + K-feldspar zone melting takes place according to a reaction analagous to the granite mimimum. This results in a lowering of X_{H_2O} towards the values estimated for the cordierite + K-feldspar zone. Reaction (31) represents the production of large quantities of melt. The absence of correspondingly large numbers of contact migmatite leucosomes is attributed to the distribution of melt along grain boundaries by shearing associated with the intrusion of the granodiorite.

The pronounced asymmetry of the aureole results from a temperature gradient, increasing at 5.24^O/km towards 122°, in the area at the time of intrusion. This reflects the temperature distribution during peak Caledonian metamorphism.

The temperatures of homogenisation of garnet under aureole and Caledonian regional conditions are used to estimate the

timescale of the thermal event (t_1) relative to the regional event (t_2) as $t_2/t_1 = 10^{-1.1\pm0.7}$. This is consistent with intrusion of the complex at an early stage of regional cooling and uplift.

The Foyers complex is intruded into Moinian and Dalradian metasediments at a higher structural level in the orogenic core. Three zones are recognised; an outer sillimanite zone, a sillimanite + K-feldspar zone and an inner cordierite + K-feldspar zone. Regional assemblages range from garnet grade in the south near Loch Killin, to sillimanite grade in the northeast near Loch Ruthven.

The outer limit of the aureole is marked by a 'muscovite out' isograd produced by a combination of the reaction

muscovite + garnet$_1$ + biotite$_1$

= sillimanite + garnet$_2$ + biotite$_2$ + quartz   (44)
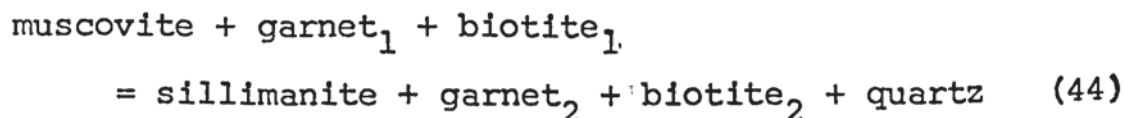
and reaction (1). Garnet disequilibrium is seen both texturally, and in zoning profiles, throughout the aureole. The sillimanite zone reflects the occurrence of relatively K-poor gneisses, and is probably consistent with sillimanite + K-feldspar zone conditions.

Conditions within the cordierite + K-feldspar zone are estimated as $660^{\circ}C$ at 3.9 kbars ($X_{H_2O} = 0.14$). Regional temperatures range from $560^{\circ}C$ near Loch Ruthven to $630^{\circ}C$ near Loch Killin. Pressures are not known with certainty, but are somewhere below 9 kbars.

Anatectic contact migmatites are rare, being associated with areas extensively injected by igneous material. The fluid phase is not buffered significantly by the 'muscovite out'

isograd reactions and X_{H_2O} values within the aureole are similar to regional values. Buffering of the fluid phase does not occur until the cordierite + K-feldspar isograd, marked by the reaction

sillimanite + garnet + quartz

$$= cordierite + garnet + K-feldspar + H_2O, \quad (2)$$
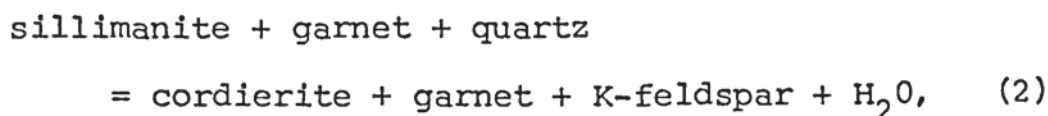
is crossed. Estimated conditions are still below those at which melting will take place.

The complex was intruded at a much later stage of regional uplift and cooling than the Strontian complex. This is reflected in the lower aureole temperatures, and in the obvious disequilibrium of regional garnet compositions within the aureole. Garnet has attempted to re-equilibrate abruptly, rather than gradually as in the Strontian aureole.

In view of the different structural levels the two complexes represent, the similar pressure estimates calculated for contact metamorphism are not consistent with them forming the mechanically separated parts of an originally continuous pluton.

The Dalbeattie complex is intruded into Silurian sediments at the margin of the orogen. Two zones are recognised; a biotite zone and an inner hornblende zone. Diopside is also seen in the hornblende zone. Cordierite is recognised at one locality. Regional assemblages are characterised by the occurrence of chlorite and calcite.

The restricted nature of the aureole, and the lower grade reactions recognised, reflect its shallower depth and the much lower background regional temperatures than those present during intrusion of the Strontian and Foyers complexes.

APPENDICES

APPENDIX I

MODAL ANALYSIS OF PELITES

Modal analysis of 38 pelites from the aureole of the Strontian granitic complex and surrounding regional assemblages are presented. Counting methods used are those recommended by Neilson & Brockman (1977). Specimens are counted in square sets of N points, each having sides of $\sqrt{N}$. Percentages of minerals present are estimated from

$$\%_i = 100 \ (\Sigma^k_{j=1} (x_j)/kN),$$

where k is the number of sets of N points counted, and x_j is the number of points falling on the ith mineral in set j.

The variance is determined by

$$s^2\%_i = (10^4/((k-1)N^2k))(\Sigma (x^2)-(\Sigma x)^2/k).$$

From this the confidence interval for each mineral, at an approximate 95 percent level of confidence, can be determined as

$$\%_i \pm 2\sqrt{s^2\%_i}.$$

APPENDIX I: MODAL ANALYSES

REGIONAL SILLIMANITE ZONE

SAMPLE	A41	A61	203C	279C	299C	359C
Quartz	19.5±3.7	20.3±5.4	16.1±4.4	14.8±4.4	22.7±7.2	14.8±3.2
Plagioclase	29.3±3.0	36.3±5.6	50.5±5.9	47.1±5.8	25.1±8.6	23.8±4.7
Biotite	26.1±4.5	25.0±4.5	23.6±5.2	31.8±2.7	14.6±4.1	31.8±3.8
Cordierite						
Garnet	0.5	pr.		pr.		0.4
Sillimanite				0.4	5.5±1.9	4.3±2.1
Andalusite						
K-feldspar		2.3±1.2				
Muscovite:P	24.2±3.7	13.0±4.6	7.6±2.2	1.8±0.9	28.0±10.2	21.1±3.4
S				0.5		0.6
Others	0.4	3.0	2.2	3.7	4.1	3.1
No.of Points	735 (15x7x7)	300 (12x5x5)	539 (11x7x7)	567 (7x9x9)	343 (7x7x7)	512 (8x8x8)
Point Interval(mm)	1.0	1.0	1.0	1.3	1.0	2.0
% Primary Muscovite	100	100	100	78	100	97
% Sillimanite + K-feldspar	0	0	0	0	0	0

REGIONAL SILLIMANITE ZONE (continued)

<table>
<tr><th>SAMPLE</th><th>362C</th><th>375C</th><th>387C</th><th>411C</th><th>A30</th><th>A32</th></tr>
<tr><td></td><td colspan="4"></td><td colspan="2">MUSCOVITE + SILLIMANITE + K-FELDSPAR ZONE</td></tr>
<tr><td>Quartz</td><td>24.7±2.0</td><td>24.7±2.0</td><td>17.7±7.2</td><td>31.4±4.5</td><td>37.6±3.1</td><td>48.1±5.1</td></tr>
<tr><td>Plagioclase</td><td>39.5±7.4</td><td>39.5±7.4</td><td>14.6±5.9</td><td>36.7±5.9</td><td>24.8±6.3</td><td>21.3±5.0</td></tr>
<tr><td>Biotite</td><td>22.7±3.8</td><td>22.7±3.8</td><td>24.5±5.4</td><td>18.4±6.5</td><td>18.7±7.2</td><td>10.4±3.0</td></tr>
<tr><td>Cordierite</td><td></td><td></td><td></td><td></td><td></td><td></td></tr>
<tr><td>Garnet</td><td>pr.</td><td>—</td><td>pr.</td><td>0.5</td><td></td><td>1.4±2.0</td></tr>
<tr><td>Sillimanite</td><td></td><td></td><td></td><td></td><td>0.3</td><td>0.2</td></tr>
<tr><td>Andalusite</td><td></td><td></td><td></td><td></td><td></td><td></td></tr>
<tr><td>K-feldspar</td><td>2.0±1.5</td><td>2.0±1.5</td><td>2.0±2.6</td><td>7.9±3.7</td><td>12.2±4.5</td><td>4.1±1.3</td></tr>
<tr><td>Muscovite: P</td><td>9.3±3.4</td><td>9.3±3.4</td><td>39.8±8.9</td><td>3.8±2.6</td><td>5.0±2.8</td><td>11.2±3.9</td></tr>
<tr><td>S</td><td>1.1±0.7</td><td>1.1±0.7</td><td></td><td></td><td>1.5±1.2</td><td>1.0±0.6</td></tr>
<tr><td>Others</td><td>0.7</td><td>0.7</td><td>1.4</td><td>1.3</td><td></td><td>2.4</td></tr>
<tr><td>No. of Points</td><td>441 (9x7x7)</td><td>441 (9x7x7)</td><td>294 (6x7x7)</td><td>392 (8x7x7)</td><td>343 (7x7x7)</td><td>588 (12x7x7)</td></tr>
<tr><td>Point Interval (mm)</td><td>1.0</td><td>1.0</td><td>1.0</td><td>1.0</td><td>1.0</td><td>1.0</td></tr>
<tr><td>% Primary Muscovite</td><td>89</td><td>89</td><td>100</td><td>100</td><td>77</td><td>92</td></tr>
<tr><td>% Sillimanite + K-feldspar</td><td>0</td><td>0</td><td>0</td><td>0</td><td>12</td><td>5</td></tr>
</table>

285

MUSCOVITE + SILLIMANITE + K-FELDSPAR ZONE (continued)

SAMPLE	A36	300C	314C	328C	364C	402C
Quartz	12.5+2.4	26.7+4.9	31.5+8.7	19.4+7.0	19.6+2.2	23.0+4.5
Plagioclase	29.5+4.8	22.8+6.2	34.7+6.1	42.1+7.6	45.1+4.6	26.5+8.4
Biotite	27.5+4.2	19.4+2.6	21.3+4.3	20.4+6.9	25.8+4.1	25.5+6.8
Cordierite						
Garnet	0.2	0.5				1.0+1.4
Sillimanite	1.2+0.8	3.6+1.3	1.8+1.4	3.1+2.6		5.0+2.0
Andalusite						
K-feldspar	0.4	5.3+2.0	1.1+0.7	4.1+1.9		3.0+2.0
Muscovite: P	4.9+1.3	18.2+6.3	7.0+4.4	8.7+5.0	5.7+3.2	10.0+2.4
S	11.9+4.1	2.6+1.8	1.8+1.1	1.5+1.0	2.7+1.3	3.5+1.8
Others	2.0	1.5	0.7	0.8	1.3	2.5
No. of Points	512 (8x8x8)	588 (12x7x5)	441 (9x7x7)	392 (8x7x7)	637 (13x7x7)	200 (8x5x5)
Point Interval (mm)	1.7	1.0	1.0	1.0	1.0	1.3
% Primary Muscovite	29	88	80	85	68	74
% Sillimanite + K-feldspar	3	28	16	38	0	25

286

SILLIMANITE + K-FELDSPAR ZONE

SAMPLE	A4	A14	A19	A29	A51	A56
Quartz	12.2±3.3	22.3±3.1	15.8±3.1	20.1±5.3	26.5±3.7	24.5±4.8
Plagioclase	46.9±10.1	27.5±3.1	42.6±3.7	44.9±7.5	46.4±4.5	54.1±3.2
Biotite	31.6±8.6	19.7±2.8	33.8±5.0	21.4±7.0	20.2±2.8	18.1±3.8
Cordierite						
Garnet		0.6	0.4			0.5
Sillimanite	1.5±2.0	2.2±0.9		6.8±4.6	0.3	
Andalusite						
K-feldspar	3.1±3.9	19.9±2.9	1.0±1.3	5.1±2.5	2.7±1.3	1.3±1.5
Muscovite: P				pr.		
S	4.6±2.0	6.3±1.5	0.6		2.4±1.1	1.0±1.1
Others		1.7	5.6	1.7	1.4	0.5
No. of Points	196 (4x7x7)	539 (11x7x7)	500 (5x10x10)	294 (6x7x7)	588 (12x7x7)	392 (8x7x7)
Point Interval (mm)	1.7	1.3	1.3	1.0	1.0	1.0
% Primary Muscovite	0	0	0	0	0	0
% Sillimanite + K-feldspar	49	51	0	100	27	0

287

	SILLIMANITE + K-FELDSPAR ZONE					CORDIERITE + K-FELDSPAR ZONE
SAMPLE	257C	291C	311C	321C	384C	A2
Quartz	18.1±5.3	18.9±5.4	22.2±5.0	30.3±5.2	28.0±11.1	12.5±3.3
Plagioclase	42.5±6.6	44.0±8.0	32.8±4.8	31.2±6.2	46.7±6.4	34.2±4.3
Biotite	33.1±4.3	33.8±8.2	34.6±2.9	17.7±5.1	15.3±8.6	34.4±6.4
Cordierite	pr.	pr.	0.6			2.6±1.7
Garnet						0.3
Sillimanite	0.6	0.7	1.9±0.8	1.5±1.5	4.0±3.6	0.5
Andalusite						
K-feldspar	0.3	0.7	4.2±1.5	3.9±1.5	1.3±1.7	5.4±2.4
Muscovite: P						
S	2.8±1.5	1.1±1.6	1.2±0.8	12.4±6.7	4.0±2.9	9.2±1.7
Others	2.8	0.7	2.6	3.0	0.7	1.0
No. of Points	360 (10x6x6)	275 (11x5x5)	686 (14x7x7)	468 (13x6x6)	150 (6x5x5)	392 (8x7x7)
Point Interval (mm)	1.0	1.0	1.0	1.0	1.7	1.3
% Primary Muscovite	0	0	0	0	0	0
% Sillimanite + K-feldspar	14	49	83	27	33	14

CORDIERITE + K-FELDSPAR ZONE (continued)

SAMPLE	A5	A7	A16	A45	270C	303C
Quartz	19.2±5.8	21.2±3.6	21.3±4.8	16.7±4.1	19.4±2.9	20.9±4.6
Plagioclase	36.7±6.0	38.7±4.3	42.6±5.5	30.0±7.9	37.4±7.6	48.5±3.3
Biotite	24.8±4.8	23.0±3.8	27.7±4.3	34.0±7.8	25.9±7.5	17.1±3.2
Cordierite	1.6±1.9	4.8±1.9	0.5	5.3±4.0	7.1±2.5	pr.
Garnet	4.4±2.1		0.2	5.3±3.4	0.7	0.3
Sillimanite	5.3±3.7		2.7±2.5	2.0±2.7	0.7	pr.
Andalusite		1.1±				
K-feldspar	5.8±1.4	1.8±0.9	1.6±0.6	0.7	5.8±2.9	3.6±1.0
Muscovite: P						
S	1.2±1.2	8.1±7.7	3.0±2.4	2.7±2.0	1.4±2.0	7.7±4.3
Others	0.9	1.2	0.5	3.3	1.7	2.1
No. of Points	343 (7x7x7)	504 (14x6x6)	441 (9x7x7)	150 (6x5x5)	294 (6x7x7)	392 (8x7x7)
Point Interval (mm)	1.3	1.7	1.3	2.0	1.0	1.3
% Primary Muscovite	0	0	0	0	0	0
% Sillimanite + K-feldspar	88	25	44	28	60	0

289

CORDIERITE + K-FELDSPAR ZONE (continued)

SAMPLE	309C	310C
Quartz	35.0±5.5	21.8±3.3
Plagioclase	42.2±9.4	28.3±4.7
Biotite	10.9±4.1	22.5±3.2
Cordierite	2.2±1.7	
Garnet	0.2	0.2
Sillimanite	1.6±0.8	8.4±3.7
Andalusite		
K-feldspar	2.7±2.4	14.7±4.3
Muscovite: P		
S	4.2±3.0	2.5±1.4
Others	0.9	1.6
No. of Points	448 (7x8x8)	441 (9x7x7)
Point Interval (mm)	1.0	1.0
% Primary Muscovite	0	0
% Sillimanite + K-feldspar	49	90

APPENDIX II

Electron Microprobe Analyses - Strontian Aureole

Analyses have been made using the Cambridge Instruments Microscan V microprobe in the Department of Metallurgy and Materials at the University of Aston in Birmingham. Additional analyses have been made with the automated energy dispersive probe at the Department of Mineralogy and Petrology, Cambridge. Analytical methods and data corrections follow the procedures given by Sweatman & Long (1969).

Feldspar compositions are estimated from partial analysis for Na, Ca and K for plagioclase, and K, Na, Ca and Ba for K-feldspar.

* indicates Cambridge E.D.S. probe analysis

a H_2O content of mica calculated assuming H = 4.00.

APPENDIX II

TABLE I

REPRESENTATIVE GARNET ANALYSES

SPECIMEN	A1 CORE	A2* CORE	RIM	A5 CORE	A8* CORE	RIM
SiO_2	36.53	37.67	37.43	37.02	37.67	37.01
TiO_2	-	-	-	-	-	-
Al_2O_3	21.19	21.30	20.88	21.29	21.38	20.83
FeO	33.56	35.36	33.67	33.81	34.42	33.20
MnO	4.44	3.48	6.54	3.88	4.60	6.68
MgO	2.91	2.46	1.60	2.95	2.78	1.95
CaO	1.29	0.81	0.81	1.28	0.95	0.81
Na_2O	-	-	-	-	-	-
K_2O	-	0.10	-	-	-	0.07
TOTAL	99.92	101.18	100.93	100.23	101.80	100.61
Si	5.92	6.02	6.04	5.97	6.01	6.00
Al	0.08	0.00	0.00	0.03	0.00	0.00
TOTAL	6.00	6.02	6.04	6.00	6.01	6.00
Al	3.97	4.01	3.97	4.01	4.00	3.98
Ti	0.00	0.00	0.00	0.00	0.00	0.00
TOTAL	3.97	4.01	3.97	4.01	4.00	3.98
Fe	4.55	4.73	4.54	4.55	4.54	4.50
Mg	0.70	0.59	0.39	0.71	0.64	0.47
Mn	0.61	0.47	0.89	0.53	0.64	0.92
Ca	0.22	0.14	0.14	0.22	0.17	0.15
Na	0.00	0.00	0.00	0.00	0.00	0.00
K	0.00	0.02	0.00	0.00	0.00	0.01
TOTAL	6.08	5.95	5.96	6.01	5.99	6.05

292

TABLE I (continued)

SPECIMEN	A45 CORE	RIM	A73 CORE	RIM	A83 CORE	RIM
SiO_2	37.25	36.91	37.02	36.88	37.61	37.33
TiO_2	0.01	0.03	–	0.03	–	–
Al_2O_3	20.89	20.68	21.29	21.03	21.26	20.93
FeO	33.51	31.57	33.13	24.41	34.59	35.27
MnO	4.78	7.28	5.31	10.17	1.80	2.95
MgO	2.82	1.91	2.86	1.84	4.56	3.20
CaO	1.10	0.91	0.89	0.90	1.13	1.13
Na_2O	0.01	0.04	–	–	–	–
K_2O	–	–	–	–	–	–
TOTAL	100.37	99.33	100.50	100.26	100.95	100.81
Si	6.00	6.03	5.96	5.99	5.97	5.99
Al	0.00	0.00	0.04	0.01	0.03	0.01
TOTAL	6.00	6.03	6.00	6.00	6.00	6.00
Al	3.97	3.98	4.00	4.01	3.94	3.94
Ti	0.00	0.00	0.00	0.00	0.00	0.00
TOTAL	3.97	3.98	4.00	4.01	3.94	3.94
Fe	4.52	4.32	4.46	3.99	4.59	4.73
Mg	0.68	0.46	0.69	0.44	1.08	0.76
Mn	0.65	1.01	0.72	1.40	0.24	0.40
Ca	0.19	0.16	0.15	0.16	0.19	0.19
Na	0.00	0.01	0.00	0.00	0.00	0.00
K	0.00	0.00	0.00	0.00	0.00	0.00
TOTAL	6.04	5.96	6.02	5.99	6.10	6.08

TABLE I (continued)

SPECIMEN	270C CORE	RIM	A10 CORE	RIM	A19 CORE	RIM *
SiO_2	37.10	36.82	37.27	37.02	37.01	37.23
TiO_2	–	0.02	0.01	0.01	0.01	–
Al_2O_3	20.99	20.70	21.03	20.93	21.32	21.06
FeO	34.93	34.63	31.13	30.54	33.95	31.35
MnO	3.52	4.72	6.71	7.99	3.38	7.20
MgO	2.43	1.90	2.13	1.50·	2.89	1.69
CaO	1.50	0.88	2.10	1.72	1.42	1.65
Na_2O	–	–	–	–	0.05	–
K_2O	–	–	–	–	–	–
TOTAL	100.47	99.67	100.38	99.71	100.03	100.18
Si	5.99	6.01	6.01	6.02	6.00	6.02
Al	0.01	0.00	0.00	0.00	0.03	0.00
TOTAL	6.00	6.01	6.01	6.02	6.00	6.02
Al	3.98	3.98	4.00	4.02	4.02	3.98
Ti	0.00	0.00	0.00	0.00	0.00	0.00
TOTAL	3.98	3.98	4.00	4.02	4.02	3.98
Fe	4.71	4.73	4.20	4.16	4.58	4.35
Mg	0.58	0.46	0.51	0.37	0.70	0.59
Mn	0.48	0.65	0.92	1.10	0.46	0.78
Ca	0.26	0.15	0.36	0.30	0.25	0.26
Na	0.00	0.00	0.00	0.00	0.02	0.00
K	0.00	0.00	0.00	0.00	0.00	0.00
TOTAL	6.03	5.99	5.99	5.93	6.01	5.98

TABLE I (continued)

SPECIMEN	A52 CORE	A55 CORE	A72 CORE	RIM	356C CORE	A32 CORE
SiO_2	37.16	37.33	37.36	36.91	37.34	37.19
TiO_2	0.02	–	0.01	0.04	–	0.01
Al_2O_3	20.79	20.96	21.01	20.80	21.17	21.24
FeO	29.23	34.40	32.41	30.14	35.43	33.40
MnO	8.03	3.64	4.36	7.12	2.38	5.86
MgO	2.61	2.95	2.90	2.07	2.60	2.63
CaO	1.14	1.16	1.92	2.00	1.95	0.92
Na_2O	0.01	0.01	–	–	0.03	0.01
K_2O	–	–	–	–	–	–
TOTAL	98.00	100.45	99.97	99.08	100.90	101.28
Si	6.05	6.00	6.01	6.02	5.98	5.96
Al	0.00	0.00	0.00	0.00	0.02	0.04
TOTAL	6.05	6.00	6.01	6.02	6.00	6.00
Al	3.99	3.98	3.99	4.00	3.98	3.97
Ti	0.00	0.00	0.00	0.00	0.00	0.00
TOTAL	3.99	3.98	3.99	4.00	3.98	3.97
Fe	3.98	4.63	4.36	4.11	4.75	4.47
Mg	0.63	0.71	0.70	0.50	0.62	0.63
Mn	1.11	0.50	0.59	0.98	0.32	0.80
Ca	0.20	0.20	0.33	0.35	0.34	0.16
Na	0.00	0.00	0.00	0.00	0.01	0.00
K	0.00	0.00	0.00	0.00	0.00	0.00
TOTAL	5192	6.04	5.98	5,94	6.04	6.01

TABLE I (continued)

SPECIMEN	402C CORE	RIM	A41[*] CORE	RIM	A65 CORE
SiO_2	37.43	36.96	37.82	36.86	37.09
TiO_2	0.01	0.02	–	–	–
Al_2O_3	30.71	20.69	21.17	20.87	21.08
FeO	34.06	28.95	32.72	29.10	31.58
MnO	4.13	9.52	4.25	9.53	6.22
MgO	2.71	1.81	2.26	1.58	2.49
CaO	1.76	1.66	2.32	1.71	1.59
Na_2O	0.01	–	–	–	–
K_2O	–	–	–	–	–
TOTAL	100.82	99.61	100.54	99.65	100.05
Si	6.01	6.02	6.05	6.01	5.99
Al	0.00	0.00	0.00	0.00	0.01
TOTAL	6.01	6.02	6.05	6.01	6.00
Al	3.92	3.97	4.00	4.01	4.01
Ti	0.00	0.00	0.00	0.00	0.00
TOTAL	3.92	3.97	4.00	4.01	4.01
Fe	4.57	3.95	4.38	3.97	4.27
Mg	0.65	0.44	0.54	0.38	0.60
Mn	0.56	1.31	0.58	1.32	0.85
Ca	0.30	0.29	0.40	0.30	0.27
Na	0.00	0.00	0.00	0.00	0.00
K	0.00	0.00	0.00	0.00	0.00
TOTAL	6.08	5.99	5.90	5.97	5.99

TABLE I (continued)

SPECIMEN	A91 CORE	RIM	205C* CORE	RIM	298C CORE	RIM
SiO_2	37.04	37.16	37.53	37.70	36.48	36.41
TiO_2	-	0.01	-	-	-	-
Al_2O_3	21.07	20.91	21.59	21.06	20.58	20.53
FeO	34.90	33.83	33.90	35.08	34.20	30.07
MnO	3.19	4.83	2.58	2.04	4.08	9.25
MgO	2.89	2.26	3.45	2.67	2.69	1.80
CaO	1.64	2.05	1.82	2.06	0.92	0.97
Na_2O	0.05	-	-	-	0.02	0.01
K_2O	-	-	-	-	-	-
TOTAL	100.78	100.05	100.87	100.61	98.97	99.04
Si	5.95	5.97	5.97	6.04	5.98	5.99
Al	0.05	0.03	0.00	0.00	0.02	0.01
TOTAL	6.00	6.00	6.00	6.04	6.00	6.00
Al	3.95	3.94	4.02	3.97	3.96	3.97
Ti	0.00	0.00	0.00	0.00	0.00	0.00
TOTAL	3.95	3.94	4.02	3.97	3.96	3.97
Fe	4.69	4.55	4.51	4.70	4.69	4.14
Mg	0.69	0.54	0.82	0.64	0.66	0.44
Mn	0.43	0.66	0.35	0.28	0.57	1.29
Ca	0.28	0.35	0.31	0.35	0.16	0.17
Na	0.01	0.00	0.00	0.00	0.01	0.00
K	0.00	0.00	0.00	0.00	0.00	0.00
TOTAL	6.10	6.10	5.99	5.97	6.09	6.03

TABLE I (continued)

SPECIMEN	572C INNER CORE	OUTER CORE	RIM	614C CORE	RIM
SiO_2	37.45	37.12	36.95	37.60	37.08
TiO_2	0.01	0.01	0.03	0.01	0.01
Al_2O_3	21.30	21.16	21.13	21.70	21.09
FeO	34.33	33.57	32.52	34.35	33.25
MnO	4.01	4.02	5.98	1.72	3.30
MgO	3.19	2.86	2.02	3.39	2.31
CaO	0.95	1.91	2.08	2.21	2.53
Na_2O	-	-	-	-	-
K_2O	-	-	-	-	-
TOTAL	101.24	100.65	100.71	100.98	99.57
Si	5.97	5.96	5.96	5.97	6.00
Al	0.03	0.04	0.04	0.03	0.00
TOTAL	6.00	6.00	6.00	6.00	6.00
Al	3.98	3.97	3.98	4.03	4.03
Ti	0.00	0.00	0.00	0.00	0.00
TOTAL	3.98	2.97	3.98	4.03	4.03
Fe	4.58	4.51	4.38	4.56	4.50
Mg	0.76	0.68	0.49	0.80	0.56
Mn	0.54	0.55	0.82	0.23	0.45
Ca	0.16	0.33	0.36	0.37	0.44
Na	0.00	0.00	0.00	0.00	0.00
K	0.00	0.00	0.00	0.00	0.00
TOTAL	6.04	6.07	6.05	5.96	5.95

298

APPENDIX II

TABLE II

REPRESENTATIVE BIOTITE ANALYSES

SPECIMEN	A1	A2*	A5	A8	A45	A73
SiO_2	34.24	34.86	34.50	34.87	34.17	35.00
TiO_2	3.81	3.76	3.18	4.07	3.34	3.13
Al_2O_3	19.48	19.48	19.90	19.46	19.34	18.57
FeO	21.61	21.82	21.30	22.12	21.61	22.28
MnO	0.24	0.17	0.19	0.32	0.29	0.42
MgO	6.84	5.75	7.06	6.64	6.74	7.08
CaO	0.01	–	0.03	0.01	0.01	0.00
Na_2O	0.17	–	0.13	0.18	0.09	0.08
K_2O	9.26	9.25	9.32	9.32	9.24	9.39
BaO	0.17	–	0.11	0.09	0.15	0.13
H_2O^a	3.90	3.89	3.91	3.95	3.87	3.90
TOTAL	99.73	98.98	99.63	101.03	98.85	99.98
Si	5.26	5.37	5.29	5.29	5.30	5.38
Al	2.74	2.63	2.71	2.71	2.70	2.62
TOTAL	8.00	8.00	8.00	8.00	8.00	8.00
Al	0.78	0.91	0.80	0.77	0.83	0.74
Ti	0.44	0.44	0.37	0.46	0.39	0.36
Fe	2.78	2.81	2.73	2.81	2.80	2.86
Mn	0.03	0.02	0.03	0.04	0.04	0.06
Mg	1.57	1.32	1.61	1.50	1.56	1.62
TOTAL	5.60	5.50	5.62	5.58	5.62	5.64
Ca	0.00	0.00	0.01	0.00	0.00	0.00
Na	0.05	0.00	0.04	0.05	0.03	0.02
K	1.81	1.82	1.82	1.80	1.83	1.84
Ba	0.01	0.00	0.01	0.01	0.01	0.01
TOTAL	1.87	1.82	1.88	1.86	1.87	1.87

TABLE II (continued)

SPECIMEN	A83	270C	A10	A19	A52	A55
SiO_2	33.77	33.55	34.47	34.76	34.42	34.00
TiO_2	3.46	3.56	4.20	2.81	3.18	3.25
Al_2O_3	18.26	19.77	19.22	19.70	19.64	19.57
FeO	19.25	23.13	22.61	21.47	19.88	21.57
MnO	0.24	0.14	0.36	0.28	0.34	0.30
MgO	8.54	5.94	6.28	6.92	7.32	6.45
CaO	-	-	-	-	-	-
Na_2O	0.23	0.22	0.10	0.21	0.17	0.19
K_2O	9.22	8.51	9.47	9.02	9.28	9.37
BaO	0.17	0.25	0.21	0.19	0.15	0.17
H_2O	3.82	3.85	3.92	3.90	3.88	3.86
TOTAL	96.96	98.92	100.84	99.26	98.26	98.73
Si	5.30	5.22	5.27	5.34	5.32	5.28
Al	2.70	2.78	2.73	2.66	2.68	2.72
TOTAL	8.00	8.00	8.00	8.00	8.00	8.00
Al	0.67	0.84	0.73	0.91	0.90	0.87
Ti	0.41	0.42	0.48	0.33	0.37	0.38
Fe	2.53	3.01	2.89	2.76	2.57	2.80
Mn	0.03	0.02	0.05	0.04	0.05	0.04
Mg	2.00	1.38	1.43	1.59	1.69	1.49
TOTAL	5.64	5.67	5.58	5.63	5.58	5.58
Ca	-	-	0.00	-	0.00	0.00
Na	0.07	0.07	0.03	0.06	0.05	0.06
K	1.85	1.69	1.85	1.77	1.83	1.86
Ba	0.01	0.02	0.01	0.01	0.01	0.01
TOTAL	1.93	1.78	1.89	1.84	1.89	1.93

TABLE II (continued)

SPECIMEN	A72	356C	A32	402C	A41	A65
SiO_2	34.70	34.46	34.71	34.16	35.20	34.57
TiO_2	4.94	3.38	3.22	2.65	2.98	3.41
Al_2O_3	18.23	19.50	19.09	19.46	19.41	19.21
FeO	20.36	22.37	22.56	21.69	22.47	20.95
MnO	0.38	0.18	0.28	0.33	0.35	0.34
MgO	6.12	6.56	6.33	7.27	7.14	7.37
CaO	-	0.01	0.00	-	0.01	0.01
Na_2O	0.12	0.19	0.13	0.00	0.16	0.13
K_2O	8.76	8.64	9.29	9.40	9.06	9.34
BaO	0.17	0.21	0.10	0.15	0.16	0.26
H_2O	3.87	3.89	3.88	3.87	3.95	3.90
TOTAL	98.15	99.39	99.59	98.98	100.89	99.43
Si	5.38	5.31	5.35	5.29	5.34	5.31
Al	2.62	2.69	2.65	2.71	2.66	2.69
TOTAL	8.00	8.00	8.00	8.00	8.00	8.00
Al	0.70	0.84	0.82	0.84	0.82	0.79
Ti	0.58	0.39	0.37	0.31	0.34	0.39
Fe	2.64	2.88	2.91	2.81	2.85	2.69
Mn	0.05	0.02	0.04	0.04	0.04	0.04
Mg	1.53	1.50	1.45	1.68	1.62	1.69
TOTAL	5.50	5.63	5.59	5.68	5.67	5.60
Ca	0.00	0.00	0.00	0.00	0.00	0.00
Na	0.04	0.06	0.04	0.00	0.05	0.04
K	1.73	1.70	1.83	1.86	1.75	1.83
Ba	0.01	0.01	0.01	0.01	0.01	0.02
TOTAL	1.78	1.77	1.88	1.87	1.81	1.89

TABLE II (continued)

SPECIMEN	A91	205C	298C	572C	614C
SiO_2	34.27	35.53	34.12	34.76	35.57
TiO_2	2.56	2.45	4.58	4.15	3.03
Al_2O_3	19.43	19.44	18.27	19.57	19.06
FeO	22.16	21.31	22.33	20.52	20.19
MnO	0.16	0.08	0.38	0.18	0.09
MgO	7.89	8.73	6.84	7.85	7.79
CaO	0.00	0.01	0.02	–	–
Na_2O	0.23	0.22	0.15	0.15	0.27
K_2O	8.98	8.72	8.87	9.09	8.97
BaO	0.13	0.21	0.25	0.25	0.22
H_2O	3.90	3.95	3.88	3.96	3.94
TOTAL	99.71	99.65	99.69	100.48	99.85
Si	5.27	5.39	5.26	5.26	5.41
Al	2.73	2.61	2.74	2.74	2.59
TOTAL	8.00	8.00	8.00	8.00	8.00
Al	0.78	0.86	0.59	0.75	0.83
Ti	0.30	0.28	0.53	0.47	0.35
Fe	2.85	2.58	2.88	2.60	2.66
Mn	0.02	0.01	0.05	0.02	0.01
Mg	1.81	1.97	1.57	1.77	1.77
TOTAL	5.76	5.70	5.62	5.61	5.62
Ca	0.00	0.00	0.00	0.00	0.00
Na	0.07	0.06	0.04	0.04	0.08
K	1.76	1.69	1.75	1.75	1.74
Ba	0.01	0.01	0.01	0.01	0.01
TOTAL	1.84	1.76	1.80	1.80	1.83

302

TABLE III

REPRESENTATIVE CORDIERITE ANALYSES

SPECIMEN	A2	270C
SiO_2	47.95	47.05
TiO_2	0.01	–
Al_2O_3	32.22	32.12
FeO	11.28	11.86
MnO	0.27	0.43
MgO	6.20	5.96
CaO	0.03	0.01
Na_2O	0.27	0.30
TOTAL	98.23	97.73
Si	5.02	4.97
Al	0.98	1.03
TOTAL	6.00	6.00
Al	2.99	2.97
Ti	0.00	0.00
TOTAL	2.99	2.97
Fe	0.99	1.05
Mg	0.97	0.94
Mn	0.02	0.04
Ca	0.00	0.00
Na	0.06	0.06
TOTAL	2.04	2.09

TABLE IV

REPRESENTATIVE MUSCOVITE ANALYSES

SPECIMEN	A2	A5	A8	A83	A10	A19
SiO_2	46.02	45.09	44.87	45.32	47.15	46.51
TiO_2	0.31	0.05	0.07	0.28	0.41	2.22
Al_2O_3	35.90	36.73	36.31	33.63	34.39	35.94
Fe_2O_3	1.34	0.97	1.34	1.56	2.12	1.05
MnO	0.01	0.02	0.00	0.04	0.02	0.01
MgO	0.60	0.32	0.66	0.83	0.80	0.37
CaO	-	0.02	0.00	-	-	0.01
Na_2O	0.50	0.49	0.69	0.47	0.28	0.49
K_2O	10.17	10.38	10.24	10.14	10.80	8.01
BaO	0.54	-	0.18	0.71	0.30	0.32
H_2O^a	4.51	4.46	4.46	4.38	4.54	4.55
TOTAL	99.90	98.53	98.82	97.36	100.81	99.28
Si	6.11	6.05	6.03	6.20	6.23	6.13
Al	1.89	1.95	1.97	1.80	1.77	1.87
TOTAL	8.00	8.00	8.00	8.00	8.00	8.00
Al	3.74	3.87	3.78	3.63	3.58	3.68
Ti	0.03	0.00	0.01	0.03	0.04	0.22
Fe	0.13	0.10	0.14	0.16	0.21	0.10
Mn	0.00	0.00	0.00	0.00	0.00	0.00
Mg	0.12	0.06	0.13	0.17	0.16	0.07
TOTAL	4.02	4.03	4.06	3.99	3.99	4.07
Ca	0.00	0.00	0.00	0.00	0.00	0.00
Na	0.13	0.13	0.18	0.13	0.07	0.12
K	1.72	1.78	1.76	1.77	1.82	1.35
Ba	0.03	0.00	0.01	0.04	0.02	0.02
TOTAL	1.88	1.91	1.95	1.94	1.91	1.49

TABLE IV (continued)

SPECIMEN	A55	356C	A32	402C	A41	A65
SiO_2	45.71	47.39	47.04	46.27	47.10	45.57
TiO_2	1.29	0.54	1.10	1.23	0.93	1.16
Al_2O_3	35.13	36.48	36.15	33.52	35.53	35.87
Fe_2O_3	1.50	1.49	1.19	1.45	1.21	1.16
MnO	0.01	0.01	0.04	0.02	0.00	0.02
MgO	0.49	0.52	0.56	0.84	0.63	0.58
CaO	-	0.01	0.00	-	-	-
Na_2O	0.40	0.47	0.58	0.54	0.46	0.47
K_2O	8.36	8.76	10.36	10.15	10.16	10.35
BaO	0.26	0.27	0.18	0.33	0.24	0.55
H_2O^a	4.46	4.59	4.61	4.46	4.57	4.51
TOTAL	97.61	100.53	101.81	98.81	100.83	100.24
Si	6.14	6.18	6.12	6.22	6.18	6.05
Al	1.86	1.82	1.88	1.78	1.82	1.95
TOTAL	8.00	8.00	8.00	8.00	8.00	8.00
Al	3.71	3.79	3.66	3.53	3.67	3.66
Ti	0.13	0.05	0.11	0.12	0.09	0.12
Fe	0.15	0.15	0.12	0.15	0.12	0.12
Mn	0.00	0.00	0.01	0.00	0.00	0.00
Mg	0.10	0.10	0.11	0.17	0.12	0.12
TOTAL	4.09	4.09	4.01	3.97	4.00	4.02
Ca	0.00	0.00	0.00	0.00	0.00	0.00
Na	0.11	0.12	0.15	0.14	0.12	0.12
K	1.43	1.46	1.72	1.74	1.70	1.75
Ba	0.01	0.01	0.01	0.02	0.01	0.03
TOTAL	1.55	1.59	1.88	1.90	1.83	1.90

TABLE IV (continued)

SPECIMEN	A91	205C	298C	572C	614C
SiO_2	45.92	46.68	44.94	46.21	45.71
TiO_2	1.41	1.27	0.96	0.79	0.95
Al_2O_3	34.01	35.02	33.37	35.83	35.42
Fe_2O_3	1.67	1.43	1.43	1.41	1.13
MnO	0.01	0.02	0.03	0.00	0.00
MgO	1.03	0.66	0.80	0.68	0.56
CaO	–	0.03	–	–	–
Na_2O	0.61	0.83	0.39	0.74	0.61
K_2O	9.95	9.55	10.14	9.82	10.22
BaO	0.27	0.21	0.24	0.45	0.40
H_2O[a]	4.48	4.54	4.36	4.54	4.49
TOTAL	99.36	100.24	96.66	100.47	99.49
Si	6.14	6.16	6.18	6.10	6.10
Al	1.86	1.84	1.82	1.90	1.90
TOTAL	8.00	8.00	8.00	8.00	8.00
Al	3.50	3.60	3.58	3.67	3.67
Ti	0.14	0.13	0.10	0.08	0.10
Fe	0.17	0.14	0.15	0.14	0.11
Mn	0.00	0.00	0.00	0.00	0.00
Mg	0.21	0.13	0.16	0.13	0.11
TOTAL	4.02	4.00	3.99	4.02	3.99
Ca	0.00	0.00	0.00	0.00	0.00
Na	0.16	0.21	0.10	0.19	0.16
K	1.70	1.61	1.78	1.65	1.74
Ba	0.01	0.01	0.01	0.02	0.02
TOTAL	1.87	1.83	1.89	1.86	1.92

APPENDIX II

TABLE V

PLAGIOCLASE COMPOSITIONS

SPECIMEN	X_{Na}	X_{Ca}	X_K
A1	0.69	0.29	0.02
A2	0.76	0.23	0.01
A5	0.74	0.25	0.01
A8	0.74	0.24	0.02
A10	0.73	0.25	0.02
A19	0.70	0.29	0.01
A28	0.64	0.34	0.02
A52	0.72	0.25	0.03
356C	0.71	0.27	0.02
A32	0.79	0.19	0.02
A41	0.81	0.17	0.02
A65	0.75	0.23	0.02
205C	0.69	0.30	0.01
572C	0.71	0.28	0.01
614C	0.62	0.37	0.01

APPENDIX II

TABLE VI

K-FELDSPAR COMPOSITIONS

SPECIMEN	X_K	X_{Na}	X_{Ca}	X_{Ba}
A2	0.87	0.12	0.01	0.00
A8	0.82	0.17	0.01	0.00
A10	0.87	0.12	0.01	0.00
A28	0.87	0.08	0.00	0.05

Electron Microprobe Analyses - Foyers Aureole

[a] H_2O content of mica calculated assuming H = 4.00.

APPENDIX III

TABLE I

REPRESENTATIVE GARNET ANALYSES

SPECIMEN	B10 CORE	RIM	B13 CORE	B77 CORE	RIM	B56 CORE
SiO_2	36.41	36.72	37.31	37.74	37.22	36.82
TiO_2	0.03	0.05	0.02	0.00	0.00	0.03
Al_2O_3	20.77	20.98	21.07	21.07	20.95	20.83
FeO	32.74	31.79	29.88	26.35	26.41	32.50
MnO	4.79	6.45	8.71	11.73	11.95	6.09
MgO	2.86	2.26	2.55	2.45	2.41	1.49
CaO	1.07	1.09	1.05	1.39	1.33	2.39
Na_2O	0.01	0.04	0.00	0.08	0.06	0.04
TOTAL	98.68	99.38	100.59	100.81	100.33	100.19
Si	5.97	5.98	6.00	6.04	6.00	5.98
Al	0.03	0.02	0.00	0.00	0.00	0.02
TOTAL	6.00	6.00	6.00	6.04	6.00	6.00
Al	3.98	4.02	4.00	3.98	3.98	3.98
Ti	0.00	0.01	0.00	0.00	0.00	0.00
TOTAL	3.98	4.03	4.00	3.98	3.98	3.98
Fe	4.49	4.33	4.02	3.53	3.56	4.42
Mg	0.70	0.55	0.61	0.58	0.58	0.36
Mn	0.67	0.89	1.19	1.59	1.63	0.84
Ca	0.19	0.19	0.18	0.24	0.23	0.42
Na	0.00	0.01	0.00	0.03	0.02	0.01
TOTAL	6.05	5.97	6.00	5.97	6.02	6.05

TABLE I (continued)

SPECIMEN	B57 CORE	RIM	B8 CORE	RIM	B44 CORE	RIM
SiO_2	38.04	37.99	37.69	37.30	37.19	37.32
TiO_2	0.02	0.03	0.06	0.08	0.06	0.00
Al_2O_3	21.06	20.72	21.07	21.01	20.71	20.30
FeO	30.86	30.06	32.01	30.73	28.60	32.50
MnO	7.26	8.21	3.73	6.83	0.88	3.62
MgO	2.70	2.54	2.21	1.73	2.13	2.32
CaO	1.01	1.15	3.59	2.87	9.27	3.43
Na_2O	0.12	0.11	0.03	0.04	0.00	0.00
TOTAL	101.06	100.81	100.39	100.59	98.84	99.49
Si	6.06	6.08	6.04	6.01	6.00	6.05
Al	0.00	0.00	0.00	0.00	0.00	0.00
TOTAL	6.06	6.08	6.04	6.01	6.00	6.05
Al	3.96	3.91	3.98	3.99	3.93	3.88
Ti	0.00	0.00	0.01	0.01	0.01	0.00
TOTAL	3.96	3.91	3.99	4.00	3.94	3.88
Fe	4.11	4.03	4.29	4.14	3.86	4.41
Mg	0.64	0.61	0.53	0.42	0.51	0.56
Mn	0.98	1.11	0.51	0.93	0.12	0.50
Ca	0.17	0.20	0.62	0.50	1.60	0.60
Na	0.04	0.04	0.01	0.01	0.00	0.00
TOTAL	5.94	5.99	5.96	6.00	6.09	6.07

TABLE I (continued)

SPECIMEN	B62 CORE	RIM	B79 CORE	INNER RIM	RIM	B83 CORE
SiO_2	38.13	37.45	37.89	37.75	37.78	37.24
TiO_2	0.01	0.00	0.00	0.00	0.00	0.02
Al_2O_3	20.68	20.76	21.19	21.00	21.06	20.90
FeO	32.49	32.26	34.47	35.90	36.36	30.68
MnO	3.85	5.08	2.75	2.36	1.80	6.76
MgO	2.85	1.96	2.39	1.67	2.24	1.87
CaO	3.30	3.24	2.45	2.13	2.47	3.21
Na_2O	-	-	0.01	-	-	0.02
TOTAL	101.31	100.65	101.15	100.81	101.71	100.70

	B62 CORE	RIM	B79 CORE	INNER RIM	RIM	B83 CORE
Si	6.06	6.03	6.04	6.06	6.02	5.99
Al	0.00	0.00	0.00	0.00	0.00	0.01
TOTAL	6.06	6.03	6.04	6.06	6.02	6.00

	B62 CORE	RIM	B79 CORE	INNER RIM	RIM	B83 CORE
Al	3.87	3.92	3.98	3.98	3.95	3.96
Ti	0.00	0.00	0.00	0.00	0.00	0.00
TOTAL	3.87	3.92	3.98	3.98	3.95	3.96

	B62 CORE	RIM	B79 CORE	INNER RIM	RIM	B83 CORE
Fe	4.32	4.34.	4.59	4.82	4.84	4.13
Mg	0.67	0.47	0.57	0.40	0.53	0.45
Mn	0.52	0.69	0.37	0.32	0.24	0.92
Ca	0.56	0.56	0.42	0.37	0.42	0.55
Na	0.00	0.00	0.00	0.00	0.00	0.01
TOTAL	6.07	6.06	5.95	5.91	6.03	6.06

APPENDIX III

TABLE II

REPRESENTATIVE BIOTITE ANALYSES

SPECIMEN	B10	B13	B77	B56	B57	B8
SiO_2	34.21	34.87	34.84	33.98	35.02	34.60
TiO_2	4.17	2.97	3.23	3.51	3.29	3.76
Al_2O_3	19.37	19.73	19.55	19.45	19.47	19.62
FeO	20.41	20.20	19.46	24.35	·20.15	21.71
MnO	0.27	0.30	0.45	0.29	0.32	0.18
MgO	6.83	7.59	8.19	5.20	7.42	7.80
CaO	-·	-	-	-	-	-
Na_2O	0.15	0.10	0.18	0.05	0.14	0.00
K_2O	9.22	9.39	9.39	8.84	9.40	8.04
BaO	0.14	0.11	0.22	0.25	0.19	0.22
H_2O^a	3.88	3.91	3.93	3.86	3.92	3.90
TOTAL	98.65	99.17	99.44	99.78	99.32	98.83
Si	5.28	5.34	5.32	5.27	5.36	5.32
Al	2.72	2.66	2.68	2.73	2.64	2.68
TOTAL	8.00	8.00	8.00	8.00	8.00	8.00
Al	0.81	0.90	0.83	0.83	0.87	0.87
Ti	0.48	0.34	0.37	0.41	0.38	0.32
Fe	2.64	2.59	2.48	3.16	2.58	2.79
Mn	0.04	0.04	0.06	0.04	0.04	0.02
Mg	1.57	1.73	1.86	1.20	1.69	1.79
TOTAL	5.54	5.60	5.60	5.64	5.56	5.79
Ca	0.00	0.00	0.00	0.00	0.00	0.00
Na	0.05	0.03	0.05	0.01	0.04	0.00
K	1.82	1.83	1.83	1.75	1.83	1.58
Ba	0.01	0.01	0.01	0.01	0.01	0.01
TOTAL	1.88	1.87	1.88	1.77	1.88	1.59

TABLE II (continued)

SPECIMEN	B44	B62	B79	B83
SiO_2	34.27	35.83	36.51	34.42
TiO_2	2.86	2.34	2.31	2.32
Al_2O_3	18.44	18.20	18.84	19.11
FeO	22.10	21.24	20.95	22.00
MnO	0.13	0.17	0.07	0.34
MgO	8.41	8.62	8.43	6.83
CaO	-	-	-	-
Na_2O	0.21	0.14	0.16	0.10
K_2O	7.86	8.49	8.28	9.06
BaO	0.12	0.20	0.20	0.22
H_2O^a	3.86	3.92	3.96	3.84
TOTAL	98.26	99.15	99.71	98.23
Si	5.32	5.48	5.52	5.37
Al	2.68	2.52	2.48	2.63
TOTAL	8.00	8.00	8.00	8.00
Al	0.69	0.77	0.88	0.89
Ti	0.33	0.27	0.26	0.27
Fe	2.87	2.72	2.65	2.87
Mn	0.02	0.02	0.01	0.05
Mg	1.94	1.97	1.90	1.59
TOTAL	5.85	5.75	5.70	5.67
Ca	0.00	0.00	0.00	0.00
Na	0.06	0.04	0.05	0.03
K	1.56	1.66	1.60	1.80
Ba	0.01	0.01	0.01	0.01
TOTAL	1.63	1.71	1.66	1.84

APPENDIX III

TABLE III

REPRESENTATIVE CORDIERITE ANALYSIS

SPECIMEN	B10
SiO_2	47.24
TiO_2	—
Al_2O_3	32.02
FeO	10.07
MnO	0.59
MgO	6.78
CaO	0.01
Na_2O	0.20
TOTAL	96.91

Si	4.99
Al	1.01
TOTAL	6.00

Al	2.98
Ti	0.00
TOTAL	2.98

Fe	0.89
Mg	1.07
Mn	0.05
Na	0.04
Ca	0.00
TOTAL	2.05

APPENDIX III

TABLE IV

REPRESENTATIVE MUSCOVITE ANALYSES

SPECIMEN	B10	B13	B56	B57
SiO_2	44.89	46.12	47.31	46.54
TiO_2	0.45	0.34	1.14	1.02
Al_2O_3	35.89	35.27	34.22	35.22
Fe_2O_3	1.06	2.21	1.90	1.20
MnO	0.01	0.01	0.01	0.03
MgO	0.47	0.81	0.11	0.50
CaO	-	-	-	0.02
Na_2O	0.28	0.25	0.30	0.74
K_2O	10.36	10.59	9.63	10.20
BaO	0.36	0.21	0.22	0.24
H_2O^a	4.44	4.52	4.51	4.53
TOTAL	98.21	100.33	99.35	100.24
Si	6.06	6.12	6.28	6.16
Al	1.94	1.88	1.72	1.84
TOTAL	8.00	8.00	8.00	8.00
Al	3.78	3.63	3.64	3.65
Ti	0.05	0.03	0.11	0.10
Fe	0.11	0.22	0.19	0.12
Mn	0.00	0.00	0.00	0.00
Mg	0.10	0.16	0.02	0.10
TOTAL	4.04	4.04	3.96	3.97
Ca	0.00	0.00	0.00	0.00
Na	0.07	0.07	0.08	0.19
K	1.79	1.79	1.63	1.72
Ba	0.02	0.01	0.01	0.01
TOTAL	1.88	1.87	1.72	1.92

TABLE IV (continued)

SPECIMEN	B62	B79	B83
SiO_2	46.65	46.93	45.93
TiO_2	0.97	0.86	1.13
Al_2O_3	34.56	34.78	33.93
Fe_2O_3	2.00	1.13	2.03
MnO	0.01	0.00	0.02
MgO	1.10	0.61	0.83
CaO	-	-	-
Na_2O	0.54	0.64	0.36
K_2O	9.76	9.21	10.47
BaO	0.34	0.39	0.41
H_2O^a	4.54	4.51	4.47
TOTAL	100.47	99.06	99.58
Si	6.16	6.24	6.15
Al	1.84	1.76	1.85
TOTAL	8.00	8.00	8.00
Al	3.54	3.69	3.51
Ti	0.10	0.09	0.11
Fe	0.20	0.11	0.20
Mn	0.00	0.00	0.00
Mg	0.22	0.12	0.17
TOTAL	4.06	4.01	3.99
Ca	0.00	0.00	0.00
Na	0.14	0.16	0.09
K	1.64	1.56	1.79
Ba	0.02	0.02	0.02
TOTAL	1.80	1.74	1.90

TABLE V

PLAGIOCLASE COMPOSITIONS

SPECIMEN	X_{Na}	X_{Ca}	X_K
B10	0.68	0.31	0.01
B8	0.70	0.29	0.01

TABLE VI

K-FELDSPAR COMPOSITION

SPECIMEN	X_K	X_{Na}	X_{Ca}	X_{Ba}
B10	0.85	0.13	0.01	0.01

REFERENCES

REFERENCES

Anderson, D.E. & Buckley, G.R.,1973. Zoning in garnets - diffusion models. Contrib. Mineral. Petrol. 40, 87-104.

Anderson, D.E. & Olimpio, J.C., 1977. Progressive homogenisation of metamorphic garnets, South Morar, Scotland: evidence for volume diffusion. Can. Mineral. 15, 230-242.

Arzi, A.A., 1978. Critical phenomena in the rheology of partially melted rocks. Tectonophysics 44, 173-184.

Ashworth, J.R., 1972. Myrmekites of exsolution and replacement origins. Geol. Mag. 109, 45-62.

Ashworth, J.R., 1975. Sillimanite zones of the Huntly-Portsoy area in the northeast Dalradian, Scotland. Geol. Mag. 112, 113-136.

Ashworth, J.R., 1976. Petrogenesis of migmatites in the Huntly-Portsoy area, northeast Scotland. Mineral.Mag. 40. 661-682.

Ashworth, J.R., 1979. Discussion of B.W.D. Yardley on: genesis of the skagit gneiss migmatites. Bull. geol. Soc. Am.

Ashworth, J.R. & Chinner, G.A., 1978. Coexisting garnet and cordierite in migmatites from the Scottish Caledonides. Contrib. Mineral. Petrol. 65, 379-394.

Atherton, M.P., 1965. The composition in garnet in regionally metamorphised rocks. In Pitcher, W.S. & Flinn, G.W. (eds.) The controls of metamorphism. Geol. J. Spec. Issue No.1, 281-290.

Atherton, M.P. & Edmunds, W.M., 1966. An electron microprobe study of some zoned garnets from metamorphic rocks. Earth Planet. Sci. Lett. 1, 185-193.

Bailey, E.B. & Maufe, H.B., 1916. The geology of Ben Nevis

and Glen Coe. Mem. Geol. Surv. G.B., 1st Ed.

Blythe, D.F., 1975. A gravity survey of the Strontian granite complex, Argyllshire, Scotland. M.Sc. Dissertation, Univ. Leeds. (unpubl).

Bradbury, H.J., Smith, R.A. & Harris, A.L., 1976. Older granites as timemarkers in Dalradian evolution. J. geol. Soc. Lond., 260, 515-517.

Brewer, M.S., Brook, M. & Powell, D., 1970. Dating the tectono-metamorphic hostory of the southwestern Moine, Scotland. In Harris, A.L. et.al. (eds.) Caledonides of the British Isles - reviewed. Spec. Pub. geol. Soc. Lond. 8, 129-138.

Brook, M., Brewer, M.S., & Powell, D., 1976. Grenville age for rocks in the Moine of northwestern Scotland. Nature, Lond. 260, 515-517.

Brook, M., Powell, D., & Brewer, M.S., 1977. Grenville events in the Moine rocks of the Northern Highlands, Scotland. J. geol. Soc. Lond. 133, 489-496.

Brown, G.G., 1979. Geochemical and geophysical constraints on the origin and evolution of Caledonian granites. In Harris, A.L. et.al. (eds.), Caledonides of the British Isles - reviewed. Spec. Pub. geol. Soc. Lond. 8, 645-652.

Brown, P.E., Miller, J.A. & Grasty, R.L., 1968. Isotopic age of late Caledonian granitic intrusions in the British Isles. Proc. Yorks. geol. Soc. 36, 251-276.

Brown, R.L., 1964. The structure and metamorphism of east Moidart and west Sunart, Argyll and Inverness-shire. Ph.D. Thesis, Univ. Edinburgh (unpubl).

Brown, R.L., Dalziel, I.W.D. & Johnson, M.R.W., 1970.

A review of the structure and stratigraphy of the
Moinian of Ardgour, Moidart and Sunart - Argyll and
Inverness-shire. Scott. J. Geol. 6, 309-335.

Burnham, C.W., Holloway, J.R. & Davis, N.F., 1969. Thermo-
dynamic properties of water to $1000^{\circ}C$ and 10,000 bars.
Geol. Soc. Am. Spec. Paper 132.

Butler, B.C.M., 1965. A chemical study of some rocks of the
Moine series of Scotland. Q.J. Geol. Soc. Lond., 121,
163-208.

Chatterjee, N.D. & Johannes, W., 1974. Thermal stability
and standard thermodynamic properties of synthetic 2M,
- Muscovite, $KAl_2(AlSi_3O_{10}(OH)_2)$. Contrib. Mineral.
Petrol. 48, 89-114.

Cheney, J.T. & Guidotti, C.V., 1979. Muscovite - plagioclase
equilibria in sillimanite + quartz bearing metapelites,
Puzzle Mountain area, northwest Maine. Am. J. Sci., 279,
411-4341

Clark, G.C., 1961. The structural and metamorphic history
of the Lochailort (Moidart) area. Ph.D. Thesis, Univ.
Edinburgh. (unpubl).

Clifford, T.N., 1957. The stratigraphy and structure of part
of the Kintail District of southern Ross-shire.
Q. J. Geol. Soc. Lond., 113, 57-92.

Cook, D.R., 1976. The geology of the Cairnsmore of Fleet
granite and its environs, southwest Scotland.
Ph.D. Thesis. Univ. St. Andrews. (unpubl).

Cressey, G., Schmid, R. & Wood, B.J., 1978. Thermodynamic
properties of almandine - grossular garnet solid solutions.
Contrib. Mineral. Petrol, 67, 397-404.

Currie, K.L., 1971. The reaction 3cordierite = 2garnet +

4sillimanite + 5quartz as a geological thermometer in the Opinicon Lake Region, Ontario. Contrib. Mineral. Petrol., 55, 215-226.

Dalziel, I.W.D., 1963. A structural study of the granitic gneiss and associated Moinian rocks between Loch Shiel and Loch Eil, Argyll and Inverness-shire. Ph.D. Thesis Univ. Edinburgh (unpubl).

Dalziel, I.W.D.,. 1966. A structural study of the granitic gneiss of western Ardgour, Argyll and Inverness-shire. Scott. J. Geol., 2, 125-152.

Dalziel, I.W.D. & Brown, R.L., 1965. The structural dating of the sillimanite -grade metamorphism of the Moines in Ardgour (Argyll) and Moidart (Inverness-shire). Scott. J. Geol., 1, 304-311.

Davis, J.C., 1973. Statistics and data analysis in Geology. J. Wiley & Sons, 322-352.

de Bethune, P., Laduron, D., & Bocquet, J., 1975. Diffusion processes in resorbed garnets. Contrib. Mineral. Petrol. 66, 113-117.

Dewey, J.F., 1969. Evolution of the Appalachian/Caledonian orogen. Nature, Lond., 222, 124-129.

Edmunds, W.M.& Atherton, M.P., 1971. Polymetamorphic evolution of garnet in the Fanad aureole, Donegal,Eire. Lithos. 4, 147-161.

Evans, B.W. & Guidotti, C.V., 1966. The sillimanite - potash feldspar isograd in western Maine, U.S.A. Contrib. Mineral. Petrol., 12, 25-62.

Ferry, J.M., 1978. Fluid interaction between granite and sediment during metamorphism, south-central Maine. Am. J. Sci., 278, 1025-1056.

Ferry, J.M. & Spear, F.S., 1978. Experimental calibration of the partitioning of Fe and Mg between biotite and garnet. _Contrib. Mineral. Petrol._ 66, 113-117.

Fettes, D.J., 1979. A metamorphic map of the British and Irish Caledonides. _In_: Harris, A.L. et.al. (eds). _Caledonides of the British Isles - reviewed. Spec. Pub. geol. Soc. Lond._ 8, 307-321.

Freer, R., 1979. An experimental measurement of cation diffusion in almandine garnet. _Nature, Lond._ 280, 220-222.

Ghent, E.D., 1976. Plagioclase - garnet - Al_2SiO_5- quartz, A potential geobarometer-geothermometer. _Am. Mineral._, 61, 710-714.

Giletti, B.J., Moorbath, S., & Lambert, R.St.J., 1961. A geochronological study of the metamorphic complexes of the Scottish Highlands. _Q. J. geol. Soc. Lond._, 117, 233-272.

Gould, D., 1966. _Geochemical and mineralogical studies of the granitic gneiss and associated rocks of western Ardgour, Argyll._ Ph.D. Thesis, Univ. Edinburgh. (unpubl).

Grant, J.A. & Weiblen, P.W., 1971. Retrograde zoning in garnet near the second sillimanite isograd. _Am. J. Sci._, 270, 281-296.

Greenwood, H.J., 1975. Buffering of pore fluids by metamorphic reactions. _Am J. Sci._ 275, 573-593.

Greig, D.C., 1971. The south of Scotland. _Brit. Reg. Geol._ H.M.S.O.

Grew, E.S., 1981. Granulite - facies metamorphism at Molodezhnaya Station, East Antartica. _J. Petrol._ in press.

Guidotti, C.V., 1970. The mineralogy and petrology of the

transition from the lower to the upper sillimanite zone in the Oquossoc area, Maine. *J. Petrol.* 11, 277-336.

Guidotti, C.V. & Sassi, F.P., 1976. Muscovite as a petrogenetic indicator mineral in pelitic schists. *N. Jb. Mineral. Abh.* 127, 97-142.

Halliday, A.N., Aftalion, M., Van Breemen, O. & Jocelyn, J., 1979. Petrogenic significance of Rb-Sr and U-Pb isotopic systems in the 400 m.y. old British Isles granitoids and their hosts. In: Harris, A.L. et.al. (eds). *Caledonides of the British Isles - reviewed. Spec. Pub. geol. Soc. Lond.*, 8, 653-662.

Halliday, A.N., Stephens, W.E. & Harmon, R.S., 1980. Rb-Sr and 0 Isotopic relationships in 3 zoned Caledonian granitic plutons, Southern Uplands, Scotland: evidence for varied sources and hybridisation of magmas. *J. geol. Soc. Lond.*, 137, 329-348.

Harris, A.L., Baldwin, C.T., Bradbury, H.J., Johnson, H.D., and Smith, R.A., 1978. Ensialic basin sedimentation: The Dalradian supergroup. *Geol. J. Spec. Issue 10*, 118-138.

Harry, W.T., 1954. The composite granitic gneiss of western Ardgour. *Q. J. geol. Soc. Lond.* 109, 285-309.

Harte, B. & Henley, K.J., 1966. Occurrence of compositionally zoned almanditic garnets in regionally metamorphosed rocks. *Nature, Lond.*, 210, 689-692.

Helgeson, H.C., Delany, J.M., Nesbitt, H.W., & Bird, D.K., 1978. Summary and critique of the thermodynamic properties of rock forming minerals. *Am. J. Sci.*, 278A.

Hensen, B.J. & Green, D.H., 1975. Experimental study of the stability of cordierite and garnet in pelitic compositions

at high pressures and temperatures. Contrib. Mineral. Petrol. 38, 151-166.

Holdaway, M.J., 1971. Stability of andalusite and the aluminium silicate phase diagram. Am. J. Sci., 271, 97-131.

Holdaway, M.J., 1980. Chemical formulae and activitymodels for biotite, muscovite and chlorite applicable to pelitic metamorphic rocks. Am. Mineral. 65, 711-719.

Holdaway, M.J. & Lee, S.M., 1977. Fe-Mg cordierite stability in high-grade pelitic rocks based on experimental, theoretical and natural observations. Contrib. Mineral. Petrol. 63, 175-198.

Hollister, L.S., 1966. Garnet zoning: An interpretation based on the Rayleigh fractionation model. Science, 154, 1647-1651.

Hollister, L.S., 1969. Contact metamorphism in the Kwoiek area of British Columbia: An end member of the metamorphic process. Bull. Geol. Soc. Amer. 80, 2465-2494.

Hollister, L.S., 1977. The reaction forming cordierite from garnet, the Khtada Lake metamorphic complex, British Columbia. Can. Mineral., 15, 217-229.

Hovis, G.C., 1972. A solution calorimetric and X-ray investigation of Al-Si distribution in monoclinic potassium feldspars. In: MacKenzie, W.S. & Zussman, J. (eds). The Feldspars. Manchester University Press. 114-144.

Howkins, J.B., 1961. The structural and metamorphic history of Moidart, southwest Inverness-shire. Ph.D. Thesis, Univ. Edinburgh. (unpubl).

Hutcheon, I, Froese, E. & Gordon, T.M., 1974. The assemblage

quartz - sillimanite - garnet - cordierite as an indicator of metamorphic conditions in the Daly Bay complex, N. W. T. <u>Contrib. Mineral. Petrol</u>, 44, 29-34.

Johnson, M.R.W., 1963. Some time relations of movements and metamorphism in the Scottish Highlands. <u>Geol. En. Mijnb.</u>, 42, 121-142.

Johnson, M.R.W., Sanderson, D.J. & Soper, N.J., 1979. Deformation in the Caledonides of England, Ireland and Scotland. <u>In</u>: Harris, A.L. (eds). <u>Caledonides of the British Isles - reviewed</u>. Spec. Pub. Geol. Soc. Lond. 8, 165-186.

Johnstone, G.S., 1973. The Moine Succession. <u>In</u>: Harris, A.L. et.al. (eds). <u>A correlation of Precambrian rocks in the British Isles</u>. 30-42. <u>Spec. Rep. geol. Soc. Lond.</u> 6.

Johnstone, G.S., Smith, D.I. & Harris, A.L. 1969. The Moinian assemblage of Scotland. <u>In</u>: Kay, M. (ed). <u>Mem. Am. Ass. Petrol. Geol.</u> 12, 159-180.

Kennedy, W.Q., 1946. The Great Glen Fault. <u>J. geol. Soc. Lond.</u> 102, 41-76.

Kennedy, W.Q., 1949. Zones of progressive regional metamorphism in the Moine schists of the Western Highlands of Scotland. <u>Geol. Mag.</u> 86, 43-56.

Kerrick, D.M., 1972. Experimental determination of muscovite + quartz stability with P_{H_2O} P_{TOTAL}. <u>Am. J. Sci.</u>, 272, 946-958.

Lambert, R. St. J., 1969. Isotopic studies relating to the Precambrian history of the Moinian of Scotland. <u>Proc. geol. Soc. Lond.</u> 1652, 243-245.

Lambert, R.St.J. & McKerrow, W.S., 1976. The Grampian orogeny. <u>Scott. J. Geol.</u> 12, 271-292.

Lambert, R.St.J., Winchester, J.A. & Holland, J.G., 1979. Time, space and intensity relationships of the Precambrian, and Lower Palaeozoic metamorphisms of the Scottish Highlands. In: Harris, A.L. et.al. (eds). Caledonides of the British Isles - reviewed. Spec. Pub. geol. Soc. Lond. 8, 363-368.

Lee, G.W. & Bailey, E.B., 1925. The Pre-Tertiary geology of Mull,Loch Aline and Oban. Mem. Geol. Surv. G.B.

Lee, S.M. & Holdaway, M.J., 1977. Significance of Fe - Mg cordierite stability relations on temperature, pressure and water pressure in cordierite granulites. Geophysic. Monogr. 20, 79-94.

Leedal, G.P., 1952. The Cluanie Igneous intrusion, Inverness-shire and Ross-shire. Q.J. geol. Soc. Lond. 108, 35-63.

Leggett, J.K., McKerrow, W.S. & Eales, M.H., 1979. The Southern Uplands of Scotland: A lower Palaeozoic accretionary prism. J. geol. Soc. Lond. 136, 755-760.

Long, L.E., & Lambert, R. St. J., 1963. Rb - Sr isotopic ages from the Moine series. In: Johnson, M.R.W. & Stewart, F.H. (eds). The British Caledonides. Oliver & Boyd, Edinburgh. 217-247.

Loomis, T.P., 1975. Reaction zoning of garnet. Contrib. Mineral. Petrol. 52, 285-305.

Loomis, T.P., 1978. Multicomponent diffusion in garnet. Am. J. Sci. 278, 1099-1137.

Lundgren, L.W. Jr., 1966. Muscovite reactions and partial melting in southeastern Connecticut. J. Petrol. 7, 421-453.

MacGregor, A.G. & Kennedy, W.Q., 1932. The Morvern - Strontian 'granite'. Sum. Prog. Geol. Surv. 1931, 105-119.

MacGregor, M., 1937. The western part of the Criffel - Dal-
    beattie Igneous Complex. Q. J. geol. Soc. Lond. 93,
    457-486.

MacQueen, J.A. & Powell, D., 1977. Relationships between
    deformation and garnet growth in Moine (Precambrian)
    rocks of western Scotland. Bull. geol. Soc. Am., 88
    235-240.

Marston, R.J., 1970. The Foyers granitic complex, Inverness-
    shire, Scotland. Q. J. geol. Soc. Lond, 126, 331-336.

Mehnert, K.R., 1968. Migmatites and the origin of granitic
    rocks. Elsevier Publishing Company, Amsterdam.

Mould, D.D.C.P., 1946. The geology of the Foyers 'granite'
    and the surrounding country. Geol. Mag., 83, 249-265.

Munro, M., 1965. Some structural features of the Caledonian
    granite complex at Strontian, Argyllshire. Scott. J.
    Geol., 1, 152-175.

Munro, M., 1973. Structures in the southeastern portion of
    the Strontian granite complex, Argyllshire. Scott. J.
    Geol., 9, 99-108.

Neilson, M.J. & Brockman, G.F., 1977. The error associated
    with point counting. Am. Mineral. 62, 1238-1244.

Newton, R.C. & Wood, B.J., 1979. Thermodynamics of water in
    cordierite and some petrologic consequences of cordierite
    as a hydrous phase. Contrib. Mineral. Petrol. 68,
    391-405.

Ohmoto, H. & Kerrick, D., 1977. Devolatization equilibria
    in graphitic systems. Am. J. Sci. 277, 1013-1044.

Okrusch, M., 1971. Garnet - cordierite - biotite equilibria
    in the Steinach aureole, Bavaria. Contrib. Mineral.
    Petrol. 32, 1-23.

Orville, P.M., 1972. Plagioclase cation exchange equilibria with aqueous chloride solutions: results at 700°C and 2000 bars in the presence of quartz. Am. J. Sci. 272 234-272.

Osberg, P.H., 1971. An equilibrium model for Buchan-type metamorphic rocks, south-central Maine. Am.Mineral. 56, 569-576.

Pankhurst, R.J. & Pidgeon, R.T., 1976. Inherited isotope systems and the source region prehistory of the early Caledonian granites in the Dalradian series of Scotland. Earth Planet. Sci. Lett.31, 55-68.

Parsons, L.M., 1979. The state of strain adjacent to the Great Glen Fault. In: Harris, A.L. et. al. (eds). The Caledonides of the British Isles - reviewed. Spec. Pub. geol. Soc. Lond., 8, 287-289.

Peach, B.N. & Horne, J., 1899. The Silurian rocks of Britain, Vol. 1., Scotland. Mem. Geol. Surv. G.B.

Phemister, J., 1936. Scotland - The Northern Highlands. Brit. Reg. Geol. 1st Edns. H.M.S.O.

Phillips, W.E.A., Stillman, C.J. & Murphy, T., 1976. A Caledonian plate tectonic model. J. geol. Soc. Lond. 132, 579-609.

Phillips, W.J., 1955. The metamorphic rocks associated with the Criffel-Dalbeattie granodiorite. Geol. Mag. 92, 1-20.

Phillips, W.J., 1956. The Criffell-Dalbeattie granodiorite complex. Q. J. geol. Soc. Lond. 112, 221-239.

Phillips, W.J., Fuge, R. & Phillips, N., 1981. Convection and crystallisation in the Criffell-Dalbeattie pluton. J. geol. Soc. Lond. 138, 351-366.

Piasecki, M.A., 1980. New light on the Moine rocks of the Central Highlands of Scotland. J. geol. Soc. Lond.

137, 41-60.

Piasecki, M.A.J. & Van Breeman, O., 1979. The 'Central Highland Granulites': cover-basement tectonics in the Moine. In: Harris, A.L. et.al. (eds). Caledonides of the British Isles - reviewed. Spec. Pub. geol. Soc. Lond. 8, 139-144.

Pidgeon, R.T. & Aftalion, M., 1978. Cogenetic and inherited zircon U-Pb systems in granites: Palaeozoic granites of Scotland and England. In: Dowes, D.R. & Leake, B.E. (eds). Crustal evolution in northwestern Britain and adjacent regions. Geol. J. Spec. Issue No. 10, 183-248.

Powell, D., 1974. Stratigraphy and structure of the western Moine and the problem of Moine orogenesis. J. geol. Soc. Lond. 130, 575-593.

Richardson, S.W., Gilbert, M.C. & Bell, P.M., 1969. Experimental determination of kyanite - andalusite and andalusite - sillimanite equilibria: the aluminium silicate triple point. Am. J. Sci. 267, 259-272.

Richardson, S.W. & Powell, R., 1976. Thermal causes of the Dalradian metamorphism in the Central Highlands of Scotland. Scott. J. Geol. 12, 237-268.

Robie, R.A., Hemingway, B.S. & Fisher, J.R., 1978. Thermo-dynamic properties of minerals and related substances at 298.15K and 1 bar $(10^5$ pascals) pressure and at higher temperatures. U.S. Geol. Surv. Bull. 1452.

Sabine, P.A., 1963. The Strontian granite complex, Argyll-shire. Bull. Geol. Surv. G.B., 20, 6-42.

Schmid, R., Cressey, G. & Wood, B.J., 1978. Experimental determination of univariant equilibria using divariant solid-solution assemblages. Am. Mineral. 63, 511-515.

Smith, D.I., 1979. Caledonian minor intrusions of the
N. Highlands of Scotland. In: Harris, A.L. et.al. (eds).
Caledonides of the British Isles - reviewed. Spec. Pub.
geol. Soc. Lond. 8, 683-698.

Stephens, W.E., 1972. The geochemistry of the Dalbeattie
granodiorite complex and associated rocks. Ph.D. Thesis
Aberystwyth (unpubl).

Sturt, B.A., 1962. The composition of garnets from pelitic
schists in relation to the grade of regional metamorphism.
J. Petrol. 3, 181-191.

Sweatman, T.R. & Long, J.V.P., 1969. Quantitative electron-
probe microanalysis of rock forming minerals. J. Petrol.
10, 332-379.

Tanner, P.W.G., 1970. The Sgurr Beag slide - a major tectonic
break within the Moinian of the Western Highlands of
Scotland. Q. J. geol. Soc. Lond. 126, 435-63.

Tanner, P.W.G., Johnstone, G.S., Smith, D.I. & Harris, A.L.,
1970. Moinian stratigraphy and the problem of the
central Ross-shire inliers. Bull. geol. Soc. Am. 81,
299-306.

Thompson, A.B., 1976.a, Mineral reactions in pelitic rocks:
I. prediction of P-T-X (Fe - Mg) phase relations.
Am. J. Sci. 276, 401-424.

Thompson, A.B., 1976.b, Mineral reactions in pelitic rocks:
II. Calculations of some P-T-X (Fe - Mg) phase relations.
Am. J. Sci. 276, 425-454.

Thompson, A.B. & Algor, J.R., 1977. Model systems for
anatexis of pelitic rocks. I. Theory of melting reactions
in the system $KAlO_2 - NaAlO_2 - Al_2O_3 - SiO_2 - H_2O$.
Contrib. Mineral. Petrol. 63, 247-269.

Thompson, A.B. & Tracy, R.J., 1979. Model systems for
anatexis of pelitic rocks II. Facies series melting
and reactions in the system CaO - $KAlO_2$ - $NaAlO_2$ - SiO_2
- H_2O. Contrib. Mineral. Petrol. 70, 429-438.

Tracy, R.J., Robinson, P. & Thompson, A.B., 1976. Garnet
composition and zoning in the determination of temp-
erature and pressure. Am. Mineral. 61, 762-775.

Turner, F.J., 1968. Metamorphic petrology: mineralogical
and field aspects. McGraw-Hill.

Van Breeman, O, Pidgeon, R.T. & Johnson, M.R.W., 1974.
Precambrian and Palaeozoic pegmatites in the Moines of
Northern Scotland. J. geol. Soc. Lond. 130, 493-507.

Van Breeman, O, Halliday, A.N., Johnson, M.R.W. & Bowes, D.R.
1978. Crustal additions in late Precambrian times.
In: Bowes D.R. & Leake, B.E. (eds). Crustal evolution
in northwestern Britain and adjacent regions. Geol. J.
Spec. Issue. No. 10 81-106.

Van Breeman, O, Aftalion, M., Pankhurst, R.J., Richardson, S.
W., 1979. Age of the Glen Dessary syenite, Inverness-
shire: diachronous Palaeozoic metamorphism across the
Great Glen. Scott. J. Geol. 15, 49-62.

Van der Molen, I. & Paterson, M.S., 1979. Experimental
deformation of partially melted granite. Contrib.
Mineral. Petrol. 70, 299-318.

Waldbaum, D.R. & Thompson, J.B., Jr., 1969. Mixing properties
of sanidine crystalline solutions: IV phase diagrams
from equations of state. Am. Mineral. 54, 1274-1298.

Watson, J., 1964. Conditions in the metamorphic Caledonides
during the period of late orogenic cooling. Geol. Mag.
101, 457-465.

Wells, P.R.A., 1979. P-T conditions in the Moines of the Central Highlands, Scotland. J. geol. Soc. Lond. 136, 663-671.

Wells, P.R.A., 1981. Discussion on P-T conditions in the Moines of the Central Highlands Scotland; a reply to J. A. Winchester. J. geol. Soc. Lond. 138, 206-209.

Wells, P.R.A. & Richardson, S.W., 1979. Thermal evolution of metamorphic rocks in the Central Highlands of Scotland. In: Harris, A.L. et. al. (eds). Caledonides of the British Isles - reviewed. Spec. Pub. geol. Soc. Lond. 8, 339-344.

Winkler, H.G.F., 1976. Petrogenesis of metamorphic rocks. Springer-Verlag.

Winchester, J.A., 1974. The zonal pattern of regional metamorphism in the Scottish Caledonides. J. geol. Soc. Lond. 130, 509-524.

Wood, B.J., 1973. Fe^{2+} - Mg^{2+} partition between coexisting cordierite and garnet - a discussion of the experimental data. Contrib. Mineral. Petrol. 40, 253-258.

Wood, B.J. & Fraser, D.G., 1977. Elementary thermodynamics for geologists. Oxford University Press.

Woodsworth, G.J., 1977. Homogenisation of zoned garnets from pelitic schists. Can. Mineral. 15, 230-242.

Yardley, B.W.D., 1977. An empirical study of diffusion in garnet. Am. Mineral. 62, 793-800.

Yardley, B.W.D., 1978. Genesis of the Skagit gneiss migmatites, Washington, and the distinction between possible mechanisms of migmatisation. Bull. geol. Soc. Am. 89, 941-951.

Yardley, B.W.D., Leake, B.E. & Farrow, C.M., 1980. The metamorphism of Fe-rich pelites from Connemara, Ireland. J. Petrol. 21, 365-399.

MAP I

I.M. TYLER   Ph.D.   THESIS

THE METAMORPHIC ENVIRONMENTS OF THE
STRONTIAN, FOYERS AND DALBEATTIE INTRUSIONS,
SCOTLAND.

MAP II

I.M. TYLER   Ph.D. THESIS

THE METAMORPHIC ENVIRONMENTS OF THE
STRONTIAN, FOYERS AND DALBEATTIE INTRUSIONS,
SCOTLAND.

MAP III

I.M. TYLER   Ph.D. THESIS

THE METAMORPHIC ENVIRONMENTS OF THE
STRONTIAN, FOYERS AND DALBEATTIE INTRUSIONS,
SCOTLAND.

Page removed for copyright restrictions.